# VARIATIONS IN ROOT SYSTEM ARCHITECTURE AND ROOT GROWTH DYNAMICS OF *BRASSICA RAPA* GENOTYPES USING A NEW SCANNER-BASED PHENOTYPING SYSTEM

**MICHAEL OSEI ADU**

Teachers' Certificate 'A' Agricultural & General Science, PTC Akropong
BSc. (Hons.) Agricultural Science, Univ. of Cape Coast
MSc. Crop Improvement, Univ. of Nottingham

Thesis submitted to the University of Nottingham for the degree of Doctor of Philosophy

University of Nottingham
School of Biosciences
Sutton Bonington Campus
Leicestershire, LE12 5RD

July 2014

**Abstract**

There is a need to breed for root systems architectures (RSAs) that optimise soil resource acquisition. This requires high resolution and high-throughput quantification of RSA in as natural an environment as possible. Current imaging techniques are limited by cost, reproducibility, throughput and complexity. This thesis describes (1) the construction of a low cost, high-resolution, root phenotyping platform that requires no sophisticated equipment which is adaptable to most laboratory and glasshouse environments and (2) its application to quantify environmental and temporal variation in RSA between genotypes of *Brassica rapa* L.

The high resolution root phenotyping system (HRP) that was constructed employed 24 scanners and could screen up to 72 individual plants at any time, with the possibility of capturing thousands of root images daily depending on the operational number of scanners and scanning periodicity. Plants were supplied with a complete nutrient solution through the wick of a germination paper. Images of RSA were acquired automatically, over extended periods, using multiple scanners controlled by customised software. The RSA data was used to validate a mechanistic model and mixed effects models were used to describe the sources of variation in traits contributing to RSA. Plants were also grown in rhizoboxes and under varying concentrations of P ($[P]_{ext}$).

Broad-sense heritability ($H^2$), was highest (≥ 0.70) for shoot biomass, length of primary roots (PRs), number of lateral roots (LRs). Coefficients of variation in RSA traits within a genotype were large and ranged between 5 and 103%. It was found that between 4 and 48 replicates were needed to detect a significant difference (95% CI, 50% difference between trait means). Significant differences were found between genotypes in root traits with strong positive correlations among RSA traits and between biomass and RSA traits. Principal component analyses identified 5 significant axes of variation, accounting for approximately 86 and 78% of the variation in the genotypes on paper and soil substrates, respectively. Cluster analysis of the genotypes produced 5 discrete groups. Genotypes with more or less shoot biomass or with bigger or smaller RSA could be distinguished.

A density-based 2D model reproduced experimental results accurately by simulating PR length and total length of LRs. Mixed-effects statistical models demonstrated that root traits show temporal variations of various types with significant effects of genotype. All genotypes followed a similar growth pattern with time, but differed in their maximum total root length (TRL), primary root length (PRL) and LR growth. A 3-parameter logistic model satisfactorily described TRL and PRL when genotypes were grown on both paper and soil substrates. On paper substrate, TRL required only a single, random-effect parameter (asymptote), describing maximum TRL. On soil substrate, TRL required two random-effects parameters, asymptote and inflection, describing maximum TRL and time at which ½ of maximum TRL occurs, respectively. Primary root length on both paper and soil substrates required only a single, random-effect parameter, describing maximum PRL. The growth rate of LRs of all ages followed a quadratic function and required only a single, random-effect parameter, describing maximum growth rate.

There was variation in specific RSA traits and plasticity in response to $[P]_{ext}$ among genotypes. Length of the apical un-branched zone of the PR increased with increasing $[P]_{ext}$. Total root length, total LR length and number of LRs was positively correlated with total plant tissue P concentration at low $[P]_{ext}$ but not at high $[P]_{ext}$. Paper substrate was more suitable for screening seedling root traits but root phenotypes must be validated *in situ* in the field or in soil media because some differences were evident between data observed on paper and soil substrates.

Scanner-based phenotyping of RSA provides economical means of studying the mechanisms underlying the plant-soil interactions and can be used to quantify environmental and temporal variation in traits contributing to RSA. The HRP system can be extended to screen the large populations required for breeding for efficient resource acquisition. The necessity for high replication and time-consuming image analysis could however limit throughput in the phenotyping system.

**Research article from this thesis (Appendix 8)**

**Adu, M.O**., Chatot A., Wiesel, L., Bennett, M.J., Broadley, M.R., White, P.J., Dupuy, X.L. (2013) A scanner system for high-resolution quantification of variation in root growth dynamics of *Brassica rapa* genotypes*. Journal of Experimental Botany* **65** (8): 2039-2048. doi: 10.1093/jxb/eru048.

**Table of Contents**

**Declaration**

I certify that except where specific reference to other study is stated, this thesis is based on the results of study conducted by myself and it is my own composition. Neither this thesis, nor any part of it, has been previously presented or is being presented for any degree.

**Michael O. Adu**

*Unto God be the Glory*

*To the memory of Grandma, Maa Agnes Clara Abena Brepo.*

*" Maa, ɛkaa me nko a na anka ɛnɛ da yi wowɔ yɛn nkyɛn ha, nanso nea Onyame yɛ na eye.*
*Nhoma yi kyerɛ sɛ wobrɛ anyɛ kwa. Nea wofii ase no, ɛnɛ, ayɛ nhyira.*
*Onyame mfa wo nsie".*

***"It always seems impossible until it's done"***

*Nelson Madiba Rolihlahla Dalibhunga Mandela*

**Acknowledgements**

I firstly wish to express my sincere gratitude to the UK Biotechnology and Biological Sciences Research Council (BBSRC) Crop Improvement Research Club and BBSRC Professorial Fellowship and University of Nottingham (UoN) Vice-Chancellor's Scholarship for Research Excellence for funding this study. Student travel grants from the British Society of Soil Science (BSSS), Society for Experimental Biology (SEB) and UoN Kesteven WVS Scholarship are duly acknowledged. My utmost gratitude also goes to my supervisors, Dr Lionel X. Dupuy (James Hutton Institute, JHI) for his comprehensive feedback, steadfast enthusiasm in this work and his unbridled patience in mentoring me, Prof. Philip J. White (JHI) for his constructive criticisms, advice and guidance, Prof. Malcolm J. Bennett (UoN) for his interest in this work and Prof. Martin R. Broadley (UoN) for believing in me from the outset, assistance in getting funding and admitting me into his research group.

My PhD would have been impossible without the support and generosity from many colleagues and to them I would like to express my deepest appreciation. The help of Jim Anderson was invaluable in building the Scanner banks, Ken Loades introduced me to *ImageJ*, Glen Bengough allowed unrestrained usage of his Perspex plates, Tim George and Lawrie Brown taught me tissue P analyses, Jacky Thompson helped with ICP analyses, Dimitris Kalogilos was very instrumental in density-based modelling and Guillaume Lobet and his group at Université catholique de Louvain, Belgium, allowed me to use *SmartRoot* even before its publication and provided prompt feedback anytime I needed it. I am grateful to Amy Gibson, Sophie Hiel, Linda Ford, Gill Banks and Bruna Arruda who provided priceless help for laboratory work. I am also grateful for advice from Jim McNichol, Christine Hackett and Katharine Preedy on statistical analyses.

For the prayers and support of many friends, including members of Mountain of Glory Church, Milton Keynes and members of Jeff Ellis' cell group, Gate Church International, Dundee, God richly bless you all. To Belinda Sampong, Prince Biribi, Edem Tamakloe, Michael Boakye, Michael Agyapong, Silas Quashie, Joseph Agyei Obeng, Annor Berefo, Kwadwo Dei, John Mensah, Wilberforce Ashie Dsane and Daniel Dzidzienyo, I am forever grateful. David Oscar Yawson, thank you for your friendship in a land of few genuine friends and keeping me sane throughout this process. I am immortally indebted to all my family members who ceaselessly provided encouragements and support whenever I needed it. Finally, I am particularly indebted to my beautiful wife, Georgina Osei-Adu (La belle), who has had to endure many sacrifices for a husband in absentia. I love you honey. To our gorgeous daughter, Maame Afua Ayeyi Osei-Adu, your arrival and associated challenges are a source of motivation for me to press on to success regardless of the difficulties, thank you sweetheart.

## List of Figures

## List of Tables

## List of Abbreviations

| | |
|---|---|
| $[P]_{ext}$ | External phosphorus concentration |
| $\Delta P_{app}$ | Difference in amount of P applied as fertilizer between high and low P treatments |
| $\mu$ | Magnitude of a root system |
| $\alpha$ | Altitude of a root system |
| AIC | Akaike information criterion |
| ANOVA | Analysis of variances |
| APUE | Agronomic phosphorus use efficiency |
| BIC | Bayesian information criterion |
| CCD | Charge Coupled Device |
| CI | Confidence interval |
| CLSM | Confocal Laser Scanning Microscopy |
| COP | Castor Oil Penetration |
| CR | Crown root |
| CV | Coefficient of variation |
| DAS | Days after sowing |
| DM | Dry matter |
| dpi | Dots per inch |
| *E* | External link of a root system |
| ENR | Efficient and nonresponsive genotypes |
| ER | Efficient and responsive genotypes |
| GPR | Ground penetrating radar |
| HP | High external phosphorus concentration (high $[P]_{ext}$) |
| HRP | High-resolution root phenotyping |
| *I* | Internal link of a root system |
| ITGV | Intra-genotypic variability |
| ICP-MS | Inductively Coupled Plasma - Mass Spectrometry |
| Int. Dist. | Inter-branch distance of lateral roots |
| LED | Light-Emitting Diode |
| LP | Low external phosphorus concentration (low $[P]_{ext}$) |
| logLik | Log-Likelihood |
| LR | Lateral root |
| LR Diam. | Mean lateral rots diameter |
| LRGR | Mean growth rate of lateral roots |
| LRL | Lateral root length |
| LSD | Least significant difference |
| LSFM | Light Sheet Fluorescence Microscopy |
| MER | Mean Extension Rates |
| MG | Malachite Green |
| MRI | Magnetic Resonance Imaging |
| NENR | Non-efficient and nonresponsive genotypes |
| NER | Non-efficient and responsive genotypes |
| ns | Not significant |
| OPT | Optical Projection Tomography |
| P. Dens. | Primary root child density or branching density |
| PAR | Photosynthetically active radiation |
| PER | Phosphorus efficiency ratio |
| $P_f$ | Phosphorus fertilizer |
| $P_{high}$ | Tissue P concentration on a P fertilized soil |
| Pi | Phosphate |
| $P_{low}$ | Tissue P concentration with little P fertilization |

| | |
|---|---|
| PPUE | Physiological phosphorus use efficiency |
| PR | Primary root |
| PR Diam. | Primary root diameter |
| PRL | Primary root length |
| PUE | Phosphorus use efficiency |
| PUpE | Phosphorus acquisition (uptake) efficiency |
| PUtE | Phosphorus utilization efficiency |
| PVC | Polyvinylchloride |
| Q-Q | Quantile-quantile |
| QTL | Quantitative trait locus |
| R:S | Root-to-shoot biomass ratio |
| RDW | Root dry weight |
| REML | Residual maximum likelihood |
| RFW | Root fresh weight |
| RGB | Red green blue |
| RIL | Recombinant inbred line |
| RMR | Relative multiplication rate |
| RP | Rock phosphate |
| RRE | Relative rate of extension |
| RSA | Root system architecture |
| RTD | Root tissue density |
| s.e. / s.e.d. / s.d. | Standard error / Standard error of differences of means / Standard deviation |
| SDW | Shoot dry weight |
| SFW | Shoot fresh weight |
| SOM | Soil organic matter |
| SPIM | Single Plane Illumination Microscopy |
| SRL | Specific root length |
| TI | Topological index |
| TLRL | Total lateral root length |
| TRL | Total root length |
| X-ray CT | X-ray computed tomography |
| $Y_{high}$ | Yield on P fertilized soil |
| $Y_{low}$ | Yield on a soil with low P fertilisation |

# CHAPTER 1 : BACKGROUND AND LITERATURE REVIEW

## 1.0 Background

The growth, morphology and physiology of roots are intimately linked to plant genotype and the properties of the soil or medium in which they grow. Crop plants have evolved many root adaptations for acquiring soil nutrients such as nitrogen (N), potassium (K) and phosphorus (P). This adaptability (plasticity) of roots is of particular importance for acquiring resources with low phytoavailability such as P (George *et al.*, 2011a; Hammond *et al.*, 2009; Hammond and White, 2008; Lynch, 2011; White *et al.*, 2009). *Brassica* crops, for example, adapt to P limiting conditions through the initiation and rapid growth of lateral roots (LRs; Hammond *et al.*, 2009; Lynch and Brown, 2008; White *et al.*, 2005). Accurate measurements of root system features can be used to predict plants' ability to acquire water and nutrients and help screen for root architectural traits that might increase agricultural productivity (Gregory *et al.,* 2009). Root system measurements will provide data with which growth and developmental patterns of roots can be formalised for the development of architectural models for resource acquisition. Accurate and precise root phenotyping strategies would provide for training genomic selection models in plant improvement (Cobb *et al.*, 2013).

Ideally, root systems must be studied continually, directly and non-destructively in the soil in which they grow. Unfortunately, the opaque nature of the soil makes these sorts of measurements difficult. Traditional methods for measuring roots in the soil such as excavation of the root system (Harrington *et al.*, 1989; Jackson, 1995; Trachsel *et al.*, 2011), coring methods (Kücke *et al.*, 1995; Nadelhoffer and Raich, 1992), soil monoliths (Buman *et al.*, 1994; Kücke *et al.*, 1995) and trench profiles (Bohm, 1979; Kücke *et al.*, 1995) are

destructive, slow and difficult (Smit *et al.*, 2000). As a result there is still paucity of reference data for many crops on within and between-genotype variations in root traits.

Recent advances in imaging using Neutron or X-ray imaging for example is providing new ways to measure roots in soil (Pierret *et al.*, 2003a). These emergent technologies however have limitations due to cost, reproducibility, throughput and complexity of installation. If the generation of phenotypic data will be at par with that of genotypic information, it is vital that new cost-effective, increased throughput and easily accessible approaches of studying root systems are developed. The development of phenotyping procedures capable of generating accurate, precise and pertinent information is now vital and this requires easily automated phenotyping pipeline. This thesis describes the development of a low cost, high-resolution root phenotyping (HRP) system that employs commonly used optical scanners to generate data to characterise genotypic variations in root system. This thesis further describes the application of the HRP system to generating data for statistical and mechanistic modelling and its application to phenotypic selection of root phenotypes with efficient P acquisition.

### *1.1 Phosphorus sustainability of crop production*

Agriculture faces tremendous challenges due to escalating world population and looming change of the climate. Also very prominent among the constraints to global food security is imminent threats of water scarcity and limited availability of plant nutrients, the mineral elements required for plants growth (Roy *et al.*, 2006). Out of the 17 elements required by plants to achieve optimal growth and productivity, 14 are acquired primarily from the soil solution (Vance *et al.*, 2003; White *et al.*, 2005). These include six macro elements namely N, P, K, calcium (Ca), magnesium (Mg) and sulphur (S) and eight microelements namely

chlorine (Cl), boron (B), iron (Fe), manganese (Mn), copper (Cu), zinc (Zn), nickel (Ni) and molybdenum (Mo) (White *et al.*, 2005; White and Brown, 2010). Crop production is often limited by low phytoavailability of essential mineral elements (White and Brown, 2010) with P being the second most limiting essential element after N in the majority of soils (Osivand *et al.*, 2009; Ramaekers *et al.*, 2010; Vance, 2001). An estimated third of total arable land contains inadequate P for sustainable crop production (Vance *et al.*, 2003). Based on cereal production, global average yield and total production losses arising from P deficiency is approximately 1093 kg $ha^{-1}$ and 491.5 x $10^6$ kg $y^{-1}$ respectively (Tan *et al.*, 2005). Development of high yielding crop genotypes capable of acquiring and using P efficiently is thus considered a vital task for the attainment of global food security.

The availability of any soil nutrient to the plant is primarily dependent on the soil's capacity to release that nutrient into the region of the soil subject to the influence of plant roots, the rhizosphere. Phosphorus is acquired as phosphate (Pi), mainly in the form of orthophosphate ($H_2PO_4^-$) (Amtmann *et al.*, 2005; Vance *et al.*, 2003) and although there is substantial quantity of P in the lithosphere, Pi is sparingly available to plants. The concentration of Pi in the rhizosphere solution generally ranges between 2 and 10 µM (Marschner, 1995; Schachtman *et al.*, 1998; Vance, 2001; Yang and Finnegan, 2010). Some amount of soil P is present as labile Pi bound to soil particles, but most soil P often form complexes with aluminium (Al) and Fe under acidic conditions (George *et al.*, 2011a; Vance, 2001; Vance *et al.*, 2003). In alkaline environments, P forms complexes with Ca (King, 2005; Vance, 2001; Vance *et al.*, 2003). Greater amount of P is thus fixed particularly in calcareous soils (Akhtar *et al.*, 2007; Akhtar *et al.*, 2008a; Akhtar *et al.*, 2009; George *et al.*, 2011a; Raghothama, 1999; Schachtman *et al.*, 1998; Vance, 2001).

Low phytoavailability of P in the soil solution has consequently necessitated increased application of P fertilizers. Approximately 85% of the processed P is used as agricultural fertilizer and as a mineral source for animal nutrition (Dawson and Hilton, 2011). Phosphorus fertilizers are however produced from finite supplies of rock phosphate (RP) (Cordell *et al.*, 2009; Hammond *et al.*, 2009; White and Brown, 2010). Unfortunately, while the quality of RP is said to be rapidly declining, its extraction is also estimated to peak soon (Cordell *et al.*, 2009). Recent estimates of RP reserve suggest that at the current rate of use of P, the expected time-frame of availability of reserves is between 300 and 400 years (Dawson and Hilton, 2011). Moreover, viable sources of RP are found only in limited places worldwide, which may cause economic and geopolitical crises (Cordell *et al.*, 2009).

The exploitation of P fertilizers could also become non-viable for many farmers around the world, with severe implications for small scale farmers in developing nations (Kumar *et al.*, 2009; Vance *et al.*, 2003). Moreover, the financial costs involved in the use of P fertilizers might rise with possible introduction of financial instruments aimed at achieving goals of climate change, the water framework directives, and other soil management targets (Hammond *et al.*, 2009). Accordingly, high P fertilizer prices will constraint low-input systems and amount to a substantial production cost in high-input systems (Vance *et al.*, 2003).

Potentially, environmental implications could also arise from greenhouse gas emissions resulting from the quarrying, production and transport of the RP. In the USA for example, continuous application of P fertilizers is creating soil P accumulation to levels in surplus of

crop needs (Daniel *et al.*, 1998; Sharpley *et al.*, 2003). The excess P could move to enrich neighbouring surface waters (Hammond *et al.*, 2009; Lambers *et al.*, 2006; Vance, 2001). The resulting eutrophication has negative effects on both aquatic and terrestrial habitats (White *et al.*, 2005; Yang and Finnegan, 2010). Furthermore, cadmium (Cd), a toxic substance to man has been shown to be contained in phosphatic fertilizers and RP has been suggested to be the sole source of the fertilizer Cd (Williams and David, 1973). Rising levels of Cd in soils increases the amounts of Cd available for plant uptake and could be harmful to human health (Lambers *et al.*, 2006; Modaihsh *et al.*, 2001; Rafiq *et al.*, 2006; Williams and David, 1973). In addition to the current problem of climate change, these trends pose a threat against the attainment of world food security goals and therefore necessitate urgent remedial actions (Raven, 2008).

### *1.2 Phosphorus use efficiency (PUE)*

Nutrient-efficient plants are capable of producing higher yields per unit of nutrient applied or absorbed from the soil solution compared with other plants grown under similar agro-ecological conditions (Fageria *et al.*, 2008; Wang *et al.*, 2010). Phosphorus efficient plants could either produce comparable yields with lower inputs of inorganic Pi fertilizers or have reduced physiological P requirements and tissue P concentrations (Hammond *et al.*, 2009). Breeding for root traits to increase the efficiency with which P is acquired thus offer a promising route to minimise the use P fertilizers. Phosphorus acquisition efficiency (PUpE) represents the increase in the P content in a plant tissue in relation to unit of added P fertilizer (g P $g^{-1}$ $P_{fertlizer}$), whereas P utilization efficiency (PUtE) denotes the increase in crop yield as a result of a unit increase in the crop's P content (g DM $g^{-1}$ P). Among the common propositions of phosphorus use efficiency (PUE), agronomic PUE is commonly used (Hammond *et al.*, 2009; White *et al.*, 2005). Agronomic PUE reflects plant's ability to

produce higher yield per unit of P applied as fertilizer or available in the soil. It is equivalent to the product of PUpE and PUtE (Table 1.1).

***Table 1.1:*** *Definitions of phosphorus use efficiency (Hammond et al., 2009) ($Y_{high}$=yield on a high P/fertilized soil; $Y_{low}$ = yield on a low P/unfertilized soil; $P_{high}$ = tissue P concentration on a high P/fertilized soil; $P_{low}$ = tissue P concentration on a low P/unfertilized soil; $\Delta P_{app}$ = difference in amount of P applied as fertilizer between high and low P treatments; DM = dry matter; $P_f$ = fertilizer P).*

| Name | Abbreviation | Calculation | Units |
|---|---|---|---|
| Agronomic P use efficiency | APUE | $(Y_{high}-Y_{low})/\Delta P_{app}$ | g DM $g^{-1}$ $P_f$ |
| P uptake efficiency | PUpE | $[(P_{high} x\ Y_{high})-(P_{low} x\ Y_{low})]/\Delta P_{app}$ | g P $g^{-1}$ $P_f$ |
| P utilization efficiency | PUtE | $(Y_{high}-Y_{low})/[(P_{high} xY_{high})-(P_{low} xY_{low})]$ | g DM $g^{-1}$ P |
| Physiological P use efficiency | PPUE | $Y_{high}/P_{high}$ or $Y_{low}/P_{low}$ | $g^2$ DM $g^{-1}$ P |
| P efficiency ratio | PER | $Y_{high}/(P_{high} x\ Y_{high})$ or $Y_{low}/(P_{low} x\ Y_{low})$ | g DM $g^{-1}$ P |

Genetic approaches to increase crop yield on soils deficient in P have targeted enhancing P acquisition by roots and tissue P utilisation (White and Hammond, 2008b). Moreover, crop plants differ in their agronomic PUE and plants' PUpE is positively correlated with root architecture (Akhtar *et al.*, 2008a, b; Hammond *et al.*, 2009). For example, root gravitropism determines the relative distribution of roots in the soil profile and therefore may influence PUpE (Liao *et al.,* 2004). Furthermore, the acquisition of P by plants and the efficient use of P in the plant are genetically determined and the genetic variation is largely attributable to PUpE (Akhtar *et al.*, 2008a, b; White *et al.*, 2005). Since, P acquisition efficiency can be improved by plant breeding; the exploitation of genetic variation in root architecture and its plastic responses to mineral elements in the soil thus presents a promising tool to cope with plant P limitation (Akhtar *et al.*, 2008a; Beebe *et al.*, 2006; Hammond *et al.*, 2009; White *et al.*, 2005). It is essential therefore to understand the genetic variation and the biology of root architectural traits in order to identify mechanisms which could be used to design crops for efficient acquisition and use of soil P (Liao *et al.*, 2001).

### *1.3 Variation in PUE*

Differential response of several crops to P nutrition has been reported (Akinrinde and Gaizer, 2006; Fageria and Baligar, 1997; Fageria *et al.*, 1988; Hammond *et al.*, 2009; Hammond and White, 2008; Ozturk *et al.*, 2005; White *et al.*, 2005). Extensive natural variation for several parameters including PUE, root uptake, root-shoot translocation and seed P content has been reported in many species (Alonso-Blanco *et al.*, 2009). For example, out of 35 cowpea lines assessed for P response on soil of a P-deficient alfisol, P fertilizer significantly enhanced shoot, root, grain dry weights and nodule weight, with over 50% of the lines showing significant response to P (Kolawole *et al.*, 2002). Environment and genotype interaction play a major role in the variation of P acquisition and PUE (Iqbal *et al.*, 2001). Thus, crop genotypes behave differently at low and high soil P levels and high yielding crop varieties need suitable soil environment to achieve optimum yield.

Efficient and responsive crop genotypes could be described in terms of two situations namely P-limited ($P_{lim}$) or P-optimum ($P_{opt}$) soil conditions. P-efficient genotypes are capable of producing higher yield in $P_{lim}$ conditions (i.e.: with lower supply of P fertiliser than commonly used for the crop). P-responsive genotypes are capable to attain economically significant increases in productivity in $P_{opt}$ conditions (i.e.: with quantities of P fertiliser higher than normally used in a given environment) (Parentoni *et al.,* 2012). Based on a presentation by Fageria and Baligar (1993), crop genotypes could consequently be categorised into four groups using their performance under $P_{opt}$ and $P_{lim}$ soils: i) efficient and responsive (ER)-genotypes which produce more than average yield and higher than average P-use both in $P_{lim}$ and $P_{opt}$ environments; ii) efficient and non-responsive (ENR)- genotypes which produce more than average yield, but PUE is less than average in $P_{opt}$ conditions.

Thus, these have high productivity under $P_{lim}$ but do not respond to increases in P supply; iii) non-efficient and responsive (NER)-genotypes which produce less than average dry matter yield, but PUE is higher than average. Thus, these produce below average yield under $P_{lim}$ but they respond positively to increases in P supply with above average yield in $P_{opt}$ conditions and iv) non-efficient and nonresponsive (NENR) - genotypes which produce less than average yield and less than average PUE both in $P_{lim}$ and $P_{opt}$ condtions (Cock *et al.*, 2002; Fageria and Baligar, 1993, 1997; Parentoni *et al.,* 2012; Shenoy and Kalagudi, 2005; White *et al.*, 2005). In general, ER genotypes are the most desirable for production purposes, but more importantly these differences in P-use have been observed to be genetically controlled (Cock *et al.*, 2002; Fageria and Baligar, 1993) and thus, potentially could be harnessed to enhance crop productivity on P-limited soils.

Sufficient tissue P concentration is required for plant cell functions. The tissue P concentration that produces 90% of the maximum yield is termed the "critical" P concentration. In other words, the critical P value is reached when 10% of the maximum yield is lost due to P deficiency. Maximum yield here may be defined as the highest yield when growth is not limited by factors including deficiencies in other mineral elements, diseases or pests, soil water, acidification and compaction. The critical P concentration can be determined statistically from the relationship between yield and tissue P concentration (Bolland, 2007; Liu, 2007). Genetic variation in tissue P concentration has been reported for many crop plants (Broadley *et al.*, 2004) including ryegrass (Breeze and Hopper, 1987); rice (Fageria *et al.*, 1988); tomatoes (Lee, 1998); wheat (Ozturk *et al.*, 2005); maize (Chen *et al.*, 2009) and (Akhtar *et al.*, 2007; Akhtar *et al.*, 2008a; Akhtar *et al.*, 2009; Broadley *et al.*, 2010; Hammond *et al.*, 2009). Factors that alter the critical tissue P concentration include

growth rate, plant tissue age, and genotype (Liu, 2007; White and Hammond, 2008b). Greenwood *et al.* (1980) noted that the essential tissue P for maximum growth usually declines as plants get larger because in older plants, a greater proportion of photosynthate is directed towards structural support of the plant.

Crop plants also differ in the efficiency by which they acquire P from the soil (Hammond *et al.*, 2009; Lambers *et al.*, 2006; White *et al.*, 2005; White and Hammond, 2008a; White and Hammond, 2008b). Phosphorus acquisition efficiency is associated with the ability of crops to mobilise Pi from poorly soluble sources or to take up Pi in the soil (Gahoonia and Nielsen, 1996; Narang *et al.*, 2000; Ramaekers *et al.*, 2010; Zhang *et al.*, 2009). Phosphorus acquisition efficient plants employ a number of genetically determined adaptive mechanisms including alterations in their root systems for better growth on poor P soils (Gahoonia and Nielsen, 1996; Lambers *et al.*, 2006; Narang *et al.*, 2000). Genotypic differences in the morphology of root systems points to the possibility of exploiting selection and breeding of crop genotypes with extensive root systems for efficient use of soil P resources and increased agricultural yield.

### *1.4 Phosphorus acquisition*

Three processes may be involved in the uptake of P: root interception, diffusion and mass flow (Barber, 1984; Marschner, 1995; Syers *et al.*, 2008). Whilst these processes may be mutually inclusive, prevailing soil conditions determines which is exploited at any point in time. For successful root interception, root must grow into the region rich in the nutrient. Given that roots occupy only small space in the soil volume, root interception of Pi is often inadequate to supply the full plant P needs (Barber, 1984). During mass flow, soluble P present in the soil solution flow to the root as water and is taken up by the roots. Mass flow

is thus influenced by water movement to the root, and P concentration in the soil solution (Syers *et al.*, 2008). Unfortunately, P concentration in the soil solution is very low and so majority of P moves to root surface through diffusion (Hinsinger, 2001). The absorbing power of the root is dependent on the metabolism of the root and the P status of the plant and the amount of P required at the root surface as determined by the depletion profile that develops with time (Barber, 1984; Hinsinger, 2001; Syers *et al.*, 2008; Tinker and Nye, 2000).

### *1.5 Root system architecture (RSA)*

Roots grow through elongation and branching, both the magnitude and direction of their elongation depend on local environmental conditions, physiological status of the plants and the type of root (Malamy, 2005). This leads to formation of complex arrangement, in space and time, of numerous interconnected roots, which is termed the Root System Architecture (RSA). RSA is thus the three dimensional geometry of the root system (Lambers *et al.*, 2006; Lynch, 1995; Vance *et al.*, 2003). Three features of the root system combine to form its architecture; the root system topology, distribution and the morphology (Fitter, 1985, 1991; Lynch, 1995).

Topology represents how individual roots are branched and he ecologist Alastair H. Fitter is among the pioneers in exploring the details of root system topology (Fitter, 1985, 1986, 1987, 1991, 2002; Fitter *et al.*, 1991). Employing a simulation model of root growth, he described roots as a branching tree with the links or internodes as its unit of classification. Two links are distinguishable: an external link (*E*) - a root between a meristem and secondary root and an internal link (*I*) - a root lying between two secondary root axes or an axis and stem (Fitter, 1986). Features of links include lengths and diameters, number of

roots originating from a node, root insertion angles, magnitude ($\mu$, the number of root tips) and the altitude ($\alpha$, number of branching points from the base to the extreme root tip) (Fitter, 1986; Glimskar, 2000). Although, the $\mu$ is indicative of the root system size, multiple root systems of same $\mu$ may vary in soil exploration efficiency depending on the length of their links. Longer links that exhibit predominant branching on the main axis (herringbone) may be more efficient at soil exploration than root systems where all *E* form new branches with equal probability (dichotomous) (Figure 1.1). Herringbones structures are however associated with large tissue volumes and hence high construction cost (Fitter, 1991). Estimates of topology may however be dependent on the plant's ontogeny. Glimskar (2000) observed that topology estimates changed with plant size in grasses, a phenomenon that may make regression-based topological indices difficult to interpret. This observation raises questions about the relevance of root topology for plant performance particularly for dynamic traits such as dynamics of root growth angles that may change with the growth of the plant.

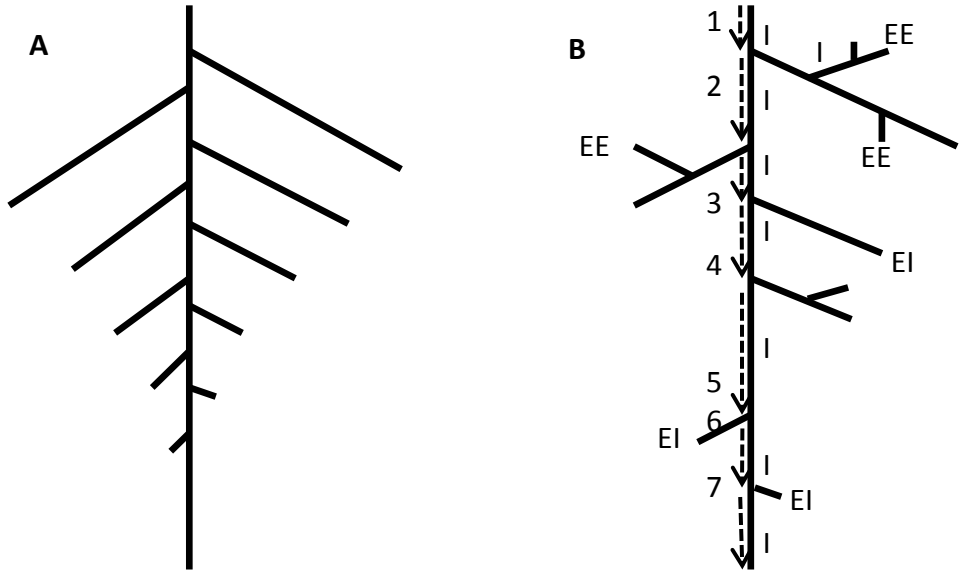


***Figure 1.1:*** *Schematic representation of (A) herringbone and (B) dichotomous topological patterns showing link structure, I = internal, E = external and altitude, which is the number of links in the longest pathway through the root system, and has a value of seven in this illustration (after (Fitter, 1991))*

Measures of the spatial distribution of roots simplify the dissection of root systems (Lynch, 1995). Root distribution is affected by soil physical properties such as bulk density, drainage, porosity and soil compaction. It indicates the soil health status and could so inform soil management practices. Root distribution often is measured from traits such as biomass and length and is expressed as a function of soil depth or position in the rhizosphere. Unlike topology and morphology, the distribution of root system could be obtained via destructive sampling and this is often measured to quantify the fraction of soil resources available to roots (Bengough *et al.*, 2000).

Root morphology on the other hand refers to the external features of a root axis considered as an organ and may include properties of roots hairs, root diameter and trend of secondary root emergence. Most general descriptions of RSA have however only concentrated on the entire root system or bigger sub sets of it at the expense of minute root features such as root hairs. In order to obtain a complete picture of RSA, the three features of the root system mentioned above must be measured. A description of the topology is important because of it functional significance. Other variables that may alter the functioning of RSA such as the duration or longevity of individual root parts and the presence of symbiotic associations are also important to measure (Fitter, 1987). Specific root length (SRL), the root length per unit dry weight measures the soil exploited per unit root biomass. The SRL measures the allocation strategy within-roots and could be a good indicator of the relative soil exploitation but not of root diameter for which it is sometime used (Atkinson, 2000).

### *1.6 Root structure and function*

Primarily, functions of roots include subterranean anchorage and the absorption of soil-based resources such as water and nutrients (Fitter, 1987; Kramer and Boyer, 1995; Osmont *et al.*, 2007). Other roles of the root system are considered secondary and may include phyto-hormone synthesis of essential compounds such as cytokinins, and photo-assimilate storage of food reserves common in plants such as onion (bulbs), cocoyam (corms), yam (tubers) and pineapples (rhizomes). Some roots, particularly tap roots of desert plants also have the capacity to store large amounts of water (Graham and Nobel, 1999). Smucker (1993) noted that root systems may function in respiration of photosynthesis and in the maintenance of balance between below- and above-soil biomass. Root respiration is particularly common in epiphytic orchids and aerial roots of mangrove. The vital functions served by root systems are closely linked to the soil in which they reside. Thus, depending on the soil's composition, differences in root system morphology may affect root function capabilities in the soil (Fitter, 1987; Osmont *et al.*, 2007).

Roots axes are categorised into four classes depending on the site of emergence on the plant. The tap or primary root (PR) is the embryonic first root to emerge from the seed and may be visible two or three days after germination. Anatomically, the structure of PR is simple and defined, showing little variability and thus possesses a stable morphological system (Hochholdinger *et al.*, 2004a; Hochholdinger *et al.*, 2004b; Zobel and Waisel, 2010). Lateral roots (LRs) refer to post-embryonically formed and branched roots from other roots and may initiate from the pericycle in about four days after germination (Hoecker *et al.*, 2006). Shoot-borne and basal roots respectively originate from the shoot tissues and the hypocotyl (Zobel and Waisel, 2010).

In simple terms, plants are distinguished into dicots and monocots. This gives rise to two types of root systems: tap and fibrous root systems (Figure 1.2). In tap root systems, exemplified by crop plants such as brassicas, legumes and *Arabidopsis*, there is a single main root axis, the PR which remains the largest root with smaller LRs originating from it (Figure 1.2a) (Dickison, 2000; Doussan *et al.*, 2006). Tap root systems, also termed allorhizic systems, usually lack adventitious roots although these can arise from the hypocotyl especially when the plant is wounded (Osmont *et al.*, 2007). Conversely, fibrous root systems (Figure 1.2b), exemplified by grasses have many adventitious roots of nearly equal size emerging from the seed with multiple branches parallel to the PR (such adventitious roots are referred to as seminal roots in monocots). Fibrous root systems, also called homorhizic systems, are relatively shallower and can be differentiated based on diameter class classifications (Bohm, 1979; Osmont *et al.*, 2007).

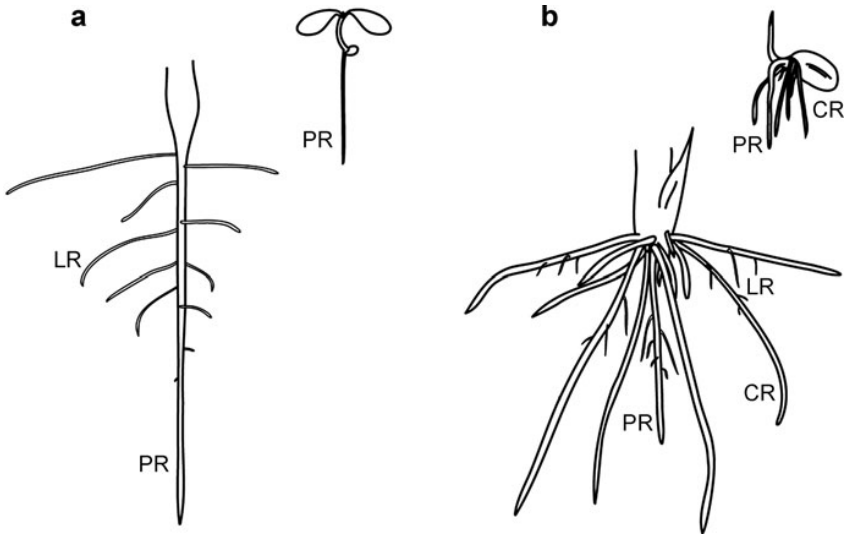


***Figure 1.2:*** *Schematic representation of root system types (a) a typical tap root system in 5-day-old and 12-day-old seedlings; (b) a typical fibrous root system in 7-day-old and 14-day-old seedlings. Root hairs are not represented; PR, primary root; LR, lateral root; CR, crown root (from (Osmont et al., 2007))*

### *1.7 Root-soil interactions*

Rhizosphere refers to the zone of soil under the control or direct influence of root systems. Modifications of soil properties in the rhizosphere are essential for efficient resource

capture (Cheng and Kuzyakov, 2005). For example, through rhizodeposition, C compounds are released into the surrounding soil, consequently altering the physio-chemical composition of the soil. Roots also serve as host for many soil microbes whose proliferation in or outside of the surface of roots are inadvertently catalysed by the release of C from root cells to the rhizosphere (Gregory, 2006; Lambers *et al.*, 2009). Increased rhizodeposition can in turn stimulate mineralization of N from recalcitrant soil organic matter (SOM) pools (de Graaff *et al.*, 2009).

Fageria and Moreira (2011) have distinguished three changes in the rhizosphere: physical, chemical and biological. Physical changes include changes in temperature, water availability, and soil structure. Modification of soil pore space geometry is for instance one of the dominant ways by which root systems affects the physical properties of the soil. This in turn may have important implications for the bulk density, drainage and other fluid properties as well as aggregation of the soil which also controls soil biological and hydrologic properties. Chemical changes include changes in pH, redox potential, root exudates and allelopathy. Other main chemical soil properties likely to be influenced by root system growth include SOM decomposition and nutrient concentration. Biological changes such as microbial association and nitrogen fixation are also common root-induced changes in the local soil environment.

Soil properties also impact greatly on root systems. For example, a greater proportion of root biomass of arable crops is found in the 0 - 20 cm topsoil, an occurrence that may be associated with greater SOM, nutrients, aeration, and water availability in the topsoil

compared to lower soil depths. For most crops, physical constraints exerted by the soil affect water retention, soil aeration and root growth, whilst chemical constraints mostly influence nutrient status of the soils and hence the plant. These constraints however differ spatially and temporally (Bengough *et al.*, 2006; Bengough *et al.*, 2011; Whitmore and Whalley, 2009).

Root system growth is an irreversible and ontogenetic change in the biomass of different root axes measured in size, form or number (Hunt, 2003; Paine *et al.*, 2012). During root growth, new cells are formed at the root tip and elongated at the zone proximal to the meristem, leading to a permanent stream of new cells through the growth zone of root tips (Walter and Schurr, 2005). Environmental effects on root growth dynamics are very complex. In very simple terms, the environmental factors that affect dynamic root growth behaviour either act independently or in combination, directly through the effects of physical and chemical conditions on primary cell growth processes, or indirectly via developmental adaptation to promote or limit root elongation. For example, roots in compacted or dry soils have slow growth (Bengough *et al.*, 2006; Bingham *et al.*, 2009). An investigation on the effect of soil compaction on the dynamics of root growth in barley (*Hordeum vulgare* L.) revealed that soil compaction reduced the total length of root produced but not mortality (Figure 1.3). Indirect constraints on root growth are exemplified by developmental plasticity of root systems (Bingham *et al.*, 2009).

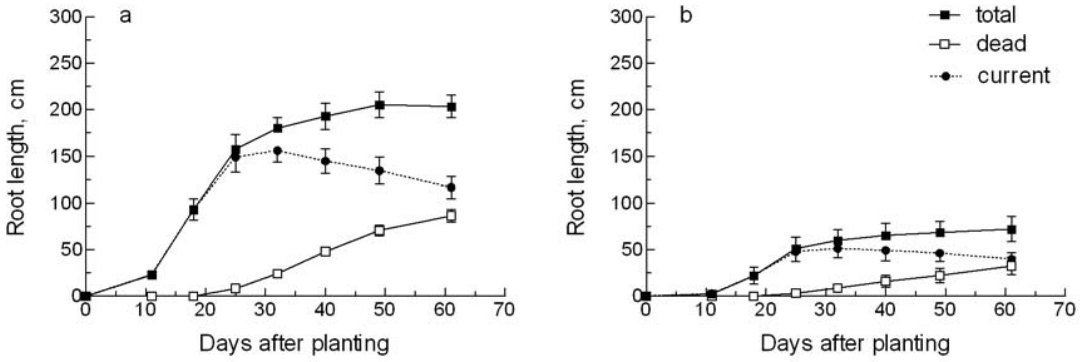


***Figure 1.3:*** *Visible root length (current), cumulative total length produced and length of dead and decayed root at the observation window (a section of rhizotron constructed with transparent acrylic sheet to facilitate visualisation of roots) 20-28 cm below the soil surface in loose (a) and compacted (b) soil (Bingham et al., 2009)*

### *1.8 Root Plasticity*

Quantitative traits are expressed differently in diverse environments. Phenotypic plasticity is the capacity of a single genotype to express variable phenotypes in different environments (Whitman and Agrawal 2009). For example, plasticity in the phenotype of a plant occurs when a single genotype produces different phenotypes in different environments. This exemplifies genotype-by-environment interaction (G×E) by plants. Plasticity could thus be said as a subset of G x E where G x E is the effect of a locus (i.e.: a chromosomal region) that changes in magnitude or direction across environments (Des Marais et al., 2013). Thus, G x E occurs when a single genotype differ in magnitude or direction of the expressed plasticity.

Root development is also highly dependent on the environment (Bell and Sultan, 1999; Gerald *et al.*, 2006). The plasticity of RSA arises due to responses of individual root meristems to factors including light regime (Yazdanbakhsh and Fisahn, 2009) temperature fluctuations (Walter and Schurr, 2005), soil water status (Eapen *et al.*, 2005) or nutrient availability and concentration (Bai *et al.*, 2013). For example, under constant temperature, no diurnal variation in root growth was observed in maize (*Zea mays* L.) seedlings but

velocity and relative growth rate at 21 °C and 26 °C were different (Walter *et al.*, 2002). Similarly, with adequate provision of water, roots of maize (*Zea mays* L.) elongated to a soil depth of 60 cm with the greatest percentage of total root length (TRL) found between 20 and 40 cm. In contrast, suboptimal provision of water restricted root growth in the top soil and increased deeper root penetration resulting in higher soil water depletion rates at depth, compared with the soil of the well watered plants (Sharp and Davies, 1985). Plasticity accounts for a large fraction of the variability in the RSA and it demonstrates an adaptation to intra- and inter-specific competition. For example, crop species with faster root growth may respond more efficiently to nutrient-rich patches in the soil than species with slower root system growth. In nutrient-deficient conditions, plasticity in root system growth may be positively correlated with soil resource acquisition and species with faster root system growth might thus be superior in adjusting their RSA in resource-limited environments.

Root development is highly sensitive to changes in the supply and distribution of inorganic nutrients in the soil. The nutrient supply can affect root development either directly, as a result of changes in the external concentration of the nutrient, or indirectly through changes in the internal nutrient status of the plant (Forde and Lorenzo, 2001). When external nutrient supply is sensed by plants, the roots integrate and translate the cues into a range of developmental outputs. These include changes in root growth and branching rate, root diameter size, root growth angles, root hair length and density and regulation of root gravitropism (Forde and Lorenzo, 2001). For example, when roots encounter nutrient rich zones, they often proliferate via increased production of root biomass (Hodge *et al.*, 2000a); elongation of individual roots (Zhang *et al.*, 1999); increased TRL (Hodge *et al.*, 2000b); and

increased initiation of LRs (Farley and Fitter, 1999; Hodge, 2004). Also, bean roots may change their geotropic curvature and the proportion of root system in the topsoil in response to low P availability in order to explore the topsoil where concentration of P is normally greater than in the subsoil (Bonser *et al.*, 1996; Lynch and Beebe, 1995).

Most of the P available in the soil is also restricted to the topmost layers of the soil (Bates and Lynch, 2000). Root systems that are able to proliferate in volumes of high nutrient availability will thus acquire more P than those that proliferate less or in other volumes. For example, shallower root growth angles of axial, basal, seminal or crown roots in maize, common bean (Lynch, 2011; Lynch and Brown, 2001) and soybean (Wang *et al.*, 2010; Watt and Evans, 2003; Zhao *et al.*, 2004) can increase topsoil exploration and may enhance P acquisition. Besides, spatial competition for P among roots of the same or different plants may result when the volume of the soil is depleted by root branches present. Under such conditions, RSA that minimises competition is expected to be more efficient at P acquisition. In common bean for example, shallower root systems had greater P acquisition per unit carbon cost than deeper root systems due to greater inter-root competition in deeper root systems (Ge *et al.*, 2000).

### *1.9 Phenotyping*

A fundamental step towards breeding for improved crop roots is the ability to accurately measure root traits of crop plants from their genetic composition (genotype). The process of measuring the phenotype from a genotype is generally referred to as phenotyping (Subramanian, 2012). Connecting the genotype to phenotype is faster pathway to selecting for superior genotypes in plant breeding programmes (Walter *et al.*, 2012; White *et al.*, 2012). There have been tremendous advances in the capacity; cost efficiency and speed of

genotyping techniques such as “next generation” DNA sequencing, however, phenotyping has made relatively less progress in the past three decades especially for complex traits such as abiotic stress tolerance and yield potential (Cobb *et al.*, 2013; Jackson *et al.*, 2011; Shendure and Ji, 2008) and this has become a major bottleneck in developing crop cultivars conferred with improved resource acquisition traits.

Generally, the aim of phenotyping is to measure or find the differences among several genotypes under defined environmental conditions. This usually requires several hundreds or thousands of genotypes to be compared with each other (Fiorani and Schurr, 2013; Subramanian, 2012). High-throughput phenotyping procedures capable of phenotyping large numbers of lines or individual plants accurately with a fraction of the time, cost and labour of current techniques are thus needed (White *et al.*, 2012). It is through high-throughput phenotyping that new genes and complex interactions are likely to be revealed and this particularly is essential for quantifying root traits due to the high plasticity of root systems. Moreover, root phenotypes may be manifested transiently, only at specific times and under varying environmental conditions, hence any developed technique of phenotyping must be non-invasive and incorporate high spatio-temporal resolution (Subramanian, 2012).

Studying root systems is difficult. The opacity of the soil is the main limitation to root studies. Not only do the measurements of roots growing in soil destroy the soil habitat but it is also extremely difficult or in some instances not feasible to extract an entire root system from soil without damaging its structure or its finer elements (Smith and De Smet, 2012). Trachsel *et al.* (2011) recently employed excavation and washing to study crown roots of

maize (*Zea mays* L.). Such approaches are laborious, time consuming and may fail to recover parts of the root system. Although very vital, studying mature root systems raises additional challenges. The size of the root system is larger and more difficult to excavate.

Sampling of the root system can be used; however, sampling introduces large variability (Araujo *et al.*, 2004; Bengough *et al.*, 2000). The reported large variations between samples could be attributable to abiotic and biotic factors, which unpredictably influence RSA and root development. Root system plasticity thus constrains root studies. Studying root systems is also very difficult not only because RSA and root growth are the consequence of local conditions, but also, roots are composed of many complex structures of varying developmental, physiological and morphological structures (Lynch, 1995). As a result, it is very difficult to have any form of standardised methods or protocols of evaluating root traits across sites, root features and plant genotypes. All these attendant characteristics have culminated in lack of reliable root phenotyping methods.

### *1.10 Methods of quantifying root systems*

Regardless of the challenges involved in root system studies, many attempts have been made. Studies of root systems date back to the 18$^{th}$ century. Duhamel du Monceau has been credited as the possible pioneer with his work on the root systems of trees from 1764-1765 (Kramer and Boyer, 1995). The earlier work mainly involved digging up roots and manually measuring their weight and length. The ecologist J.E Weaver is one of the pioneers of root research by field excavation. Weaver excavated entire root systems by using pick axes to dig big trenches (up to 3 x 10 x 20 feet) by the side of the plants. Plants studied by Weaver and colleagues included *Rosa arkansana, Lygodesmia juncea, Petalostemon purpureus, Liatria punctala* and during the studies roots of the plants were drawn in place

with pencil on a large drawing-sheet ruled to scale. Drawings were made simultaneously with the excavation of the root, to exact measurements and subsequently retraced with ink when the whole root has been excavated (Figure 1.4) (Weaver, 1919, 1920, 1925, 1926; Weaver and Bruner, 1927). Many others also cultured plants in containers in order to study their root systems (Bohm, 1979). This included Hiltner (1904), Bates (1937), Kutschera (1960) and others who quantified root systems of crop plants in the field or in pots by observation, sketching or tracing.

Excavation of roots from the soil and washing them in order to measure their length and architecture is the most common and simplest method of studying roots in the field. Other classical methods to study roots are based on destructive sampling of soil techniques including core, monolith, and profile wall (Zhu *et al.*, 2011). Auger methods are suitable for taking volumetric soil-root samples with no attempt to keep the roots in their natural positions (Bohm, 1979). Perhaps the greatest advantage of these systems is that the measurements are normally carried out in the field. Trench profiles can also be used to measure root spatial distribution and more importantly, the environment surrounding the root system. Trench profiles also have potential to provide quantitative information on the roots system but unfortunately it also involves a major disturbance of the soil and provides measurements for a small fraction of the root system (Pierret *et al.*, 2003b). Classical techniques are not often suitable in investigating root developmental processes (Liedgens *et al.*, 2000) and may lead to loss of information on finer root parts such as root hairs (Smit *et al.*, 2000).

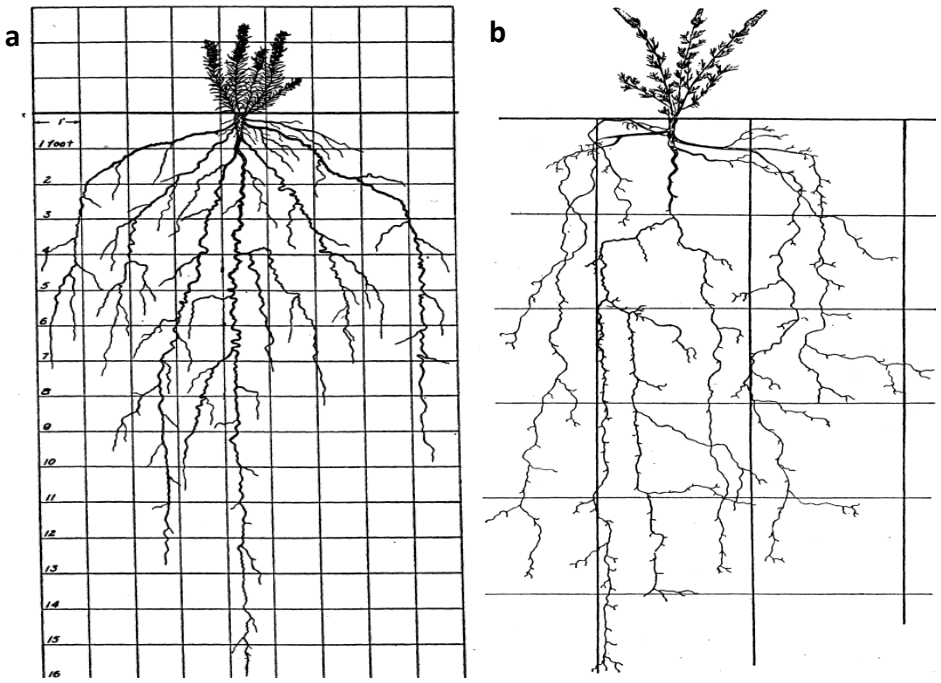


***Figure 1.44:*** *Examples of root systems analysed by excavation and drawing; (a) Liatria punctala and (b) Petalostemon purpureus (Weaver, 1919; 1920)*

### *1.11 The use of imaging in phenotyping root systems*

More recently, techniques for studying RSA have progressed from sampling-based techniques to *in situ* imaging systems some of which were derived from medical sciences (Xuecheng and Xiwen, 2009). There are many reasons in support of this shift. Given the limitations in classical sampling techniques, quantifying the temporal and spatial root distribution has been challenging. Since local conditions have strong effects on the RSA, environmental stimuli may only be manifested transiently. Additionally, it would be advantageous for phenotyping techniques to be compliant with screening many plants at any point in time, given that a single phenotypic root trait may be determined by several genes. Imaging permits the time-lapse observations of root systems at very minuscule scales that approach dimensions of single cells in plant tissues (Connelly *et al.*, 1987).

*In situ* imaging of roots refers to imaging techniques, carried out either in the field (Rodgers *et al.*, 2004) or in controlled environments in which the rooting medium for the plant is soil (Volkmar, 1993). Popular *in situ* root observations and measurements employ rhizotrons or minirhizotrons. Both techniques use transparent soil-air interfaces for the observation of plant roots (Taylor *et al.*, 1990). Rhizotrons have larger flat transparent windows and may be constrained by setup and operational cost. Minirhizotrons on the other hand are small-diameter transparent tubes inserted into the soil at either a vertical, horizontal or at an angle to observe and measure roots and soil processes (Figure 1.5) (Herrera *et al.*, 2012; Rewald and Ephrath, 2013). Minirhizotrons imaging usually combine a light source, a small camera constructed to fit into cylindrical tubes (Faget *et al.*, 2010) and store the images on a computer equipped with software to capture and label pictures (Figure 1.5). There are many variants of rhizotron methods (Smit *et al.*, 2000), with different imaging devices or techniques having been applied. Variants setups applicable to high throughput imaging include growing plants on small-sized 2D rhizotrons (Devienne-Barret *et al.*, 2006). For a comprehensive review on minirhizotrons see (Rewald and Ephrath, 2013).

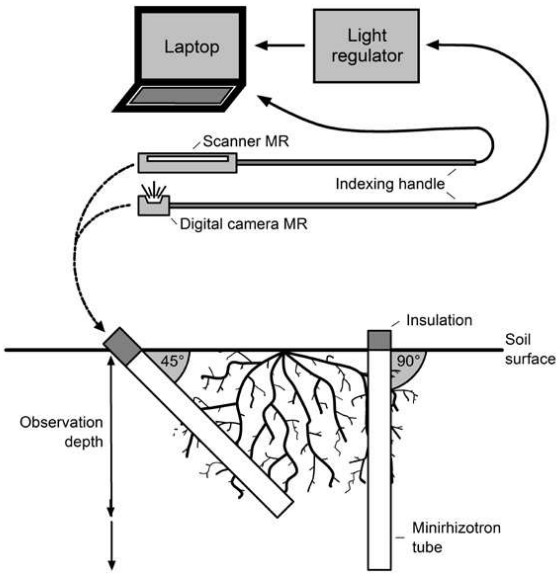


***Figure 1.5:*** *Schematic diagram of minirhizotrons tubes in both angled and vertical position. Images are captured by either digital camera- or scanner-based minirhizotron (MR) systems connected to a laptop(Adapted from: (Rewald and Ephrath, 2013))*

The incorporation of various imaging technologies has generally enabled the conduction of faster experiments and more comprehensive measurements and capture of highly resolved images. However, many imaging techniques employ 2-dimensional imaging and influence root growth since it is forced to grow at the surface of the imaging window. With developments in radiation tomography, such as X-ray computed tomography (X-ray CT), X-ray microcomputed tomography, neutron tomography and magnetic resonance imaging (MRI), it is now possible to image the 3D architecture of soil and root structures non-destructively and with great resolution (Asseng *et al.*, 2000; Moradi *et al.*, 2009; Perret *et al.*, 2007; Tracy *et al.*, 2010). Following the pioneering efforts of Willatt and Struss (1979) and Bois and Couchat (1983), use of medical scanners has grown rapidly in roots and soil research (Hainsworth and Aylmore, 1983; Hamza and Aylmore, 1992). Subsequently, the use

of industrial scanners mostly developed for materials research have been employed to improve the resolution obtainable in visualizing root systems in soil (Tracy *et al.*, 2010).

MRI uses signals of nuclear magnetic resonance from hydrogen nuclei in root tissues and soil matrix to differentiate between roots and soil (Berger, 2002), and to provide 3D architecture of roots and their rhizosphere. The approach is considered beneficial in providing exact locations of the various structures within the soil with high spatial resolution (0.39 mm) (Stingaciu *et al.*, 2013). For example, Nagel *et al.* (2009) could observe response of root structure and gradient of carbon transport to root zone and observed that low temperature induced smaller branching angles between PR and LRs. Using the technique, they could conclude that the volume explored by roots is reduced at low temperatures. MRI is however limited in soils rich in ions of Fe and Mn as these may provide interference (Pierret *et al.*, 2003a).

In X-ray CT, the physical density of the medium is probed via the acquisition and reconstruction of images from thin cross sections or slices of root and rhizosphere on the basis of measurements of attenuation of an electromagnetic wave (the gradual loss of electromagnetic wave through the soil medium) (Mahesh, 2002; Mooney *et al.*, 2012). Among the methods of radiation tomography, X-ray CT is currently the preferred 3D imaging approach in soil-root studies. Image quality is not influenced by Fe or Mn in the soil matrix (Tracy *et al.*, 2010). It provides the best contrast between soil and roots. For example, fine root systems of wheat plants measured with X-ray tomography were generally within 10% range from those obtained from destructive samples and with a flat-bed scanner (Gregory *et al.*, 2003). However, X-ray CT has difficulties resolving with diameters of less than 100 µm

(Kaestner *et al.*, 2006). Water content of soil also has an influence on the contrast between root and soil. Particularly, pore saturated with water can be confounded with roots and organic matter (Tracy *et al.*, 2010).

Methods for field based 3D non-destructive imaging are also developing rapidly (Luster *et al.*, 2009). These methods include ground penetrating radar (GPR). GPR uses high frequency radio waves. Contrast is created by differences in material dielectric constants (Zhu *et al.*, 2011). The approach has been developed for geophysical methods and can provide 2D and 3D live images (al Hagrey, 2007). Using this approach, al Hagrey (2007) produced images of root systems growing in the field using information on soil moisture distribution. Ground penetrating radar could however be extremely dependent on soil type.

Radiation based imaging are not suitable to study biological processes. For this reason the use of artificial substrates in imaging is common (Bengough *et al.*, 2004; Hargreaves *et al.*, 2009). These artificial substrates mostly utilise economical, non-invasive and high-throughput imaging facilities including scanners, video and digital cameras (Ortiz-Ribbing and Eastburn, 2003). Digital cameras and scanner are common in *ex situ* applications where they are usually combined with experimental systems in which plants are grown or cultured on moist germination papers (Hund *et al.*, 2009; Lee and Woolhouse, 1969; Yorke and Sagar, 1970), in hydroponic systems (Chen *et al.*, 2011; Sena *et al.*, 2011) and in aeroponic systems (Lobet *et al.*, 2011; Waisel, 1996, 2002) and transparent substrates (Downie *et al.*, 2012; Iyer-Pascuzzi *et al.*, 2010). Agar-filled petri dishes were for example used to undertake automatic screening of complex root systems of rice (*Oryza sativa*) varieties (Iyer-Pascuzzi *et al.*, 2010).

Although the use of experimental setups such as aeroponic and hydroponic culture may be a limitation in their inability to offer the same mechanical impedance inherent in the soil matrix to root growth, such approaches are still very useful because they are 3-D. Root development in aeroponics for example may be more extensive and more anatomically similar to soil grown roots than is achievable with hydroponics and may be due similar exodermis development in aeroponic and soil substrates (Redjala *et al.*, 2011). More recently, a transparent soil approach was developed. This uses a low refractive index polymer to simulate soil and made transparent upon saturation with water. This technique allows control of moisture content during plant growth in a granular, unsaturated substrate and thus incorporates the physical heterogeneity of soils (Downie *et al.*, 2012). Transparent substrates can be used in combination with a number of powerful imaging techniques such as Confocal Laser Scanning Microscopy (CLSM; Roberts *et al.*, 2010; Smith, 2008; Yu *et al.*, 2001), Single Plane Illumination Microscopy (SPIM) or Light Sheet Fluorescence Microscopy (LSFM; Huisken *et al.*, 2004; Huisken and Stainier, 2009; Sena *et al.*, 2011; Yang *et al.*, 2013) and Optical Projection Tomography (OPT; Downie *et al.*, 2012; Lee *et al.*, 2006; Sharpe, 2004; Sharpe *et al.*, 2002). These microscopic techniques give different scale of data to that pursued in this thesis and will not be reviewed here.

Although both 2D and 3D imaging are possible in these microscopic techniques, it may however not represent accurately the natural 3D nature of RSA in soil (Zhu *et al.*, 2011). Again, the size of the imaging area of most of these techniques is usually small and therefore restricted to small specimens. Furthermore, most of the emerging platforms often incorporate robotics and conveyor belts which enable the movement and positioning of plants in front of imaging devices and sensors (Tsaftaris and Noutsos, 2009). Unfortunately,

these infrastructures make installation of such platforms complex and complicated. The complexity of instrumentation is such that it is usually difficult to obtain sufficient throughput or to collect time lapse data and even in cases where they are not proprietary, such platforms are difficult to replicate elsewhere (Iyer-Pascuzzi *et al.*, 2010; Smith and De Smet, 2012). For screening purposes where large numbers are required to be phenotyped within short time, these techniques may thus be of low throughput, and its usage may be constrained by increased screening times, installation complexity and cost.

### *1.12 Image analysis*

Image acquisition is only the first step in a series of processes involved in computed image analysis. What follows include image enhancement and analyses of geometric features (Duncan and Ayache, 2000). Root images, 2D or 3D, colorimetric or grayscale, normally come with artefacts that complicate processing and extraction of information (Lobet *et al.*, 2011). Image enhancement is the process of modifying the attributes of digital images to improve the quality so that the results are more suitable for display or further analysis (Maini and Aggarwal, 2010). The conversion of each pixel of an image into one bit with two possible values (making a binary image) is often the second stage in most systems of image analysis. Image segmentation follows and is performed to discriminate (segment or threshold) root structures from non-root objects or artefacts on the image (Chen and Zhou, 2010; Zhang *et al.*, 2008). Thus, root image segmentation is an image processing step by which whole or part of root system is extracted from the image data for purposes of visualization and measurement. It involves associating a pixel with a root, based on the local intensity, spatial position, neighbouring pixels, or prior information about the shape characteristics of the root systems (Budinger *et al.*, 1996).

There are many ways to segment an image as different images require different segmentation procedures (Smit *et al.*, 2000). While current developments in computer capabilities mean that segmentation of digital images could be automated and accelerated, there is no off-the- shelf solution for all data sets (Sezgin and Sankur, 2004). Segmentation by thresholding for example is prone to high degree of subjectivity (Zhang et al., 2008) but this is true especially for diameter measurements but not for length measurements. Standardisation of these processes is one that is very vital but also very challenging to achieve.

Software dedicated to root image analyses are now increasingly available (Le Bot *et al.,* 2010). These software which are either designed to analyse minirhizotron pictures of roots growing in soils (e.g.: *MR-RIPL* (http://rootimage.msu.edu/MR-RIPL/), *RMS* (Ingram and Leers, 2001) or images of roots grown on gels or paper substrates (e.g.: *SmartRoot* (Lobet *et al.*, 2011), *EZ-Rhizo* (Armengaud *et al.*, 2009), *DART* (Le Bot e*t al.,* 2010) or for harvested and washed roots analysis (e.g. *WinRHIZO*® (http://www.regent.qc.ca/)) and can be grouped based on their mode of operation.

The first set of software operates by first segmenting a complete network of root system, followed by a skeletonisation (thinning or morphological erosion) so that measurements are made on the resultant pixel-wide centreline or perimeter of the root system (skeleton of the root) (Kirbas and Quek, 2004). Segmentation techniques employed include filtering and edge operator techniques, pixel classification techniques and mathematical morphology approaches. Skeleton-based software work well with high quality images or may require extensive processing of image pixels, followed by extracting boundaries or centrelines. They

extract centrelines of root axes and operate by identifying the pixels located on the specific areas of the image covered by the root structures (Boroujeni *et al.*, 2010). Example includes *WinRHIZO*, (Arsenault *et al.*, 1995) and *EZ-Rhizo* (Armengaud *et al.*, 2009). *EZ-Rhizo* for example is a Windows-based semi-automated root analyses software with functionality for user-defined image enhancements capabilities (filtering and thresholding) and was applied to evaluate natural variation in RSA across accessions *Arabidopsis thaliana* (Armengaud *et al.*, 2009).

A second category of software operates by tracking. Algorithms that incorporate a search procedure which keeps track of the centreline of the root axis and progress along the root track based on certain properties to determine the future path of the root. For example, *RootTrace* uses iterative algorithm of density functions to track moving objects, in order to track the line of the root from a user-defined start location to the tip of the root (French *et al.*, 2009; Naeem *et al.*, 2011). *RootTrace* for example, was applied to quantify the effect of 10 µM dexamethasone treatment on the root system growth of 3-d-old transgenic *Arabidopsis* seedlings (French *et al.*, 2009). Another example of tracking-based root analyses software is the *RootflowRT* which employs optical flow procedures (Van der Weele *et al.*, 2003). *RootflowRT* was for example employed to identify two distinct growth zone regions of root system of several plants including *Arabidopsis*, tomato (*Lycopersicon esculentum*), lettuce (*Lactuca sativa*), alyssum (*Aurinia saxatilis*), and timothy (*Phleum pratense* (van der Weele *et al.*, 2003).

Tracing-based software usually avoid low level pre-processing steps and instead, locate a number of initial seed points and only process the pixels which are close to the feature of

interest. These approaches often rely on user-defined or automatic detection of seed points which are assumed to be located on the centreline of the root axis (Boroujeni *et al.*, 2010). *SmartRoot* is an example of tracing-based root image analysis software and combines a vector representation of root objects with a powerful tracing algorithm. The software has an underlying wireframe model of connecting image vertices with lines and utilizes an algorithm that determines the midline of the root near a user selected seed position and proceeds with stepwise construction of segmented line to the root tip by approximating the root midline (Lobet *et al.*, 2011). *SmartRoot* was used to generate data from 20-day old maize root systems grown in rhizotrons (Lobet and Draye, 2013).

Many of these programs are available freely, but others are also proprietary. *WinRhizo* (http://www.regent.qc.ca), Lemnatec's Scanalyzer3D (http://www.lemnatec.de) and *Rootsnap*, an accompaniment to the CI-600 *in-situ* root imager from CID Bio-Science (http://www.cid-inc.com) are common examples of proprietary root image analyses software. Table 1.2 provides some examples of current root image analyses software and brief description of their applicability but this list is not exhaustive. Although these programs have increased the throughput of image analyses, there are still major limitations. Automation works only with high contrast images and manual feature extraction are still very slow.

***Table 1.2:*** *Examples of available software used for analysing root images (Source: [http://www.root-image-analysis.org/; Lobet et al., 2013](http://www.root-image-analysis.org/; Lobet et al., 2013))*

| Software | Degree of User Interaction | Availability / input format / Export Format / Platform | Type of Analyses (Examples of Measured Root traits) |
|---|---|---|---|
| ***WinRHIZO***™ (Arsenault *et al.*, 1995) | Automated | Commercial / txt / Windows | Local, global (length, area, volume and topological, and colour analyses) |
| ***RootTrace*** (French *et al.*, 2009; Naeem *et al.*, 2011) | Automated | Freeware / cvc / Windows | Time-lapse (Length, curvature, number, gravitropism) |
| ***RootflowRT*** (van der Weele *et al.*, 2003) | Automated | Freeware / ppm, tiff / txt / Windows, Mac | Time lapse (Growth, spatial velocity profile) |
| ***KineRoot*** (Basu *et al.*, 2007) | Automated | Freeware / jpg Matlab / txt / Windows, Mac, Linus | Time-lapse (Spatio-temporal patterns of growth and curvature) |
| ***Growth Explorer*** (Basu and Pal, 2012) | Automated | Windows /Image Unknown / Matlab | Global (velocity profiles) |
| ***RootScan*** (Burton *et al.*, 2012) | automated | Freeware / no image requirement / Windows, Mac, Linus | Global / root morphology |
| ***Root System Analyser*** (Leitner *et al.*, 2013) | automated | Freeware / windows, Mac/ Matlab | Root architectural parameters (length, angle, diameter, count) |
| ***IJ_Rhizo*** (Pierret *et al.,* 2013) | automated | Freeware / jpg/ windows, Mac, Linus | length, diameter, |
| ***SmartRoot*** (Lobet *et al.*, 2011) | Semi-automated | Freeware / gif, jpg, tiff, bmp / csv / sql database / Windows, Mac, Linus | Local, time-lapse (Length, diameter, angle, insertion point, root direction, architecture, topology) |
| ***Rootnav*** (Pound *et al.*, 2013) | Semi-automated | Freeware/ Windows | Root system architectures |
| ***DigiRoot*** (Stefanelli *et al.*, 2009) | Semi-automated | Commercial /jpg, bmp, tiff, png, gif / xml / Windows | Local (Length, area, volume, number of branches, branches angle and branching hierarchy) |
| ***RooTSnap*** (www.cid-inc.com/ci-690.php) | Semi-automated | Commercial / jpg, bmp, tiff, png, gif etc / csv /Windows | Local, global, time lapse (Root development, architecture, and morphology) |
| ***RootReader2D*** (www.plantmineralnutrition.net/rootreader.htm) | Semi-automated | Freeware (as Java Web Start / modified xml / Windows, Mac, Linus | Local, global (Lengths, number of laterals) |
| **EZ-*Rhizo*** (Armengaud *et al.*, 2009) | Semi-automated | Freeware / bmp / sql database /Windows | Global (Length, vector length, angle, number of laterals, position etc.) |
| ***Growscreen_Root*** (Nagel *et al.,* 2009) | Semi-automated | on-demand/ no image type / Windows | length, angle, number |
| ***RootScape*** (Ristova *et al.*, 2013) | Semi-automated | Freeware / no image requirement /Windows, Mac | Global (capture root system architecture as one integrated trait) |
| ***WinRHIZO*** **Tron**™ (www.regent.qc.cac) | Manual | Commercial / rhizotron images / txt / Windows | Local, global (Length, area, volume, diameter, number) |

| | | | |
|---|---|---|---|
| ***RootView*** (www.mv.helsinki.fi/aphalo/RootView) | Manual | Unknown / jpg / txt / Windows | Time lapse (Length, diameter, growth) |
| ***DART*** (Le Bot *et al.*, 2010) | Manual | Freeware / gif, jpg / stat program / Windows, Mac, Linus | Local, time-lapse (Length, order, insertion point) |
| ***Rootfly*** (Zeng *et al.*, 2008, 2010) | Manual | Freeware / minirhizotron images, jpg/csv/ Windows | Local, time-lapse (length, diameter, colour of roots, birth and mortality) |
| ***RootLM*** (Qi *et al.*, 2007) | Manual | Freeware / jpg, colour image / Matlab / Windows, Mac, Linux | Length |

### *1.13 Summary*

Root system architecture (RSA) exhibit high degree of plasticity and represents a key plant trait that could condition plants' ability to respond to nutrient stress. In this thesis, phosphorus (P) is employed as a case study because whilst P is an essential mineral nutrient for plant productivity and its availability regulates RSA in many crops, its phytoavailability is however low and resources for P fertilisers are finite. Identifying the variations in RSA traits or root growth between crop genotypes therefore represents a promising route towards genetic improvement of crops and ultimately for producing elite ideotypes for improved P acquisition and use. Past work on root systems revealed that the structure is complex and greatly influenced by soil environment. There are also different types of root systems for different crop plants. Although progress has been made in root measurement methodology to observe and quantify RSA, methods employed in the past still have some limitations.

i. Most current methods are not suitable to capture temporal data on root growth dynamics;
ii. Current methods are not adequate to phenotype large numbers of plants;
iii. Some high throughput imaging technologies involve complex installation systems and are too expensive;
iv. Correlation between measured data and actual root system is not often.

### *1.14 Aims*

The present study aims to develop a cost-effective and highly resolved root phenotyping methodology that integrates automated temporal data acquisition with limited engineering complexity. It also aims to study root system dynamic and root system response of *Brassica rapa* seedlings to external P concentration.

This project utilizes *Brassica rapa* L. (syn. *Brassica campestris* L.) commonly referred to as field mustard as a model crop. The genus *Brassica* comes from the family *Brassicaceae* and includes some of the most important vegetable and oilseed crops grown globally. These include three elementary diploid species namely *B. rapa* (2n=20; AA), *B. nigra* (2n=16; BB) and *B. oleracea* (2n=18; CC). Also included are three amphidiploid species which originated through interspecific hybridization between any two of the diploids and are *B. juncea* (2n=36; AABB), *B. napus* (2n=38; AACC) and *B. carinata* (2n=34; BBCC) (Song *et al.*, 1990; Song *et al.*, 1988). *Brassica* in general show considerable genetic variation in their adaptations to P limited conditions including changing their root morphology, changes in the amount of biomass invested into the root system and secretion of enzymes and metabolites in the rhizosphere to increase the availability of Pi (Hammond *et al.*, 2003; Hammond *et al.*, 2004; Hammond and White, 2008). *Brassica rapa* is a non mycorrhizal plant and is considered a good candidate for research due to their characteristic rapid cycling and close relation to the model plant *Arabidopsis thaliana* and the widely cultivated *B. napus* (Wang *et al*., 2011*)*. The relatively small genome size of *B. rapa* (468 - 516 Mbp) also make research using the crop preferable. There are extensive resources available for *B. rapa* including a complete *Brassica* A genome sequence (Wang *et al.*, 2011), rapid cycling

Brairri mapping population (Iniguez-Luy *et al.,* 2009) and Genetic Diversity Foundation Set (BraDFS) (White and Brown, 2010).

### *1.15 Objectives*

i. To develop 2-dimensional root phenotyping system that uses a flatbed optical scanner and enables non-destructive high resolution phenotyping of growing *B. rapa* seedlings with high spatial and temporal resolution and repeatability.

ii. Generate relevant data to validate 2-dimensional root system density based models.

iii. Investigate the effect of environment or growth media on the dynamics of RSA traits and root growth.

iv. Quantify root system architecture to evaluate within and between genotype variations in root traits.

v. Analyse the response of root system architecture of *B. rapa* genotypes grown under varying P availability on non-soil and soil rooting media.

vi. Analyse root growth dynamics using mixed-effects models in order to establish the variation in root traits attributable to effects of genetic factors and environmental effects.

# CHAPTER 2 : DEVELOPMENT OF A LOW-COST HIGH RESOLUTION ROOT PHENOTYPING SYSTEM

## 2.0 Introduction

This chapter describes the development of a root phenotyping platform. We chose to design a root phenotyping platform based on flatbed scanners because:

i. it is inexpensive and the design is simple which can be assembled in many places;

ii. it has high image quality;

iii. it can be automated easily (Dannoura *et al.*, 2008; 2012).

The root phenotyping platform is made of three main components, namely: the physical system, the image acquisition control system which consist of software and thirdly the data analyses system (Figure 2.1). The following sections describe the development and testing of each of the three components of the phenotyping system. Finally, we conclude this chapter with a discussion on the components described.

### *2.1 Physical System*

#### 2.1.1 Growth chamber

The imaging system was developed in a 2.40 m x 4.15 m x 2.15 m growth room equipped with heavy duty wire mesh grid of 3.85 m x 1 m raised 30 cm above the floor to accommodate scanner banks (Figure 2.2). This growth chamber provides light, temperature and humidity control. Lighting in the growth room was initially provided by a Philips SON-T Agro 400-W high pressure sodium lamp (http://www.eltacnet.com/philips5.pdf) with an illumination of 550 µmol $m^{-2}$ $s^{-1}$ photosynthetically active radiation (PAR) (s.d. ±12 µmol $m^{-2}$ $s^{-1}$) at plant height (about 90 cm). These lamps produced excessive heat and excessive condensation on the scanner window.

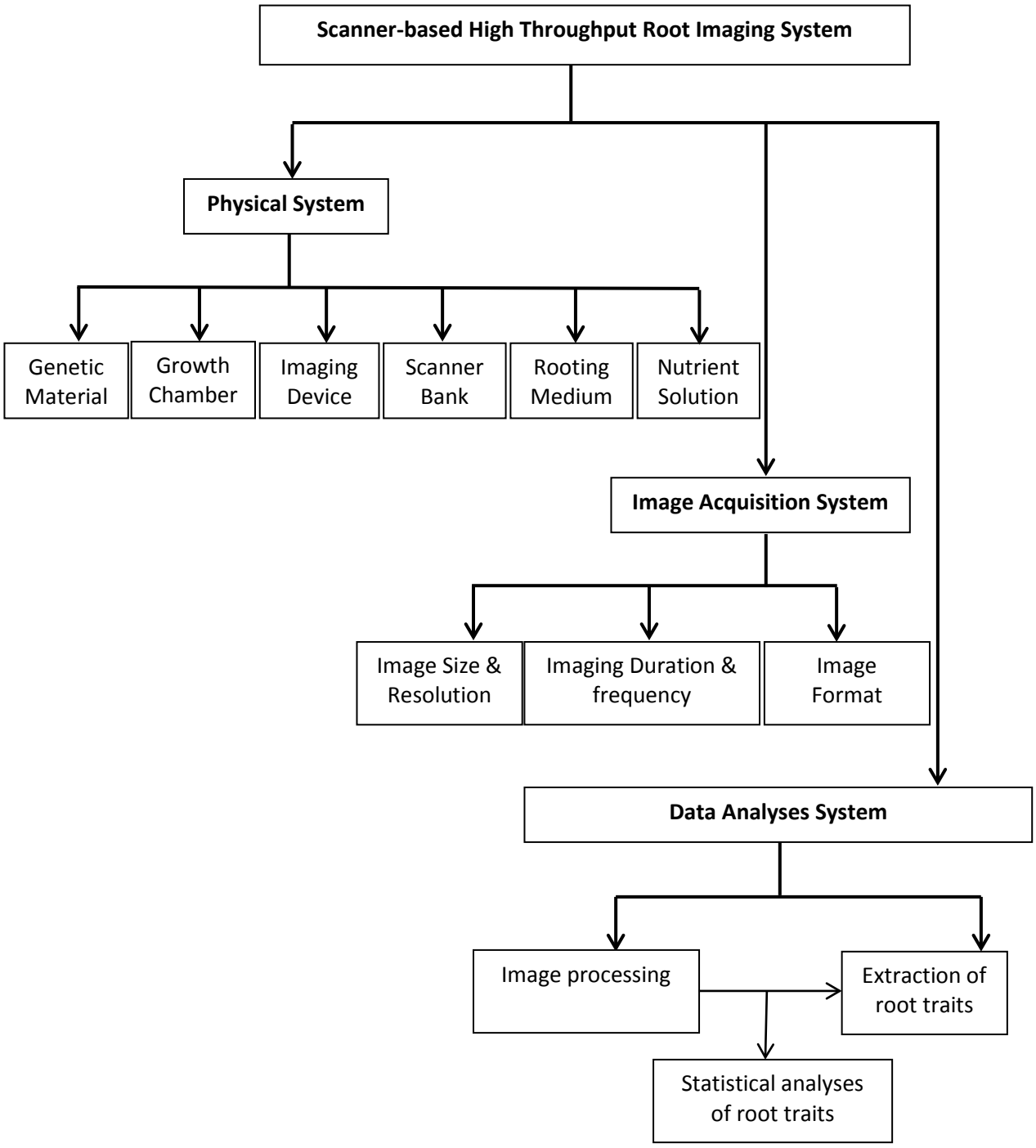


***Figure 2.1:*** *Workflow for the development of the high throughput scanner-based root phenotyping system*

Subsequently, we employed two banks of 3 each 100-W cool-white fluorescent tubes (Philips, Eindhoven, Netherlands), providing PAR of 100 µmol $m^{-2}$ $s^{-1}$ (s.d. ±15 µmol $m^{-2}$ $s^{-1}$) at plant height (Figure 2.2). These cool light sources enabled the light source to be closer to plant leaves. The fluorescent lights also provided even light and temperature distribution

over the plants and scanners. The experiments in this thesis were conducted with a 16/8 h light/dark cycle. The growth room air temperature was maintained at 20°C (s.d. ± 1°C) during the light/dark period seemed optimal also for fungal growth on the seed germination paper (see Section 2.1.6 for description of germination paper). A constant temperature of 15 °C (s.d. ± 1°C) was adopted to limit fungal growth with a relative humidity of 60% (s.d. ± 5%).

***Figure 2.2:*** *Growth chamber showing light source and wire grid on which the scanner banks were assembled.*

### 2.1.2 Imaging Device

The imaging device used in this study is a Canon flatbed scanner CanoScan 5600F (Figure 2.3) which at the time of writing this thesis was priced at £91.97 per unit (http://www.canon.co.uk). This scanner uses an advanced Charge Coupled Device (CCD) technology incorporating a reflective cold cathode fluorescent lamp with a white Light-Emitting Diode (LED) as its light source. It reads images of objects placed on its glass surface

through a lens after reflected light is consolidated in a mirror (Dannoura *et al.*, 2008). The scanner provides a 2-dimensional imaging panel of 216 x 297 mm. Other features and specifications given by manufacturer include 4800 x 9600 dots per inch (dpi) resolution and 48-bit colour image as well as zero warm-up time during imaging. It is easily operated using a USB interface for image capture. The CanoScan 5600F is supported by several versions of Windows and Mac operating systems with an optimal operating temperature range of 10 - 35 °C and humidity of 10 - 90%.

***Figure 2.3:*** *Flatbed scanner used in the study (Source: www.canon.co.uk/)*

To facilitate the fixing of germination papers on scanners, the top cover of the scanners was detached. Black polyvinylchloride plates, (215 × 300 mm) were used as covers for the scanners (Figure 2.4). The plates were initially fixed with magnetic tape but the adhesive was not strong enough to hold plates and germination papers during the course of experiments. Plates were therefore attached with duct tape, with the duct tape being replaced for each new experiment.

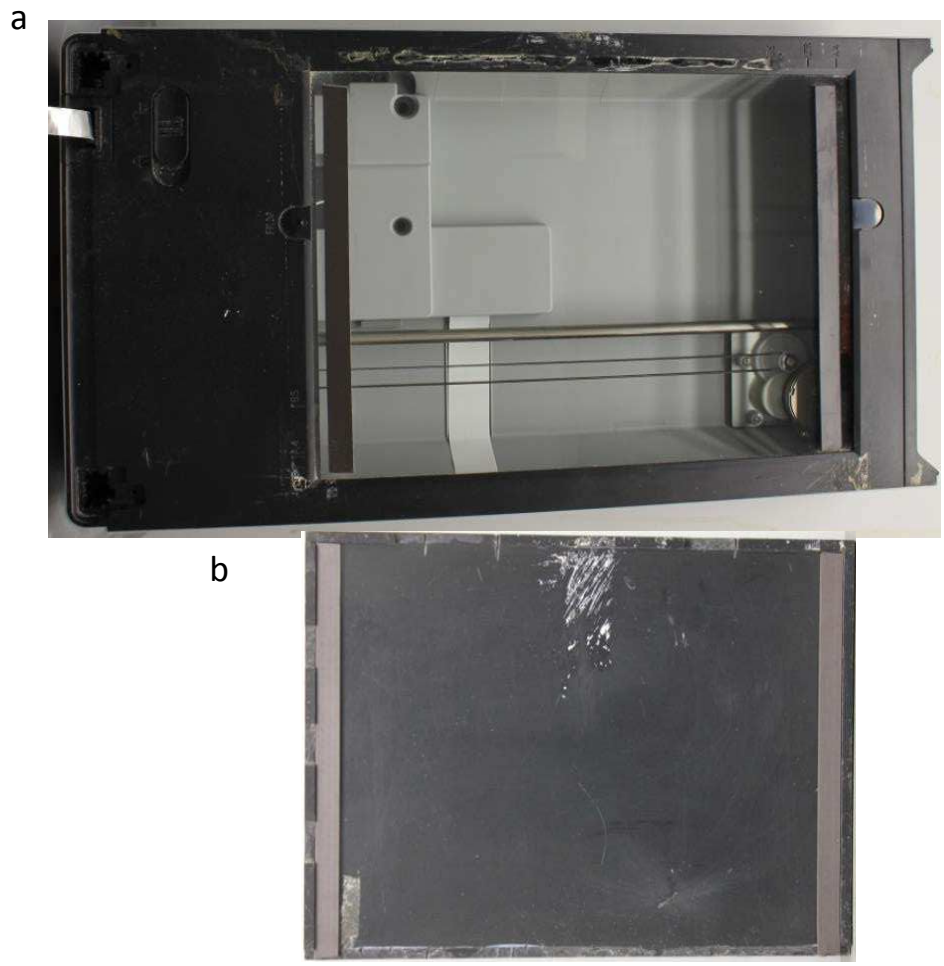


***Figure 2.4:*** *(a) Modified flatbed scanner with cover detached and magnetic strips fixed at both ends of its width; (b) Black Perspex plates used as scanner cover and also to hold rooting medium vertically on scanner surfaces - two magnetic strips used to attach plates to scanners are shown.*

### 2.1.3 Effects of scanning on seedling RSA

Potential influence of the spectral effects of scanner LED on RSA could increase for individual seedlings. This is because the scanners incorporated white LED and repeated scans were done on same plants over longer periods of time. Moreover, given that root systems of seedlings are in close proximity to the light source in our setup, it is plausible that conclusions drawn from root system data obtained may be confounded by the effects of the scanners' light. Here, we assessed the influence of the scanners' lighting on root system traits.

Environmental conditions (Sections 2.1.2; 2.1.6; 2.1.7 & 2.1.8) other than scanning frequency were uniformly maintained among seedlings grown for 10 days on flatbed scanners. Seeds of *Brassica rapa* genotype R-o-18 were pre-germinated for 72 h. For germination, seeds were sown on 12 × 12 cm germination papers (Anchor Paper, Saint Paul, MN, USA) sprayed with deionized water and placed vertically in a Sanyo MIR153® incubator at 20 °C. Three days after sowing (DAS), seedlings of similar size with radicles 2-3 cm in length were transferred to large sheets of germination paper (30 × 42 cm; Anchor Paper Company, St. Paul MN., USA, http://www.anchorpaper.com/) (Section 2.1.7.1) attached to flatbed scanners using 30 × 20 cm clear-Perspex plates. The germination paper surrounding each radicle was cut and transferred with the seedling to minimize disturbance during this process (Adu *et al.,* 2014). The genotype used for this experiment, R-o-18, is a diploid self-fertile inbred line of the *B. rapa* subsp. *trilocularis* (Yellow Sarson) closely related to *B. rapa* oilseed crops grown in Pakistan (Stephenson *et al.*, 2010). The germination paper with the seedlings were held in place by 30 cm x 20 cm opaque / transparent Perspex plates and then fixed to Canon CanoScan 5600F flatbed scanners (Sections 2.1.1, 2.1.3; Figure 2.3).

Roots of the seedlings grew vertically on the rooting medium. Nutrient solution was supplied through the germinating papers (Section 2.1.7). Two independent experiments were run and for each, there were two treatments. In experiment 1, roots of seedlings were scanned every 12 hours (Section 2.2) for the whole 10 d duration of the experiment. The resolution for scanners was set at 300 dpi. In experiment 2, seedlings also grown on germination papers fixed to Perspex plates abutting flatbed scanners but were not periodically scanned except ones on the 10$^{th}$ day after sowing (DAS), just before the

seedlings were harvested. For each experiment, there was two independent run and 12 scanners were used in each run with six scanners per scanner bank ('Scanner bank' will be explained in Section 2.1.5). Treatments were randomly placed within scanner banks. Two plants were grown on each scanner giving 12 replicates per treatment for each run. Seedlings were harvested 10 days after sowing (DAS) and were separated into shoot and root parts for fresh weight measurements and dry weights, following drying at 60 °C for 72 h. *SmartRoot* (Lobet *et al.*, 2011) was used to extract root traits (see Section 2.3.3.1 for description of *SmartRoot*) from all images captured on the final day of the experiments. Analyses of variances (ANOVA) were performed on shoot and root traits using *R* (R Core Team, http://www.R-project.org).

Total root length (TRL), total lateral roots length (1$^{st}$ order lateral roots, TLRL), primary root length (PRL) and mean length of all laterals (mean LRL) were measured, along with shoot biomass (shoot fresh weight, SFW; shoot dry weight, SDW) and root biomass (root fresh weight, RFW; root dry weight, RDW). Also, diameter of primary (PR Diam.) and lateral roots (LR Diam), branching density, (B. Dens), number, mean insertion angle (angle) and inter-branch distance of laterals (Int. Dist.) were measured. Root-to-shoot biomass ratio (R:S) was also calculated from SDW and RDW.

No seedling mortality was recorded for the 48 individual seedlings studied. There was no significant difference between the two experiments except in 3 traits (i.e.: LR diameter, number of LRs and R:S; $p<0.05$; Figure 2.5). Lateral roots of seedlings that were periodically scanned for example recorded higher diameters (Figure 2.5; $p=0.05$). It is also seen in Figure 2.5 that that there was large variation within these traits. This may suggest that the sample

size (n = 6) was not adequate, traits investigated here were unstable or control of environmental conditions may have been sub-optimal.

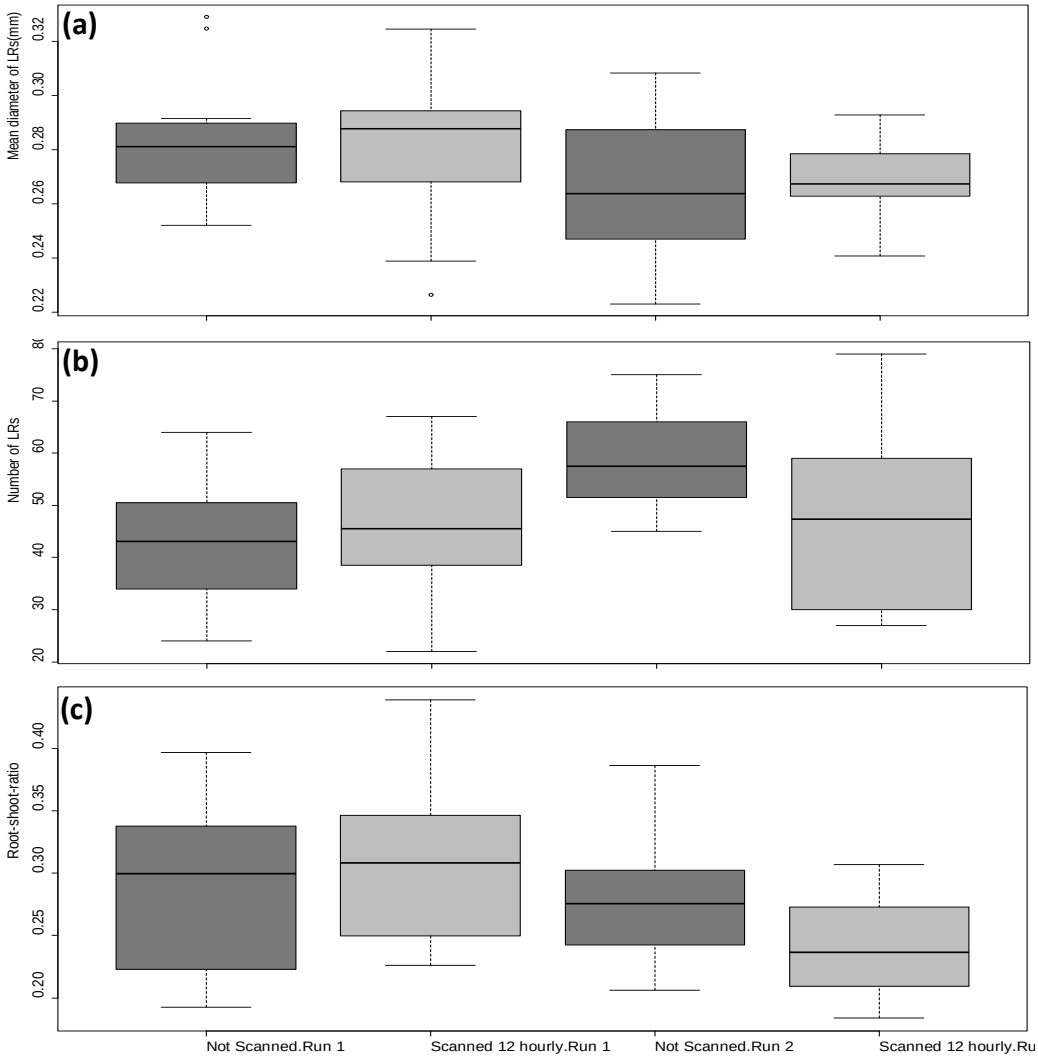


***Figure 2.5:*** *The effect of run on (a) mean diameter of LRs; (b) Number of LRs and (c) root-to-shoot ratio of* Brassica rapa *seedlings grown for 10 DAS under with or without periodic scanning with flatbed scanners*

Scanner light did not affect growth of plants (Figure 2.6). Seedlings which were not periodically scanned recorded 5.71 mg, 1.62 mg, 54.10 cm, 39.0 cm, 15.12 cm and 0.83 cm, respectively for SDW, RDW, TRL, TLRL, PRL and mean LRL. Periodically-scanned seedlings recorded 5.66 mg, 1.60 mg, 59.0 cm, 45.20 cm, 13.74 cm, and 1.03 cm, respectively for SDW, RDW, TRL, TLRL, PRL and mean LRL (Figure 2.6). Estimates of number of LRs, P Dens., LR Diam., Int. Dist., angle and R:S for 'Not-Scanned' seedlings were 51 roots, 4.82 roots $cm^{-1}$,

0.27 mm, 0.27 cm, 75.30 ° and 0.28, respectively. Estimates of number of LRs, P Dens., LR Diam., Int. Dist., angle and R:S for 'Periodically-Scanned' seedlings were respectively 47 roots, 5.32, roots $cm^{-1}$, 0.27 mm, 0.25 cm, 75.68°, 0.28 ( Figure 2.6). The results showed that cool white LED light source of flatbed scanners does not significantly alter root growth.

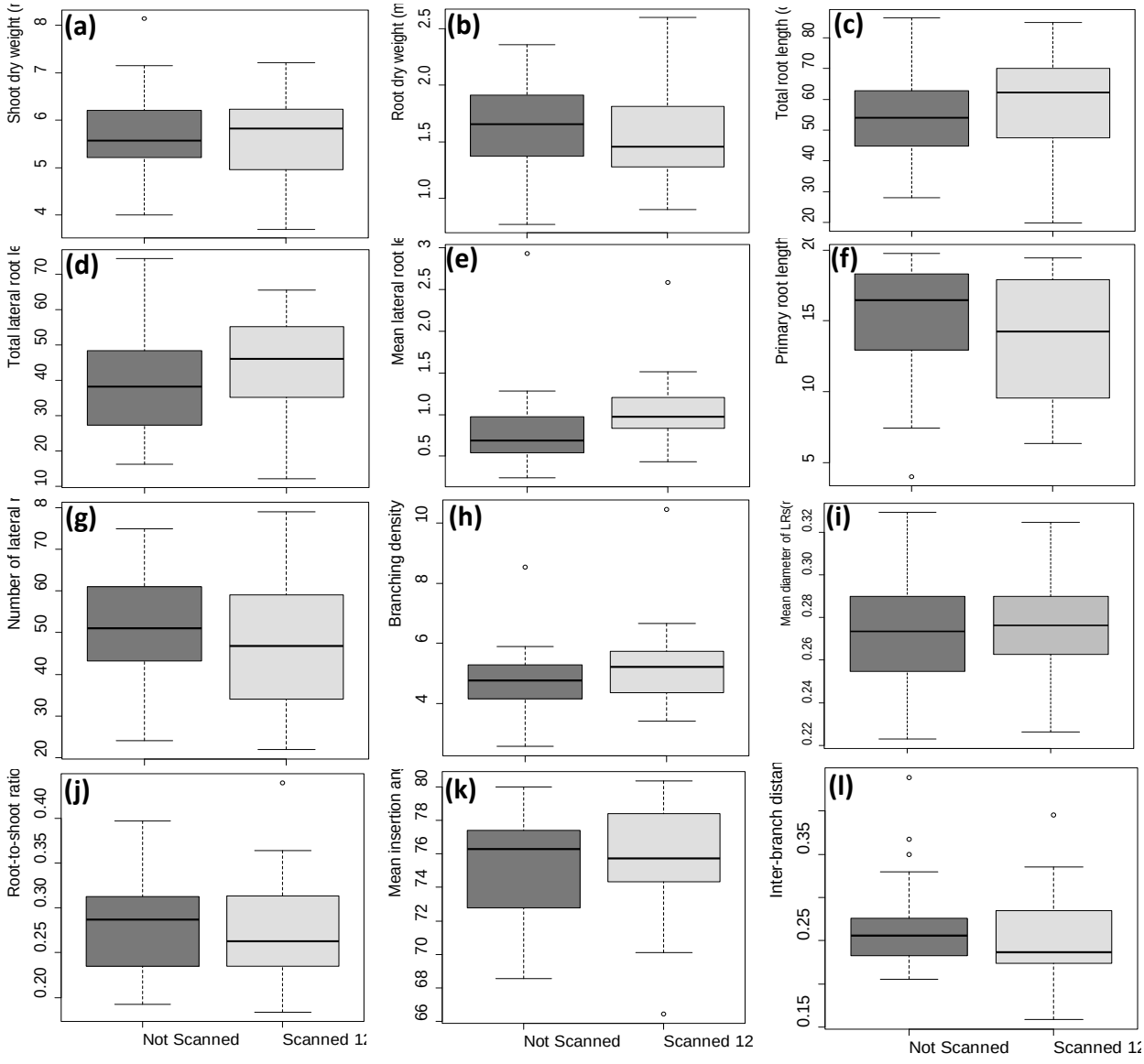


***Figure 2.6:*** *The effects of scanner white light emitting diode (LED) on shoot dry biomass (a), root dry biomass (b), total root length (c), total lateral root length (d), mean lateral root length (e), primary root length (f), number of lateral roots (g) branching density (h), mean diameter of lateral roots (i), root-shoot-ratio(j), mean insertion angle of lateral roots (k) and mean inter-branch distance of lateral roots (l) of* Brassica rapa *seedlings grown for 10 days after sowing on seed germination paper fixed to flatbed scanners with or without scanning by the flatbed scanners. (n=24).*

### 2.1.4 Rhizobox experiments

During this thesis, root growth were also studied using rhizoboxes (root observation chambers) filled with soil. Rhizoboxes were constructed after the design of Bengough *et al.* (2004). Boxes were constructed from two Perspex plates, one of which was opaque and the other transparent. Each plate measured 30 × 21.5 × 0.3 cm (Figure 2.7). Strips of Perspex (0.3 cm thick) were used as spacers around each plate, giving a plate separation of 0.6 cm. Three gaps, each approximately 3 cm long, were left along the top surface to allow gas exchange with the surrounding atmosphere and unimpeded shoot growth (Figure 2.7a). Rhizoboxes were initially oriented in landscape format for the growth of seedlings (Figure 2.7a) but primary roots grew faster in soil (e.g.: 21 cm could be reached after 8 days). Boxes were therefore re-oriented (Figure 2.7b). Root growth was captured by flatbed scanners. Rhizoboxes were fixed on scanners with the transparent wall aligned with the scanning glass.

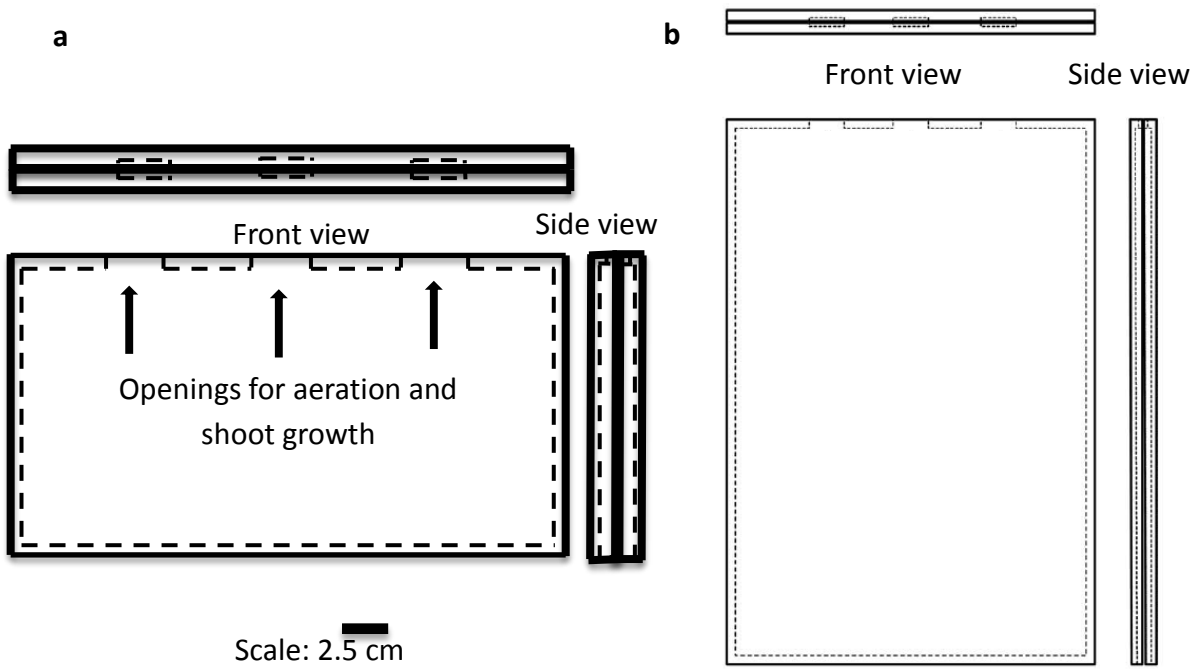


***Figure 2.7:*** *Schematic of the rhizobox used as observation-chamber for experiments involving soil; (a) rhizobox when scanners are used in landscape mode; (b) rhizobox when scanners are used in portrait mode (Bengough et al., 2004)*

### 2.1.5 Scanner Bank

Scanner bank refers to the equipment used to provide support for the ensemble of scanners and also to provide adequate support for plants by supplying nutrients onto the seed germination papers. Two types of scanner banks were used in this thesis. The first generation of scanner banks was constructed using transparent polyvinylchloride plates (Figure 2.8). These banks consist of a tank measuring 100 x 60 x 24 cm for holding nutrient solution. The tanks had a tap for drainage and were covered with black plastic sheets to limit exposure to light in order to prevent the proliferation of green algae (Figure 2.8). Each bank could hold 8 scanners and scanners were held vertically above nutrient solution on supports within the tanks (E-F, Figure 2.8). Five removable scanner supports, three of which could house two scanners each at opposite ends and the remaining, one scanner each, were also constructed from transparent polyvinylchloride plates. During an experiment, scanners were placed on these supports within the tanks (Figure 2.8).

The size of this first generation scanner banks was a severe limitation. It was difficult to move and wash after each experiment. It made them quite fragile and susceptible to leakage after several uses. Consequently, a lighter and simple tank (Figure 2.9) was used. The tanks measured 60 x 40 x 17.5 cm could accommodate 6 scanners at a time. Scanners were larger than these tanks so scanners could simply be held on the top of the tanks at various angles (Figure 2.9).

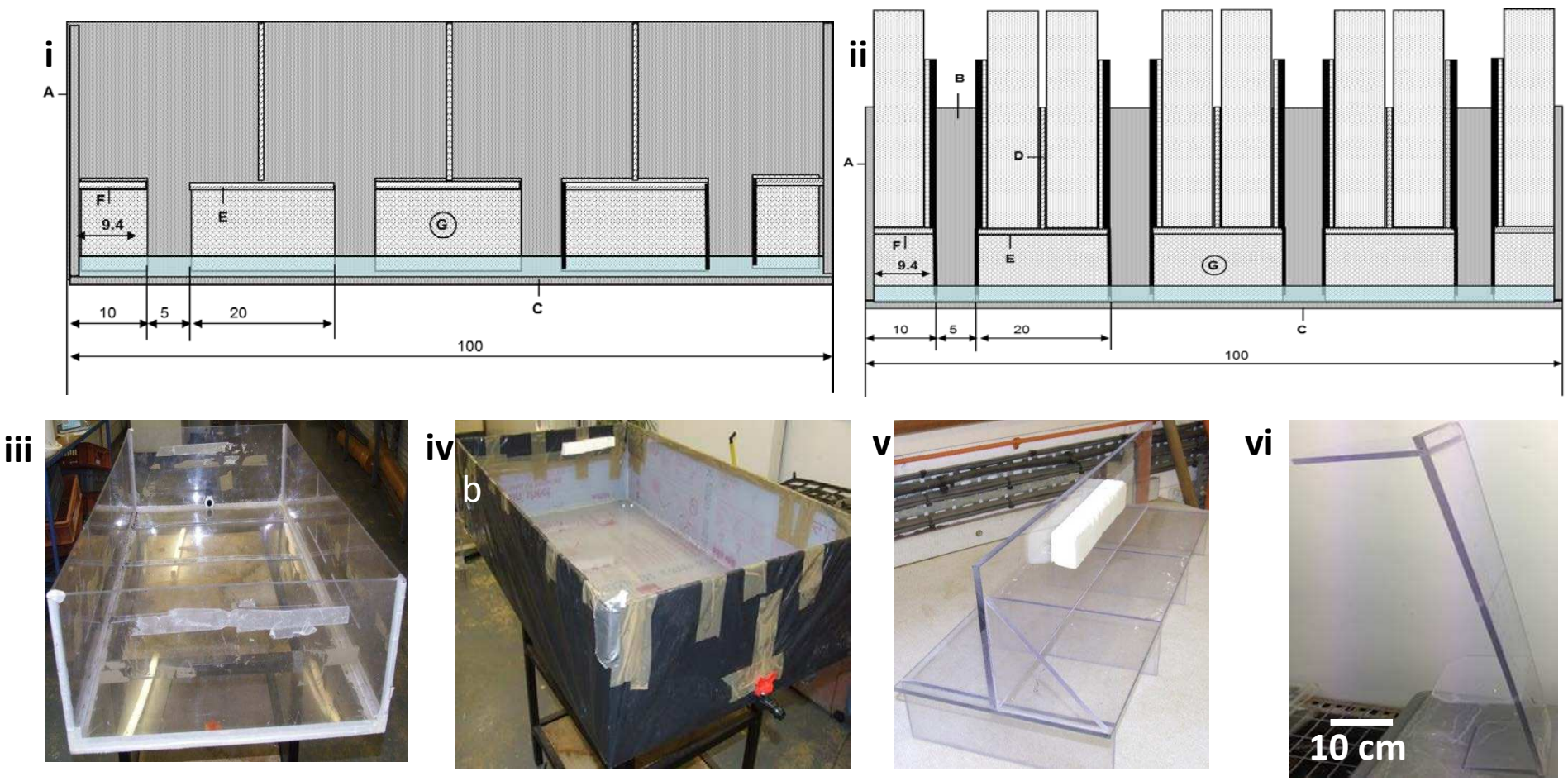


***Figure 2.8:*** *Schematic of the scanner banks; (i) with scanner platforms within the tank but without scanners (ii) with scanners mounted on platforms within the tank. A-C: Bottom and side plates; D: vertical support for scanners; E - F: horizontal support for scanners; All dimensions are in centimetres. (iii) tank for nutrient solution; (v) tank for nutrient solution covered with black plastic sheet; (v) support for 2 scanner (i-G); (vi) support for 1 scanner (i-F).*

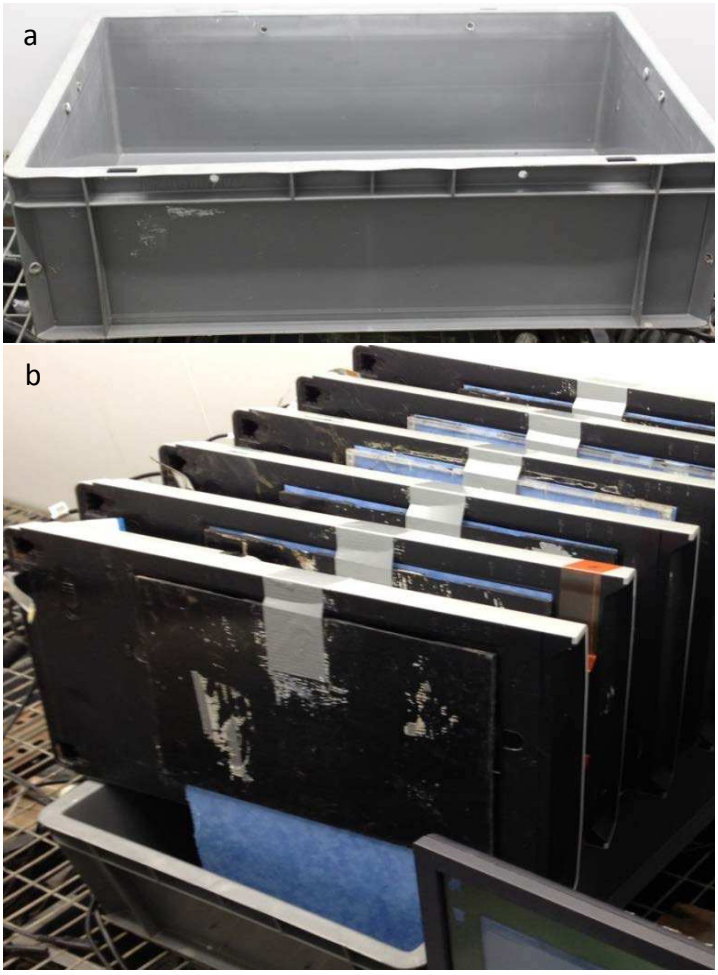


***Figure 2.9:*** *a) Polypropylene tanks for the 2nd generation scanner bank; b) scanners held on top of the tanks of nutrient solution.*

### 2.1.6 Rooting Medium

#### *2.1.6.1 Paper*

Seed germination paper was the primary substrate used in the scanner banks. This is similar to pouch systems where plant roots grow at the surface of germination blotters (Hund *et al.*, 2009; Liao *et al.*, 2001). In this project, seedlings were grown on a germinating paper, placed on a polycarbonate plate and attached to the scanners. Observing root growth on germination papers was on some occasions problematic because roots can occasionally grow within the paper. This phenomenon was observed when the germination paper was in

tight contact with another surface. For example, we initially covered the growing root systems with the transparent films to facilitate two-dimensional root growth on the surface of the paper and also to reduce some of the potential effect of light emitted by scanners onto the live root system. It has been suggested that there could be light-induced effects on root growth (Webb, 1982). The exposure of white light to the elongating zone of growing maize (*Zea mays* L.) induced a very rapid inhibition of the elongation rate (Pilet and Ney, 1978). So in an attempt to reduce this effect, we covered the growing roots with the transparent films but this promoted the tendency for fine roots to grow within the paper which made weighting and other analyses more difficult. The use of the transparency covers was thus terminated. Besides, roots grew two-dimensionally on the surface of the papers with no observed difficulty. Moreover, the transparencies were also hydrophobic, leading to increased condensation on its surface and introducing more artefacts on the images of root systems.

Root growth on different paper types was tested and paper types that were tried included: (i) Black construction paper (http://shop.hobbylobby.com). This paper is a 100% recycled material made from wood pulp and has a slightly coarse texture on its surface. The black construction paper provided very good contrast and was ideal for imaging fine root structures. Root growth was also vigorous. Due to its lighter weight, this paper type was not adequately hydrophilic and couldn't transport enough water and nutrients to the root zone and roots could be subjected to drought. Moreover, the paper was subject to discoloration which also affected the colour of roots during the course of experiments. For this reason,

black construction paper was not used beyond simple root growth experiments (system testing stage of this thesis).

(ii) Steel blue seed germination blotter (Anchor Paper Company, St. Paul MN., USA, http://www.anchorpaper.com/). This 30 x 42 cm paper standard seed germination paper is produced from 100% recycled cellulose fibre. It is a nontoxic paper with an open and porous structure free from mechanical pulp content, bacteria and other impurities. The steel blue seed germination blotter provides good contrasts and roots are easy to see. It also has good water retention properties (Dutt *et al.*, 2005) (Table 2.1) and can store water 14 to 16 time of its dry weight. The minimum capillary rise above water surface after immersion for 5 minutes is approximately 4 cm.

(iii) The third paper type was a Versapack or Kimpak paper (Anchor Paper Company, St. Paul MN., USA). Apart from being brown in colour, this paper shared most of the properties of the steel blue anchor paper. For brevity, the three paper types described above hereafter will be called construction, blue and brown papers.

***Table 2.1:*** *Absorbent properties of a seed germination blotter ([1]Minimum Castor Oil Penetration (COP) values are preferred in water Absorption measurements as higher values adversely affect water Klemm. [2]Water Klemm: the degree of water absorption of a paper and is related to water rise in capillaries (Dutt et al., 2005)*

| Particulars | Specifications |
|---|---|
| Basis weight ($g/m^2$) | 155 ± 3 |
| [1]Average COP (at 35 ± 1 °C, s) | 11.5 |
| [2]Average water klemm (mm/4min) | 24 |
| Wet strength (g/cm) | 200 |

The P concentration of the paper was determined. The construction (black) paper was not used further so the [P] assessment here was made on the remaining two paper types. A 3 x 3 cm dry paper sample from the two germination papers (3 replications each) was weighed, digested in MARS® microwave sample digester (CEM Corporation, Matthews, NC, USA) and the P concentration determined by Inductively Coupled Plasma Mass Spectrometry (ICP-MS) method (Ivanov *et al.*, 2010) (Section 2.3.3.4.3). Results show that both paper types naturally contain some levels of P (Figure 2.10). A small fraction of this P might be available to the roots.

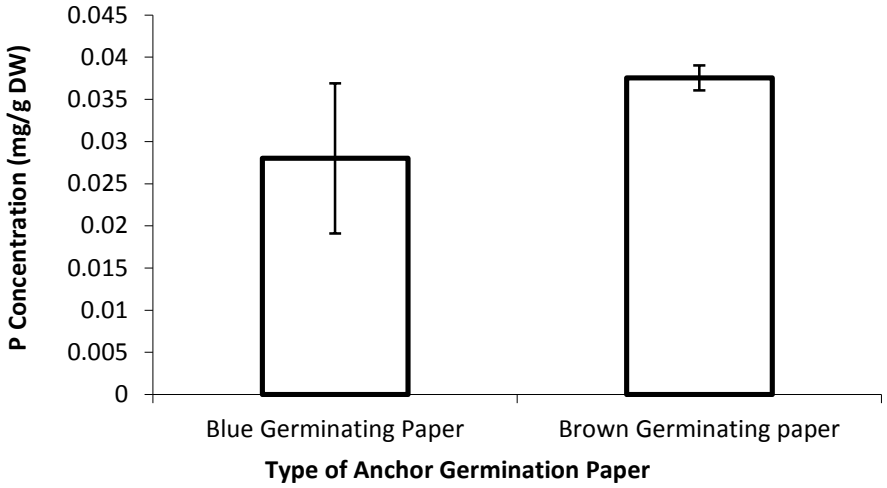


***Figure 2.10****: P concentration in unused germination papers*

In the scanner bank, the bottom quarter of the paper is in contact with the nutrient solution during an experiment. In order to determine if adequate quantities of P are transported to the rooting zone on the paper, the P concentration of the portion of germination paper not in contact with nutrient solution was measured. The papers were subjected to nutrient solutions containing P concentrations of 10, 30, 50, 100, 150 and 300 µM. Samples of the

papers were taken and solution extracted from them using a pair of cleaned flat edge tweezers. Concentrations of P in the solutions were then determined by the Malachite Green (MG) method (Van Veldhoven and Mannaerts, 1987). Concentrations of P in the rooting zone of the paper correlated with the externally imposed P regimes, although the observed [P] was in most cases greater than the actual $[P]_{ext}$ in original nutrient solution (Figure 2.11). It seemed that the germination papers were providing additional sources of P to the nutrient solution.

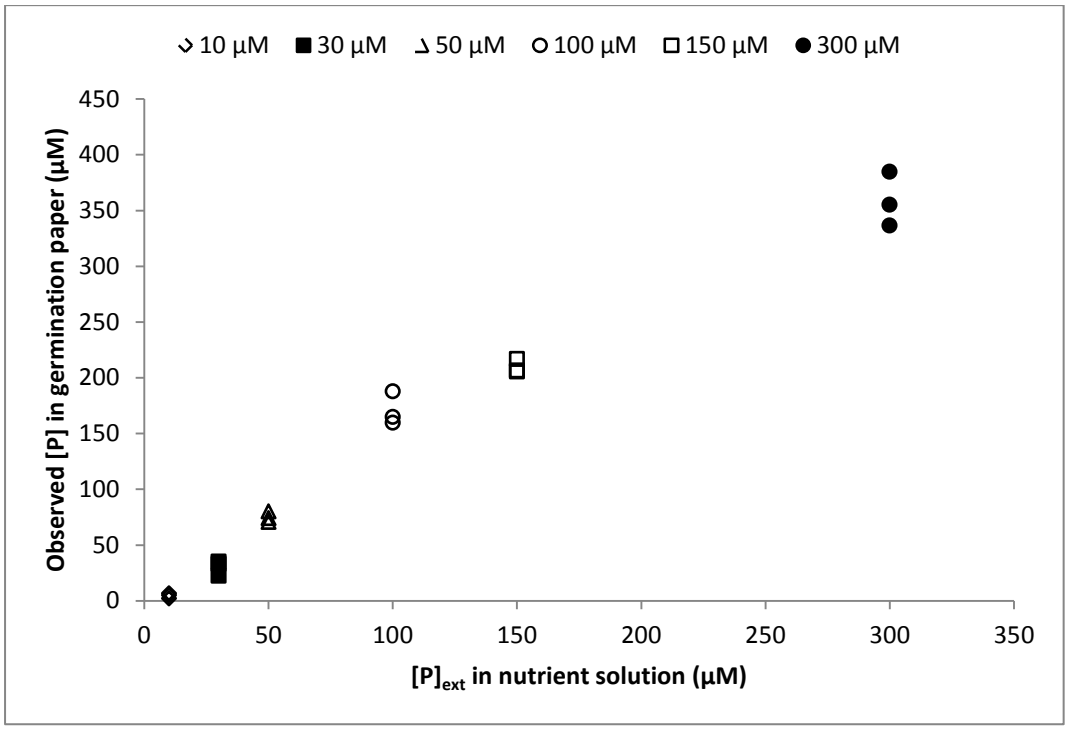


***Figure 2.11****: External P concentration of nutrient solution and the P concentration in the rooting zone of used germination papers*

#### *2.1.6.2 Soil rooting medium*

Topsoil from 0 to 10 cm depth was collected from Tayport (56.45° N, 2.88° W), a site near the James Hutton Institute, Dundee, Scotland. The soil was typical of arable soil of the region and defined as a Cambisol (George *et al.*, 2011a). The soil was a sandy loam with a pH

of 6.3 and contained total digestible P of 1475.0 mg P $kg^{-1}$ of which 40.8% was in organic moieties (Table 2.2). The soil had a relatively high Olsen P content of 84.5 mg P $kg^{-1}$ (probably due to recent additions of pig manure) and water extractable P was relatively low (Pi = 6.3 mg P kg-1 and Po = 0.5 mg P kg-1) (Table 2.2) (Brown *et al.*, 2012). Soils were air-dried, mixed and passed through a 2 mm sieve to remove coarse material and vegetative matter. Soils were subsequently put into rhizoboxes to approximately 0.4 to 0.5 cm deep. Soils were loosely packed into rhizoboxes at a dry bulk density of approximately 1.0 g $cm^{-3}$ and a volume of approximately 300 $cm^3$ per rhizobox. All soils were watered to approximately 80% field capacity as determined by gravimetric water content. Depending on the nature of the experiment, soils were either amended with additional nutrient solution or left un-amended.

***Table 2.2:*** *Summary of soil properties used to fill rhizoboxes (Brown, 2011).*

| **Soil property** | **Value** |
|---|---|
| pH ($Ca Cl_2$) | 6.0 |
| Olsen P (mg P $kg^{-1}$) | 84.5 |
| Total P ( mg P $kg^{-1}$) | 1175.7 |
| Inorganic P (mg P $kg^{-1}$) | 696.1 |
| Organic P (mg P $kg^{-1}$) | 479.5 |
| Organic C (%) | 2.0 |
| Clay (%) | 5.0 |
| Course Silt (%) | 11.0 |
| Fine Silt (%) | 29.0 |
| Sand (%) | 55.0 |

#### *2.1.6.3 Case study: Effect of rooting media on root system growth*

##### 2.1.6.3.1 Methods

*Brassica rapa* genotypes, R500 and IMB211 were used to study the effect of rooting media on root growth parameters. IMB211 and R500 are the parents of the BraIRRI mapping population (Iniguez-Luy *et al.*, 2009). Genotype IMB211 is a highly inbred rapid cycling

Chinese cabbage *B. rapa* subsp. *pekinensis* and R500 is a highly inbred annual yellow sarson *B. rapa* subsp. *trilocularis* (Iniguez-Luy *et al.*, 2009; Xu *et al.*, 2010). The experiment used 3 of the first generation scanner banks and 2 plants were grown on each scanner with 6 replications per genotype and rooting media. Rooting media treatments namely construction paper, blue paper, brown paper and soil were randomised within scanner banks. Two independent experiments were run and time-lapse images were taken at twelve-hour intervals using the fixed flatbed scanners abutting the plates and rhizoboxes. All plants were harvested 10 DAS.

Root traits were extracted with *ImageJ* software (http://rsb.info.nih.gov/ij/) from each image (Section 2.3.3.2). Traits extracted included TRL, PRL, TLRL and R:S, the quotient of RDW/SDW. Time-lapse emergence of LRs was also extracted from images by counting the number of LRs that emerged each day. The number of root tips on each seedling was counted to calculate root topological indices. The topological index (TI) was calculated as the slope of the linear regression between log(altitude) and log(magnitude) (Fitter, 1987; 1991). The Relative Rates of Extension (RRE) of total, primary and total LRs, Relative Multiplication Rate (RMR) of LRs and Mean Extension Rates (MER) of seedlings grown with the different rooting media were calculated as described by (May *et al.*, 1965; Tennant, 1976):

$$RMR = \frac{\log_e n_2 - \log_e n_1}{t_2 - t_1} \approx \frac{n_2 - n_1}{t_2 - t_1} \approx \frac{d_n}{d_t} \qquad (\mathbf{2.1})$$

$$RRE = \frac{\log_e l_2 - \log_e l_1}{t_2 - t_1} \approx \frac{l_2 - l_1}{t_2 - t_1} \approx MER \qquad (\mathbf{2.2})$$

where, *n, l* and *t* for each parameters refer to root number, root length and time (measured in DAS) image was acquired. The data were analysed in Genstat 15$^{th}$ edition using residual maximum likelihood (REML) and employing the model below:

$$y_{ij} = \mu + \alpha_i + \beta_j + \alpha\beta_{ij} + \varepsilon_{ij} \qquad \textbf{(2.3)}$$

where $y_{ij}$ is the trait value of the $i^{th}$ genotype (i = 1,2) grown on the $j^{th}$ media (j = 1,…,4) ; $\alpha$ is the main effect of the genotype , $\beta$ the main effect of the rooting media , $\alpha\beta$ the genotype-by-rooting media interaction and $\varepsilon_{ij}$ the residual.

#### 2.1.6.3.2 Results

*Brassica rapa* genotype R500 attained the greater biomass and root system size than the IMB211 genotype. For IMB211, shoot biomass was significantly higher on soil than on the other rooting media (*p<0.001*). Shoot biomass of R500 on the blue paper was greater than on the other rooting media although there was no significant difference between that and the biomass recorded on soil. Root dry matter was highest for genotypes on the blue paper (Table 2.3). However, the higher root biomass on the blue paper does not appear to be a consequence of root length as the greatest root length was not recorded on blue paper. Root-to-shoot ratios were higher on construction paper for both genotypes. There was a significant genotype × rooting media interaction for root biomass and R:S, but no such interaction for shoot biomass (Table 2.3). There was significant difference between genotypes, rooting media and genotype × media interaction for topological index (TI) values derived from the data (Table 2.3; Figure 2.12 A, B).

***Table 2.3:*** *Probability levels for treatment main effects and interactions, and treatment mean values for shoot and root biomass, root: shoot ratio and topological index for 12 replicates of two* Brassica rapa *genotypes grown for 10 DAS on blue seed germination, brown Kimpack, construction paper and on soil-filled rhizoboxes ( ns: not significant)*

| | | Shoot dry weight (mg) | Root dry weight (mg) | Root: shoot ratio | Topological index ± s.e. |
|---|---|---|---|---|---|
| Genotype effect *(s.e.d.)* | | *P<0.001 (0.965)* | *P<0.001 (0.136)* | *P<0.001* | *P<0.001* |
| Media type effect *(s.e.d.)* | | *P<0.05 (1.322)* | *P<0.001 (0.187)* | *P<0.001* | *P<0.001* |
| Genotype x media type effect *(s.e.d.)* | | ns | *P<0.001 (0.264)* | ns | *P<0.001* |
| IMB211 | Construction paper | 2.16 | 0.72 | 0.34 | 0.93 ± 0.008 |
| | Blue paper | 2.47 | 0.73 | 0.30 | 0.95 ± 0.005 |
| | Brown paper | 1.87 | 0.44 | 0.23 | 1.00 ± 0.006 |
| | Soil-filled rhizobox | 6.88 | 0.35 | 0.09 | 1.0 ± 0.011 |
| R500 | Construction paper | 6.57 | 2.57 | 0.39 | 0.82 ± 0.004 |
| | Blue paper | 10.07 | 3.77 | 0.37 | 1.0 ± 0.006 |
| | Brown paper | 6.97 | 2.41 | 0.35 | 0.9 ± 0.005 |
| | Soil-filled rhizobox | 9.97 | 1.75 | 0.24 | 0.99 ± 0.003 |

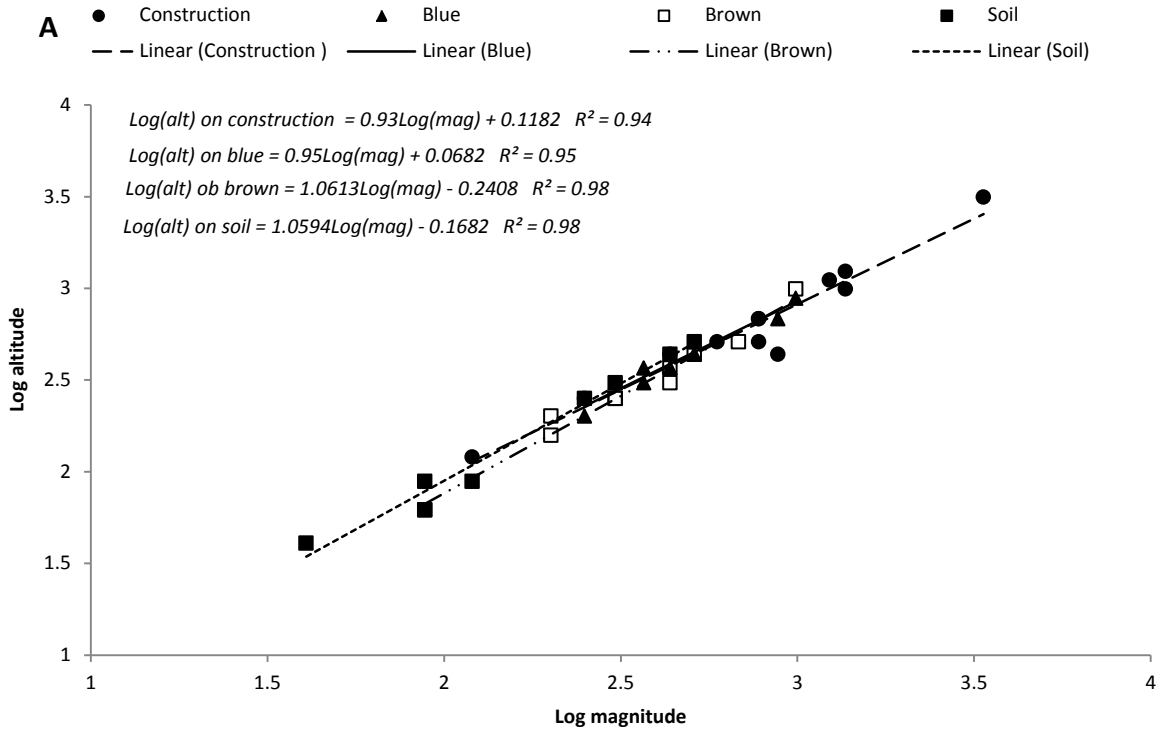

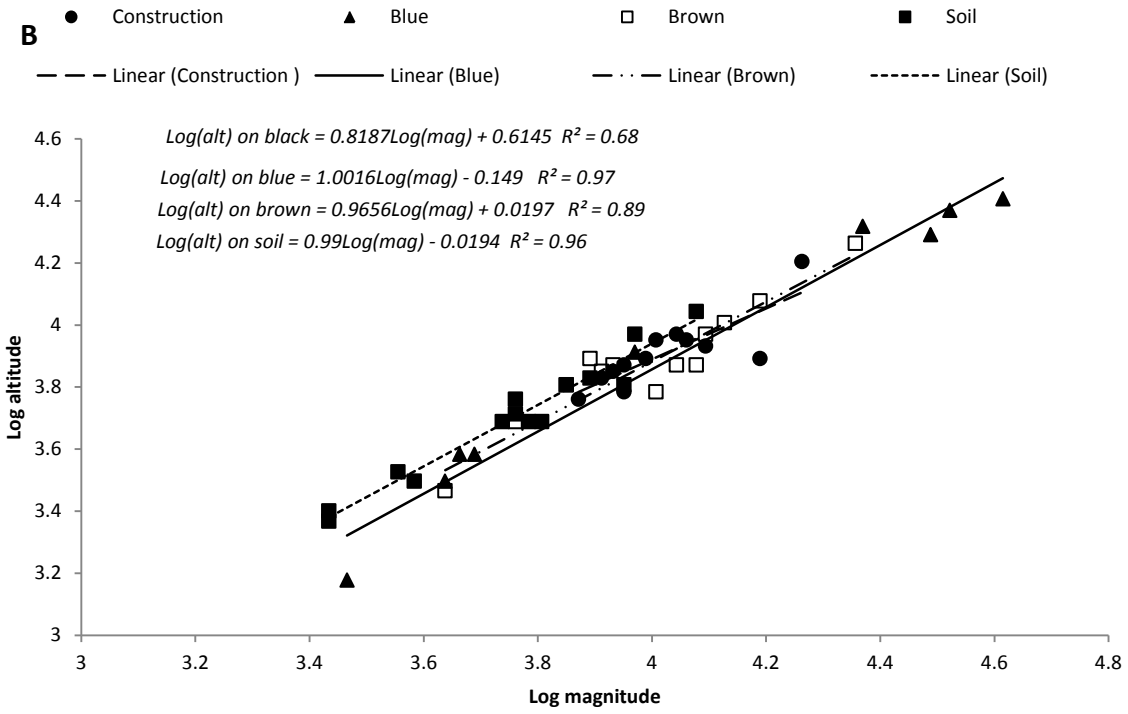


***Figure 2.12****: Linear regression plots of log altitude (number of branching points from the base of the root system to the extreme root tip) on log magnitude (the number of root tips on the root system) for (A) IMB211 and (B) R500* Brassica rapa *genotypes grown on three paper cultures and on soil rooting media.*

Lateral roots emerged generally from 3 DAS. Emergence of LRs for the R500 genotypes was greater on the blue paper whereas that of the IMB211 genotype is greater on the construction paper (Figure 2.13B). Derived RMR however show that emergence on LRs on the black and brown papers are higher for the R500 genotype. The lowest LR number was recorded on soil media at almost all time points for both genotypes (Figure 2.13A). Relative rates of increase in LR number were highest initially and decreased with time for both genotypes and for each rooting media. The decrease in RMR approached constant levels and fell to zero during the period of the experiment particularly for the R500 genotypes (Figure 2.13B).

Type of rooting media significantly affected TRL and PRL ($p<0.05$). Generally, seedlings grown on the construction paper showed faster root growth. The effect of medium on root length was evident from six DAS (Figs. 2.13 C - D; Figure 2.14 A - D). On all rooting media, the highest relative rates of increase occurred over the first 6 DAS and subsequently fell until nearly constant, mainly with the PRs. On all media, RRE values during the periods of constant relative increase were higher for LRs than for PRs and the total root system. Soil medium however seem to favour PR growth than LR growth as RRE of PR on soils was generally greater. Paper rooting media, particularly the construction and brown papers seem to favour LR growth.

There was significant variation ($p<0.05$) between treatments in mean extension rate (MER), as a function of time for LRs (Figure 2.15). In the R500 genotype, MER increased with time to a peak at 6 to 7 DAS after which it declined but the decline was sharper on the construction paper. For the IMB211 genotype, MER appears to be constant with time and significantly higher on the blue paper. In both genotypes, MER recorded on soil medium is generally the lowest.

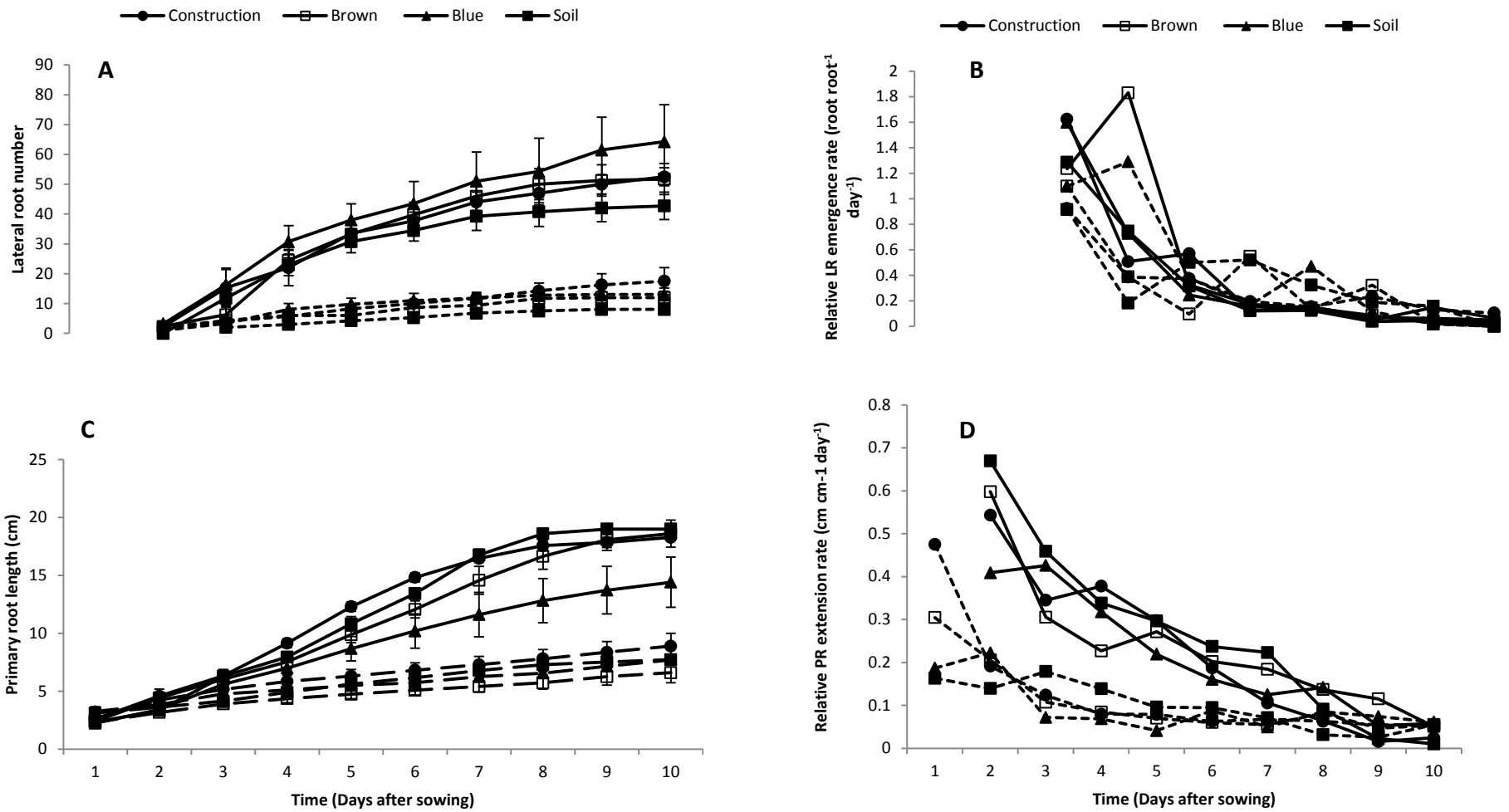


***Figure 2.13:*** *(A) 1. Lateral root number (LR); (B) relative LR emergence rates of LR; (C) primary root length and (D) relative extension rate of primary root during the first 10 days of growth on four different rooting media. (Continuous or solid lines: R500; Dashed lines: IMB211)*

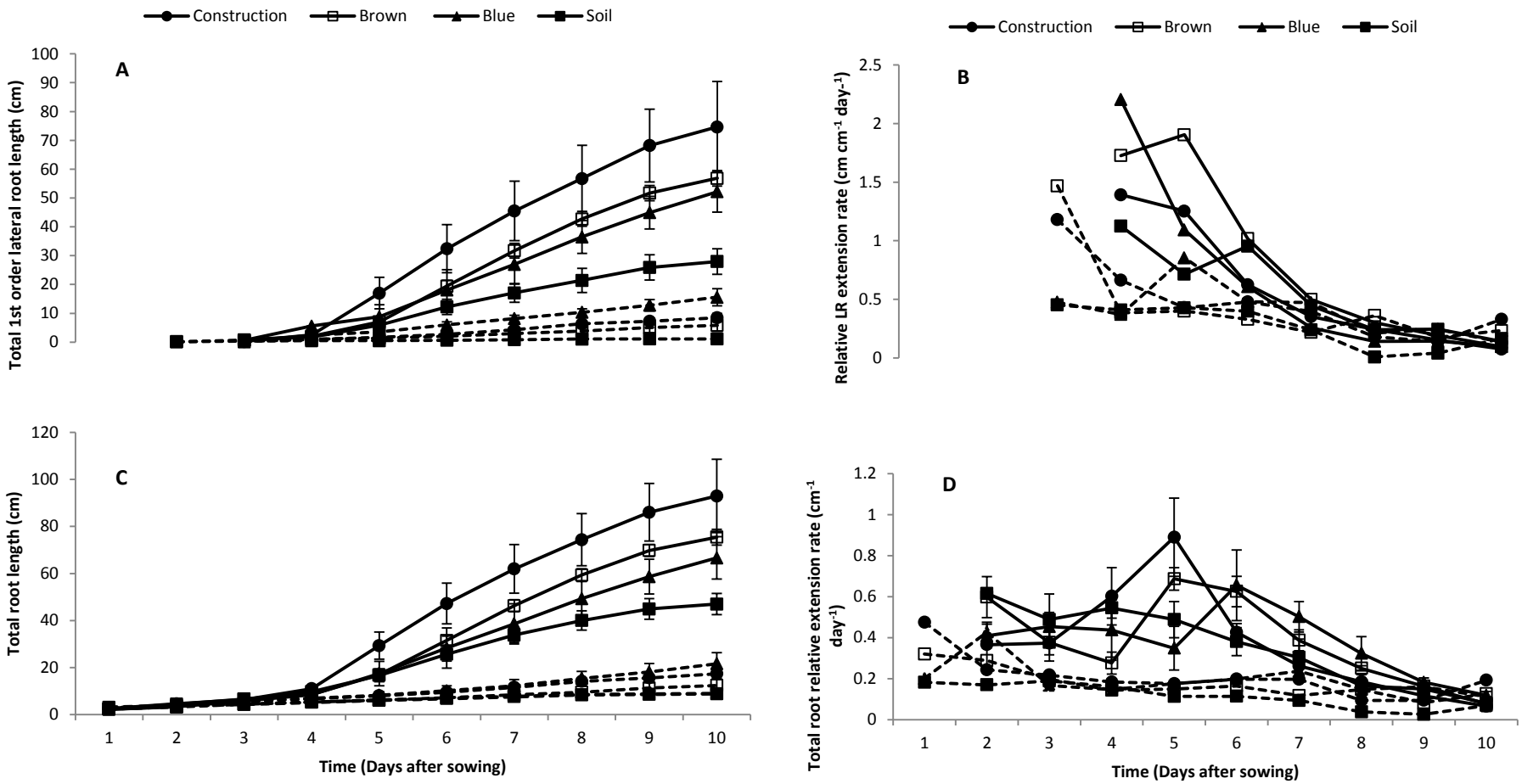


***Figure 2.14:*** *(A) Total length of LR; (B) relative extension rates of LR;(C) length of the total root system and (D) relative extension rate of the total root system during the first 10 days of growth on four different rooting media. (Continues lines: R500; Dashed lines: IMB211)*

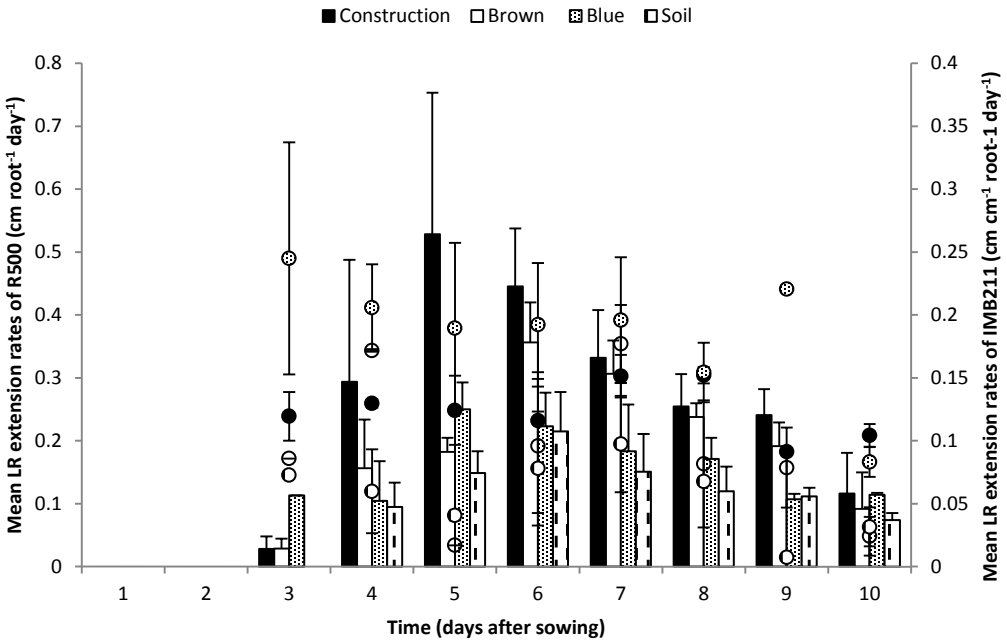


***Figure 2.15:*** *Mean extension rates of LR during 10 days of growth of two* B. rapa *genotypes on four different root media. (Bars & primary axis: R500; Circles & secondary axis: IMB211)*

### 2.1.7 Nutrient Supply to Plants

The HRP system employs a modified pouch systems (Hund *et al.*, 2009) in which a germination paper is attached to a scanner. The bottom of the germination paper is submerged in the nutrient solution (Figure 2.16). Scanners were fixed in near-vertical positions 5 cm above 20 l of nutrient solution contained in opaque polyvinyl plastic tanks, each supplying six scanners. Approximately 10 cm of the germination paper was submerged in the nutrient solution (Adu *et al.,* 2014). In this thesis, nutrient solutions were not changed and replaced during experiments. In this system, nutrients and water are transported to the region of the roots via capillary action. The default nutrient solution was prepared with deionised water and was composed of the macronutrients [in mM]: $KH_2PO_4$ [0.25], $MgSO_4$ $7H_2O$ [0.75], FeNa EDTA [0.1], Ca $(NO_3)_2$ $4H_2O$ [2], $NH_4NO_3$ [2] and micronutrients [in µM] $H_3BO_3$ [30], $MnSO_4$ $4H_2O$ [10], $ZNSO_4$ $7H_2O$ [1], $CuSO_4$ $5H_2O$ [3], and $Na_2MO_4$ $2H_2O$ [0.5] (Broadley *et al.*, 2003). The nutrient solution was adjusted to pH 6 (s.d. ± 0.5) at the start of

the experiment using $H_2SO_4$. Since the nutrient solution was stagnant, air pumps connected to porous stones were used for aeration.

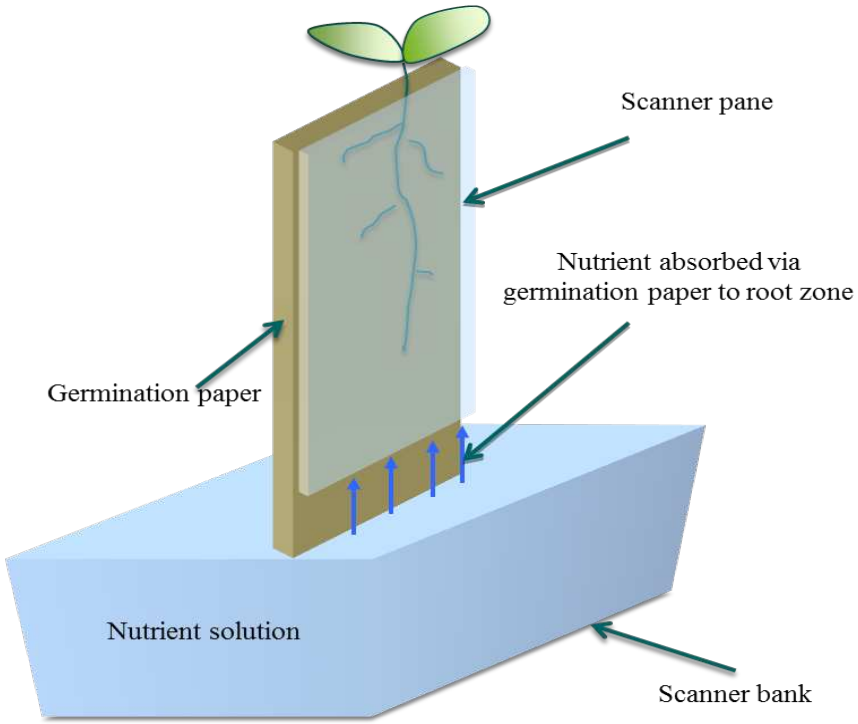


***Figure 2.16:*** *Schematic of nutrient absorption onto root zone.*

In order to quantify the depletion of nutrients in the solution, plants were grown under six external P nutrient concentrations. For each, micro-samples (10 µL) of nutrient solutions were collected from each concentration on the first, fifth and tenth day of plant growth. Phosphorus concentration in each solution and at the three time points was analysed by the Malachite Green (MG) P assay method (Van Veldhoven and Mannaerts, 1987). At the end of 10 DAS, solution concentrations generally decreased by approximately 20 -27%, except for solutions containing 10 and 50 µM P for which $[P]_{ext}$ increased (Figure 2.17). These results show that there is decline in $[P]_{ext}$ in the initial solutions but this decline is not likely to affect plant growth.

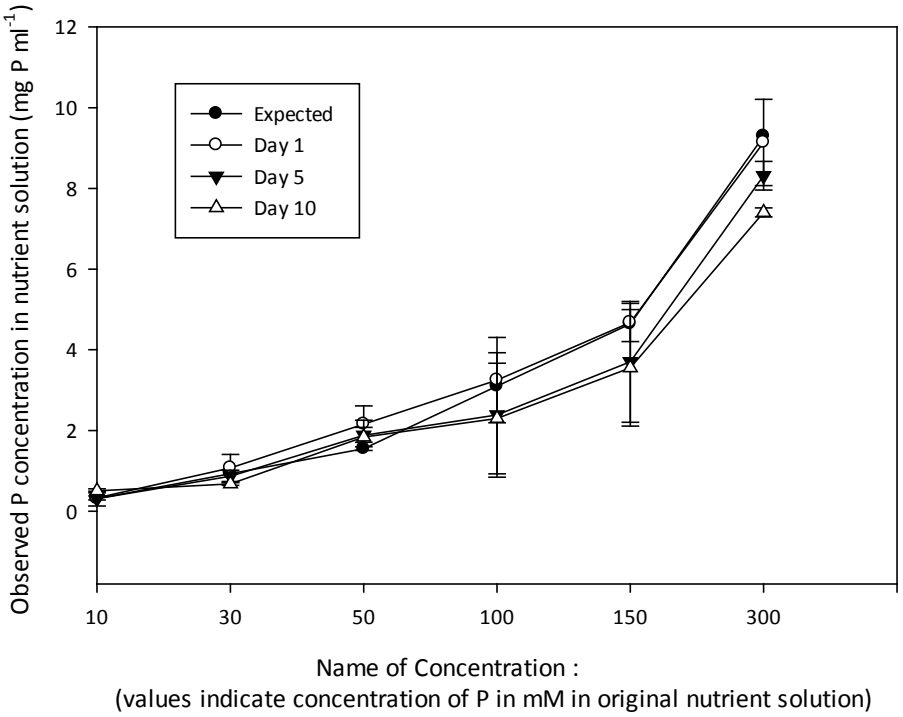


***Figure 2.17:*** *Depletion of P in nutrient solutions*

### *2.2 Image acquisition tool:* ArchiScan

*ArchiScan* was authored by Lionel X. Dupuy and Antoine Chatot and is programmed in Python employing libraries such as *wxPython* for graphical user interface, the *Python TWAIN* module (http://twainmodule.sourceforge.net/). The software uses the *TWAIN* driver provided by the constructor to access built-in functionality for the scanner such as image type, format, and resolution. *ArchiScan* is generic and can be used with any other type of scanners, provided a twain driver is available. An additional key feature of *ArchiScan* is its utility in controlling an assembly of numerous scanners with one or more computers for scheduled image acquisitions. *ArchiScan* provides an environment for setting image acquisition parameters. Thus, it enables user-defined image feature setting with the graphical interface allowing control of most image properties relevant to phenotyping such

as image resolution, format and frequency of image capture. Following the setup of a project, image acquisition and data storage proceeds automatically.

### 2.2.1 Running and user-defined feature setting in *ArchiScan*

The acquisition interface is Windows-based software and must be installed on a computer directory on which there is sufficient space to save images. To operate *ArchiScan*, the program must be opened and a new project created from a file menu (Figure 2.18a). Details of the project must then be specified. Details may include initial scanning time, duration of scanning or project duration, period between serial scans (Figure 2.18d). Scanner properties can also be set (Figure 2.18e). Image features including, colour (black and white, greyscale or red green blue-RGB channel images), resolution (dpi), scaling (percent) and frame size (x10, inch) can be chosen. The brightness, contrast and file format (bmp, jpeg etc.) can also be set here (Figure 2.18e). Image acquisition (Figure 2.18g) can then proceed.

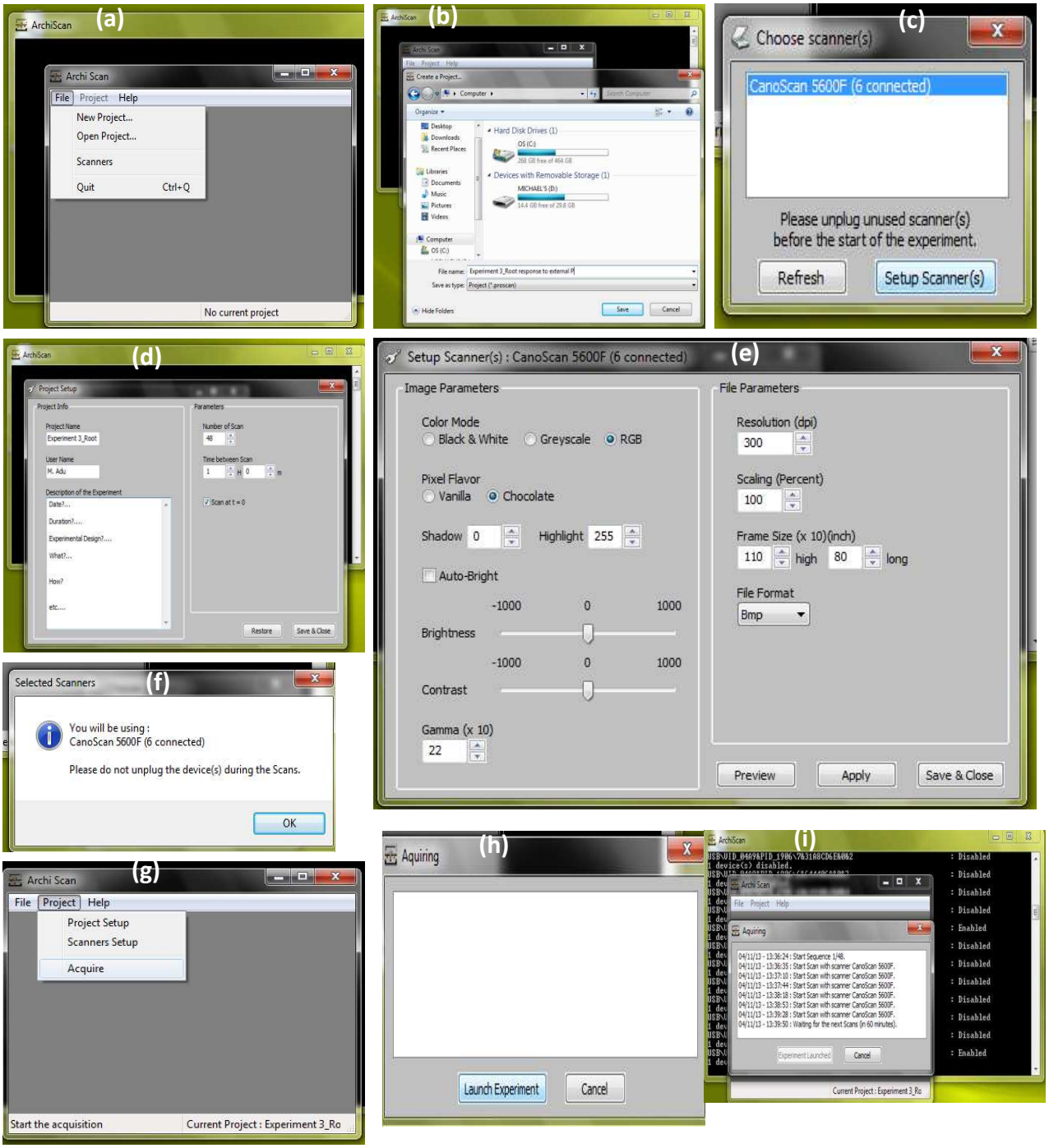


***Figure 2.18**: Screenshots of setting an a project in* ArchiScan*: dialogue boxes for (a) project creation; (b) saving new project; (c) chosen scanners; (d) specifying project details; (e) setting up scanner parameters; (f) confirming scanner that have been selected and setup; (g-h) acquiring time-lapse images; (i) progress of image acquisition during and end of project.*

### 2.2.2 Image Resolution

Wires of varying diameters and length were scanned at different scanner resolutions in order to determine if the scanners could adequately resolve the fine root structures of the seedlings. Five types of wires at three replications each were selected and their actual diameters were measured with callipers. The wires were then moulded into caricatures of roots systems and their actual length determined with thread and ruler. Subsequently, the artificial root systems were scanned at 150, 300 and 600 dpi. From the images obtained, the diameter and the total length were extracted (observed length and diameter) using *SmartRoot* (Lobet *et al.,* 2011).

The results indicated that resolution has no effect on the length of the scanned images (Figure 2.19a). However, actual and observed diameters of the wires at different resolutions seemed to vary ($p = 0.027$) and there also appear to be difference in the observed diameters of the wires at the three different resolutions ($p = 0.002$). The disparity between the actual and observed diameters could possibly be due to the overestimation of the observed diameter at 150 dpi (Figure 2. 19b). Seeing that at 300 dpi, even the wire with the least diameter (0.2 ± 0.005 mm) was accurately resolved and quantified, this resolution was chosen for my experiments.

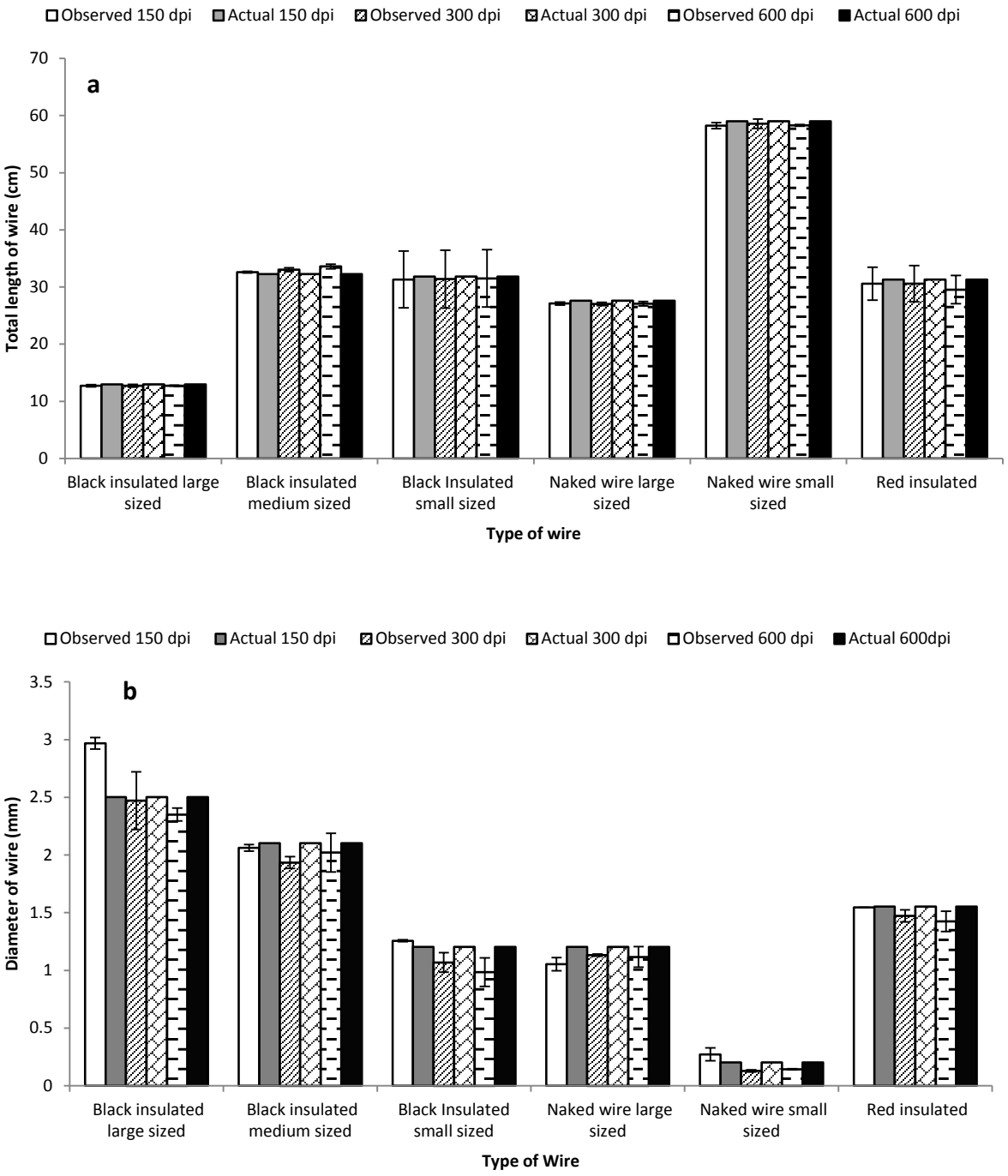


***Figure 2.19:*** *Effect of resolution on (a) total length and (b) diameter on wires.*

### *2.3 Image processing and geometric feature extraction*

Scanners generate digital images. Digital images consist of grid of pixels. Each pixel is associated with unique pixel intensity. For example, an 8-bit greyscale image can take any integer value between 0 (black) and 255 (white) and a 16-bit image can take values between

0 (black) and 65535 (white) (Megahed, 2012). Root data is not directly accessible from digital images and therefore requires analyses of the image to extract the needed information. Image analyses prior to extraction of root traits data from images are also meant to improve the image by reducing artefacts on the image. An image artefact is any feature which appears in an image which is not present in the original imaged object. Artefacts may result from improper operation or practical limitations of the imaging device, or are a consequence of natural processes or properties of the imaging environment (Hornak, 2008; Martinez-Ortiz, 2010). Artefacts can obscure, and be mistaken for a root feature and can result in false negatives and false positives, confounding the reliability of the data obtained. The following sections describe the chain of analysis procedures developed to process and extract root trait data from images.

### 2.3.1 Image enhancement

The objective of this step is to correct for noise and defect in the image. All processing routines were performed with algorithms implemented in *ImageJ* (http://rsbweb.nih.gov/ij/). Images were captured in the RGB image format. Analysis was hence based on 8 bit greyscale images obtained from the red channel of the colour images. Images were restored from two types of image imperfections namely short range and long range variations in pixel intensity.

Short range variation in pixel intensity can be attributed to interferences on the surface of the imaging device or on the rooting medium. Short range variations are introduced for example by water droplets due to condensation at the surface of scanners, or due to inhomogeneity on the surface of the germination paper. Such variations in the images were

minimised with a median filter. The median filter is considered robust average and is more suited to image edge preservation since it does not create new unrealistic pixel values when the filter straddles an edge (Marion, 1991). The filter works by finding the median value of the pixel intensity of a neighbourhood whose size is smaller than the size of objects of interest in the image. The median value is then replaced by the initial pixel intensity value. Figure 2.20 illustrates how the median filter works using a 3 x 3 square in this example. The central pixel value here 149, is not representative of the eight other neighbouring pixel values around it. The median pixel value of 120 could thus be used instead (i.e.: 115, 116, 119, **120**, 123, 126, 127, 130 and 149).

| | | | | | |
|---|---|---|---|---|---|
| | 111 | 128 | 129 | 136 | 139 | |
| | 118 | 126 | 115 | 127 | 140 | |
| | 125 | 116 | 149 | 120 | 133 | |
| | 117 | 119 | 123 | 130 | 121 | |
| | 129 | 110 | 122 | 134 | 131 | |
| | | | | | | |

***Figure 2.20****: Calculating the median value of a pixel neighbourhood.*

Long range intensity profile variations may be the variations that remain after short range intensity profile variations are removed. Long range variations are corrected by a background subtraction technique. The background subtraction algorithm starts with the plotting of intensity profile of the image background. This is followed by the calculation of the mean pixel intensity over a neighbourhood with size larger than the object of interest in the image i.e. root diameter. The mean value is then subtracted from the original value (Figure 2.21). A Gaussian filter (convolution with a Gaussian function) was subsequently

applied to ensure smooth root edges and in turn more precise estimation of the root perimeter.

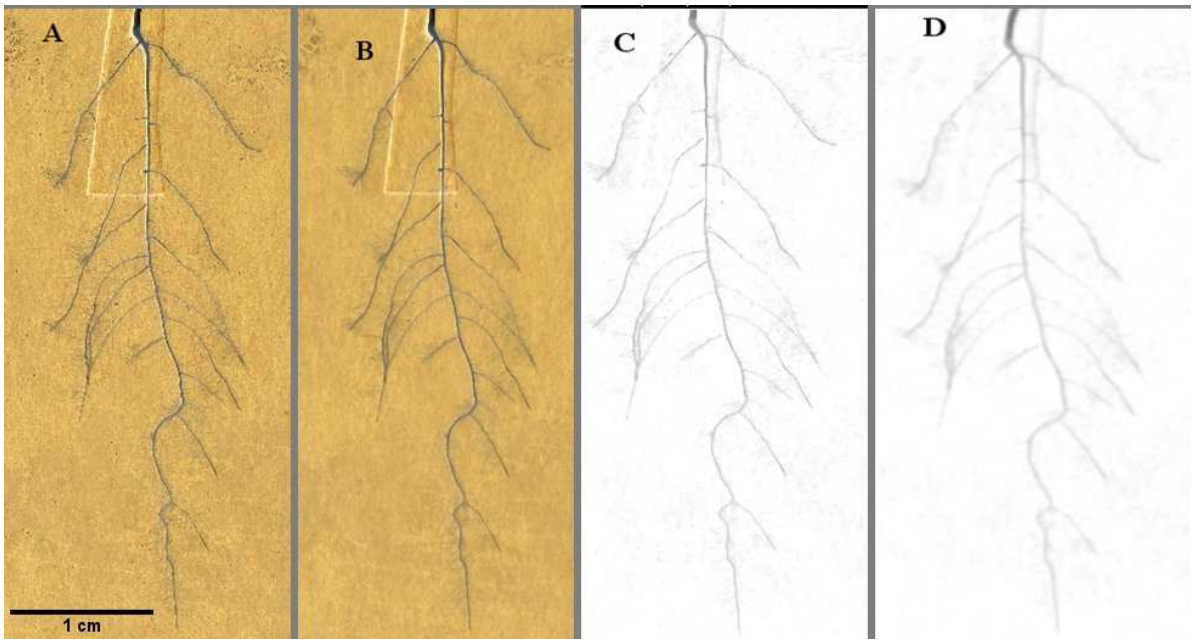


***Figure 2.21:*** *Image pre-processing routings: (A) an original RGB colour image showing the presence of short range pixel intensity variations; (B) RGB image with short range variations reduced with the median filter; (C) images with long range variations reduced through background subtraction procedures; (D) image with Gaussian blur filter applied. Images have been inverted for clarity.*

### 2.3.2 Image segmentation

Segmentation involves associating an image pixel with an object in order to decompose the image into meaningful parts with respect to a particular application (Barrow and Tenenbaum, 1978; Haralick and Shapiro, 1992). Parts of an image are distinguished or segmented by local intensity, spatial position, neighbouring pixels, or prior information about the shape characteristics of the object (Sekulska-Nalewajko and Goclawski, 2009; NIFA-NSF- USDA, 2011). Segmentation by thresholding was employed in this thesis. In order to choose the most suitable thresholding technique, we evaluated all sixteen thresholding algorithms implemented in *ImageJ* on images of 14 d root system of *Brassica rapa* seedlings.

For these images, five of the algorithms recognised and segmented the root systems satisfactorily. These were Isodata (Ridler and Calvard, 1978), Li (Li and Lee, 1993; Li and Tam, 1998), Moments (Tsai, 1985), Otsu (Otsu, 1979), and Triangle algorithms (Zack *et al.*, 1977) (Figure 2.22). Further, we measured the TRL of the segmented images as (i) 50% of the root perimeter (one pixel-wide edge around the root image) from the products of the five satisfactory threshold routines and (ii) length of the topological skeleton of the images obtained using *ImageJ*. Topological skeleton of the root system is a pixel-wide version of the root system obtained from the iterative removal of pixels from the edges of the root system in a binary image (Zhang and Suen, 1984). In order to compare the ensuing data with some kind of a standard, TRL data were also extracted from the same images using root analyses software, called *SmartRoot* (Lobet *et al.*, 2011).

Results obtained from the five threshold algorithms were generally comparable, but they underestimated the TRL when compared with data obtained from the *SmartRoot* (Figure 2.23). Some features of the root system are possibly lost following segmentation. On my data, we generally found that the Moment-preserving threshold algorithm (Tsai, 1985), performed consistently well and so was employed in subsequent analyses. The Moment algorithms use the grey level image histogram to determine an optimal threshold in the image. The optimal threshold is the one that best preserves moment of the thresholded image. A Gaussian blur filter that uses convolution with a Gaussian function was then employed to smooth edges of the ensuing root image.

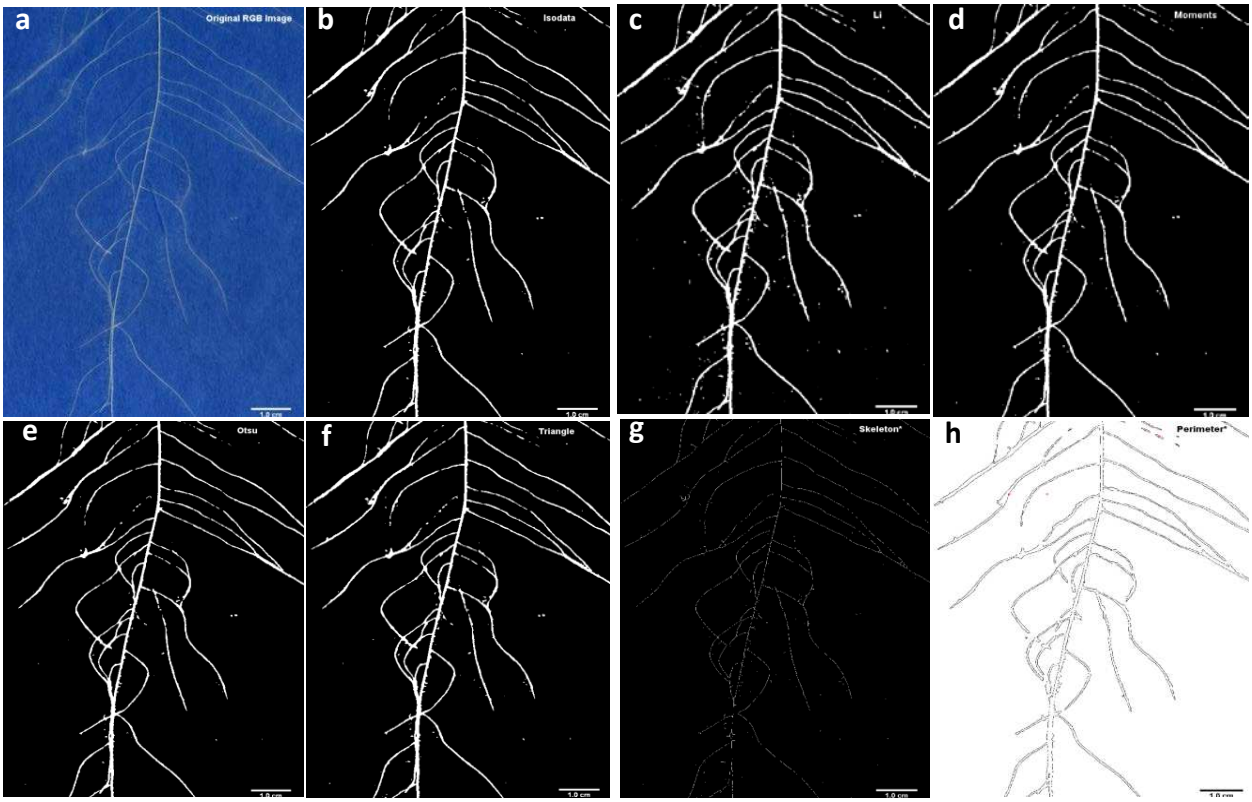


***Figure 2.22:*** *RGB image of a root system segmented with* ImageJ *automated threshold-based algorithms. Original RGB image (a) segmented with Isodata (b), Li (c), Moment (d), Otsu (e), Triangle algorithms (f); Pixel-wide root skeleton (g) and pixel-wide boundary perimeter of root system (h). Root skeleton and boundary perimeter were obtained from triangle threshold algorithm.*

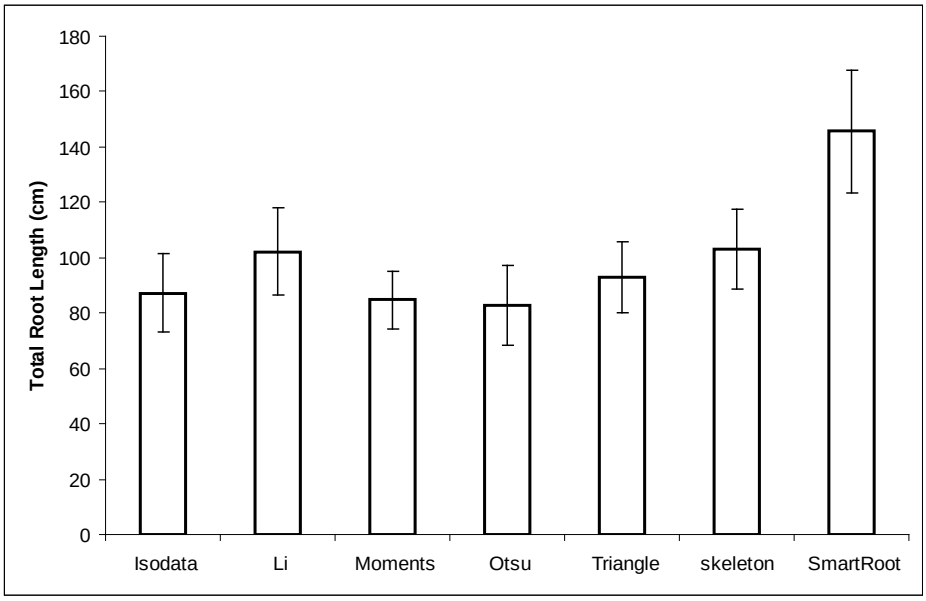


***Figure 2.23:*** *Total root length of 14 d* Brassica rapa *seedlings computed from root images processed with different automated threshold-based algorithms in* ImageJ *and* SmartRoot *root analysing software (n=10).*

### 2.3.3 Extraction of geometrical features

*ImageJ* was employed as the first procedure to extract features of the root geometry from the processed images. Root traits including root lengths, elongation rate, root diameter and LR angle were extracted from the images. For example, daily root emergence and growth were measured by tracing the new growth increments on the images. Here, time-lapse root images were imported into *ImageJ* and point selections were placed manually on the tip of each root axis in successive images using mouse clicks. Root tip displacement (Δ*u*) was recorded and calculated using:

$$\Delta u = u_f - u_o \qquad (\mathbf{2.4})$$

where $u_f$ = original *x* co-ordinate and $u_o$ = *x* co-ordinate of the point selection in next image in the sequence. Vertical patch (Δ*v*) displacement was calculated as:

$$\Delta v = v_f - v_o \qquad (\mathbf{2.5})$$

where $v_f$ = original *y* co-ordinate and $v_o$ = *y* co-ordinate of point selection in the next image of the sequence.

The daily root elongation rate (cm $d^{-1}$) of each root axis was calculated using movement in both *x* and *y* co-ordinates as:

$$y = \frac{\sqrt{(\Delta u)^2 + (\Delta v)^2}}{px} \qquad (\mathbf{2.6})$$

where *y* = growth rate (cm $d^{-1}$), *px* = scale factor calibration value (pixel/cm). Although the technique yielded highly reproducible data, it was too slow to be employed in extracting a high throughput data.

#### *2.3.3.1 Extraction of root features using* SmartRoot *software*

Second procedure employed in extracting root traits is an *ImageJ* plugin called *SmartRoot* (Lobet *et al.*, 2011). *SmartRoot* is a root image analysis tool which tracks root objects and

sends measurement to a standardised access database. *SmartRoot* has an underlying wireframe model of connecting image vertices with lines. *SmartRoot* describes root images by a vector representation of the root system using coordinates of connected nodes along various axes of the root system (Figure 2.24). The software incorporates an algorithm that determines the midline of the root near a user selected seed position and proceeds with stepwise construction of segmented line to the root tip by approximating the root midline. The list of specific attributes captured in *SmartRoot* root descriptions includes: a unique root axis identification number, the branching order, *x* and *y* co-ordinates of root axis, the distance of LR position in relation to the PR's base and tip, and the root length and diameter at each observation date. Thus, *SmartRoot* has the capability to obtain static root traits including topological description of the root system.

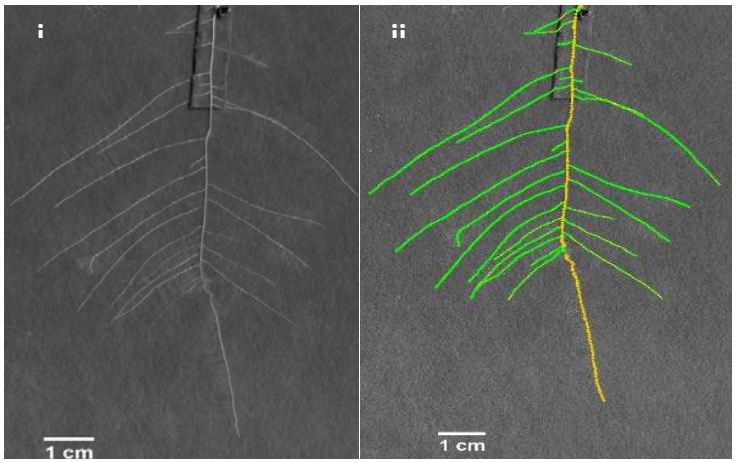


***Figure 2.24****: Analysis of RSA by* SmartRoot *Software (i) original grey-scale image; (ii) image traced with* SmartRoot *showing primary root (yellow) and lateral roots (green)*

*SmartRoot* can also be used to analyse developmental processes of complex RSA from images across time-series (Lobet *et al.,* 2011) but the procedure could be slow by repeating the whole process for each image. In this thesis, *SmartRoot* was used to extract root growth information by tracing all root axes (primary and lateral roots) on the last image. The initial tracing was then used as the starting point for the tracing of the preceding image which is

obtained by removing the portion of roots that have been created between the penultimate and last images. The same process was repeated until the root system from of DAS 1 is traced.

#### *2.3.3.2* **ImageJ** *macro for extracting dynamic root features*

Dynamic root traits were extracted from successive images using custom routines developed in *ImageJ* (Figure 2.25). Particle analyses extracts non connected regions of the image on which it is possible to calculate shape descriptors. An example of shape descriptors is the circularity descriptor (*circ*) which gives a measure of similarity between a given shape and a perfect circle. Circularity ranges between 0-1 and is a dimensionless shape descriptor which is a function of the object perimeter and the area (*circ* = perimeter$^2$/4π. *area*) (Bottema, 2000).

Following image enhancement routines, the macro converts the series of time-lapsed images to 8-bit greyscale formats after which the images are restored and segmented using the moment-preserving threshold algorithm of (Tsai, 1985). Next, the stack of images is converted to mask where all slices are converted to black and white images and then threshold levels re-calculated for each individual slice. Subsequently, an edge-tracing algorithm implemented in the macro which utilises a user-defined size and shape descriptors are employed to define the boundary (perimeter) of root tissues and removes objects external to the root system from the image. Size of 0.2 and circularity of 0.00-0.2 was identified as the best threshold to discriminate non-root objects from of root tissues.

The macro further implements an algorithms to estimate global traits of the root system (total root length, total root cross-sectional area, total root perimeter, convex hull of the root system, root length density) on 2D images. Convex hulls are the smallest polygon whose vertices are all points in the root image (Figure 2.25). The convex hull macro incorporated a loop in its script capable of determining the local maxima in all root system images in the stack from slice one to the final slice. Based on the identified local maxima, a band (convex hull) was then wrapped tightly around the maxima points that define the rectangular selection that is the same size as the root system images in each slice ( Figure 2.25c).

**a**

```
n = nSlices;
run("Duplicate...", "title=[Sample Data-1] duplicate range=1-" + (n+1) );
run("8-bit");
run("Median...", "radius=2 stack");
run("Subtract Background...", "rolling=50 stack");
run("Gaussian Blur...", "sigma=2 stack");
//run("Threshold...");
setAutoThreshold("Moments dark");
run("Convert to Mask", " black");
run("Analyze Particles...", "size=0.2-Infinity circularity=0.00-0.2 show=Outlines display add stack");
```

**b**

```
n = nSlices;
run("Duplicate...", "title=[Sample Data-1] duplicate range=1-" + (n+1) );
run("8-bit");
//run("Median...", "radius=3 stack");
//run("Subtract Background...", "rolling=40 stack");
run("Gaussian Blur...", "sigma=1 stack");
setAutoThreshold("MaxEntropy dark");

run("Convert to Mask", " black");
run("Gaussian Blur...", "sigma=3 stack");
run("ROI Manager...");

for (i=0; i<n; i++)
{
        setSlice(i+1);
        run("Find Maxima...", "noise=0 output=[Point Selection];// exclude");
        run("Convex Hull");
        roiManager("Add");
        run("Select None");
        //run("Clear");
}
roiManager("Measure");
```

**c**

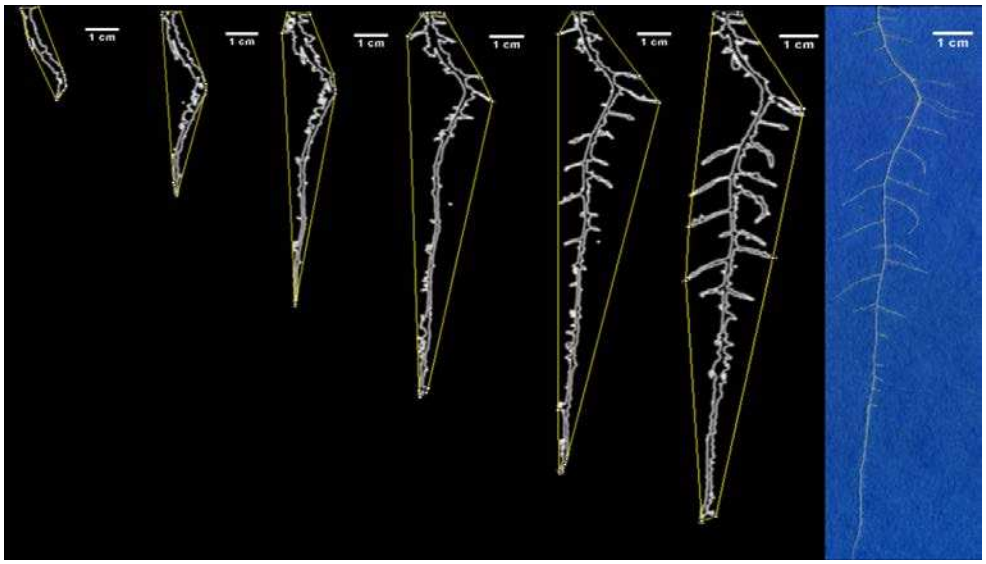


***Figure 2.25:*** *(a)* ImageJ *macro script for particle analysis (b) macro script for fitting convex hull on root system perimeter; (c) resultant analyses of root system by the* ImageJ *macros showing time-lapse images of RSA of 2, 4, 6, 8, 10, 12 DAS* B. rapa *seedling. The RGB image of the root system at 14 DAS is shown at the end of figure C.*

#### *2.3.3.3 Feature extraction of data from rhizobox using* WinRhizo

To verify that most roots were visible on the surface of rhizobox, root systems from experiments performed in soil-filled rhizoboxes were also measured with the image analysis system *WinRhizo* Version 2012b (www.regentinstruments.com). At the end of experiments, shoot parts were removed and the soil-root sample was suspended in water. Roots were washed from the soil by hand and brush and cautiously taken out by tweezers. Root samples were transferred into large clean petri dishes (150 mm) with no markings or scratches on it. Petri dishes were half-filled with water, ensuring that root axes do not overlap and are separate from each other as much as possible. Each washed root sample was scanned using an Epson Expression 10000 XL scanner. Morphological features including length, area, volume and diameters were then measured with the *WinRhizo*.

#### *2.3.3.4 Measurement of other seedling parameters*

##### 2.3.3.4.1 Shoot and root biomass

Depending on experimental objective, experiments lasted 10 to 21 days after sowing on scanners. In addition to the extraction of root trait data as described previously, other measurements obtained in this thesis included shoot biomass and phosphorus concentration is plant tissues. Results of these measurements will be presented in the subsequent chapters but a brief description of the methodology used is here described. At the end of experiments, shoot were severed from roots at the root-shoot junction. The SFW and RFW were recorded immediately. Shoot and root plant samples were then oven dried at 60 °C for 72 hours and SDW and RDW determined.

#### 2.3.3.4.2 Phosphorus concentration in plant tissues

Total shoot-P and root-P concentrations (Shoot [P] and Root [P]) were determined by the MG phosphate assay method (Van Veldhoven and Mannaerts, 1987). Firstly, whole, oven dried and weighed plant materials were digested in MARS® microwave sample digester (CEM Corporation, Matthews, NC, USA). Two samples of standards made up of 30 mg 1573a tomato leaves, (National Institute of Standards and Technology (NIST), Gaithersburg, MD, USA) were also put into digester tubes to go through the entire digestion process in order to test the quality of the digestion. There were two round of digestion and for the first round, 3 ml of concentrated nitric acid (15 M $HNO_3$) (Aristar, VWR International Ltd., Poole, UK) was added to each sample and left to digest in a fume hood for approximately 15 minutes. Nitric acid was included in two tubes as a blank sample to take through the entire extraction procedure. The samples were digested using the STD-NO3 40 Digest programme (Table 2.4). The samples were then heated in steps to 180°C and held at same temperature for 20 min to allow the complete digestion of the material.

***Table 2.4:*** *STD-NO3 Digest programme for microwave acid digestion of plant materials*

| Ramp Time (min) | Temperature (°C) | Hold Time (min) |
|---|---|---|
| 3 | 100 | 2 |
| 1 | 120 | 1 |
| 3 | 160 | 2 |
| 2 | 180 | 20 |

Samples were then allowed to cool for 20 min and digester tubes were carefully opened in a fume hood to allow nitrogen oxide fumes to vent for about 20 min. For the second round of digestion, 1 ml hydrogen peroxide solution (30% $H_2O_2$, Aristar, VWR International Ltd., Poole, UK) was added to each sample and the samples left to digest in a fume hood for 15 min. The samples were digested again in the microwave using the STD-NO3 Digest

programme as described above (Table 2.4). Digested samples were cooled in fume hood and were subsequently topped up to a final volume of 50 ml using Milli-Q water (Millipore (U.K.) Ltd., Watford, UK).

A solution of 2 µg $ml^{-1}$ P was used for calibration by dissolving 0.8789 g $KH_2PO_4$ in 1 L ultrapure water and diluted 100 times. Standard curve of 0, 5, 10, 15, 20, 30, 40, 50, 60 and 80 µL of P standard in one row of a 96 well plate was prepared, adding 10 µL of blank to each standard well. Ten microliters of digest was pipetted into remaining wells on the plate and each well made up to 200 µL with Milli-Q water (Millipore (U.K.) Ltd., Watford, UK). Hundred microliters of MG solution was added and left for 20 minutes for colour to develop after which absorbance was read at 595 nm using $EL_x$ 800 Universal microplate reader (BioTek Instruments Inc. USA). Table 2.5 shows an example dilution of the standard solution included in each run and Figure 2.26 shows an example of a calibration curve obtained. The P concentration was calibrated to the tomato leaves standard included in the extraction process. Thus, the tomato leaf standard provided the analytical error for each run and its actual readings were used to determine the decrease or increase in P concentrations in each step of the run in order to correct for it.

***Table 2.5:*** *An example of dilution for the preparation of standard curve*

| № | Volume (µl) | | | |
|---|---|---|---|---|
| | Standard | Blank | Milli-Q water | Malachite green |
| 1 | 0 | 10 | 190 | 100 |
| 2 | 5 | 10 | 185 | 100 |
| 3 | 10 | 10 | 180 | 100 |
| 4 | 15 | 10 | 175 | 100 |
| 5 | 20 | 10 | 170 | 100 |
| 6 | 30 | 10 | 160 | 100 |
| 7 | 40 | 10 | 150 | 100 |
| 8 | 50 | 10 | 140 | 100 |
| 9 | 60 | 10 | 130 | 100 |
| 10 | 80 | 10 | 110 | 100 |

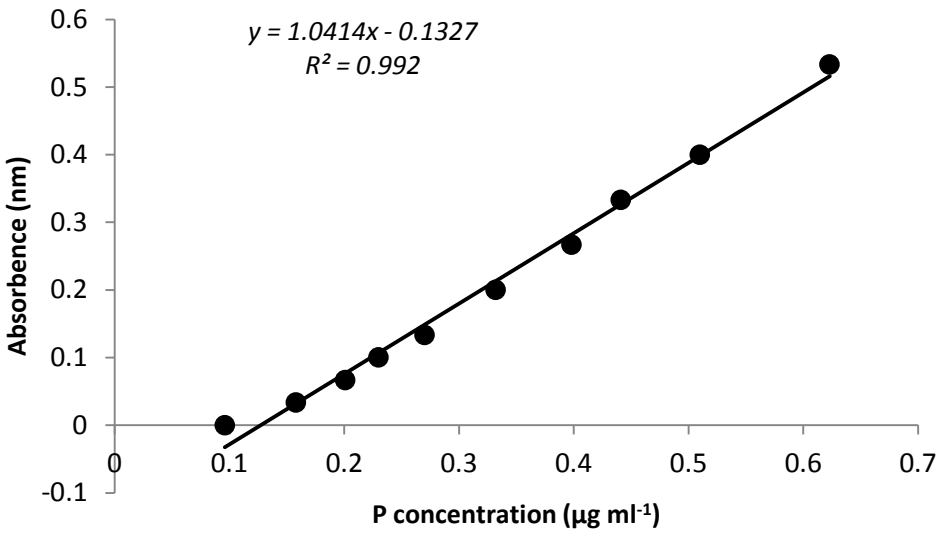


***Figure 2.26:*** *Calibration curve for P concentration: Absorbance values are plotted against P concentrations [µg ml$^{-1}$]*

#### 2.3.3.4.3 Phosphorus concentration in seeds and paper rooting medium

Concentrations of P in the paper rooting medium and that in the seeds of the parents of the BraIRRI population were determined using ICP-MS instrument (ICP-MS, ELAN DRC-e, PerkinElmerSCIEX, Massachusetts, USA, www.perkinelmer.com/). In PerkinElmer's technical note, an explanation of how ICP-MS is performed has been provided. Briefly, samples are first introduced into ICP-MS instrument via nebulizer and spray chamber which also convert the samples into minute droplets. An argon plasma serving as an ion source of the ICP-MS ionises the droplets and directs them into a mass filtering device known as quadrupole mass spectrometer. The mass spectrometer rapidly scans the mass range of the ions and separates them based on mass-to-charge ratio allowing only one ratio to exit the spectrometer. Ions that exit the spectrometer then strike a dynode of an electron multiplier, serving as a detector. Electrons released from the impact of the strike are amplified into a

measureable pulse. Software, ELAN (PerkinElmerSCIEX, Massachusetts, USA), converts the counts for the ions to ppm or ppb values according to standard curves. Here, digested paper samples or seed and nitric acid blanks were placed in the ICP-MS. The volume of the digest and DW of the paper or seeds were used to calculate the amount of P in mg $g^{-1}$ DW.

## *2.4 Discussion*

Roots are hidden in the soil and do not lend itself easily to empirical methods to quantitatively describe its growth and architecture. Methods of phenotyping root systems do not currently have the same degree of sophistication or throughput as genomes or processes more proximate to the genome and frequently limit functional genomic studies. Efforts to understand interactions of roots and their environments are frequently constrained by increased root plasticity, high impacts of ontogenetic variations as well as strong influence of plants' internal status (carbon and minerals) on root growth and architecture (Oborny, 2004). There is therefore the tendency of instantaneous variables such as root length to offer poor descriptions of the root system. Complex integrated traits such as root growth dynamics must therefore be measured and this will require improvements in the phenotyping process. Reproducible, methodological and technical alternatives which are also simple, economical and widely accessible must be sought.

### 2.4.1 High resolution low cost scanner-based 2-D phenotyping system

Work in this thesis shows that a low cost imaging facility enables rapid acquisition of high resolution root system images. The design comprises a simple Windows-based interface for automatic 2D image capture of root system growth which also permits the managements of several scanners at any point in time. The system has no or limited engineering requirements and could potentially be scaled-up to increase the throughput. In this thesis,

up to 72 plants can be phenotyped simultaneously for up to 21 days after sowing. The scanner-based phenotyping described here system combines hydrophilic germination paper and nutrient solution to mimic soil conditions. By design, it has the capacity to measure static and global root characteristics. It also provides a simple means for continuous observations of seedling root development enabling detailed observations of dynamics of root growth and development. Thus, root development can be monitored at the macroscopic or microscopic level at intervals ranging from minutes, days or weeks (Futsaether and Oxaal, 2002). The system can also be adapted to observe root growth in soil and could be adapted for the quantification of root growth dynamics in response to various stimuli such as the effects of different physical environments and nutrient supply.

The interaction of quantity and quality of light could affect several plant morphological parameters including root system growth and architecture. Cope and Bugbee (2013) for example have reported that light from white LEDs increased stem elongation and leaf expansion and initial plant growth in radish, soybean, and wheat. In this thesis, scanning did not affect growth of plants (Figure 2.6). Cope and Bugbee (2013), have suggested that normal plant development under cool white LEDs is attributed to high percentage (25%) of blue light (400 to 500 nm) contained in white LEDs. Images captured by the system could however be susceptible to small amounts of artefacts but it is possible to extract the data with simple image analyses routines. Macros written in *ImageJ* are able to automatically processes and extract root features such as root perimeter and convex hull area from sequential images. In a normal soil environment, segmentation of roots from their background is an onerous task and usually limits throughput and number of samples (Basu and Pal, 2012). To a large extent, images captured here have uniform background and

facilitate the segmentation process, accelerating the analyses of RSA traits. Fine root features such as root hairs are visible (Figure 2.27) and show potential for fast analysis of their morphology in the future.

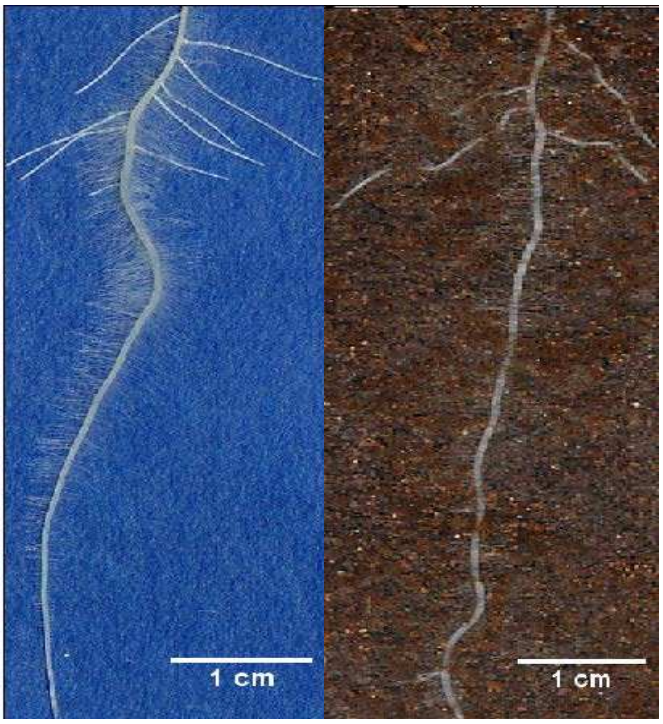


***Figure 2.27:*** *Example of images on the two selected root growth substrates used in this thesis (blue seed germination paper and soil in rhizoboxes) showing highly resolved fine root features (root hairs and first order laterals) on 6 d after sowing* Brassica rapa *(R500) seedlings.*

### 2.4.2 Effect of rooting media on root topological indices

It is important that information is given about how closely data produced in controlled environments relates to that produced in soil or under field conditions. Dubrovsky and Forde, (2012) have stressed the importance of adequately characterising the growth conditions, especially the rooting medium employed in the quantification processes of root features. This would give confidence that any manifested phenotypes are the result of the imposed treatments rather than environmental factors, such as growth medium,

temperature, light, and aeration. It would also facilitate inferences and extrapolating of data across both spatial and temporal scales.

As part of developing the scanner-based root phenotyping system, different paper cultures and soil growth media were evaluated to determine their suitability. This also enabled the response of the early phase of root growth in brassica to environmental factors, in this case, the rooting media, to be examined. The results indicated that simple indicators such as topological indices of root systems can be used to characterise variations in seedling root traits. It is worth noting that the present results are based on growth media of different physio-chemical properties and may thus have varied water and nutrient retention properties.

When topological index (TI) was plotted for the two *B. rapa* genotypes, strong linear relationships were established. The TI values tended to be comparable and higher for both genotypes. Mean TI values of 0.93, 0.95, 1.0, and 1.0 for IMB211 grown on construction, blue, brown and soil media respectively indicated that root media had little effect on the typical herringbone pattern of 10 d after sowing *B. rapa* seedlings. Similarly, mean TI values of 0.82, 1.0, 0.97 and 0.99 for the R500 genotype grown on construction, blue, brown and soil media for 10 days respectively in general suggest little alteration in the inherent root topology by the rooting media at early stages of the plants' growth. *Brassica* cultivars grown in rhizoboxes showed similar TI values but the TI values increased when cultivars were constrained with limited external P supply (Akhtar *et al.*, 2009).

Relatively, lower TI values were however recorded on the construction paper. Given that the construction paper was not originally manufactured for growing plants, it is not entirely surprising that the branching pattern of the root systems grown on it changed from a herringbone pattern to random branching. The responses observed here may be explained by root systems reacting to inadequate water or perhaps increased innate mineral originating from the dye or the raw material of production. The construction paper was lighter and less hydrophilic and the plants may have been subjected to drought. Moreover, the significant genotype x root medium type interactive effects for TI observed here may be explained exclusively by difference in the extent of response by the two genotypes. It is seen that IMB211, the genotype with smaller root system, was relatively less responsive to a change in rooting medium than R500 genotype with longer root length and highly branched. The results show that *Brassica* lines x root medium interactions are likely to occur more frequently in highly branched inbred lines with older and therefore most probably bigger root systems (Crush *et al.*, 2005). In these circumstances choice of root medium become more critical especially in empirical studies targeting the phenotypic selection of exploratory root systems characterised by increased lateral root emergence and growth.

### 2.4.3 Effect of rooting media on root growth

Growth media effects were observed on primary and total root length and their corresponding relative extension rates. On all rooting media, rates of extension for both the primary root and total root system begun to approach constant following initial higher extension rates. These experiments lasted only 10 DAS but the constant root growth in the later stages irrespective of the rooting medium suggests that the rate of root growth may be under stable internal control, and perhaps large responses to variations in the environment

occur only during the early stages of growth. This confirms the suggestion that the responsiveness of plants to variations of the environment decreases with the age of the plant (May *et al.*, 1965; May *et al.*, 1967). Roots systems analysed by May *et al.,* (1965; 1967) were however from monocots.

As expected, lateral root numbers and lengths increased with time to a point beyond which root growth was suppressed. There were consistent patterns of root number and length increase in the *Brassica rapa* seedlings. This trend has long been established in many crops including barley (May *et al.*, 1965; Rahman *et al.*, 1975) and wheat (Tennant, 1975). An interesting feature however is the observation here that numbers and RMR of 1$^{st}$ order laterals was altered by the nature of the medium in which the roots were growing and that media effect on RMR is evident between 2 and 5 DAS for R500 and between 2 and 8 DAS for IMB211. Irrespective of the genotype, the brown and construction paper media induced the greatest number of laterals and the mechanism operated within 8 days following germination. As indicated earlier, these paper types were relatively lighter in weight and may so have suboptimal capillarity and water retention capacities. Nutrition and water retention status of these media types could therefore be implicated in the increased lateral rooting (Malamy and Ryan, 2001).

When lateral root number was however compared with total lateral length, it was seen that during early growth (up to 10 days after germination), the number of 1$^{st}$ order lateral roots was higher than the total length of lateral roots expressed in cm on the blue paper culture and in the soil but not on the construction and brown paper cultures. This is consistent with Wahbi and Gregory (1995) and May *et al.* (1965) for barley seedlings where there was rapid

increase in the length of laterals in comparison with number such that mean length increased. It is thus possible that during the early growth of brassica roots, there is increased emergence of 1$^{st}$ order LRs which extends relatively faster than the production of new LRs of the same order so that relative rates of extension decreased with time but this trend is subject to suitable environmental conditions. Further, differences in MER with respect to time give evidence of changing rate of cell division in LR meristems resulting in MER that at first, increases and then declines with time. This observation suggests that assigning a single value of elongation rate to LRs of different ages may be impractical.

In general, the differences between roots grown in soil and on blue paper culture were relatively small in general. Consequently, it would be advantageous to use the blue paper culture for screening brassica seedlings for RSA and root growth traits especially in my case when the physical effect of a solid root medium on roots was important.

### *2.5 Summary*

- Two-dimensional low cost scanners coupled with windows-based image acquisition interphase (*ArchiScan*) allows root growth phenotyping of the same plant for several days.
- *ArchiScan* allows the management of multiple scanners concurrently, increasing the throughput of plants that can be screened at any time. We have developed a system employing 24 scanners which can screen up to 72 individual of plants at any time.
- Scanners are of high resolution enabling finer root features to be adequately resolved.
- Scanner resolution of 300 dpi adequately resolved fine root features of seedlings.

- White light emitting diode light of the flatbed scanners had no effects on root system features of *Brassica rapa* seedlings.
- There were growth media effects on topological indices (TI), attributable to roots branching more on construction paper rooting medium with possible suboptimal water retention properties. Mean root topological index of 0.82 - 0.93 respectively recorded for R500 and IMB211 on the construction paper medium indicated that root growth media could have effect on the herringbone pattern of brassica roots in their early stage of growth.
- First order lateral root numbers and lengths followed consistent patterns of increase on all root medium treatments, recording their highest rates of relative increase in length and number immediately after sowing. Whilst root extension rates and multiplication of lateral roots were responsive to rooting medium, both fell and approached constant with time. Mean extension rates of lateral roots vary with time and would be more rewarding if root system analyses procedures could account for this time-dependent variability rather than assigning single extension rate values to lateral roots of different ages.
- Differences between roots grown in soil and on Anchor blue germination blotter were relatively small suggesting that the blue blotter is ideal for phenotyping *Brassica rapa* seedlings for RSA traits and root growth when the physical effects of a growth medium on root system is essential.

## CHAPTER 3 : PHENOTYPIC VARIABILITY WITHIN A GENOTYPE

### 3.0 Introduction

Genetic improvement of rooting traits in crop species requires knowledge of intra-species variability in significant root parameters and its genetic control (O'Toole and Bland, 1987). For example, root diameter is highly variable within a root system and this in turn influence root growth rate (Lecompte *et al.*, 2005; Pagès, 1995; Thaler and Pagès, 1996). In *Brassica*, LRs are secondary roots that emerge from the primary root (PR) (Hammond *et al.*, 2009). Lateral roots (LRs) emerge consecutively and variation exists in the growth rate of successive LRs related to anatomical variations or root diameter (Pagès, 1995; Zhang *et al.*, 2003). Understanding this variation is important because whilst roots of different orders may be implicated in differences in acquisition of soil-based-resources, roots segments of different ages may also vary in their acquisition capacity and physiological activity (Zhang *et al.*, 2003).

Unfortunately, characterising the variability of root traits is difficult. Root system architectural traits and growth vary in time and in space. For example, root traits vary in response to soil nutrients (Gaudin *et al.*, 2011), soil water (Ober and Sharp, 2007) and in response to stresses due to temporal variation in soil physical conditions (Gregory, 2006). Root growth also varies spatially due to changes in soil physical and / or chemical properties (Gregory, 2006) such as soil compaction (Montagu *et al.*, 2001) and also due to physiological and developmental processes or variation in tissue differentiation associated with root segments (Hodge *et al.*, 2009). Modelling approaches can be used to simplify the complexity of root system descriptions using processes and dynamic parameters instead of using a multitude of variables to describe a system that is inherently dynamic.

The primary aim of this chapter was to estimate phenotypic variation for morphological root traits for a single genotype of *Brassica rapa*. The second aim was to evaluate the ability of a mechanistic model to represent the complexity of this root system. My specific objectives were (i) to quantify the coefficients of variation within a single *B. rapa* genotype and determine the required number of replications needed to detect significant differences between root trait means; (ii) to estimate the variation in the growth of PR and LRs of differing ages and provide a general descriptive overview of the root growth patterns of different root axes of a single genotype; (iii) to apply a density-based model to assess if a RSA can be represented accurately using a limited number of morphological variables.

## *3.1 Materials and methods*

Seedlings of a *Brassica rapa* genotype R-o-18 were grown on seed germination paper (Section 2.1.6.1) and were imaged with flatbed scanners (Sections 2.1.2; 2.2.1) in eight independent experiments (runs) under the same environmental conditions as described in Chapter 2 (Section 2.1.1). Two experiments employed 16 scanners each with the remaining using 8 scanners per experiment. There were two seedlings per scanner for each run, and a total of 160 individual plants. Seedlings were grown for 14 days after germination and geometric data were extracted from images using *SmartRoot* (Lobet *et al.*, 2011) (Section 2.3.3.1).

### 3.1.1 Data Analyses

Each run was treated as an independent population for analysis. Data were entered into GenStat (GenStat Release 14.1, VSN International, Oxford, UK) and descriptive statistics was performed on each population. For each population, we obtained an estimate of the standard deviation and the mean (± standard error) and used these estimates to determine

the coefficient of variation (CV). The CV was estimated as the percentage of the ratio of the standard deviation to the mean.

### 3.1.2 Determination of required sample size (replication)

We estimated the number of replicates required to detect significant differences in measured traits in two-sided 95% confidence interval (CI) t-test. The following equation was applied:

$$N = \frac{4\sigma^2(z_{crit})^2}{D^2} \qquad (\mathbf{3.1})$$

*N* is the number of replicates, $\sigma$ is the measured standard deviation, $Z_{crit}$ is the standard normal deviate corresponding to selected significance level and CI, and *D* is the total width of the selected CI. Calculations were initially based on a difference of the means of 50% and with a 95% CI. It must be noted that this is a test with two virtual genotypes or treatments based on the variability of root traits measured from a single genotype. Equation 3.1 therefore does not depend on statistical power because this concept only applies to statistical comparisons (Eng, 2003).

### 3.1.3 Estimation of variance components and correlation between traits

Variances in the static root traits were then analysed using a linear random effect model with run and scanner considered as random factors:

$$y_{ij} = m + a_i + b_j + \epsilon_{ij} \qquad (\mathbf{3.2})$$

$$i \in \{1, \dots, n\}, j \in \{1, \dots, r\},$$

$$a_i \sim N(0, \sigma_a^2), b_j \sim N(0, \sigma_b^2), \epsilon_{ij,} \sim N(0, \sigma^2\ ).$$

where $y_{ij}$ represents the root trait from the $i^{th}$ run or population from the $j^{th}$ scanner number with *m* denoting the overall mean trait value; $a_i$ is the effect of the run, $b_j$ is the

effect of scanner and $\epsilon_{ij}$ is the residual error; *n = 8* is the number of runs; *r = 16* is the total number of scanners used during the experiments. Phenotypic correlations between pairs of traits and significance of correlation pairs were respectively estimated using the functions cor() and cor.test() in *R* (R Core Team, 2008). These functions allow the computation of correlation and testing for association between paired traits, using either Pearson's product moment correlation coefficient, the Kendall's *tau* or the Spearman's *rho* (http://stat.ethz.ch/R-manual/). Here, the Pearson's product moment correlation coefficient was used and significant correlations with $0.2 \leq r^2 \leq 0.5$, $0.5 < r^2 \leq 0.8$, $0.8 < r^2$, were defined as weak, moderate and strong, respectively.

### 3.1.4 Variability in root growth

The root elongation rates (cm $d^{-1}$) of the PR and first-order LRs were obtained from time-lapse root images. Lengths and elongation rate of LRs is dependent on the time of emergence from the pericycle of the PR. Variability in LR root growth was analysed by taking into account the time of emergence of individual LRs on the PR. Lateral root elongation rate were calculated separately for laterals that emerged 2, 3, 4 and 5 d after sowing hereafter referred to as 1st, 2nd, 3rd and 4th laterals, respectively. Growth of PR was analysed with mixed effects linear models with days after sowing (DAS) as covariate (Equation 3.3a):

$$y_i = b_i + \beta_1 + \beta_2 DAS_i + \epsilon_i, \qquad (\mathbf{3.3a})$$
$$i = \{1, \ldots, 9\},$$
$$b_i \sim N(0, \sigma_b^2), \epsilon_i \sim N(0, \sigma^2).$$

where $y_i$ is the growth rate of the PR on the $i^{th}$ DAS, $b_i$ is the random effects on the intercept and $\beta_1$, *and* $\beta_2$ are the fixed effect parameters of the linear function. We restricted the analyses of PRs to 9 DAS because PRs usually reached the bottom of the scanner at 10 days after sowing. Similarly, growth of LRs were analysed with mixed effects linear models with

DAS as covariate but included a quadratic function and the time of LR emergence as fixed effects (Equation 3.3b).

$$y_{ij} = b_i + \beta_1 + \beta_2 DAS_j + \beta_3 DAS_j^2 + \epsilon_{ij}, \qquad \textbf{(3.3b)}$$
$$i = \{1, \dots, 4\}, j = \{1, \dots, 9\},$$
$$b_i \sim N(0, \sigma_b^2), \quad \epsilon_{ij} \sim N(0, \sigma^2).$$

where $y_{ij}$ is the LR growth rate for type of root $i$ on the $j^{th}$ day after sowing (time of LR emergence), $\beta_1$ *(general mean or intercept),* $\beta_2$ and $\beta_3$ are the fixed effect parameters for the quadratic function and $b_i$ is the random effects on the intercept of the quadratic function. Data for primary and lateral root growth were normalised by square root prior to analyses and analyses were done in *R* (R Core Team, 2008). Log-likelihood (logLik) and Akaike and Bayesain information criteria (AIC and BIC) were used to select best performing model. The AIC and BIC are measures of the relative quality of a statistical model. The AIC is defined as -2 × Log-likelihood + 2 × df, where df is the number of parameters in the model. The BIC is defined as -2 × Log-likelihood + 2 × df × log (N), where N is the total number of observations (Guan *et al.*, 2006; Posada and Buckley, 2004). A model with higher value of the logLik and smaller AIC and BIC indicates the best fit model. Models quality was also assessed visually using quantile-quantile (Q-Q) plots to check for normality and residual plots to check that the variance of residuals was constant (Pinheiro and Bates, 2000).

### 3.1.5 Density-based models of root growth dynamics

In this section, a mechanistic approach was used to model root systems so that the dynamics of root development can be represented as a set of process-based parameters. The modelling approach is based on the density representation of root systems proposed by (Dupuy *et al.*, 2005; Dupuy *et al.*, 2010a; Dupuy *et al.*, 2010b), and modified by Kalogiros *et al* (unpublished). The model is calibrated on datasets presented earlier in this chapter using

a method developed by Kalogiros et al (unpublished). A brief background and basic definitions of generalised density functions are presented here.

#### *3.1.5.1 Definitions of generalised density functions for density-based RSA modelling*

In density-based models, root growth is represented through the trajectory of root apical meristems. This includes properties of both the geometry and topology of the root system. Three types of root density distribution functions suitably describe the geometry-topology relationship of the root system. These are root length density ($\rho_{n,}\ cm^{-2}$) which is the total root length per unit soil volume; root branching density ($\rho_b\ cm^{-3}$), which defines the root topology or linkages between roots of two consecutive branching orders and the root apical meristem density ($\rho_{a,}\ cm^{-3}$), which defines the root tips where cells more or less continuously divide for growth. These densities may also vary according to depth ($z$), incline angle of individual roots ($\alpha$) and time ($t$) (Dupuy *et al.*, 2010a).

Root system growth through apical meristem activity is either by initiation of new meristems (visible and non-visible new meristems at a given location in the reference rooting volume) or through changes in the position of already emerged meristems by root elongation and gravitropism (Figure 3.1).

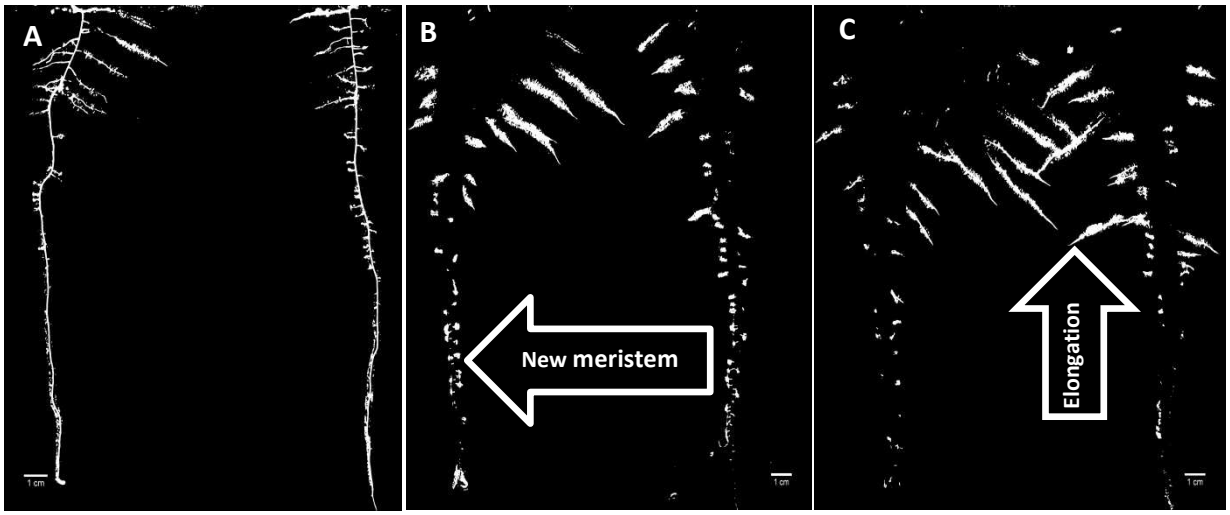


***Figure 3.1:*** *Illustration of root system growth through apical meristem activity: Figure shows A: Images of two whole* Brassica rapa *seedlings imaged 6 days after sowing (DAS); B & C: root meristem locations and newly emerged lateral roots of same root systems in A at 8 and 10 DAS, respectively.*

Dynamics in $\rho_n$ and $\rho_b$ consequently evolve through time as a function of three parameters: root elongation rate $e$ (cm $d^{-1}$), branching rate $b$ ($cm^{-2}$ $d^{-1}$) and gravitropic rate $g$ (° $d^{-1}$). Changes in meristem density distribution is then determined from a classical conservation equation that links these growth parameters (Equation 3.4).

$$b - d = \frac{\partial \rho_a}{\partial t} + \frac{\partial \rho_a g}{\partial \alpha} + \frac{\partial \rho_a e cos\alpha}{\partial x} + \frac{\partial \rho_a e sin\alpha}{\partial z} \qquad (\mathbf{3.4})$$

This equation states that change with time ($\partial/\partial t$) due to meristems entering and leaving the reference volume ($\frac{\partial}{\partial x}, \frac{\partial}{\partial y}$) through elongation rate $e$, in the direction of growth (cos α, sin α), but also through reorientation ($\partial/\partial\alpha$) of meristems due to root gravitropism $g$, and through the creation of new meristems from root branching $b$ as well as loss of meristems due to death of roots axes per unit time $d$ (Dupuy *et al.*, 2005; Dupuy *et al.*, 2010a). Thus, if the space of defined root distribution is generalised, developmental parameters describing the dynamics of RSA can be combined in single equation (Equation 3.4) (Dupuy *et al.*,

2010a). Further details of the density-based modelling and mathematical representations can be referred from (Dupuy *et al.*, 2005) and (Dupuy *et al.*, 2010a).

### *3.1.5.2 Modelling Procedure*

*SmartRoot* (Lobet *et al.,* 2011) digitised each root axis into subcomponents or nodes and generated files containing coordinates which define the spatial location of the extremities of each root segment (called node, Figure 3.2). The coordinate for the nodes of each root segment for all root systems were transferred into a unique database. Information merged in the database included image file name, root ID, position or root nodes, the orientation of the root segment, root diameter at the node (Figure 3.2). The root systems in the database were then centred so that the first node of all root systems was positioned at the same point (Kalogiros et al., unpublished). Then, root length density was obtained using kernel density estimation method (Dupuy *et al.*, 2005; Kalogiros et al., unpublished; Silverman, 1996).

**A**


**B**

| Root | X | Y | theta | Diam |
|---|---|---|---|---|
| root_51 | 20.22562 | 1.414158 | 2.891656 | 0.055055 |
| root_51 | 20.18354 | 1.403414 | 2.891668 | 0.019026 |
| root_51 | 20.1661 | 1.398964 | 3.549982 | 0.019026 |
| root_51 | 20.13147 | 1.41395 | 3.54998 | 0.018844 |
| root_51 | 20.09688 | 1.428917 | 3.569457 | 0.018844 |
| root_51 | 20.06191 | 1.444867 | 3.527908 | 0.0254 |
| root_51 | 20.01474 | 1.464054 | 3.502004 | 0.014815 |
| root_51 | 19.9877 | 1.474243 | 3.448841 | 0.014815 |
| root_51 | 19.96085 | 1.482764 | 3.486624 | 0.019048 |
| root_51 | 19.92356 | 1.496165 | 3.445757 | 0.019048 |
| root_51 | 19.88861 | 1.507135 | 3.491148 | 0.023289 |
| root_51 | 19.84503 | 1.523022 | 3.491149 | 0.023289 |
| root_51 | 19.80127 | 1.538975 | 3.387413 | 0.023289 |
| root_51 | 19.49412 | 1.616037 | 3.647667 | 0.0288 |
| root_51 | 19.4088 | 1.663322 | 3.672298 | 0.014819 |
| root_51 | 19.38258 | 1.678706 | 3.672301 | 0.016932 |
| root_51 | 19.35338 | 1.695846 | 3.652273 | 0.019049 |
| root_51 | 19.32079 | 1.714105 | 3.701722 | 0.021166 |
| root_51 | 19.28524 | 1.736398 | 3.749746 | 0.014813 |
| root_51 | 19.25967 | 1.754202 | 3.696606 | 0.014813 |
| root_51 | 19.23573 | 1.769045 | 3.734399 | 0.019051 |
| root_51 | 19.20286 | 1.791185 | 3.714373 | 0.019051 |

***Figure 3.2:*** *A) An example of* SmartRoot-*traced root system showing primary root nodes (yellow) and lateral root nodes (green); B) Sample nodes dataset generated by* SmartRoot- *The* SmartRoot *algorithm estimates the root diameter (Diam) at each node (X,Y) of the segmented line and uses this information to set the orientation (theta) of the segmented line from the root base of the root tip*

The final stage of the modelling process was to calibrate the density model, calculating the optimal values of substantial model parameters (Kalogiros *et al.,* unpublished). The simulation program was written in the Python programming language (http://www.python.org/) and programme syntaxes were authored by Dimitris Kalogiros, a colleague with whom I worked on this part of the thesis. Simulated and experimental root systems were compared using mean root length of PRs and mean total root length of LRs.

## *3.2 Results*

### 3.2.1 Variability in root traits within a single *Brassica rapa* genotype

The variability of quantitative root traits employed 8 (6 runs) or 16 scanners (2 runs) across 8 independent runs. With two plants per scanner, a total of 160 seedlings were grown. Analyses of variability in root traits within the genotype was however carried out on 133 seedlings (Table 3.1) with approximately 17% of seedlings discarded due to mortality or unusual RSA arising from the death of the PR immediately after sowing. In the present study, time of emergence differed between plants but generally LRs became visible on the PR from 2 DAS. Lateral root emergence declined from 10 DAS unless the PR tip touched the boundaries of the plates on which the rooting media were fixed. Root emergence followed a typical acropetal root growth for a dicot with roots systems normally consisting of a central main root which had developed from the radicle herein called PR and first-order LRs defining the roots which emerged from the PR. Observations of subsequent orders of LRs were rare at the end of the experiments and were therefore excluded from the analysis.

For the majority of the traits measured, the combined effect of the run and the scanner explained the greater proportion of the variation (Table 3.1). Largest variations attributable to run and scanner effect were 86.25% and 47.50% for PR diameter and root dry weight,

respectively. For PR surface area, root-to-shoot ratio, PR volume, LR insertion angle, number of LRs and branching density, the estimated unexplained variations were large and were 69.57%, 64.56%, 64.19%, 63.65%, 61.28 and 55.84%, respectively (Table 3.1).

***Table 3.1:*** *Sources of variation in shoot and root traits assayed 14 DAS among 133 surviving seedlings of* Brassica rapa L. *subsp.* trilocularis *cv. R-o-18 grown for 14 DAS in the phenotyping platform. The experiment was performed in 8 runs employing up to 16 scanners per run and two plants per scanner. (**SDW:** Shoot dry weight; **SFW**: Shoot fresh weight; **RFW**: Root fresh weight; **RDW**: Root dry weight; **TRL**: Total root length; **TLRL**: Total length of LRs; **PRL**: PR length, **PR area**: Surface area of PRs; **PR vol.**: PR volume; **PR diam**.: diameter of PRs; **B. Dens**: Branching density; **LR No**.: Number of LRs; **Mean LRL**: mean length of LRs; **LR diam**.: Diameter of LRs; **Angle**: mean LR insertion angle; **Int. Dist.**: Mean inter-branch distance of LRs; **LAUZ**: Length of the apical un-branched zone of the PR; **R:S**: Root-to-shoot ratio; **SRL**: Specific root length)*

| | | Variance Components | | | Percentage Variation | | |
|---|---|---|---|---|---|---|---|
| **TRAIT (Unit)** | **Mean ± se** | **Run** | **Scanner** | **Residual** | **Run** | **Scanner** | **Residual** |
| SFW (mg) | 102.77 ± 11.012 | 837.34 | 987.60 | 330.42 | 38.85 | 45.82 | 15.33 |
| SDW (mg) | 9.03 ± 0.679 | 3.07 | 4.07 | 2.43 | 32.10 | 42.56 | 25.35 |
| RFW (mg) | 40.17 ± 5.184 | 175.64 | 259.71 | 157.83 | 29.61 | 43.78 | 26.61 |
| RDW (mg) | 3.44 ± 0.334 | 0.70 | 1.30 | 0.74 | 25.45 | 47.50 | 27.05 |
| TRL (cm) | 117.52 ± 12.00 | 888.45 | 1720.85 | 1096.69 | 23.97 | 46.43 | 29.59 |
| TLRL (cm) | 101.95± 11.580 | 829.28 | 1579.86 | 1034.93 | 24.08 | 45.87 | 30.05 |
| PRL (cm) | 15.51 ± 0.914 | 5.52 | 4.76 | 10.08 | 27.10 | 23.37 | 49.53 |
| PR area ($mm^2$) | 154.92 ± 8.967 | 257.45 | 455.33 | 1629.89 | 10.99 | 19.44 | 69.57 |
| PR vol. ($mm^3$) | 14.74 ± 0.804 | 1.72 | 6.31 | 14.39 | 7.66 | 28.16 | 64.19 |
| PR diam. (mm) | 0.39 ± 0.038 | 0.01 | 0.00 | 0.00 | 86.25 | 4.20 | 9.55 |
| B. Dens.(LR $cm^{-1}$) | 3.20 ± 0.263 | 0.38 | 0.76 | 1.44 | 14.65 | 29.51 | 55.84 |
| LR No. | 46.89 ± 3.305 | 72.48 | 36.85 | 173.01 | 25.67 | 13.05 | 61.28 |
| Mean LRL (cm) | 2.89 ± 0.413 | 1.15 | 1.06 | 1.45 | 31.48 | 28.89 | 39.63 |
| LR diam. (mm) | 0.32 ± 0.026 | 0.01 | 0.00 | 0.00 | 39.04 | 33.91 | 27.05 |
| Angle ( °) | 78.40 ± 0.814 | 3.59 | 5.97 | 16.74 | 13.65 | 22.70 | 63.65 |
| Int. Dist. (cm) | 0.49 ± 0.037 | 0.01 | 0.02 | 0.02 | 16.47 | 35.37 | 48.16 |
| LAUZ (cm) | 1.50 ± 0.297 | 0.30 | 0.79 | 1.04 | 13.98 | 37.05 | 48.98 |
| R:S | 0.40 ± 0.021 | 0.00 | 0.00 | 0.01 | 13.94 | 21.50 | 64.56 |
| SRL (cm $mg^{-1}$) | 37.42 ± 4.742 | 103.86 | 36.36 | 78.00 | 47.60 | 16.66 | 35.74 |

The coefficients of variation in the measured traits of the reference genotype varied 5 - 103% (Table 3.2). The CVs across the runs were fairly constant for majority of the traits except for the last two runs which recorded greater CVs for most traits. Root traits generally had greater variability than shoot traits; largest CVs tended to be associated with LR-related traits. Within-genotype trait variability could be ranked as: LAUZ > TLRL > mean LRL >TRL > RFW > Int. Dist. > SRL > RDW > B. Dens. > LR No. > LR Diam. > SFW. Occasionally, PRs of seedlings reached the bottom of the rooting medium before the completion of a run and

therefore, the LAUZ in such cases could be underestimated. This may explain the greater variability observed and hence higher CVs for the trait in all the runs. Lateral root insertion angle recorded smallest CV throughout all the runs.

***Table 3.2:*** *Mean trait value (± s.e) and coefficient of variation in shoot and root traits assayed 14 DAS among 133 surviving seedlings of* Brassica rapa *L. subsp.* trilocularis *cv. R-o-18 grown for 14 days in the phenotyping platform. The experiment was performed in 8 runs employing up to scanners per run and two plants per scanner*

| | | **Run 1 (n = 13)** | | **Run 2 (n = 15)** | | **Run 3 (n = 16 )** | | **Run 4 (n = 16)** | |
|---|---|---|---|---|---|---|---|---|---|
| ***Measured Trait*** | **Unit** | **Mean ± se** | **CV (%)** | **Mean ± se** | **CV (%)** | **Mean ± se** | **CV (%)** | **Mean ± se** | **CV (%)** |
| SFW | *mg* | 127.82 ± 8.273 | 23.34 | 97.15 ± 7.005 | 27.93 | 75.76 ± 2.693 | 14.22 | 143.83 ± 7.668 | 19.95 |
| SDW | *mg* | 9.90 ± 0.663 | 24.13 | 10.04 ± 0.398 | 15.35 | 8.82 ± 0.285 | 12.94 | 7.92 ± 0.413 | 19.52 |
| RFW | *mg* | 33.90 ± 5.266 | 56.01 | 37.57 ± 3.145 | 32.42 | 24.69 ± 2.705 | 43.83 | 42.23 ± 3.986 | 35.32 |
| RDW | *mg* | 3.04 ± 0.419 | 49.72 | 4.34 ± 0.282 | 25.19 | 2.74 ± 0.178 | 25.91 | 2.51 ± 0.227 | 33.71 |
| TRL | *cm* | 89.19 ± 13.202 | 53.37 | 150.99 ± 14.216 | 36.46 | 65.08 ± 6.332 | 38.92 | 142.13 ± 10.932 | 30.77 |
| TLRL | *cm* | 76.71 ± 12.624 | 59.34 | 130.69 ± 13.981 | 41.43 | 48.76 ± 5.689 | 46.67 | 128.28 ± 10.844 | 33.81 |
| PRL | *cm* | 12.48 ± 1.159 | 33.49 | 20.30 ± 0.798 | 15.23 | 16.32 ± 0.784 | 19.21 | 13.85 ± 1.072 | 30.96 |
| PR area | $mm^2$ | *na* | *na* | *na* | *na* | *na* | *na* | 151.05 ± 9.691 | 25.66 |
| PR vol. | $mm^3$ | *na* | *na* | *na* | *na* | *na* | *na* | 15.57 ± 1.136 | 29.18 |
| PR Diam. | *mm* | 0.45 ± 0.012 | 9.90 | 0.55 ± 0.012 | 8.27 | 0.55 ± 0.010 | 7.13 | 0.34 ± 0.013 | 15.23 |
| B. Dens. | *root* $cm^{-1}$ | 3.47 ± 0.439 | 45.72 | 2.77 ± 0.152 | 21.28 | 2.37 ± 0.089 | 15.08 | 4.37 ± 0.705 | 64.58 |
| LR No. | | 62.46 ± 3.684 | 21.27 | 45.47 ± 2.330 | 19.84 | 29.38 ± 1.749 | 23.81 | 44.25 ± 3.817 | 34.51 |
| Mean LRL | *cm* | 1.41 ± 0.232 | 59.40 | 2.87 ± 0.251 | 33.83 | 1.60 ± 0.130 | 32.57 | 5.10 ± 0.796 | 62.52 |
| LR Diam. | *cm* | 0.30 ± 0.005 | 6.24 | 0.44 ± 0.006 | 5.39 | 0.44 ± 0.005 | 4.75 | 0.29 ± 0.030 | 41.53 |
| Angle | ° | 76.54 ± 1.100 | 5.18 | 76.85 ± 1.100 | 5.54 | 74.12 ± 1.481 | 7.99 | 78.58 ± 1.222 | 6.22 |
| Int. Dist. | *cm* | 0.25 ± 0.019 | 28.04 | 0.47 ± 0.027 | 21.89 | 0.46 ± 0.032 | 28.40 | 0.59 ± 0.064 | 42.90 |
| LAUZ | *cm* | 2.55 ± 0.541 | 76.58 | 3.24 ± 0.499 | 59.78 | 3.66 ± 0.476 | 52.00 | 2.92 ± 0.685 | 93.96 |
| R:S | | 0.31 ± 0.040 | 46.29 | 0.44 ± 0.026 | 23.34 | 0.31 ± 0.021 | 26.76 | 0.31 ± 0.021 | 25.17 |
| SRL | *cm* $mg^{-1}$ | 31.01 ± 2.465 | 28.66 | 34.84 ± 2.517 | 27.99 | 24.22 ± 2.156 | 35.61 | 56.04 ± 3.269 | 21.83 |

Table 3.2 (cont'd)

| *Measured Trait* | Unit | Run 5 (n = 16) | | Run 6 (n = 15) | | Run 7 (n = 20 ) | | Run 8 (n = 22) | |
|---|---|---|---|---|---|---|---|---|---|
| | | Mean ± se | CV (%) | Mean ± se | CV (%) | Mean ± se | CV (%) | Mean ± se | CV (%) |
| SFW | *mg* | 85.56 ± 5.561 | 26.00 | 136.79 ± 7.960 | 22.54 | 122.82 ± 11.560 | 42.09 | 48.70 ± 5.265 | 50.71 |
| SDW | *mg* | 9.73 ± 0.669 | 27.48 | 8.59 ± 0.516 | 23.30 | 12.14 ± 0.847 | 31.22 | 6.01 ± 0.428 | 33.42 |
| RFW | *mg* | 50.13 ± 5.031 | 40.15 | 36.78 ± 3.116 | 32.81 | 69.35 ± 7.180 | 46.30 | 26.51 ± 3.644 | 64.47 |
| RDW | *mg* | 3.79 ± 0.322 | 33.92 | 3.46 ± 0.228 | 25.50 | 5.11 ± 0.519 | 45.50 | 2.68 ± 0.269 | 47.16 |
| TRL | *cm* | 125.19 ± 13.314 | 42.54 | 123.89 ± 7.303 | 22.83 | 159.12 ± 17.044 | 47.90 | 75.62 ± 10.761 | 66.75 |
| TLRL | *cm* | 111.13 ± 12.671 | 45.61 | 108.67 ± 7.390 | 26.34 | 141.07 ± 16.240 | 51.48 | 62.27 ± 10.448 | 78.69 |
| PRL | *cm* | 14.06 ± 1.116 | 31.73 | 15.22 ± 1.126 | 28.66 | 18.05 ± 0.880 | 21.81 | 13.35 ± 0.641 | 22.53 |
| PR area | $mm^2$ | 139.12 ± 14.396 | 41.39 | 157.99 ± 11.340 | 27.80 | 184.33 ± 10.639 | 25.81 | 135.08 ± 7.983 | 27.72 |
| PR vol. | $mm^3$ | 14.17 ± 1.079 | 30.46 | 14.71 ± 1.131 | 29.77 | 16.31 ± 1.161 | 31.86 | 12.16 ± 0.930 | 35.87 |
| PR Diam. | *mm* | 0.33 ± 0.007 | 8.84 | 0.32 ± 0.009 | 11.11 | 0.31 ± 0.008 | 11.37 | 0.31 ± 0.011 | 16.53 |
| B. Dens. | $root\ cm^{-1}$ | 2.80 ± 0.339 | 48.38 | 4.07 ± 0.226 | 21.52 | 2.41 ± 0.335 | 62.17 | 3.52 ± 0.262 | 34.89 |
| LR No | | 42.44 ± 3.626 | 34.18 | 51.67 ± 4.535 | 34.00 | 52.55 ± 3.887 | 33.08 | 46.64 ± 3.363 | 33.82 |
| Mean LRL | *cm* | 3.52 ± 0.376 | 42.72 | 3.17 ± 0.404 | 49.42 | 3.38 ± 0.331 | 43.90 | 2.07 ± 0.209 | 47.31 |
| LR Diam. | *cm* | 0.28 ± 0.026 | 37.14 | 0.27 ± 0.026 | 37.62 | 0.27 ± 0.020 | 32.63 | 0.32 ± 0.021 | 30.43 |
| Angle | ° | 79.43 ± 1.159 | 5.84 | 80.67 ± 1.254 | 6.02 | 80.16 ± 1.059 | 5.91 | 80.24 ± 0.925 | 5.41 |
| Int. Dist. | *cm* | 0.49 ± 0.051 | 41.31 | 0.59 ± 0.055 | 36.17 | 0.52 ± 0.060 | 51.80 | 0.57 ± 0.040 | 32.78 |
| LAUZ | cm | 1.17 ± 0.234 | 80.26 | 1.97 ± 0.276 | 54.44 | 1.02 ± 0.186 | 81.33 | 0.97 ± 0.213 | 103.27 |
| R:S | | 0.39 ± 0.015 | 15.73 | 0.40 ± 0.015 | 14.26 | 0.40 ± 0.021 | 23.23 | 0.44 ± 0.029 | 31.52 |
| SRL | $cm\ mg^{-1}$ | 32.49 ± 2.119 | 26.08 | 37.58 ± 2.926 | 30.15 | 32.19 ± 1.900 | 26.40 | 29.23 ± 2.537 | 40.71 |

### 3.2.2 Minimum replication

Replication needed to detect difference between the means of each trait was largely consistent across runs (Table 3.3) but large variability for some traits was evident. Data from the eight runs were pooled to calculate the replication numbers for respective traits. Depending on the trait, 4 to 37 replicates are sufficient to detect a 50% significant difference in trait means in a 2-sided 95% CI t-test (Table 3.3). However, in many cases, 50% differences between mean is unrealistic. Some traits in particular, for example, PR diameter and LR insertion angle usually exhibit low degree of genotypic variability. The number of replicates increases drastically when the difference between the mean is reduced. Nevertheless, a few traits can retain manageable replication number when the difference between the means drops to 30% (Figure 3.3).

***Table 3.3:*** *Number of replicates required to detect a 50% significant difference in a measured trait between two populations with identical standard deviations in the trait using a two-sided 95% confidence interval t-test.*

| Measured shoot or root trait | Run 1 | Run 2 | Run 3 | Run 4 | Run 5 | Run 6 | Run 7 | Run 8 | Mean replication per line |
|---|---|---|---|---|---|---|---|---|---|
| LAUZ | 36 | 22 | 17 | 54 | 40 | 18 | 41 | 66 | 37 |
| TLRL | 22 | 11 | 13 | 7 | 13 | 4 | 16 | 38 | 16 |
| Mean LRL | 22 | 7 | 7 | 24 | 11 | 15 | 12 | 14 | 14 |
| RFW | 19 | 7 | 12 | 8 | 10 | 7 | 13 | 26 | 13 |
| TRL | 18 | 8 | 9 | 6 | 11 | 3 | 14 | 27 | 12 |
| B. Dens. | 13 | 3 | 1 | 26 | 14 | 3 | 24 | 8 | 11 |
| RDW | 15 | 4 | 4 | 7 | 7 | 4 | 13 | 14 | 8 |
| Int. Dist. | 5 | 3 | 5 | 11 | 11 | 8 | 17 | 7 | 8 |
| PR volume | na | na | na | 5 | 6 | 6 | 6 | 8 | 6 |
| SFW | 3 | 5 | 1 | 3 | 4 | 3 | 11 | 16 | 6 |
| PR area | na | na | na | 4 | 11 | 5 | 4 | 5 | 6 |
| SRL | 5 | 5 | 8 | 3 | 4 | 6 | 4 | 10 | 6 |
| LR No. | 3 | 2 | 4 | 7 | 7 | 7 | 7 | 7 | 6 |
| LR Diam. | 0 | 0 | 00 | 11 | 9 | 9 | 7 | 6 | 5 |
| R:S | 13 | 3 | 4 | 4 | 2 | 1 | 3 | 6 | 5 |
| PRL | 7 | 1 | 2 | 6 | 6 | 5 | 3 | 3 | 4 |
| SDW | 4 | 2 | 1 | 2 | 5 | 3 | 6 | 7 | 4 |
| PR Diam. | 1 | 0 | 0 | 1 | 1 | 1 | 1 | 2 | 1 |
| Angle | 0 | 0 | 0 | 0 | 0 | 0 | 0 | 0 | 0 |

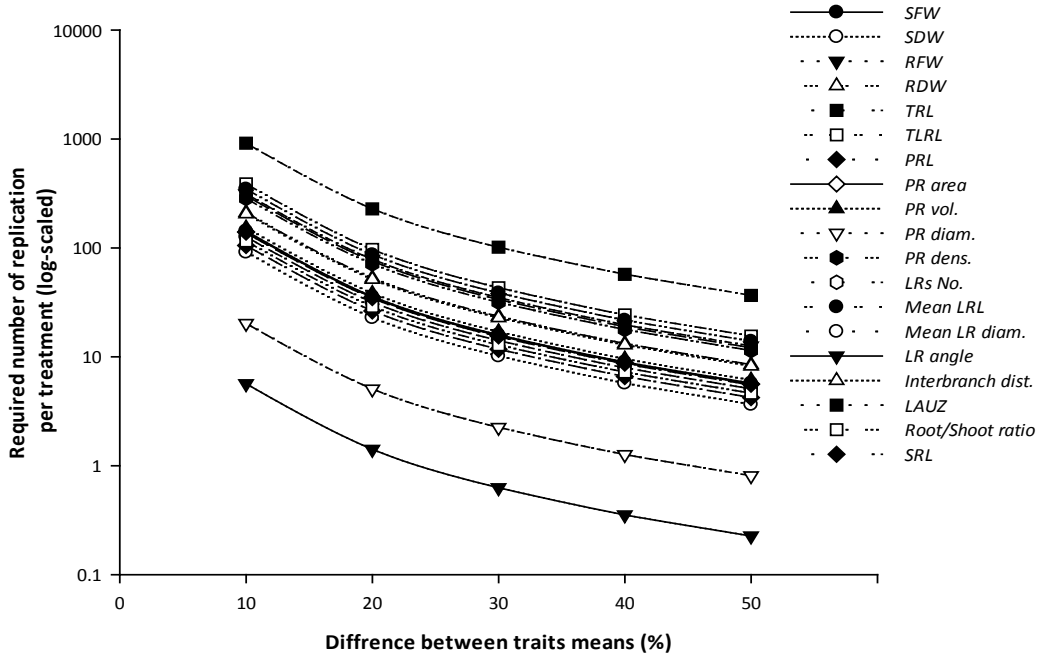


***Figure 3.3:*** *Relationship between the numbers of replicates required to detect a significant difference in a measured trait and the require difference between traits means.*

### 3.2.3 Correlations among seedling shoot and root traits

A total of 47 significant correlations were classified as weak, 35 as moderate and 4 as strong (Figure 3.4). In general, Figure 3.4 shows that bigger plants produced bigger root systems with greater number of lateral roots. Shoot FW exhibited weak to moderate correlations (*r* ranged from 0.22 to 0.69) for 13 of the traits evaluated, with all the significant correlations being positive except for LR diameter. Shoot DW showed weak to strong significant correlations with 13 other traits correlations (*r* ranged from 0.29 to 0.90). All correlations for SDW were positive except with LR inter-branch distance. Root FW had moderate and positive correlations with RDW, TRL, PRL, and PR volume. Root DW had relationship with other parameters except with PR diameter, branching density, LR diameter, angle and LAUZ. Expectedly, TRL strongly and positively correlated with total lateral root length (TLRL) (*r* = 0.98) and showed moderate correlations with PRL, root surface area and root volume. Significant positive correlations were found between TLRL and other parameters including

PRL ($r$ = 0.52), PR surface area ($r$ = 0.53) and PR volume ($r$ = 0.51). The length and the volume of the PR both strongly correlated with its surface area ($r$ = 0.85). The PRL further showed moderate positive correlation with PR volume ($r$ = 0.68) and number of LRs ($r$ =0.80), with PR surface area also correlating with number of LRs ($r$ = 0.75) and LR number also correlating with PR volume ($r$ = 0.65). The diameter of the PR moderately correlated with its volume ($r$ = 0.51). Other correlations were either weak or non-significant (Figure 3.4).

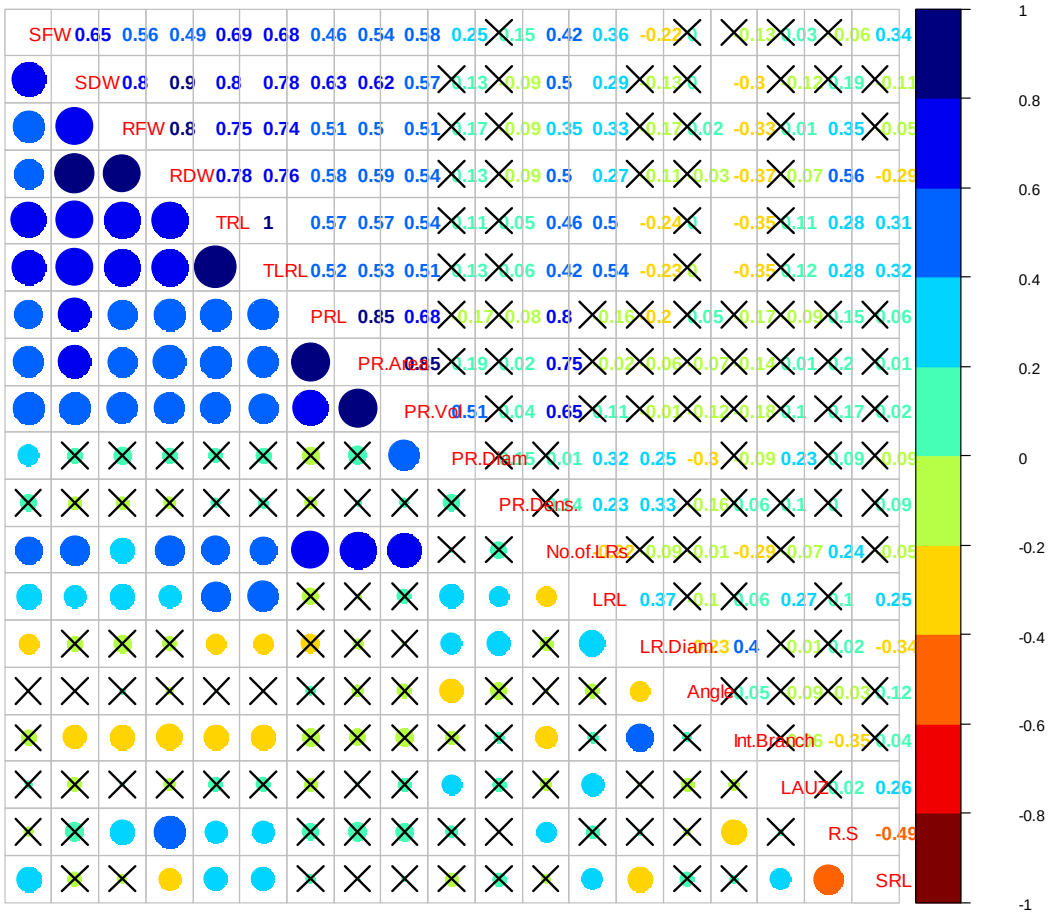


***Figure 3.4:*** *Pearson's correlation coefficients for 19 seedling shoot and root traits. The correlation coefficients are indicated by the colour and size of the circles in lower section of the matrix and the exact corresponding correlation coefficients are indicated in the upper section of the matrix. Boxes with crosses indicate non-significant correlations (p <0.05). The scale is indicated in the bar at the right-hand side of the matrix.*

### 3.2.4 Variability in growth rate of different root axes

Growth rate for both PRs and LRs were not constant over time. The mean growth rate of PRs was 1.24 cm $d^{-1}$ and linearly declined over time (Figure 3.5). Model for PR was initially

fitted with DAS covariate as the only fixed effect parameter (PR model 1). The AIC, BIC and REML logLik were respectively 290.85, 313.11 and -139.42. The PR model subsequently included a quadratic function (PR model 2). The AIC, BIC and REML logLik were 297.55, 323.50 and -141.77, indicating that the previous model (PR model 1) performed better and therefore the model without the quadratic term (PR model 1) was preferred. The intercept ($b_{i1} + \beta_1$) for the fitted PR model was 1.47 but ranged between 0.70 and 2.34 for individual seedlings analysed. The random slope ($b_{i1}$) estimated from the fitted PR model was -0.10 and ranged between -0.01 to 0.06 for individual seedlings analysed. The model was satisfactory as seen in the residual and Q-Q plots which are shown in Figure 3.6.

Lateral roots generally started to emerge 2 DAS. It appeared that 1$^{st}$ laterals generally had faster elongation rates than those that emerged later but all LRs of all ages seem to peak roughly at the same time, between DAS 6 and 9. Among the LRs, it is also evident from Figure 3.5 that older LRs may be separated from younger LRs by their growth rate. For example, 1$^{st}$ LRs initially exhibit faster growth than the remaining LRs but its rate declines from the DAS 6. For the 2$^{nd}$ LRs, growth rate is still increasing 6 days after sowing, and a maximum growth rate is obtained 8 or 9 DAS. Mean growth rates of 0.64, 0.55, 0.27 and 0.16 cm d$^{-1}$ were recorded for 1$^{st}$, 2$^{nd}$, 3$^{rd}$ and 4$^{th}$ laterals respectively.

The mixed-effects model for LR growth was first fitted with DAS considered as a fixed covariate (LR model 1). The AIC, BIC and REML logLik were 44.98, 63.88 and -18.49, respectively. The model subsequently included a quadratic function (LR model 2). The AIC, BIC and REML logLik were 14.03, 47.10 and -0.02, respectively. To check if the growth rates were different among lateral roots based on time of emergence, a third model was fitted

including the categorical variable, type of LR, as a fixed effect (LR model 3). The new values for AIC, BIC and REML logLik were 16.43, 54.19 and -0.22, respectively. Based on these estimated parameters, LR model 2 had better performance. Moreover, the analyses of variance of the models showed that the covariate DAS and the quadratic function were significant (*p<0.0001*) in all models but the type of LR had a non-significant p-value (*p= 0.4541*) in LR model 3, indicating growth rates were not different among LR that emerged on different DAS. Thus, growth rate of LRs generally increased quadratically to an optimum for all types of LRs (Figure 3.5) and the most informative model did not include the effect of time of LR emergence. The fitted LR model (LR model 2) indicated that random intercept had positive or negative values and the curves for each type of LR had different intercepts (Table 3.4). The model was satisfactory as seen in the residual and Q-Q plots which are shown in Figure 3.6.

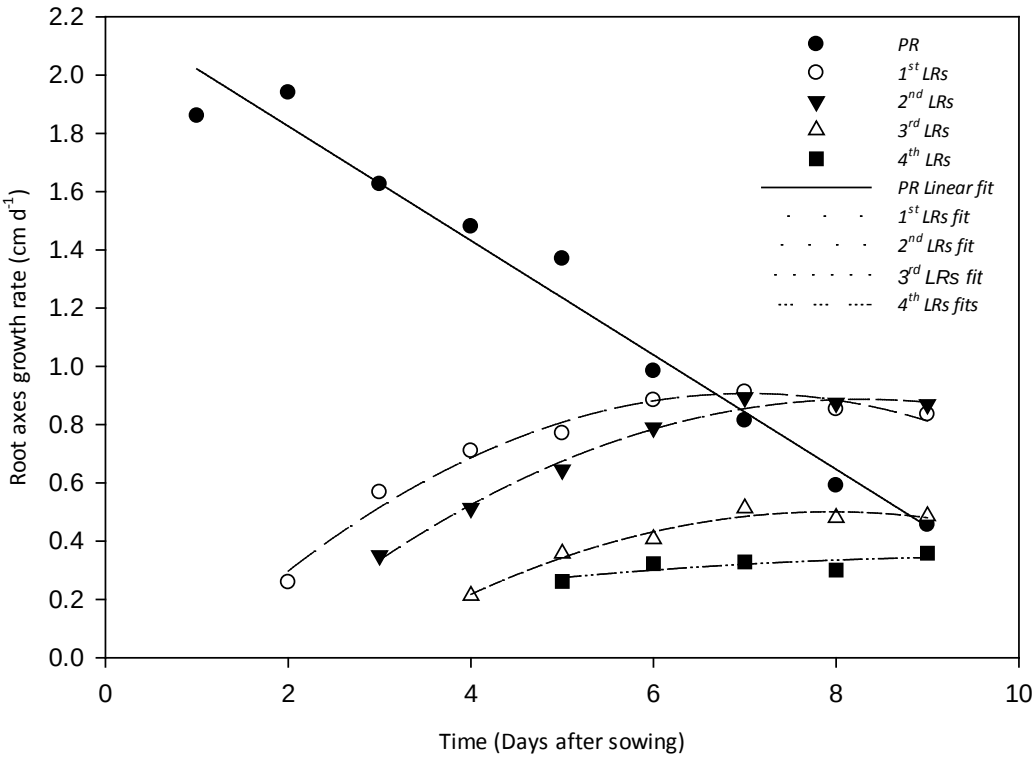


***Figure 3.5:*** *Growth rate of primary and first order lateral roots of seedlings of a* Brassica rapa cv. *R-o-18 grown over a period of days after sowing on germinating paper.*

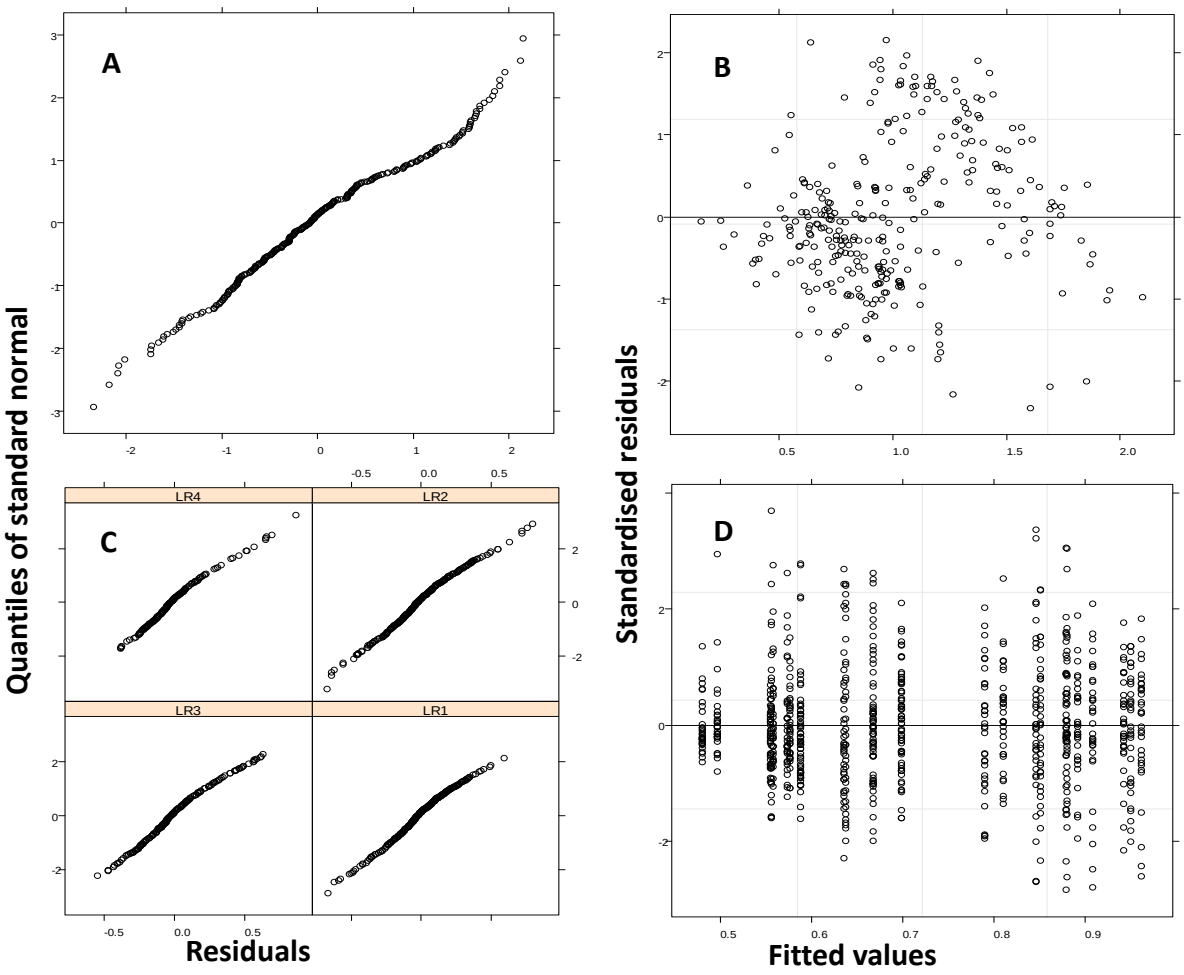


***Figure 3.6:*** *Diagnostic plots for assessing model adequacy of primary and lateral root growth rate of seedlings of a* Brassica rapa *genotype (cv. R-o-18) grown over a period of days after sowing on germinating blotter paper. (A): normal plots of residuals of PR fitted model for all seedlings, (B): residuals versus fitted values for PR linear mixed-effects model for all seedlings, (C) normal plots of residuals of LR fitted model for each type of lateral root and (D) residuals versus fitted values for linear mixed-effects LR model for all seedlings.*

***Table 3.4:*** *Parameters estimates (Equation 3.3b) for mixed effects models describing the growth rate of LRs that emerged 2 (1st LR), 3 (2nd LR), 4 (3rd LR) and 5 (4th LR) DAS from a* Brassica rapa *genotype (R-o-18) grown for 14 days on paper.*

| Type of lateral root | Intercept ($b_{i1} + \beta_1$) | DAS (Random slope, $b_{i1}$) | $DAS^2$ (Fixed slope, $\beta_1$) |
|---|---|---|---|
| 1st LRs | 0.176 | 0.221 | -0.015 |
| 2nd LRs | 0.023 | 0.231 | -0.015 |
| 3rd LRs | -0.202 | 0.233 | -0.015 |
| 4th LRs | -0.273 | 0.231 | -0.015 |

### 3.2.5 Density-based model

The density based model predicted that total primary root length was 13.81 cm, while the estimated total primary root length was 15.28 cm. Thus, the model appeared to

underestimate the primary root length density by 10.2%. Model output and the estimate from real 14 d *Brassica* root systems for total lateral root length per plant were similar. The simulated total lateral root length per plant was 125.32 cm, and was 0.43% greater than the 124.78 cm obtained from the measured data of real *Brassica rapa* roots. Qualitatively, the spatial mapping of root length density distribution for both primary and first order lateral roots with regards to radial distance (*x*) and depth (*z*) showed similar distributions between real roots from experimental data and model-simulated root systems (Figure 3.7). Minor inconsistencies are however observed between experimental and predicted root length density and this is more evident in the primary root length density than lateral rot length density (Figure 3.7). For example, the region of high primary root density appears to be inconsistent between measured and simulated data, with measured data seemingly showing higher values to the results of the simulated data. Root length density provides good descriptions of the local geometrical properties of root systems to model root-soil interactions (Dupuy *et al.,* 2010a). Only root length density was therefore considered in this thesis to demonstrate the utility of scanner-based non-destructive measurement of roots to modelling of root system architecture. Nevertheless, it can be expected that the main root growth parameters such as elongation rate, gravitropic rate, and branching rate can be estimated using density-based models and in each case, data acquired via scanner-based imaging will be very relevant.

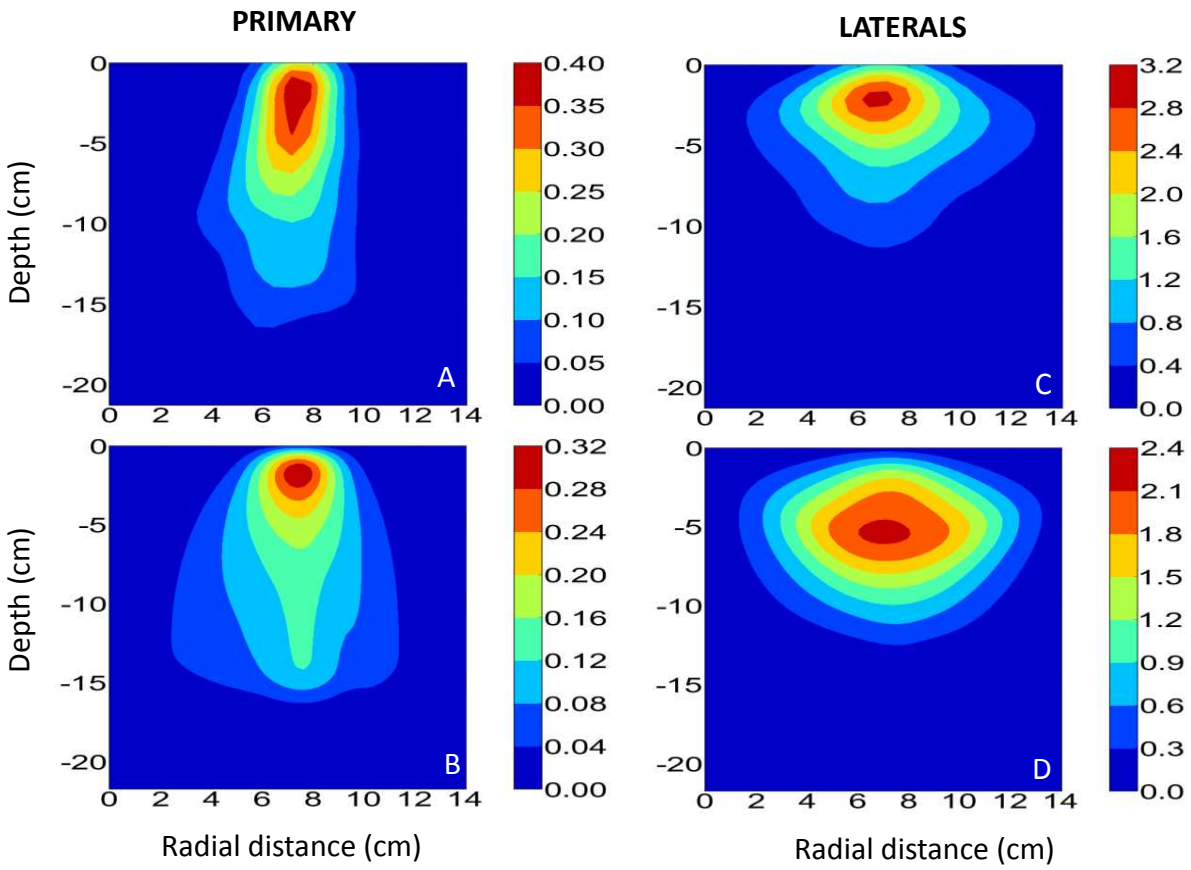


***Figure 3.7:*** *Experimental and predicted root length density distribution as a function of depth and radial distance. The global shape of the (a) experimentally measured primary root length density distribution is highly similar to the root length density distribution estimated from (b) simulated root systems. The global shape of the (c) experimentally measured lateral root length density distribution is highly similar to the lateral root length density distribution estimated from (d) simulated root systems.*

## *3.3 Discussion*

### 3.3.1 Within-genotype variability in shoots and root traits of seedlings

There were wide variation between runs for some traits but close correspondence was also observed between some root traits across most runs. In general, the result suggests that uniform conditions were largely achieved across runs and that the experimental set-up provide results that are reproducible. My search did not produce any published information on variability of root traits within seedlings of a *Brassica rapa* genotype. This limits comparison of the results here with published results from other laboratories. The within-

genotype variations recorded in my study were relatively less than those observed by Armengaud *et al.* (2009) who had reported up to 130% CV for LR density in 23 accessions of *Arabidopsis*. However, my estimated variations are consistent with those recorded by Araujo *et al.* (2004) for common bean genotypes under low P conditions.

The correlations of pairs of root traits and with shoot traits observed in this study are consistent with those found by Seiler (2008), for sunflower seedlings. However, only one genotype has been employed here so all variations observed are due to environmental effects and not genetic. Results here demonstrate that due to substantial environmental effects, within-genotype variability in root systems can be very large for many traits. Also, some traits showed larger variability within a genotype than others, such that limited number of selected traits could account for most of the variability in a genotype. For example, root biomass, total and mean length of LRs might account for most of the variability in the traits measured here (Table 3.2). de Dorlodot *et al.* (2007) have stated that a few carefully selected traits could be used to explain most variability in RSA, indicating for example that variability in root branching could be accounted for by variations of root diameter.

Due to the large variation within a genotype for many root traits, different replication numbers are required to detect significant differences. For some traits such as LAUZ and LR mean length, it may be necessary to increase replication substantially to provide the necessary statistical power. Without due considerations for statistical power and effect size in detecting phenotypic variability, root phenotyping could be futile even if data are generated from the most elegant and robust of phenotyping platforms. In all root

phenotyping protocols, the natural variability in a trait of interest determines number of individuals or replication (sample size) to be selected (Cornelissen *et al.*, 2003). Due to high plasticity in roots, it is common that replication required in root studies exceeds that required in shoot studies (Bengough *et al.*, 2000). For example, it was found that up to 120 replications may be necessary to detect 10% difference between root traits when coefficient of variation is 40% (Bengough *et al.*, 2000). In this example, a too small a sample size might not allow the detection of small but relevant differences between treatment effects, whereas an excessively large sample size may lead to the wastage of already limited time and resources (Bros and Cowell, 1987; Costa *et al.*, 2000).

### 3.3.2 Within-genotype variation in the growth rate of different root axes

Growth data indicated that root elongation is coordinated between PRs and first order LRs such that plants appear to inherently switch root growth from the PR to LRs. This may support the hypothesis that variations in the growth of the total root system are more linked to variations in LR growth than PR growth (Armengaud *et al.*, 2009). Lecompte *et al.* (2001) suggested that root elongation rate is variable within a genotype or within a single plant and for LRs, the age or time of emergence could be important in explaining this variability. Amongst all the covariate tested, this study showed however that time of emergence or age of LRs was not significant in explaining within-genotype variability. This however require further validation as the model here had incorporated only a few laterals sampled form plants grown for short a period. Most first order LRs seemed to grow initially at the same rate and peak roughly at the same time after sowing (Figure 3.5).

### 3.3.3 Scanner-based root phenotyping and density-based model

Models are useful in synthesising knowledge to produce more global representations of the complexity of root systems and for testing hypothesis on the interactions in experimental results (Pagès *et al.*, 2000). Root architecture models enable dynamic representation of the dynamics of the development of a root system (de Dorlodot *et al.*, 2007; Pagès and Bengough, 1997), and their integration with phenotypic data from a range of genotypes would be powerful tools in plant breeding. In the present study, a density-based approach for the modelling of root architecture was tested for its ability to predict the root length distribution of *Brassica rapa* plants. The model was validated against a dataset from 89 seedlings grown for 14 DAS. The model reproduced the experimental results well, accurately simulating PR length and cumulative length of all LRs. Although, root length distributions of simulated root systems were similar to data from real root systems, there was a slight tendency to under estimate PR by approximately 10%. From the results shown here, it is expected that root growth parameters including elongation rate, gravitropic rate and branching rate can be reliably estimated using density-based models with a relatively limited number of parameters and the process would benefit greatly from scanner-based imaging.

## *3.4 Summary*

- Within-genotype variability in root systems is large for many traits.
- Large replication is needed to detect significant differences between many root trait means and the needed replication may be particularly high for lateral-root related traits.
- The growth of PRs and LRs of *Brassica rapa* seedlings are coordinated such that increased growth in LRs compensates for decline in the growth of PRs.

- Growth rate of PRs of *Brassica rapa* seedlings decline linearly with time, whiles that of first order LRs growth rate is nonlinear, with an initial increase, followed by peak and then a decline in the elongation rate.
- Differentially emerged first order LR of *Brassica rapa* seedlings exhibit differential growth rates but age or time of lateral root emergence was not significant in explaining this variability.
- Density-based mechanistic model reproduced experimental results accurately by simulating PR length and cumulative length of all LRs. Root growth parameters such as elongation rate, gravitropic rate and branching rate can be reliably estimated using density-based models.
- Time-lapsed imaging of root systems by low-cost optical scanners provides reliable empirical data for the validation and parameterisation of density-based modelling of root system analyses.

## CHAPTER 4 : GENOTYPIC VARIABILITY IN ROOT SYSTEM GROWTH DYNAMICS IN *BRASSICA RAPA* GENOTYPES

### 4.0 Introduction

To breed for crops with improved RSA, natural variation must be observed in various root traits. Exploitation of natural genetic variation in RSA allows the identification of genes which may be targets for the evolution of morphological variation (Pacheco-Villalobos and Hardtke, 2012). Variation in root traits including differences among genotypes in the ability to establish a deep root system quickly (Siddique *et al.*, 1990), in root length density (Mian *et al.*, 1994), in root distribution (Ford *et al.*, 2006), in the numbers of seminal and total roots (Box and Johnson, 1987; Robertson *et al.*, 1979), and in root-to-shoot ratio (Sadhu and Bhaduri, 1984) have been found in several crops including wheat (Herrera *et al.*, 2012) and *Brassica* crops (Hammond *et al.*, 2009; Lu *et al.*, 2008; Shi *et al.*, 2013a; Shi *et al.*, 2013b). Studies on bean, maize, and soybean have identified variation in root gravitropism and hence variation in adaptation to low P availability (Liao *et al.*, 2001; Liao *et al.*, 2004; Lynch and Beebe, 1995; Lynch and Brown, 2001; Lynch and Brown, 2008; Zhu *et al.*, 2005a; Zhu *et al.*, 2005b; Zhu and Lynch, 2004).

The root system of *Brassica* normally consists of two distinct components, the main or PR and successive orders of LRs. The depth of the PR, length and number of LR depend on the genetic background of the seedling. Intraspecific genotypic variability in root length for example has been exploited to identify key genes involved with N use efficiency and drought tolerance (Syers *et al.*, 2008). *Brassica* genotypes with long primary and lateral roots, large root volumes and heavy root weight may have an improved yield in nutrient deficient or drought prone conditions (Kumar *et al.*, 2012). With the availability of mapping populations for various crops such as the *Brassica rapa* BraIRRI mapping population (Iniguez-Luy *et al.,*

2009), rapid identification of quantitative trait loci (QTL) underlying root system architecture would be achieved quickly, provided the variation in RSA of genotypes is evaluated and understood.

The aim of this Chapter was to exploit the newly developed root phenotyping platform to collect new high resolution data on the development of the root system architecture of *Brassica rapa* at the seedling stage. The objective is to provide a detailed quantitative description of the genotypic variability of root traits amongst a selection of genotypes derived from the BraIRRI population. The genotypes studied consisted of the parents of the BraIRRI population and fourteen recombinant inbred lines (RILs). The specific objective of this Chapter were to (i) quantify the genotypic variability and broad-sense heritability in the selected lines; (ii) identify the traits accounting for most of the variation in the RSA of *Brassica rapa* genotypes; and (iii) use statistical model to describe the genotypic variations of dynamic RSA traits. This was achieved by the development of mixed-effect models.

### *4.1 Materials and methods*

The parents (cv. IMB211 and cv. R500) and 14 recombinant inbred lines (RILs) of the BraIRRI mapping population (Iniguez-Luy *et al.*, 2009) were used to study variations in root traits caused by genetic factors. The BraIRRI population is an immortal mapping population consisting of 160 RILs derived from the cross of IMB211 and R500 genotypes. Genotype IMB211 is a highly inbred rapid cycling Chinese cabbage *B. rapa* subsp. *pekinensis* and R500 is a highly inbred annual yellow sarson *B. rapa* subsp. *trilocularis* (Iniguez-Luy *et al.*, 2009; Xu *et al.*, 2010). Genotypes IMB211 and R500 have different root system characteristics and the RILs were expected to segregate for root traits. The inbred lines tested in this study were

chosen based on availability of seeds and included BraIRRI 002, 016, 030, 070, 104, 124,143, 198, 201,205, 229, 248, 360 and 380.

Growth conditions and nutrient composition were as described in Section 2 of Chapter Two. Twenty four scanners were assembled and seedlings were grown on four scanner banks with each bank containing 6 scanners and 2 seedlings per scanner (Figure 4.1). Seedlings of genotypes were grown in six replicates in two independent experiments. Since the experiments were performed under uniform and unstressed environmental conditions, all the data from the two independent experiments were combined for analyses given 12 replicates for each line. From previous Chapter (Table 3.3), requisite replication is between 1 and 37 for different traits and so depending on the trait of interest, sample size must be greater or lesser than 6. However, due to practical limitations, a compromise was made in this and subsequent Chapters to set a single replication value for all traits (n=6). This was small enough to be useful and feasible but not smaller than necessary because: (i) in this thesis, analyses were performed on continuous measurements and according to Eng (2003), statistical tests that incorporate the use of continuous values are mathematically more robust than those used for proportions, given the same sample size, and (ii) pooling together data from duplicated experiments also increased precision and reduced variability in trait measurements.

Images were taken at 12-hour intervals using the fixed flatbed scanners abutting the plates for up to 15 DAS. Fresh and dry weights of shoots and roots, lengths and diameters of primary and lateral roots, the branching density and insertion angle of LRs on the PR, and the total length of the whole root system (Table 4.1) were determined on individuals of the

parental genotypes (IMB211, R500) and 14 RILs of the BraIRRI mapping population grown for 15 days on the phenotyping platform. Images were analysed as described in Chapter 2, Section 2.3.3 using *ImageJ* and *SmartRoot* (Lobet *et al.*, 2011).

***Figure 4.1:*** *The phenotyping platform comprising 24 scanners assembled in four banks of six scanners.*

### 4.1.1 Multivariate analysis of the trait space

First, correlations and clustering of static root traits was studied using statistical multivariate analyses. Data from all genotypes were combined and trait correlations between parameters were assessed with Pearson's correlation coefficients. Correlations were considered statistically significant at $p < 0.05$. Root and shoot traits were subjected to principal components analysis (PCA). Significant components were chosen when the eigenvalue > 1 (Tabachnick and Fidell, 1996). Subsequently, cluster analysis was conducted

on all the traits pooled together to identify discrete groups of lines with similar RSA traits among the reference population studied. Clustering was performed using Ward's hierarchical approach based on minimum variance linking method with Euclidean distance as the similarity measure (Manschadi *et al.*, 2008). Optimal number of clusters was chosen based on the 'elbow-criterion' which compares the Sum of Squared Differences (SSD) for different cluster solutions (Thorndike, 1953). Generally, increases in the number of cluster are associated with decreases in the SSD because clusters are, by definition, smaller. Therefore, the SSD is plotted against the numbers of cluster in the analysis and an optimal number of clusters are determined by identifying the "elbow" in the plot where the reduction in SSD slows dramatically (Mooi and Sarstedt, 2011).

### 4.1.2 Statistical analysis of static root traits

The sources of variation in static root traits were determined using a random effects model with experimental run, scanner and genotype considered as random factors.

$$y_{ijk} = m + g_k + ag_{ik} + bg_{jk} + abg_{ijk} + \epsilon_{ijk,} \qquad (\mathbf{4.1})$$

$$i \in \{1, \dots, n\}, j \in \{1, \dots, r\}, k \in \{1, \dots, s\},$$

$$g_k/ag_{ik}/bg_{jk}/abg_{ijk} \sim N\left(0, \sigma^2_{g/ag/bg/abg}\right), \epsilon_{ij} \sim N(0, \sigma^2),$$

where $y_{ijk}$ represents the root trait from the $i^{th}$ experimental run, $j^{th}$ scanner and $k^{th}$ genotype, $m$ is the mean trait value, $g_k$ is the effect of the genotype, $ag_{ik}$ is the effect of interactions between experimental run and genotypic factors, $bg_{jk}$ is the effect of interactions between scanner and genotypic factors, $abg_{ijk}$ is the effect of interactions between experimental run, scanner and genotypic factors, $\epsilon_{ijk}$ is the residual error, *n* is the number of runs (2), *r* is the total number of scanners (24) and *s* is the number of genotypes (16). A model incorporating all individual terms (i.e.: genotype, run and scanner) with all

their interactions was over-parameterised and sub-optimal based on model assessments. Phenotypic variance was then calculated with the estimated genetic variance ($\sigma_g^2$), Genotype x Experimental run variance ($\sigma_{ag}^2$) and the error variance ($\sigma^2$) as:

$$\sigma_p^2 = \sigma_g^2 + \frac{\sigma_{ag}^2}{n} + \frac{\sigma^2}{pn} \qquad (\mathbf{4.2})$$

*p* = 6 is the number of replicates and *n* = 2 is the number of experiments. Broad-sense heritability ($H^2$) was estimated as $\sigma_g^2 / \sigma_p^2$, where $\sigma_g^2$ is the estimated variance associated with the genotypic effect and $\sigma_p^2$ is the phenotypic variance for the trait.

### 4.1.3 Analyses of root growth dynamics

Dynamic root trait analyses were performed using linear and non-linear mixed-effects models following methods described previously (Pinheiro and Bates, 2000). Models were used to ascertain (i) variation in total root length, (ii) variation in primary root length and (iii) variation in first order lateral root growth rate. Thus, the response variables were total root length, primary root length and lateral root growth rate with the fixed effect represented by days after sowing (DAS) and the random effects, the genotypes and experimental run. The growth rate of a lateral root was expressed as the quotient of the lateral root length and the length of time after its emergence from the primary root. For total root length, data was square-rooted to normalise it before fitting linear model. Data were grouped according to genotypes and the covariate DAS. The following model was applied for the linear mixed-effect analyses:

$$y_{ijk} = g_i + b_1 + b_2 das_{jk} + \epsilon_{ijk,} \qquad (\mathbf{4.3})$$
$$i = \{1, \dots, s\}, j = \{1, \dots, n\},$$
$$g_i \sim N\left(0, \sigma_g^2\right), \epsilon_{ij,} \sim N(0, \sigma^2) .$$

where

$y_{ijk}$ is the average total or primary root length for the $i^{th}$ genotype for the $j^{th}$ day after sowing in the $k^{th}$ experimental run. $g_i$, is the genotypic effect, $das_j$ is therefore the time covariate, and $b_1$ and $b_2$ represent the intercept and slope respectively, of the relationship between root length and *das*, and $\epsilon_{ij}$ is the residual error term. $s$ = 16 is the number of genotypes and $n$ = 15 is duration of the experiment in days.

Prior to fitting linear mixed-effects models, genotypic variations in the total root length, the primary root length and lateral root growth rate, among genotypes were assessed graphically to observe the trend of growth in each parameter. The data were then centred at 7 DAS in order to eliminate correlations between slopes and intercepts for each genotype. Parameter estimates were plotted and the 95% confidence intervals of the estimates were used to analyse genotypic variations. In order to account for non-linear relation between DAS and total root length and primary root length, a logistic growth function was also used to model the increases in these parameters with time. The three parameters of the logistic function were the asymptote ($\emptyset_1$), inflection point ($\emptyset_2$ ), and scale parameter ($\emptyset_3$).

$$y_{ij} = \frac{\emptyset_{i1}}{1 + \exp[-(DAS_j - \emptyset_{i2})/\emptyset_{i3}]} + \epsilon_{ij}, \qquad (\mathbf{4.4})$$

$$\emptyset_i = \begin{bmatrix} \emptyset_{i1} \\ \emptyset_{i2} \\ \emptyset_{i3} \end{bmatrix} = \begin{bmatrix} \beta_1 \\ \beta_2 \\ \beta_3 \end{bmatrix} + \begin{bmatrix} b_i \\ 0 \\ 0 \end{bmatrix},$$

$$i = \{1, \dots, s\}, j = \{1, \dots, t\},$$

$$b_i \sim N(0, \sigma_b^2), \epsilon_{ij} \sim N(0, \sigma^2).$$

where $y_{ij}$ is the total root length or primary root length for the $i^{th}$ genotype, on the $j^{th}$ DAS, and $t$ is the number of time-points at which measurements were made (15). The parameters

$\beta_1$, $\beta_2$ and $\beta_3$ are the mean values of the individual logistic parameters $\emptyset_{i1}$, $\emptyset_{i2}$ and $\emptyset_{i3}$, respectively, and $b_i$, is the random effect on the asymptote of the logistic function and $\epsilon_{ij}$ is the residual error. A likelihood ratio test was used to select the final model, which had the three parameters as fixed effects and only the asymptote as a random effect. Autocorrelation in the data was modelled using the moving average (corARMA) and autoregressive model of an order 1 (AR1) correlation structure (Pinheiro and Bates, 2000). To account for heteroscedasticity in both the linear and the non-linear models, a power variance function was used of the form:

$$Var(\epsilon_{ij}|DAS) = \sigma^2(\delta_1 + |DAS|^{\delta_2}), \quad (\mathbf{4.5})$$

where $\sigma^2$ is the variance when $j$=0 and $\delta_1$ and $\delta_2$ are the two parameters for the power variance function (Pinheiro and Bates, 2000).

The sources of variation in the growth rate of lateral roots were determined using mixed effects models with genotype and DAS considered as random factors (Eqn. 4.6):

$$y_{ij} = b_i + \beta_1 + \beta_2 DAS_j + \beta_3 DAS_j^2 + \epsilon_{ij,} \quad (\mathbf{4.6})$$

$$i = \{1, \dots, s\}, j = \{1, \dots, t\},$$

$$b_i \sim N(0, \sigma_b^2), \epsilon_{ijk} \sim N(0, \sigma^2).$$

where $y_{ij}$ is the lateral root growth rate for genotype $i$ on the $j^{th}$ day of the experiment, $\beta_1$, $\beta_2$ and $\beta_3$ are the fixed effect parameters for the quadratic function and $b_i$ is the random effects on the intercept of the quadratic function. Additional factors such as plant or scanner effects resulted in an over-parameterised model and were therefore not incorporated into the model. Data for growth rates of lateral roots were normalised by square root transformation.

#### 4.1.4 Assessment of model performance

In all analyses, the first model was compared against respective models to assess their structural adequacy using the logLik, AIC and BIC. Models quality was also assessed visually using Q-Q plots to check for normality and residual plots to check that the variance of residuals was constant (Pinheiro and Bates, 2000). Further, we investigated possible autocorrelation in the data and subsequently introduced an autoregressive model.

#### 4.1.5 Software packages

Statistical analyses of static root traits were performed using GenStat (GenStat Release 14.1, VSN International, Oxford, UK) whilst dynamic root analyses was conducted with the *R* statistical software (R Core Team, 2008). Principal component and clustering analyses were performed in *R* software with the princomp() and the dist() / hclust() functions respectively. Statistical analyses of all mixed effects models were performed using *R* software and the nlme library (Pinheiro *et al.*, 2008; R Core Team, 2008).

### *4.2 Results*

#### 4.2.1 Genotypic variability in static root traits

Significant effect of genotype was observed for all the root traits measured ($p < 0.05$) including fresh and dry weights of shoots and roots, lengths and diameters of primary and lateral roots, the branching density and insertion angle of LRs on the PR, and the total length of the whole root system (Table 4.1). No effect of genotype was observed for specific root length and root-to-shoot ratio. The quotient of the highest and lowest values for a particular trait ranged from 1.2 for LR insertion angle to 4.8 for TLRL and 4.9 for SFW (Table 4.1). The parental genotypes exhibited extreme values for many biomass and root length traits. The R500 parental genotype had the highest values for the majority of root and shoot traits assayed. Although the IMB211 parental genotype had the lowest values for TLRL and TRL, it

did not have the lowest values for all root and shoot traits, providing some evidence for transgressive segregation. Neither parental genotype had the most extreme values for branching density, mean length or diameter of LRs or the LR insertion angle (Table 4.1).

***Table 4.1:*** *Genotypic variation in shoot and root traits of parents and 14 RILs of 15 DAS seedlings of* Brassica rapa *(SFW: Shoot fresh weight; SDW: Shoot dry weight; RFW: Root fresh weight; RDW: Root dry weight; TRL: Total root length; TLRL: Total lateral root length; PRL: Primary root length; PR Diam.: Primary root diameter; B. Dens.: Branching density; No. LRs: Number of lateral roots; LRL: Mean lateral root length; LR Diam.: Mean lateral root diameter; Angle: Mean lateral root insertion angle; B. Dist: Mean Inter-branch distance; SRL: Specific root length; R:S: Root to Shoot ratio. **= significance at p<0.001; ns = not significant [a]= parents).*

| TRAIT MEASURED (n=12; d.f.= 174) | | | | | | | | | | | | | | | | |
|---|---|---|---|---|---|---|---|---|---|---|---|---|---|---|---|---|
| **Lines** | **SFW (mg)** | **SDW (mg)** | **RFW (mg)** | **RDW (mg)** | **TRL (cm)** | **TLRL (cm)** | **PRL (cm)** | **PR Diam. (mm)** | **B. Dens (r/cm)** | **No. LRs** | **LRL (cm)** | **LR Diam. (mm)** | **Angle (°)** | **B. Dist. (cm)** | **SRL (cm $mg^{-1}$)** | **R:S** |
| | ** | ** | ** | ** | ** | ** | ** | ** | ** | ** | ** | ** | ** | ** | ns | ns |
| IRRI 002 | 55.88 | 3.135 | 13.02 | 2.449 | 47.7 | 30.0 | 17.71 | 0.373 | 3.230 | 30.10 | 1.034 | 0.326 | 72.90 | 0.335 | 37.8 | 0.785 |
| IRRI 016 | 56.31 | 3.232 | 12.19 | 1.024 | 34.4 | 22.5 | 11.89 | 0.398 | 2.461 | 20.67 | 1.140 | 0.307 | 63.27 | 0.449 | 34.3 | 0.320 |
| IRRI 030 | 21.28 | 1.350 | 6.69 | 0.612 | 35.8 | 18.5 | 17.23 | 0.330 | 1.683 | 11.07 | 2.019 | 0.233 | 75.12 | 0.698 | 62.8 | 0.487 |
| IRRI 070 | 41.63 | 2.643 | 9.19 | 1.380 | 38.9 | 24.7 | 14.27 | 0.364 | 3.431 | 17.83 | 1.373 | 0.246 | 66.75 | 0.386 | 44.1 | 0.509 |
| IRRI 104 | 44.43 | 2.771 | 12.21 | 0.886 | 47.3 | 33.9 | 13.40 | 0.384 | 3.035 | 19.75 | 1.776 | 0.244 | 65.85 | 0.416 | 55 | 0.321 |
| IRRI 124 | 47.12 | 2.721 | 11.48 | 1.142 | 39.7 | 23.8 | 5.85 | 0.356 | 2.708 | 25.55 | 1.098 | 0.268 | 65.58 | 0.438 | 35.4 | 0.427 |
| IRRI 143 | 60.29 | 3.332 | 9.97 | 0.980 | 40.7 | 22.3 | 18.45 | 0.348 | 2.785 | 36.5 | 0.692 | 0.284 | 73.41 | 0.405 | 45.4 | 0.287 |
| IRRI 198 | 73.99 | 3.654 | 13.23 | 1.101 | 42.2 | 22.8 | 19.46 | 0.348 | 2.124 | 30.92 | 0.772 | 0.288 | 62.76 | 0.529 | 39.5 | 0.310 |
| IRRI 201 | 62.57 | 3.201 | 12.26 | 0.956 | 43.2 | 24.4 | 18.8 | 0.356 | 2.247 | 25.75 | 1.032 | 0.265 | 63.76 | 0.468 | 81.6 | 0.302 |
| IRRI 205 | 34.75 | 2.089 | 9.3 | 0.798 | 48.4 | 32.4 | 16.29 | 0.347 | 2.790 | 28.65 | 1.343 | 0.231 | 68.76 | 0.376 | 64.1 | 0.646 |
| IRRI 229 | 36.89 | 2.433 | 10.66 | 0.856 | 54.2 | 39.1 | 15.12 | 0.337 | 2.833 | 21.8 | 1.741 | 0.239 | 65.06 | 0.410 | 102 | 0.341 |
| IRRI 248 | 40.91 | 2.577 | 10.16 | 0.815 | 36.3 | 19.4 | 16.38 | 0.352 | 2.587 | 25.58 | 0.763 | 0.253 | 65.22 | 0.418 | 46.7 | 0.317 |
| IRRI 360 | 64.77 | 4.113 | 16.12 | 1.444 | 55.6 | 37.5 | 16.82 | 0.395 | 3.471 | 33.38 | 1.191 | 0.309 | 61.07 | 0.356 | 38.4 | 0.355 |
| IRRI 380 | 75.25 | 4.706 | 21.91 | 1.920 | 75.6 | 57.7 | 17.92 | 0.382 | 3.806 | 40.96 | 1.737 | 0.270 | 70.95 | 0.348 | 39.4 | 0.431 |
| IMB211[a] | 29.42 | 1.950 | 8.2 | 0.758 | 28.8 | 15.7 | 13.08 | 0.360 | 2.653 | 15.50 | 1.332 | 0.256 | 70.09 | 0.450 | 39.6 | 0.384 |
| R500[a] | 104.1 | 5.963 | 22.6 | 2.023 | 95.0 | 74.7 | 20.44 | 0.407 | 3.154 | 50.29 | 1.354 | 0.260 | 70.80 | 0.362 | 48.8 | 0.321 |
| | | | | | | | | | | | | | | | | |
| *LSD* | *9.632* | *0.6318* | *4.055* | *0.8078* | *13.68* | *13.32* | *2.106* | *0.01969* | *0.574* | *7.162* | *0.4918* | *0.03524* | *4.127* | *0.09568* | *41.13* | *0.3193* |

There were strong positive correlations among biomass traits among the 190 plants studied (Figure 4.2). Total root length was strongly positively correlated with shoot and root biomass, total LR length and LR number. The diameter of the PR was also correlated with shoot and root biomass, and with the diameter of lateral roots. The length of the PR positively correlated with the number of LRs but little correlation was found between LR angle, specific root length or root-to-shoot ratio and any other trait (Figure 4.2).

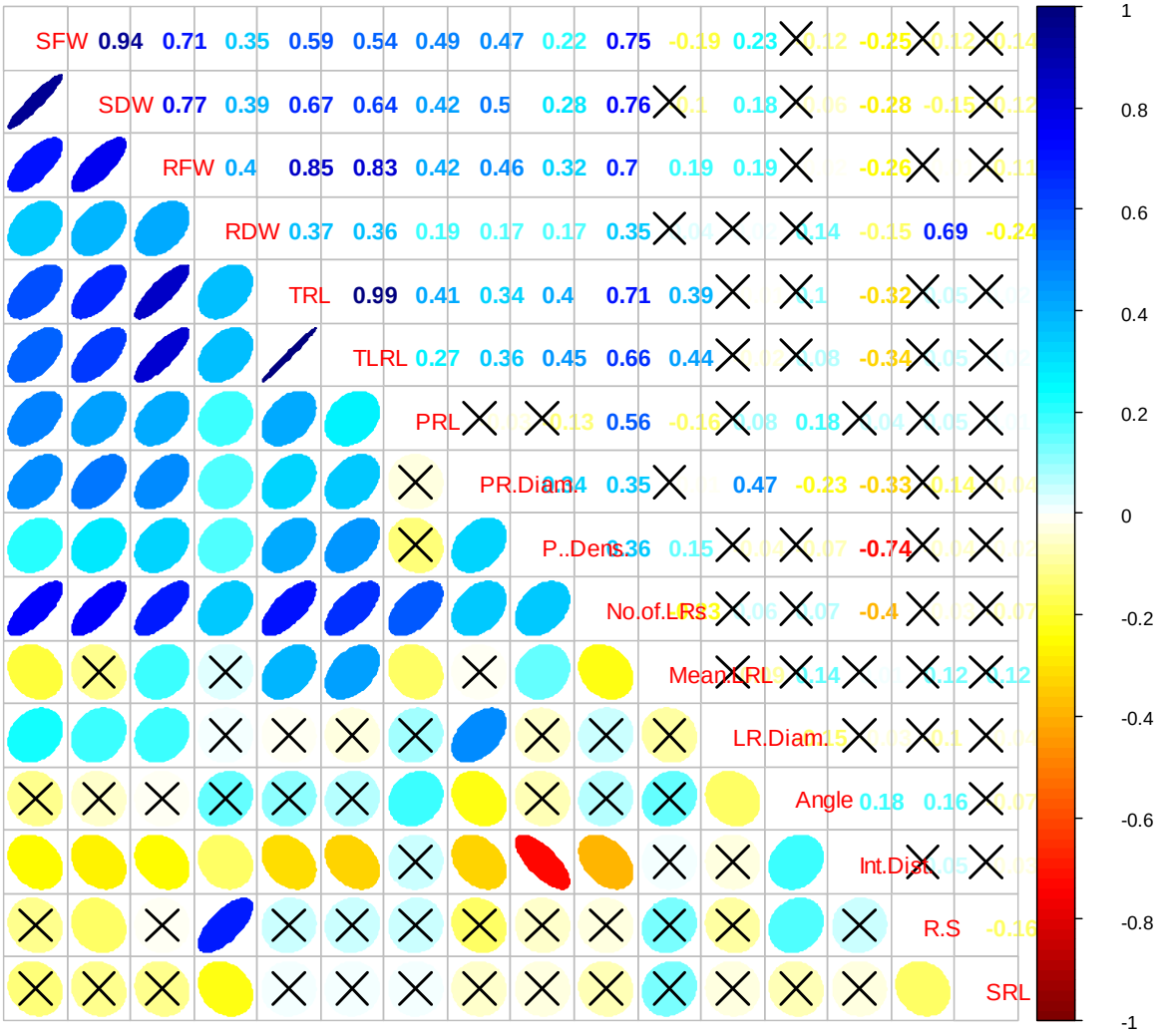


***Figure 4.2:*** *Pearson's correlation matrix for shoot and root traits of the 16 genotypes. The correlation coefficients are indicated by the colour and shape of the ellipse below the diagonal and the exact corresponding correlation coefficients are indicated above the diagonal of trait names in the matrix. The scale is indicated in the bar to right of the matrix. Non-significant correlations at p<0.05 are indicated by crosses. Trait names from top left to bottom right of the diagonal: SFW: Shoot fresh weight; SDW: Shoot dry weight; RFW: Root fresh weight; RDW: Root dry weight; TRL: Total root length; TLRL: Total lateral root length; PRL: Primary root length; PR Diam.: Primary root diameter; B. Dens.: Branching density; No. LRs: Number of lateral roots; mean LRL: Mean lateral root length; LR Diam.: Mean lateral root diameter; Angle: Mean lateral root insertion angle; Int. Dist: Mean Inter-branch distance; R:S: Root to Shoot ratio; SRL: Specific root length*

The PCA identified five significant axes of variation, accounting for approximately 86% of the variation in the genotypes studied (Table 4.2). The first and strongest principal component (PC) was mainly associated with traits related to size of the seedling, with shoot biomasses traits, total root and total LR length and number of LRs. The second PC was almost entirely associated mean LR length, whilst the third PC which could be described as the root branching component, was associated with genotype differences in PR length, branching density on the PR and inter-branch distance. The fourth and fifth PCs mainly explained differences in root-to-shoot ratio and diameters of the PR and LRs, respectively (Table 4.2).

***Table 4.2:*** *Principal components of the root traits space and the associated variation explained. Components with eigenvalues greater than 1 were considered significant (Tabachnick and Fidell, 1996). Traits contributing the most to a principal component are written in bold numbers.*

| | PC1 | PC2 | PC3 | PC4 | PC5 |
|---|---|---|---|---|---|
| SFW | **0.35** | -0.28 | 0.06 | 0.04 | -0.02 |
| SDW | **0.37** | -0.21 | 0.02 | -0.01 | 0.00 |
| RFW | **0.38** | 0.02 | 0.05 | -0.13 | 0.15 |
| RDW | 0.20 | 0.24 | **0.37** | **0.48** | 0.08 |
| TRL | **0.37** | 0.20 | 0.07 | -0.26 | 0.03 |
| TLRL | **0.36** | 0.25 | 0.01 | -0.25 | 0.06 |
| PRL | 0.18 | -0.28 | **0.41** | -0.17 | -0.15 |
| PR Diam. | 0.23 | -0.12 | -0.33 | 0.23 | **0.38** |
| B .Dens. | 0.21 | 0.28 | **-0.42** | 0.20 | -0.26 |
| No. of LRs | **0.35** | -0.16 | 0.08 | 0.02 | -0.28 |
| Mean LRL | 0.04 | **0.52** | -0.04 | **-0.39** | 0.37 |
| LR Diam. | 0.07 | -0.30 | -0.16 | 0.24 | **0.62** |
| B. Dist. | -0.19 | -0.16 | **0.40** | -0.29 | 0.35 |
| R:S | 0.00 | 0.37 | **0.45** | **0.46** | 0.09 |
| | | | | | |
| Eigen Value | 5.79 | 1.91 | 1.79 | 1.36 | 1.21 |
| % variation | 41.39 | 13.63 | 12.77 | 9.7 | 8.66 |
| Cumulative % variation | 41.39 | 55.02 | 67.79 | 77.49 | 86.15 |

Cluster analyses were conducted to evaluate if the PCA extracted features relevant to the inherent cluster structure of the data. Cluster analysis of the genotypes based on a trait space indicated that the genotypes formed 5 discrete groups with similar linkage distances

between the groups (Figure 4.3). The grouping of genotypes based on the root traits employed here appeared to be only partly related to their genetic background. For example, one of the parental genotypes (R500) was allocated toone discrete group, whilst RIL BraIRRI030 was clustered in the same group with the other parental genotype (IMB211). Inbred line BraIRRI380 also had a unique cluster, with the 4$^{th}$ and 5$^{th}$ clusters having 4 and 8 clusters respectively (Figure 4.3). Inferring from Table 4.1 and Figure 4.4, it could be seen that genotypes in groups 1 and 2 largely exhibited bigger biomass, increased TRL and increased number of LRs corresponding to traits identified on PC1. In contrast, genotypes in group 3 have reduced biomass and root length. These clusters could thus be referred to as the biomass and root size clusters. Whilst genotypes in cluster 4 appear to have longer PRs and could be located on PC3 , genotypes expressing longer inter-branch LRs with generally shorter mean LR length seem to be clustered in group 5 (Figs. 4.3 and 4.4).

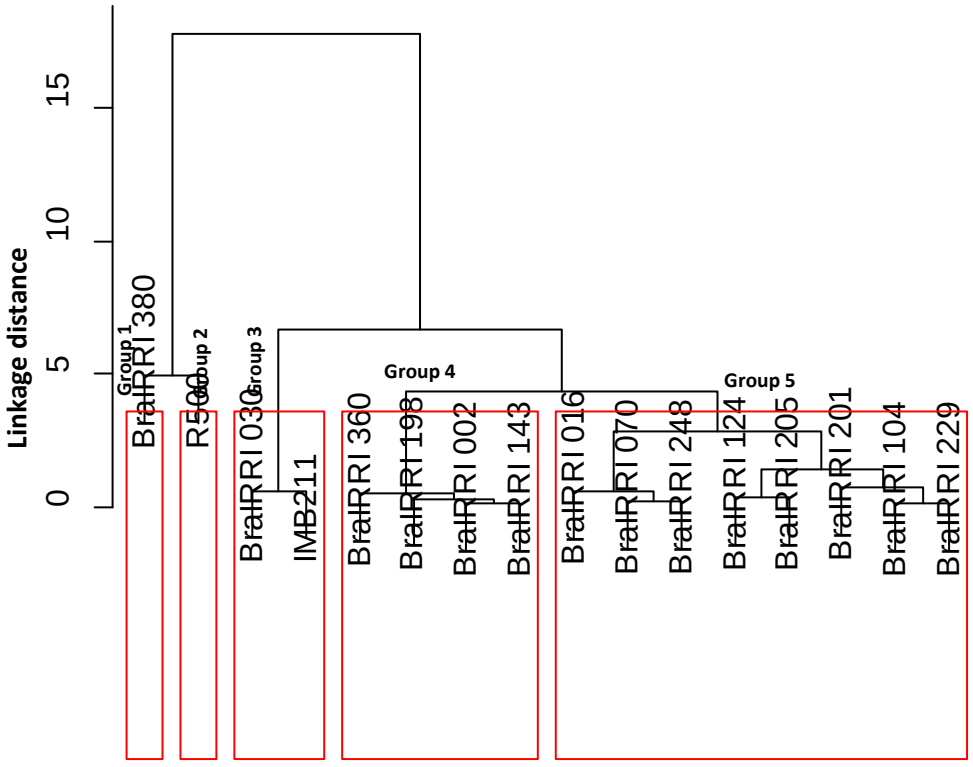


***Figure 4.3:*** *Clustering of 16* Brassica rapa *genotypes based on all measured shoot and root traits. The red-lined boxes indicate groupings of the genotypes.*

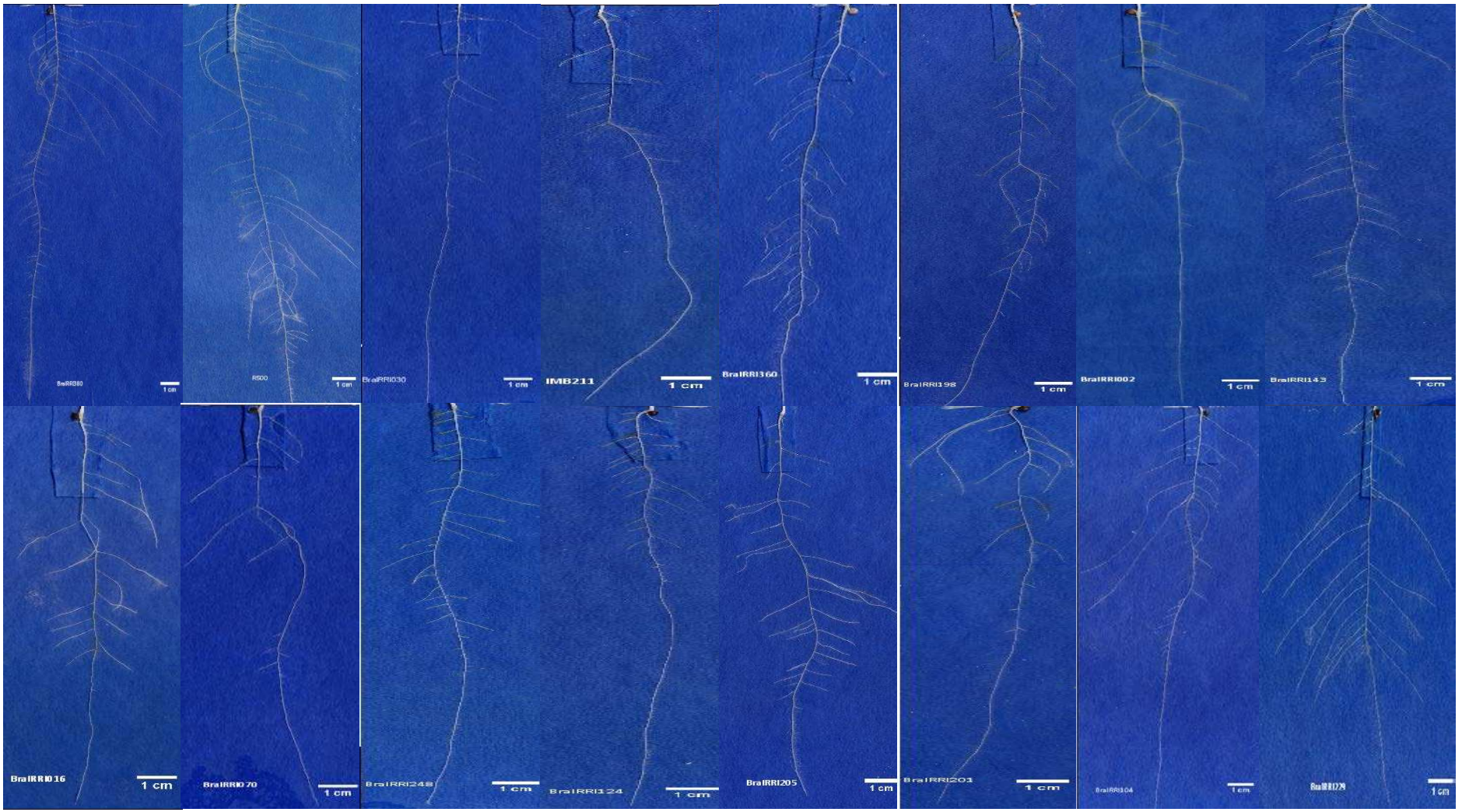


***Figure 4.4:*** *Examples of RSA images from the 16* Brassica rapa *seedlings studied. (Counting from top left, images 1 and 2 were grouped into clusters one and two respectively; images 3 & 4 in cluster three; images 5 to 8 in cluster four and images 9 to 16 in cluster five).*

The effect of genotype alone accounted for more variation in shoot traits than in root traits. The effect of genotype alone accounted for >56 % of the variation in shoot biomass, but only 8-19 % of the variation in root biomass. Genotype alone accounted for 36 % of the variation in PRL but only 13 % of the variation in TLRL. Genotype alone accounted for 27 % of the variation in LR branching density and only 6 % of the variation in the mean length of LRs. Genotype alone accounted for 34 % of the variation in PR diameter. In contrast, genotype alone accounted for none of the variation in LR diameter. The effects of genotype, and the effects of interactions between genotype x run, genotype x scanner and genotype x run x scanner accounted for most of the experimental variation (Table 4.3). A large amount of the variation in these traits was attributed to interactions between genotype x run and these traits also had the largest unexplained variation. A large proportion of the variation in root biomass (44-61 %) was attributed to interactions between genotype x run or genotype x run x scanner. The interactions between genotype x run and genotype x run x scanner accounted for 22 % and 69 % of the variation in PRL and in TLRL, respectively. The interactions between genotype x run, genotype x scanner and genotype x run x scanner accounted for 31% of the variation in PR diameter. The interactions between genotype x run and genotype x run x scanner accounted for 78 % of the variation in LR diameter. Unexplained (residual) variation was between 16 and 61 % of the total variation. Little variation in the traits assayed was attributed directly to run or scanner.

Broad-sense heritability was highest for shoot biomass traits (0.81 - 0.88), PRL (0.81) and number of LRs (0.73), Broad-sense heritability was intermediate (0.45-0.62) for root biomass, and LR insertion angle (0.56), and lowest (<0.25) for mean LR length, LR diameter and TLRL (Table 4.3).

***Table 4.3:*** *Sources of variation in shoot and root traits of seedlings of 16* B. rapa *genotypes*

| Trait | Percentage contribution by individual variance components | | | | | Heritability |
|---|---|---|---|---|---|---|
| | Genotype | Genotype x Scanner | Genotype x Run | Genotype x Scanner x Run | Residual | |
| SFW | 67.10 | 0.33 | 14.72 | 0.00 | 17.85 | 0.88 |
| SDW | 56.02 | 0.00 | 23.67 | 0.00 | 20.31 | 0.81 |
| RFW | 19.39 | 0.00 | 44.11 | 11.81 | 24.70 | 0.45 |
| RDW | 8.05 | 0.00 | 5.51 | 61.42 | 25.01 | 0.62 |
| TRL | 17.49 | 0.28 | 64.90 | 0.86 | 16.47 | 0.34 |
| TLRL | 13.32 | 0.81 | 68.51 | 0.32 | 17.04 | 0.27 |
| PRL | 36.20 | 0.00 | 10.61 | 11.64 | 41.56 | 0.81 |
| LRL | 5.51 | 3.93 | 38.79 | 5.20 | 46.57 | 0.19 |
| PR Diam. | 34.23 | 3.97 | 17.12 | 10.54 | 34.14 | 0.75 |
| B. Dens. | 26.51 | 3.07 | 13.30 | 0.00 | 57.11 | 0.70 |
| LR Diam. | 0.00 | 1.81 | 60.33 | 18.27 | 19.58 | 0.00 |
| No. LRs | 40.51 | 0.00 | 25.95 | 5.87 | 27.67 | 0.73 |
| Angle | 23.11 | 6.27 | 28.83 | 0.31 | 41.49 | 0.56 |
| B. Dist. | 24.16 | 1.24 | 13.85 | 0.00 | 60.75 | 0.67 |

### 4.2.2 The dynamics of root growth

Total and primary root lengths were first fitted with linear mixed effects model. Initial fits ignored the grouping structure in the data in order to investigate the homogeneity of variance and normality of the distribution of the residual. The plot of the residual showed that the variance of the residual varies with time (Appendix 1a), indicating a violation of the homogeneity assumption. The Normal Quantile-Quantile plot (Normal Q-Q, Appendix 1b) indicated that the distribution have a significant tail toward larger values of the TRL and PRL. To assess if there are differences among genotypes, a model with specific intercept and slope was fitted and this showed that genotype by DAS interaction had a significant effect ($p<0.05$), suggesting that growth patterns are different among genotypes (data not shown). Subsequently, suitable random effects and covariance structure for the model were determined. Results showed a negative correlation between the intercept and slope (Appendix 2). This correlation was removed by centring the data so that the intercepts of all curves are 0. Variability in parameter estimates were observed, suggesting that it was

necessary to estimate separate intercepts and, in some cases, separate slopes to account for genotype-to-genotype variability. These variations indicated it would be informative to use the genotype as a random effect. On the whole, the use of mixed effect model was also motivated by the data being repeated measures on each genotype.

#### *4.2.2.1 Total root length: linear mixed-effects model*

Linear mixed-effects model (eqn. 4.3) was first fitted considering the interaction of the covariate DAS and experimental run ($das_{jk}$) as fixed effects and including the effect of genotype ($g_i$) as a random effect. The best performing model and thus the chosen linear model incorporated random intercepts and slopes (eqn. 4.3). The estimated AIC, BIC and log-Lik values were 158.32, 204.14 and -68.16 respectively and were lower (AIC & BIC) and higher (logLik) than other models assessed. Other models that were assessed either excluded random intercepts or slopes, or incorporated a function to account for within-group heteroscedasticity (model with variance function excluded random intercepts and slopes to allow convergence) (Appendix 3). The fitted linear model (Eqn. 4.3) showed that 19.45% and 50.39% and 30.16% variability in TRL is attributable to the genotypic, experimental and residual effects, respectively. The relationship between the fitted and observed data for the TRL can be seen in appendix 4a. Root growths of many genotypes in the second run exhibited larger root system than their corresponding lines in run one (Appendix 4a). The assumption of normalised residuals for each genotype was confirmed by normal plots of residuals (Appendix 5). The final parameters estimated for fixed and random effects for the 16 genotypes screened in two runs are shown in Appendix 6.

#### *4.2.2.2 Primary root length: linear mixed-effects model*

The same linear mixed effect models tested in 4.2.2.1 were used to model PRL. Models showed that intercepts and slope differ for genotypes ($p<0.05$). Primary root length was

influenced by genotype (40%), environment (39%) with a 21% residual term. The relationship between the fitted and observed data for the PRL can be seen in appendix 4b. The AIC, BIC and logLik of the best performing and chosen model (eqn. 4.3) were 1256.47, 1302.2 9 and -617.23 respectively. This model was compared with other models which either excluded random intercepts or slopes, or incorporated a function to account for within-group heteroscedasticity (Appendix 3). The assumption of normalised residuals for each genotype was confirmed by normal plots of residuals (Appendix5b). The final parameters estimated for fixed and random effects for the 16 genotypes screened in two runs are shown in Appendix 6.

#### *4.2.2.3 Non-linear mixed effect model*

The linear model appeared to fit the data well, but initial exploration of the data had also suggested that increments in root length appear to decrease with time as seedlings grow and accumulate more biomass. Indeed, growth processes are usually better modelled using logistic growth functions partly because such functions are able to test biologically meaningful parameters (Calegario *et al.*, 2005; Hunt, 2003; Paine *et al.*, 2012; Peek *et al.*, 2002). Thus, to account for the non-linearity in root growth curves, the data was also subjected to non-linear mixed effect models. Non-linear mixed effect models considered the TRL, PRL and LRGR as response variable and DAS as covariate. Since the plots of TRL and PRL as a function of DAS were S-shaped, an extension of the model is to model the change of TRL and PRL with time using a 3-parameter logistic model. The first model incorporated random effects for all parameters. The plot of standardised residuals for this model revealed that there is an increasing variability for the within-group error (Figure 4.5a). We therefore, in the subsequent model, accounted for within-group heteroscedasticity using a power variance function (Eqn. 4.5) and this improved the predictions of the model (Figure 4.5b). To

account for autocorrelation (when there is periodicity in the error) we also included in the next model, a corAR1 correlation structure representing an autocorrelation of the order 1.

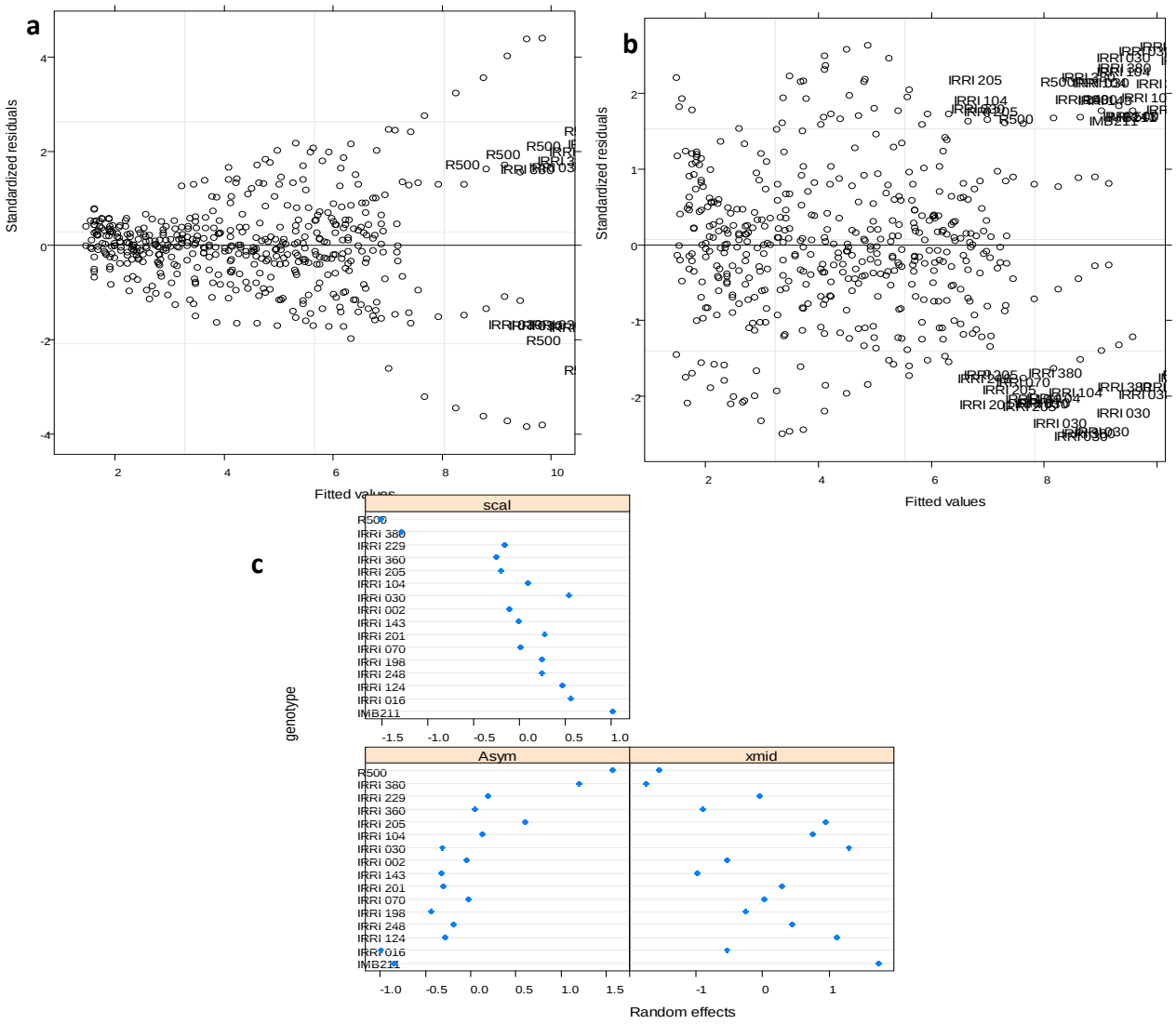


***Figure 4.5:*** *Diagnostic plot for fitted values vs. standard residual for TRL model without (a) and with (b) variance function; (c) Estimates of random effects by genotype in 1st fitted non-linear mixed-effects model for TRL*

All three parameters varied with genotype. The asymptote was larger for one of the parental genotypes (R500) and lower for inbred line BraIRI016 (Figure 4.5c). The most informative model however included only a single, random-effect parameter (the asymptote, $\emptyset_1$, Equation 4.4) describing the effect of genotype on the growth in length of the total or the primary root system. The assessment of the adequacy of the most

informative (single random effect on the asymptote) models is seen in the plot of fitted and observed data in Figures 4.6 (Figure 4.6 shows plot for 7 sampled genotypes out of 16). Normal plots of residuals for each genotype indicated that residuals are normalised for each genotype (Figure 4.8).

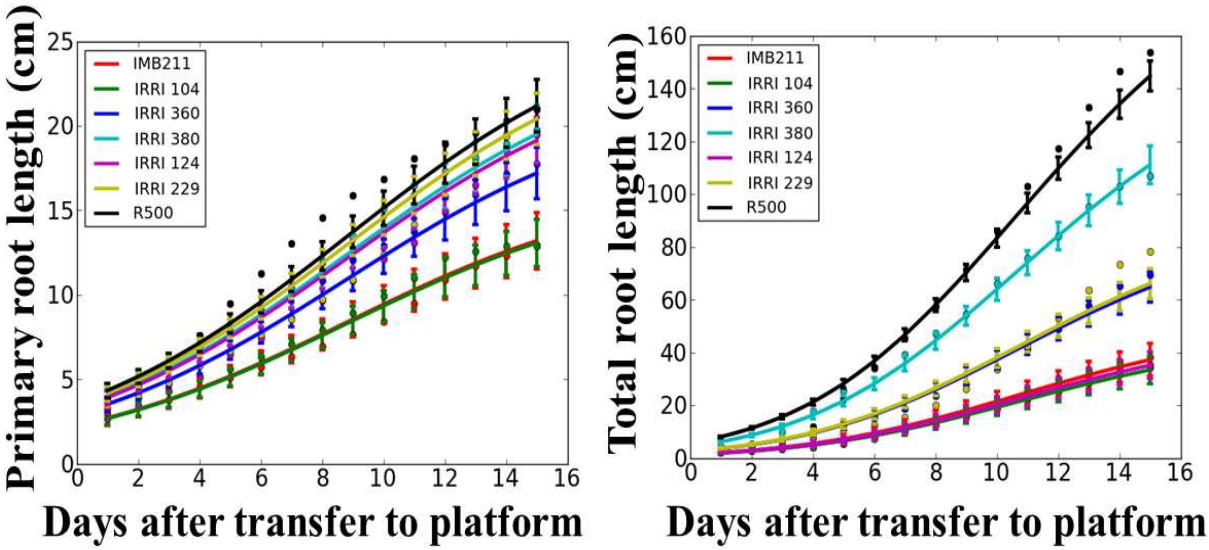


***Figure 4.6:*** *Measured (circles) and predicted (lines) values of (a) PRL and (b) TRL of the two parents and five RILs of the* Brassica rapa *BraIRRI mapping population over the 15 d following transfer to the phenotyping platform. Predicted values were estimated using a nonlinear mixed-effects model (Equation 4.4).*

A three-parameter logistic model where the lower horizontal asymptote is fixed at zero and the inflection point describes the time in DAS when absolute root growth rate (cm $d^{-1}$) is maximised was employed to analyse total and primary root length. Parameter estimates from the model was applied individually to fit total and primary root growth of each genotype. The inflection point ($Ø_2$) and scale parameter of the logistic growth function ($Ø_3$) were constants across all genotypes studied. Asymptotes for the TRL and the PRL differed between genotypes (Table 4.4). Values for the inflection point and scale parameter of the logistic growth function describing TRL were 10.4 DAS and 0.310, respectively. Asymptotes for TRL ranged from 37.3 to 126.6 cm. The parental genotype IMB211 had the lowest asymptote and the parental genotype R500 had the highest asymptote of all the genotypes assayed (Table 4.4). Values for the inflection point and scale parameter of the logistic

growth function describing PRL were 8.82 DAS and 0.211, respectively. Asymptotes for PRL ranged from 17.0 to 29.0 cm. The parental genotype IMB211 had an asymptote of 17.4 cm and the parental genotype R500 had an asymptote of 28.3 cm. These observations are consistent with the measurements of PRL and TRL assayed 15 DAS (Table 4.1).

#### *4.2.2.4 Growth rate of lateral roots*

The relationship between the growth rate of first order LRs and days after transfer to the phenotyping platform followed a quadratic function for all genotypes (Figure 4.7). Basal LRs generally had faster elongation rates than those that emerged later. The maximum LR elongation rate predicted by the model fitted to the data was 0.35 cm $d^{-1}$ for IRRI104 five days after transfer to the phenotyping system. The most informative model included only one, random-effect parameter ($b_{i1}$, Equation 4.6) describing the effect of genotype on the initial growth rate of LRs. The model also included a correlation structure and variance function. The initial growth rate ($b_{i1}$ + $\beta_1$) of LRs differed between genotypes (Table 4.4). Values for $b_{i1}$ + $\beta_1$ ranged from 0.216 to 0.307 cm $d^{-1}$. The parental genotype IMB211 had a value of 0.255 cm $d^{-1}$ and the parental genotype R500 had a value of 0.290 cm $d^{-1}$. Model assessment with plots of residuals suggested that the model was satisfactory (Figure 4.8), although unexplained residual errors were greater than those for the models for either the length of the PR or the total length of the root system.

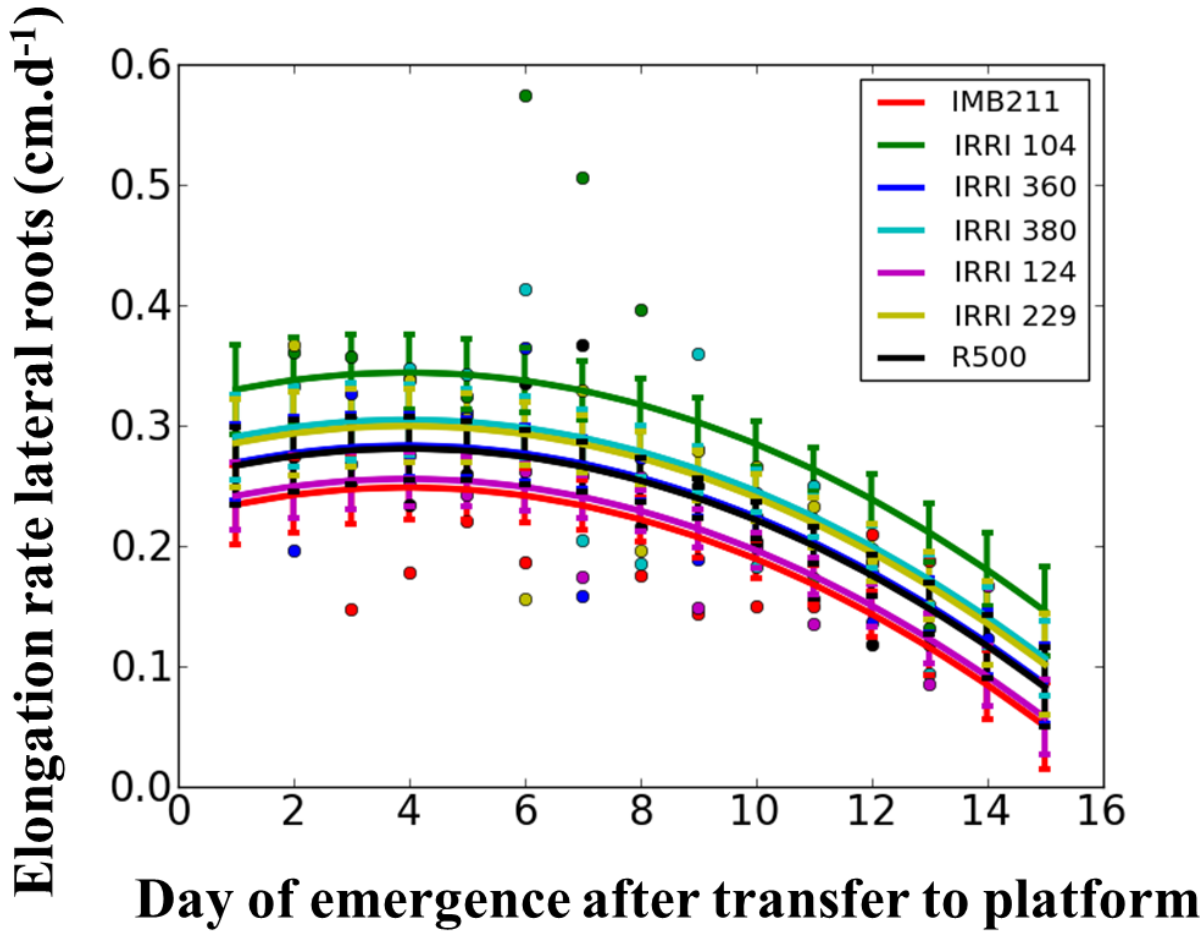


***Figure 4.7:*** *Measured (circles) and predicted (lines) values of the elongation rates of LRs of the two parents and fourteen RILs of the* Brassica rapa *BraIRRI mapping population as a function of the time of their emergence after transfer to the phenotyping platform. Predicted values were estimated using a nonlinear mixed-effects model (Equation 4.6).*

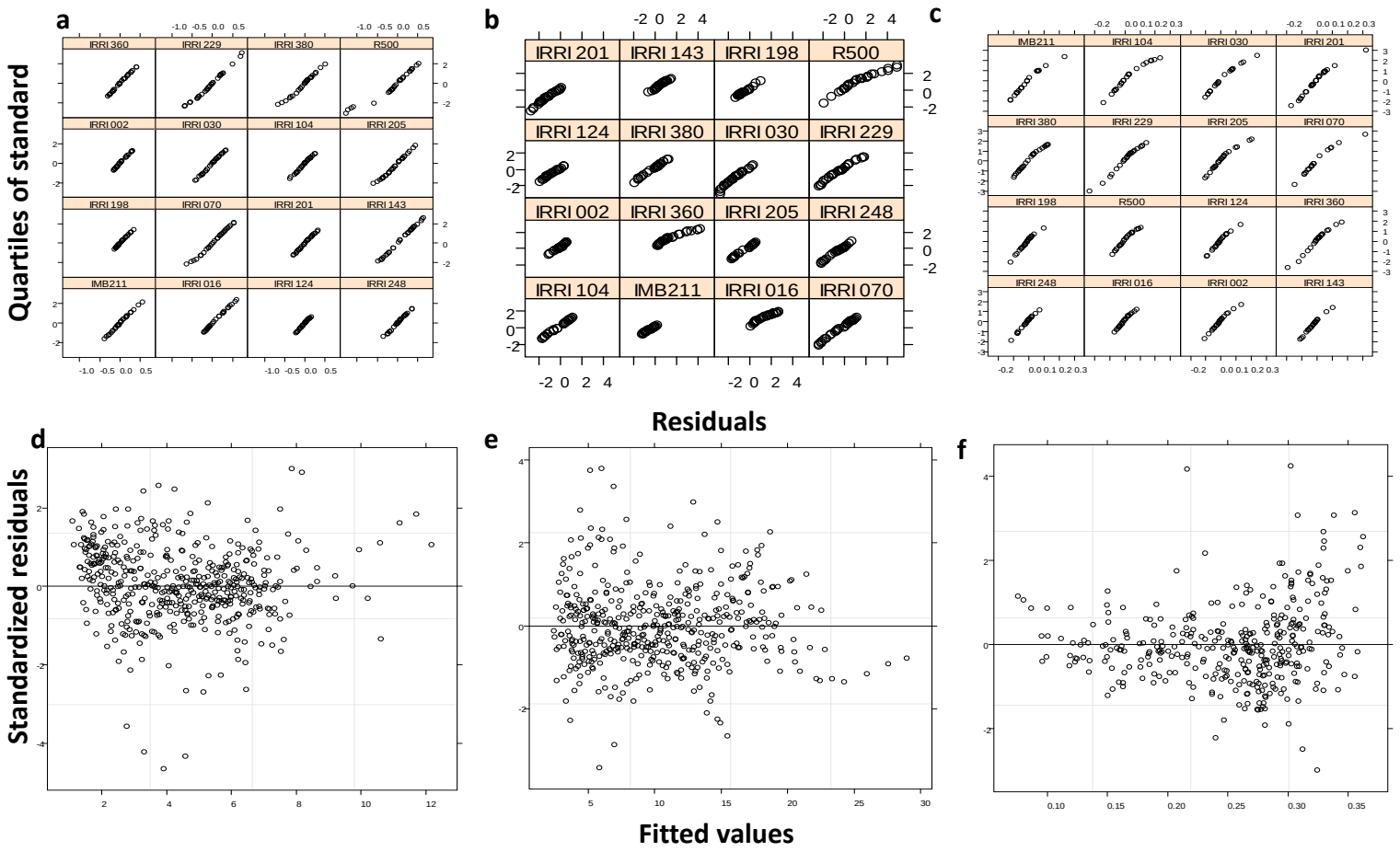


***Figure 4.8:*** *Examples of diagnostic plots for the three dynamic root traits investigated: normal plot of residuals by genotype for TRL (a), PRL (b), LRGR (c); fitted values for standardised normal for TRL (d), PRL (e) and LRGR (f).*

***Table 4.4:*** *Estimates of the asymptotes ($\emptyset_1$, Equation 4.4) for mixed effects models describing temporal variation in total and primary root length, and the intercept ($b_{i1} + \theta_1$, Equation 4.6) for the mixed effects model describing the growth rate of 1st order LRs among the parents (IMB211, R500) and 14 RILs of the* Brassica rapa *BraIRRI mapping population grown for 15 days in the phenotyping platform*

| | **IMB211** | **R500** | **IRRI 002** | **IRRI 016** | **IRRI 030** | **IRRI 070** | **IRRI 104** | **IRRI 124** | **IRRI 143** | **IRRI 198** | **IRRI 201** | **IRRI 205** | **IRRI 229** | **IRRI 248** | **IRRI 360** | **IRRI 380** |
|---|---|---|---|---|---|---|---|---|---|---|---|---|---|---|---|---|
| **Total Root Length** | 37.3 | 126.6 | 64.2 | 49.4 | 47.8 | 56.8 | 55.9 | 47.5 | 61.1 | 56.1 | 53.5 | 61.3 | 67.6 | 52.6 | 71.5 | 113.7 |
| **Primary Root Length** | 17.4 | 28.3 | 22.3 | 17.0 | 22.9 | 19.1 | 17.1 | 20.3 | 25.4 | 29.0 | 26.5 | 21.1 | 22.5 | 23.5 | 19.1 | 24.0 |
| **Lateral Growth Rate** | 0.255 | 0.290 | 0.255 | 0.273 | 0.307 | 0.285 | 0.326 | 0.262 | 0.216 | 0.234 | 0.263 | 0.296 | 0.295 | 0.233 | 0.281 | 0.297 |

### *4.3 Discussion*

Breeding for roots with efficient resource acquisition traits requires screening of large populations of genotypes, which necessitates high-throughput, low-cost phenotyping platforms. The study reported here provides an assessment of the genetic variation in root properties of *Brassica rapa* genotypes and demonstrates the potential of the high resolution root phenotyping platform developed here.

Using parents and RILs of *Brassica rapa*, we examined and observed significant differences between genotypes in static root traits including lengths of the total root system, the primary and lateral roots, and also in branching density, angles, inter-branch distances of laterals and root diameters. The range of values recorded for static root traits may not necessarily represent the full extent of genetic variation for the traits measured in BraIRRI mapping population, as we tested only the parents and selected set of inbred lines. Even so, significant variation in root traits observed here suggests that the BraIRRI population is suitable for QTL analysis (Ali *et al.*, 2000). It is difficult to compare results here with other published data as root trait information for *B. rapa* grown for similar duration and under comparable conditions is rare. Correlations among root traits observed here is however consistent with that reported by Lu *et al.* (2008). Significant positive correlation among pairs or root traits may be a sign that QTLs for certain pairs of root traits would be mapped to similar genomic regions. Highly positive correlations are also likely to be associated with QTLs with large effects (Ali *et al.*, 2000; Materechera *et al.*, 1992).

A PCA was employed to determine which combinations of traits contributed more to the phenotypic variability in the reference population. Five PCs were identified in this study and PC1 which represented 41.39% of the variation was most affected by parameters predominantly describing biomass and length and therefore related to size of the root system. Most of the traits, which are not directly describing root system size such as angle and diameter contributed less or did not significantly contribute to PC1 variation. Therefore, consistent with the report of Fita *et al.* (2008), low values of PC1 correspond to genotypes with smaller root system size. High PC2 values also appear to correspond to root systems with long lateral roots illustrated by the high weight of the mean length of the lateral roots. PC3 was negatively affected by branching density and positively by inter-branch distance and primary root length. It was not entirely surprising that root-to-shoot ratio and root dry weight was both represented also on PC3 as one is the determinant of the other. What was however interesting was the fact that the other determinant of root-to-shoot ratio, shoot biomass, was not significant on the PC3. Generally, it appears that PC3 explains variations in primary root-related traits such a length and branching density on the primary root.

Cluster analyses of the genotypes was conducted to identify inherent natural groups in the data and included all shoot and root traits measured. Results of cluster analyses were consistent with that of PCA, providing additional insights to the observed PCA-based dimension reductions of the data. Broadly, cluster analysis resulted in five groups comprising largely of genotypes with a combination of bigger shoot and root biomass / increased total root length and number of laterals or genotypes with longer primary roots or genotypes with wider inter-branch distances and shorter mean lateral root length. The group composition to some extent reflected the genetic background of the genotypes and

was consistent with the report of Manschadi *et al.* (2008). For example, inbred line IRRI030 was observed to have shorter, few and highly spaced lateral roots resulting in a smaller root system length and this was clustered with the parent, IMB211 which shares similar characteristics. Also, the inbred line IRRI380 has bigger biomass and root system length, quite similar to the parental genotype R500 and was clustered in distinct group but with similar linkage distance as R500. Similarly, RILs including IRRI198 and 360 with longer primary root length was in one group whilst, 070, 016 and 229 with shorter PR length, mid-LR length between that of the two parents, few and highly spaced laterals were also in one group. It thus suffices to say that genotypes which were grouped together may share stress similar adaptive response mechanisms. The relationships between the genotypes may therefore be important in phenotypic selection and adoption of genotypes for particular environments.

Broad-sense heritability, was highest for shoot biomass traits, the length, branching density and diameter of PRs, number and diameter of LRs (≥ 0.70), intermediate (0.45-0.67) for root biomass, LR insertion angle and inter-branch distance and lowest (<0.3 5) for total length of laterals of the whole root system , diameter and mean length of LRs (Table 4.4). Coefficient of variations obtained from previous studies (Chapter 3, Table 3.2), for traits such as primary root length (15 - 34%), branching density (15 - 65%) and number of LRs (19 - 35%) could be considered relatively high. These traits also recorded high heritability in the present study. Broadly speaking, this suggest that traits with large differences between genotypes and low variation within a genotype (i.e. high hereditability) require less replication to detect significant differences between genotypes than traits with either small differences between genotypes or low hereditability.

Many of the static traits described above also show temporal variation with significant effects of genotype on the dynamics of root growth (Table 4.4, Appendix 4; Figures 4.6 and 4.7). Root growth measured in length increments of the total root system and the primary root over time were statistically analysed by both linear and non-linear mixed-effects models. Considering that variability attributable to genotype was 19.5% for TRL and 40.0% for PR, it could be said that PRL growth is more linear than the growth of the total root system. This assertion is also supported by the fact that unexplained variation encountered by the linear model was higher for TRL (30.16%) than PRL (21.0%). Nevertheless, the length of the primary root and total length of the root system follow a sigmoidal growth function with time (Figure 4.6) and the elongation rate of lateral roots follows a quadratic function with day of emergence from the primary root (Figure 4.7). Data for primary root length and the length of the root system indicated that all genotypes follow a similar growth pattern with time, but differ in their absolute growth rate. Data for the elongation rate of lateral roots also indicated that all genotypes follow a similar pattern with time, but differ in their maximum growth rate. One utility of the non-linear modelling approach is that the parameters of the logistic equation (Eqn. 4.4), can be interpreted biologically where $Ø_{i1}$ is the asymptote parameter (maximum root length), $Ø_{i2}$ is the inflection point (time or age at which ½ of maximum root length occurs) and $Øi_3$ is the scale parameter (distance in DAS from the inflection point to the point where the height is 73% of the maximum root length (Calegario *et al.*, 2005).

The results presented in this chapter show roots show dynamic patterns. Since the elongation rate of roots is not constant, the length of a root is not directly related to the age

and the time it has been exposed to local soil resources. Root systems of plants grown in soil are exposed to temporal and spatial heterogeneity in, for example, temperature, soil strength, aeration, the availability of water and essential mineral elements, exposure to toxic substances, and contact with soil biota. Mechanisms underlying dynamic response of roots to changes in such environmental cues would be better understood with models and analyses developed to characterise these responses such as the mixed effects modelling approaches described here. Root responses could be quantified across genetic mapping populations and to identify genetic factors affecting root responses to the environment. The ability to characterise dynamic responses to environmental variables will allow researchers to develop more efficient marker-assisted selection of genotypes adapted to multiple soil types and environmental conditions (Acuña and Wade, 2013; de Dorlodot *et al.*, 2007; Gerald *et al.*, 2006; Hochholdinger and Tuberosa, 2009; Hodge *et al.*, 2009).

### *4.4 Summary*

• Significant differences were found between genotypes in static root traits including lengths of the total root system, the primary and lateral roots, and also in branching density, angles, inter-branch distances of laterals and root diameters.

• Significant positive correlations were found among pairs of root traits and could indicate the effect of closely linked genes. Chromosomal loci for certain pairs of root traits would thus be mapped to similar genomic regions and highly positive correlations observed here could be associated with QTLs with large effects.

• Five PCs explained the variability within the data. Plant size explains larger proportion of the total variability within the population. Other important factors that explain variation within the population are branching density, number of laterals, root-to-shoot ratio and root diameter.

• Cluster analysis resulted in five groups each comprising of genotypes with a combination of bigger biomass and increased total root length or longer primary roots or genotypes with wider inter-branch distances and shorter mean lateral root length. The group composition to some extent reflected the genetic background of the genotypes.

• Broad-sense heritability, was highest for shoot biomass traits, the length, branching density and diameter of PRs, number and diameter of LRs, intermediate for root biomass, LR insertion angle and inter-branch distance and lowest for total length of laterals the whole root system, diameter and mean length of LRs.

• Static root traits show temporal variation with significant effects of genotype on the dynamics of root growth. These traits include growth of the total root system, primary and lateral roots.

• Whilst primary root growth appears to be more linear than the growth of the total root system, the general trend of both follows a sigmoidal growth function with time. Elongation rate of lateral roots is quadratic and indicate that all genotypes follow a similar pattern with time, but differ in their maximum growth rate.

# CHAPTER 5 : SCANNER-BASED IMAGING OF ROOT GROWTH DYNAMICS IN SOIL-FILLED RHIZOBOX SYSTEMS

## 5.0 Introduction

Plants are adaptable and responsive to their local environment. For example, high soil bulk density decreased root growth of barley seedlings (Bingham and Bengough, 2003). Similarly, high soil water availability caused a reduction in the number and length of lateral roots in *Triticale* (Grzesiak *et al.*, 2002). Local soil P availability led to various alterations in RSA (Dai *et al.*, 2012; Lopez-Bucio *et al.*, 2002). This has led to the development of many lab-based techniques, employing root growth cultures which are approximations of field conditions to quantify RSA (Dai *et al.*, 2012; Dupuy *et al.*, 2010a; Faget *et al.*, 2013; Galkovskyi *et al.*, 2012; Gregory *et al.*, 2009; Iyer-Pascuzzi *et al.*, 2010; Lopez-Bucio *et al.*, 2002; Nagel *et al.*, 2012).

Root system phenotyping through imaging requires the use of a rooting medium that is cheap, provides repeatable root growth conditions over time (Crush *et al.*, 2005). It is also desirable that the rooting media used increase the contrast between roots and their background and so ease the process of image analyses (Mairhofer *et al.*, 2013). Artificial rooting media such as agar or gels (Gruber *et al.*, 2013; Jain *et al.*, 2009; Yazdanbakhsh and Fisahn, 2012) and paper pouches (Hund *et al.*, 2009; Liao *et al.*, 2001) have been used successfully to screen crop plants for variation in root system characteristics. However, the limitations include the absence of microbial interactions, soil structure and in most cases, absence of mechanical impedance. In some cases, it is also challenging to adequately simulate heterogeneity of water and nutrient availability typically observed along soil profiles (Hutchings and John, 2004; Nagel *et al.*, 2012). Moreover, the mineral concentrations and ionic potentials of commonly used artificial rooting media could exceed

those found in soils (Foehse and Jungk, 1983; Gruber *et al.*, 2013; Jain *et al.*, 2009). Thus, despite the ease and tractability of image analysis of root systems grown on artificial media, there are concerns regarding the effect these environments might have on root development (Mairhofer *et al.*, 2013).

Soil-filled chambers (rhizoboxes) are an alternative that provides the closest naturalistic conditions for screening plant root systems under controlled environments. Transparent soil-filled columns or rhizoboxes are popular because they permit non-invasive repeated measurements of the same roots at frequent time intervals and can be used to explore the dynamics of root water uptake of the root system (Garrigues *et al.*, 2006). Compared to soil in the field, roots can readily be recovered from soil-filled chambers and such systems can be scaled up to accommodate large numbers of plants. However, despite the extensive use of rhizoboxes and artificial rooting media, it is not certain root system data obtained from soil growth media is representative of the actual harvested root traits data or correlate with data obtained from artificial substrates such as paper pouches.

In this Chapter, the parents and 10 RILs of the BraIRRI mapping population used previously in filter-paper based studies were analysed. The soil-filled rhizobox study was used to estimate the number of replicates required to detect differences in traits contributing to RSA between genotypes of *Brassica rapa* L. The genotypic, environmental and temporal variations in root traits in soil-filled rhizobox were also quantified. Root growth dynamics was expressed as length of the total root system and the primary root, and the growth rate of first order lateral roots. We also assessed whether the part of the root system visible at the transparent face of the rhizoboxes is representative of the total root system. In addition,

we also tested for correlation between soil-based and filter-paper based techniques used previously (Chapter 4).

## *5.1 Materials and Methods*

### 5.1.1 Plant material and soil cultivation protocols

The parents (cv. IMB211 and cv. R500) and 10 RILs including BraIRRI 002, 016, 030, 104, 124, 198, 201, 229, 360 and 380 were used in this study. The rhizoboxes, adapted from Bengough *et al.* (2004) as described in Chapter 2 (Section 2.1.4; Figure 2.7), consisted of two polyvinylchloride plates (30 × 21.5 × 0.3 cm), one transparent and the other made of an opaque polythene sheet (Section 2.1.4). The rhizoboxes were filled with topsoil (0-10 cm depth) collected from a site near the James Hutton Institute, Dundee, Scotland (NO 456 265). The soil was typical of arable soil of the region and defined as a Cambisol (FAO-UNESCO Classification) (George *et al.*, 2011a). The sieved soil, prepared as described hitherto in Chapter 2 (Section 2.1.6.2), was left un-amended and was watered with deionised water to approximately 80% field capacity on gravimetric water content basis prior to planting (George *et al.*, 2011a). All environmental conditions were maintained as described in Section 2.1.1. Seedlings were grown in six replicates in two independent experiments. Twenty four scanners were employed and with three replicates per scanner, the rhizobox system allowed the imaging of the root growth of 72 seedlings for 15 days after sowing. Rhizoboxes were fixed to scanners in “portrait” orientation in near vertical position as shown in Figure 5.1 and images were captured at 12 hour intervals. Data analyses of root growth were based on daily measurements.

***Figure 5.1:*** *Setup for phenotyping roots in soil-filled rhizoboxes showing 24 scanner positions arranged in rows of 6. The inclination angle of the scanners and hence rhizoboxes was adjusted to approximately 75°.*

### 5.1.2 Extraction of geometric features and root growth information

At harvesting, roots were excised from shoots and carefully washed out of the soil. Root systems were individually placed in water-containing 150 mm sterile polystyrene Petri dishes and scanned with Epson Expression 10000 XL scanner. Morphological features including length, area, volume and diameters were measured with *WinRhizo*, (Version 2012b, Regent Instruments) with grey value threshold 30; removal of objects with an area <1 $cm^2$ and a length-to-width ratio <4 (Nagel *et al.*, 2012). Geometric information from captured images was also extracted with *SmartRoot* software (Lobet *et al.*, 2011) (Section 2.3.3.1) and total root length measured with *WinRHIZO* was compared to the total visible root length obtained with the scanners. Root growth information was extracted with *SmartRoot* (Lobet *et al.,* 2011) by first, tracing all root axes (primary and lateral roots) on the

last image (image at 15 DAS when the root axes were longest). The initial tracing was then used as the starting point for the tracing of the preceding image at DAS 14 which is obtained by removing the portion of roots that have been created between DAS 14 and DAS 15. The same process is repeated until the root system from the first day of experiment is traced.

### 5.1.3 Statistical analysis

Descriptive statistics for all traits were calculated. An estimate of the standard deviation and the mean (± standard error) were obtained and the first divided by latter to obtain an estimate of the coefficient of variation (CV) as a percentage of standard deviation to the trait grand mean. Root trait data from the parents of the population (cv. R500 and IMB211) were used to calculate the number of replicates (*R*) that would be required to detect a significant difference between the means of two populations with identical standard deviations in a trait using a two-sided, 95% confidence interval (CI), t-test, if the trait means differed by 50%. Since this involved a study comparing two means, there was slight modification of Equation 3.1 and the equation used here incorporated the desired statistical power (Eng, 2003):

$$R = \frac{4\sigma^2(z_{crit} + z_{pwr})^2}{D^2} \qquad (\mathbf{5.1})$$

where: *R* is the total sample size, $\sigma$ is the standard deviation of both groups, the $z_{crit}$ value is the standard normal deviate given in normal score tables and corresponding to the confidence interval of 95% (1.96), the $z_{pwr}$ is the standard normal deviate corresponding to 0.80 statistical power and *D* is the minimum expected difference between the two means (50%). *R* represents the sum of the sample sizes of both comparison groups and $\sigma$ is assumed to be equal for both groups.

Pearson's correlation coefficients between all trait combinations were determined and PCA analysis was performed. Significant components were chosen by the 'eigenvalue >1' rule (Tabachnick and Fidell, 1996). Cluster analysis was conducted on all the traits pooled together to identify discrete groups of lines with similar RSA traits among the reference population studied. Clustering was performed using Ward's hierarchical approach based on minimum variance linking method with Euclidean distance as the similarity measure (Manschadi *et al.*, 2008). Optimal number of clusters was chosen based on the 'elbow-criterion' which compares the Sum of Squared Differences (SSD) for different cluster solutions (Thorndike, 1953).

Genotypic variability was analysed with three-way ANOVA. The sources of variation in static root traits among the genotypes were determined using a mixed effects model with experiment (run), scanner and genotype considered as random factors using Equation 4.1. Except for *s* (the number of genotypes, i.e. 12), all parameters in Equation 4.1 remains unchanged in the present analyses. ANOVA was also performed on some traits (SDW, TRL, number of LRs and mean LRL) between data generated here and data generated in Chapter 4 when seedlings were grown on seed germination paper. Broad-sense heritability ($H^2$) was estimated as $\sigma_g^2 \ /\sigma_p^2$, where $\sigma_g^2$ is the estimated variance associated with the genotypic effect and $\sigma_p^2$ is the total variance for the trait.

The sources of variation in dynamic root traits were determined using mixed effects models with genotype and experiment considered as random factors. To account for non-linearity in growth curves, a logistic growth function was used to model the increase in total root length and primary root length with time using three parameters of the logistic function as detailed

in Equation 4.4. Due to an additional random effect parameter utilised for the modelling of total root length, Equation 4.4 was slightly modified:

$$y_{ij} = \frac{\emptyset_{i1}}{1 + \exp[-(DAS_j - \emptyset_{i2})/\emptyset_{i3}]} + \boldsymbol{\epsilon_{ij}}, \quad (\mathbf{5.2})$$

$$\emptyset_i = \begin{bmatrix} \emptyset_{i1} \\ \emptyset_{i2} \\ \emptyset_{i3} \end{bmatrix} = \begin{bmatrix} \beta_1 \\ \beta_2 \\ \beta_3 \end{bmatrix} + \begin{bmatrix} b_{i1} \\ b_{i2} \\ 0 \end{bmatrix},$$

$$i = \{1, \dots, s\}, j = \{1, \dots, t\},$$

$$b_{i1} \,\&\, b_{i1} \sim N\,(0, \sigma_b^2), \epsilon_{ij} \sim N\,(0, \sigma^2).$$

Definitions of all parameters remains unchanged from Equation 4.4 but here, $b_{i1}$ and $b_{i2}$, are respectively the random effect on the asymptote and inflection point of the logistic function. The sources of variation in the growth rate of lateral roots were determined using Equation 4.6. Data for growth rates of lateral roots were normalised by square root transformation. The structure of the mixed effects models described were chosen based on Akaike and Bayesain information criteria and model quality was also assessed visually using quantile-quantile and residual plots as in Chapter 4. Statistical analyses were performed using GenStat (GenStat Release 14.1, VSN International, Oxford, UK) and *R* software and the nlme library (Pinheiro *et al.*, 2008; Pinheiro and Bates, 2000; R Core Team, 2008).

## *5.2* Results

### 5.2.1 A rhizobox platform for high-resolution quantification of root architectural development

The low-cost and simple scanner-based root phenotyping system for high-resolution quantification of RSA development was adapted to soil-filled rhizoboxes made from PVC plates equipped with transparent root observation windows (Bengough *et al.*, 2004). The

adapted scanner-based rhizobox system allowed non-destructive measurements of root growth along the observation window and followed with time by taking images at regular intervals with scanners attached to rhizoboxes and *ArchiScan* (Section 2.2.1), the image acquisition software (Figure 5.1). Plants grew vigorously in this system, and with no apparent symptoms of mineral deficiencies. The experiment allowed also detailed quantification of architectural parameters of root systems at the end of experiments and also information on the dynamics of global characteristics of root systems from the images.

Only the roots reaching the surface of the observation windows can be observed and measured by image analysis non-destructively. The proportion of roots reaching the surface of the observation window (total visible root length) (Figure 5.3) ranged from 42.6 to 98.9% (average of 85%) of the actual or harvested total root length (total root length). On a limited number of occasions (8.3% of measurements taken), total visible root length were larger than total root length for corresponding plants. This suggests that in such occurrences, root parts may have been lost during washing or were left unidentified in the soil growth medium. There was a linear relationship ($r = 0.90$) between total visible root length and total root length with a slope of 1.24 for all the genotypes combined (Figure 5.2).

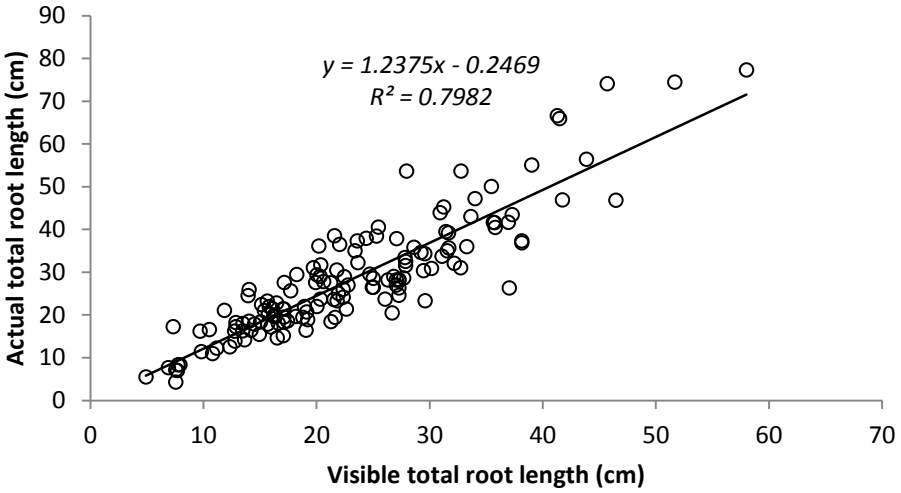


***Figure 5.2:*** *Relationship between total visible root length on transparent surface of soil-filled rhizoboxes and total harvested root length of* Brassica rapa *seedlings grown for 15 DAS after germination*

The correlation between the total root length and total visible root length was dependent on the genotype, an observation that may be due to size of the root system. Correlation coefficients between visible and harvested total root length for the parental genotypes, (cv. IMB211 and R500) were 0.60 and 0.77, respectively. The correlation between the total root length and the total visible root length for the RILs combined was 0.82. Slopes of linear regression curves also varied between genotypes with values of 1.20, 1.61 and 1.15 respectively recorded for IMB211, R500 and all RILs combined (Figure 5.4a). Total visible root length also correlated well with other traits and could therefore be proxies for other traits but this also was affected by the genotype (Figure 5.4b-d). Correlation coefficients of visible total root length with shoot biomass, root biomass and number of lateral roots were 0.68, -0.10 and 0.61, respectively for parental genotype, IMB211; 0.71, 0.06 and 0.74, respectively for parental genotype, R500; and 0.65, 0.35 and 0.82, respectively for the 10 RILs combined. Overall, correlation recorded between root biomass and visible total root length was the least, in which case, it also seemed that correlation was better for RILs and IMB211 than for R500 (Figure 5.4).

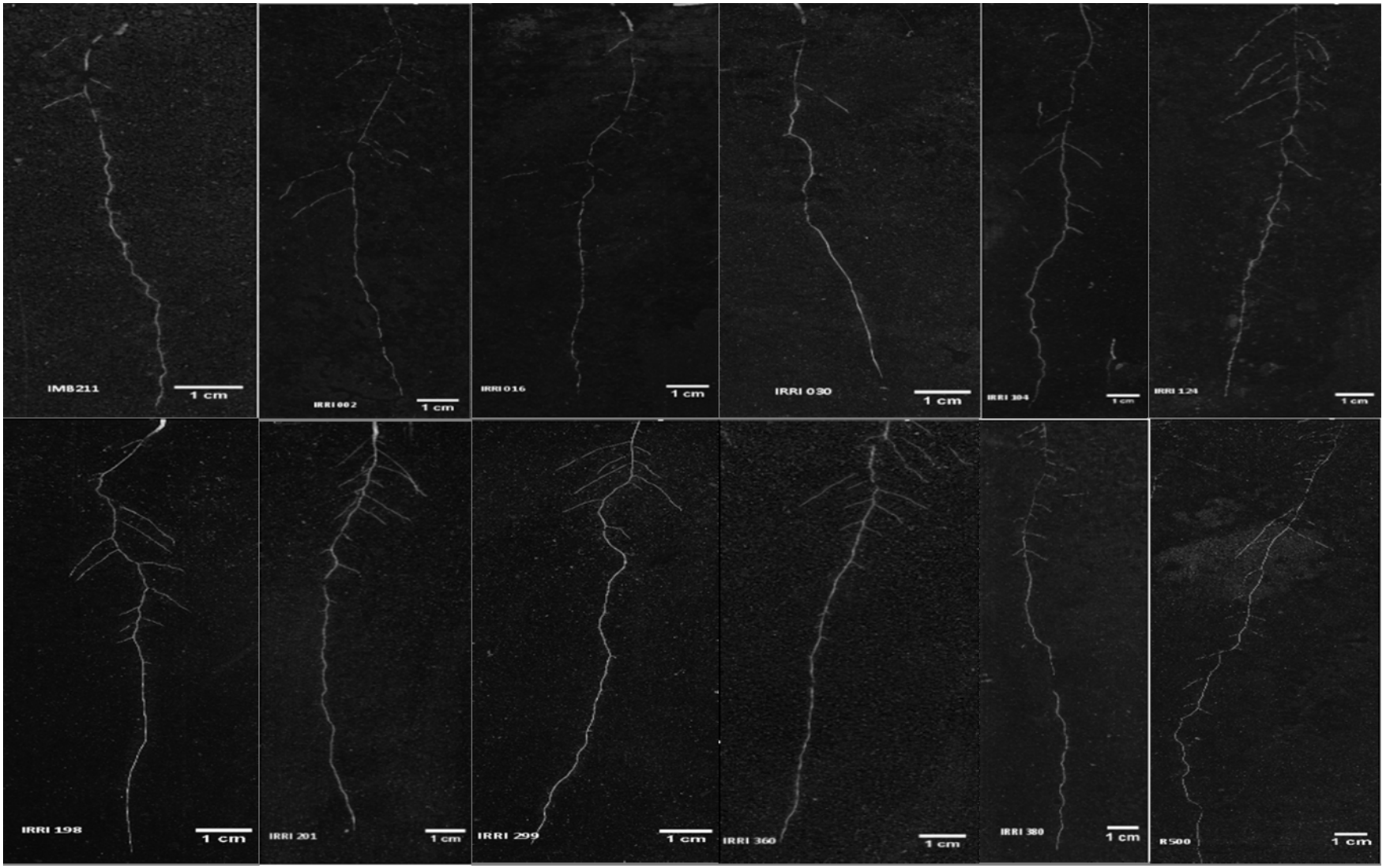


***Figure 5.3:*** *Examples of root system of* B. rapa *seedlings 15 d after sowing. R500 and IMB211 are parents and 10 RILs from the BraIRRI mapping population (For clarity, images shown here are from the blue channel of the RGB colour beams).*

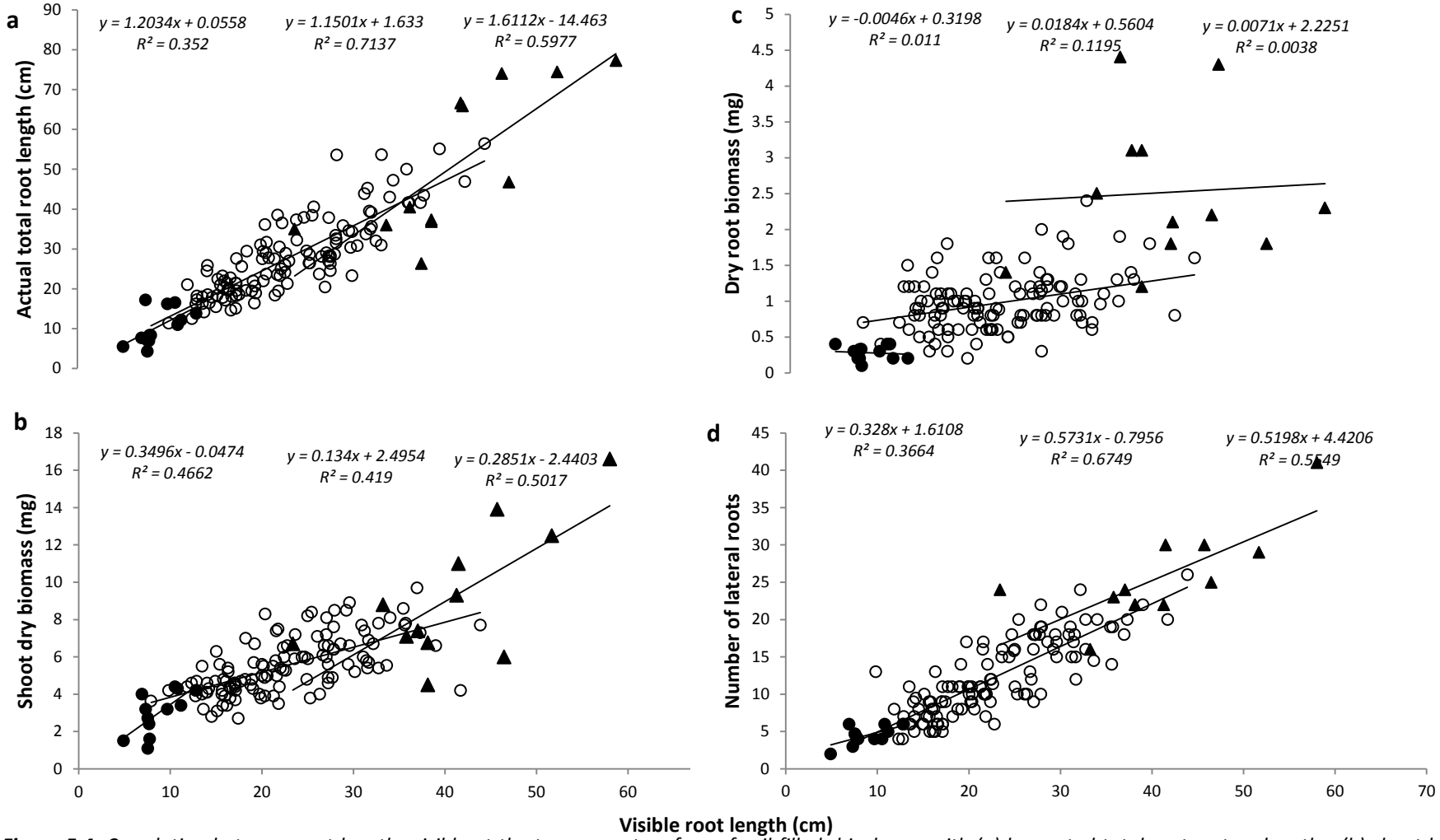


***Figure 5.4:*** *Correlation between root lengths visible at the transparent surface of soil-filled rhizoboxes with (a) harvested total root-system lengths; (b) shoot biomass; (c) root biomass and (d) number of lateral roots. Open circles, filled circles and filled triangles are data points for IMB211, RILs and R500 respectively; Equations and $R^2$ values on each plot are from left to right, the trend lines of IMB211, RILs and R500, respectively.*

### 5.2.2 Sources of variation in static root traits

A few plants had not grown and so each genotype was represented by ≥ 10 individual seedlings in the analyses. The analyses of root architectural traits were restricted to first order lateral roots as no second order lateral roots could be observed 15 d after transfer to the rhizoboxes. Coefficients of variation (CVs) was estimated on combined data for all lines on measured traits including fresh and dry weights of shoots and roots, lengths of primary root, lateral roots and whole root system. Other measured parameters included the branching density and insertion angle of lateral roots on the primary root, mean diameter of all roots, length of the un-branched apical root zone of the primary root, mean distance between laterals, root-to-shoot ratio and specific root length (Table 5.1). There was nearly an order of magnitude of variation in most of the 18 traits studied (Table 5.1). However, lateral root insertion angle, mean root diameter and root biomass showed small variations (CV = 9.46, 10.64). Most of the variation in all the traits could be attributed to the genotype and vagaries in experimental conditions (i.e. run and block).

Using Equation 5.1, it was estimated that between 4 and 48 replicates, depending upon the trait, would be generally required to detect a significant difference in means of two lines using a 2-sided, 95% CI, t-test if trait means differed by 50% (Table 5.2). Estimated sample sizes were large for certain traits including branching density, LR insertion angle, mean inter-branch distance and specific root length (Table 5.2). Differences between means for these traits were very small. This may be due to lesser or non-correlation between visible and harvested root systems caused by non-visibility of some root axes on the surface of the rhizobox.

***Table 5.1:*** *Descriptive statistics for traits measured on the parents and 10 RILs of* Brassica rapa *seedlings grown for 15 days after sowing on soil-filled rhizoboxes. (Sample size was estimated based on the difference between mean values of the parental lines for each trait. *SD: standard deviation - estimated as 50% of the sum of SDs for both groups; *represents the sum of the sample sizes of both parental lines and calculated for 50% difference between means).*

| | **Descriptive Statistics for all genotypes** | | | | | **Difference between Means of parental lines** | **SD*** | **Estimated Sample Size**** |
|---|---|---|---|---|---|---|---|---|
| **Trait** | **Unit** | **Min.** | **Max.** | **Mean** | **CV (%)** | | | |
| SFW | mg | 24.00 | 333.30 | 111.07 | 43.02 | 144.40 | 45.44 | 12 |
| SDW | mg | 1.10 | 16.60 | 5.64 | 38.39 | 6.21 | 2.38 | 18 |
| RFW | mg | 3.50 | 39.50 | 13.75 | 43.18 | 19.91 | 4.84 | 7 |
| RDW | mg | 0.10 | 4.40 | 1.05 | 63.54 | 2.24 | 0.57 | 8 |
| TRL | cm | 4.27 | 77.27 | 28.32 | 47.73 | 40.84 | 11.62 | 10 |
| TLRL | cm | 1.42 | 64.59 | 16.84 | 57.69 | 27.00 | 8.89 | 14 |
| PRL | cm | 4.69 | 28.70 | 13.93 | 30.23 | 14.65 | 3.17 | 6 |
| B. Dens. | root $cm^{-1}$ | 0.59 | 3.89 | 1.71 | 32.39 | 0.24 | 0.52 | 590 |
| LR No. | - | 2.00 | 34.00 | 12.59 | 51.18 | 19.75 | 3.54 | 4 |
| Mean LRL | cm | 0.08 | 1.93 | 0.68 | 43.11 | 0.32 | 0.18 | 39 |
| Angle | ° | 55.53 | 94.82 | 67.33 | 9.46 | 1.86 | 7.82 | 2212 |
| B. Dist. | cm | 0.30 | 3.01 | 0.80 | 47.14 | 0.11 | 0.26 | 762 |
| Mean Diam. | mm | 0.25 | 0.42 | 0.31 | 10.64 | 2.81 | 1.22 | 24 |
| Surf. Area | $cm^2$ | 2.57 | 8.84 | 6.77 | 19.02 | 28.75 | 11.74 | 21 |
| Root Vol. | $mm^3$ | 4.00 | 64.00 | 20.89 | 55.25 | 0.00 | - | - |
| LAUZ | cm | 2.48 | 18.99 | 6.15 | 37.89 | 4.03 | 2.25 | 39 |
| R:S | - | 0.03 | 0.72 | 0.19 | 53.20 | 0.21 | 0.13 | 48 |
| SRL | cm $mg^{-1}$ | 8.48 | 94.45 | 32.68 | 53.11 | 19.79 | 19.02 | 116 |

### 5.2.3 Genotypic variation in root traits on soil-filled rhizoboxes

A significant effect of genotype was observed for all the root traits measured except for mean root diameter ($p < 0.001$; Table 5.2). The parental genotypes exhibited extreme values for many biomass and root architectural traits with the R500 and IMB211 genotypes respectively having the highest and smallest values for the majority of root and shoot traits assayed. However, there was some evidence of transgressive segregation in some traits including branching density, mean LR length, LR insertion angle and LR inter-branch distance where some inbred lines recorded either smaller or higher trait values than parental lines (Table 5.2).

There were strong positive correlations among biomass traits for the 144 plants studied (Figure 5.5). There were also strong correlations between biomass and root architectural traits (Figure 5.5). Total root length was positively correlated with SFW ($r$ = 0.85; $p < 0.05$), SDW ($r$ = 0.81; $p < 0.05$), RFW ($r$ = 0.83; $p < 0.05$). Within root traits, TRL strongly correlated with root surface area ($r$ = 0.86; $p < 0.05$), PRL ($r$ = 0.75; $p < 0.05$), number of LRs ($r$ = 0.75; $p < 0.05$) and TLRL (, $r$ = 0.85; $p < 0.05$). Root FW positively correlated strongly with PRL ($r$ = 0.77; $p < 0.05$) and TLRL ($r$ = 0.77; $p < 0.05$). Other significant positive correlations included that between TLRL and number of LRs ($r$ = 0.75; $p < 0.05$), PRL and number of LRs ($r$ = 0.76; $p < 0.05$), TLRL and PRL ($r$ = 0.65; $p < 0.0$). Significant correlations were also recorded between R:S and SRL ($r$ = -0.67; $p < 0.0$).

***Table 5.2:*** *Genotypic variation in shoot and root traits assayed 15 DAS among the parents (IMB211, R500) and 10 RILs of the B. rapa BraIRRI mapping population grown for 15 days in the scanner-based soil-filled rhizobox system. (** P<0.001* or P < 0.005, n = 12 plants; d.f = 143). ns = Not Significant; LSD = Least Significant Difference.*

| Trait | IMB211 | IRRI 002 | IRRI 016 | IRRI 030 | IRRI104 | IRRI124 | IRRI198 | IRRI201 | IRRI229 | IRRI360 | IRRI380 | R500 | *P* | LSD |
|---|---|---|---|---|---|---|---|---|---|---|---|---|---|---|
| SFW | 50.40 | 105.20 | 115.30 | 56.80 | 102.50 | 102.50 | 143.70 | 130.30 | 112.10 | 114.00 | 105.00 | 194.80 | ** | 26.55 |
| SDW | 3.00 | 5.23 | 5.03 | 4.04 | 4.70 | 5.24 | 7.12 | 6.13 | 6.17 | 6.47 | 5.28 | 9.21 | ** | 1.298 |
| RFW | 5.41 | 13.65 | 11.12 | 9.52 | 14.28 | 11.62 | 13.57 | 16.4 | 15.7 | 12.76 | 15.63 | 25.32 | ** | 3.19 |
| RDW | 0.28 | 1.00 | 0.717 | 0.842 | 0.817 | 1.083 | 1.083 | 1.053 | 1.017 | 1.113 | 1.067 | 2.517 | ** | 0.3716 |
| TRL | 10.55 | 30.32 | 24.09 | 20.9 | 28.70 | 24.81 | 28.89 | 34.03 | 31.5 | 27.67 | 26.94 | 51.39 | ** | 8.415 |
| Mean Diam. | 0.306 | 0.296 | 0.315 | 0.300 | 0.318 | 0.315 | 0.312 | 0.298 | 0.296 | 0.328 | 0.323 | 0.307 | *ns* | 0.026 |
| Surf Area | 4.811 | 7.276 | 6.85 | 6.408 | 7.338 | 6.66 | 6.628 | 6.846 | 7.018 | 6.577 | 7.205 | 7.62 | ** | 0.9163 |
| Root Vol. | 8.14 | 20.9 | 18.25 | 15.25 | 22.92 | 19.58 | 22.25 | 22.52 | 22.42 | 19.18 | 22.33 | 36.92 | ** | 8.115 |
| PRL | 7.35 | 14.25 | 12.76 | 10.67 | 15.71 | 12.28 | 14.10 | 15.07 | 14.04 | 14.33 | 14.60 | 22 | ** | 2.217 |
| B. Den. | 1.868 | 2.015 | 2.022 | 1.561 | 1.149 | 1.694 | 1.728 | 1.703 | 1.785 | 1.851 | 1.489 | 1.63 | * | 0.4227 |
| LR No. | 4.47 | 15.15 | 8.58 | 7.67 | 9.88 | 12.00 | 14.42 | 14.57 | 14.33 | 15.83 | 9.92 | 24.25 | ** | 3.532 |
| mean LRL | 0.278 | 0.705 | 0.69 | 0.768 | 0.679 | 0.655 | 0.886 | 0.93 | 0.716 | 0.678 | 0.52 | 0.598 | ** | 0.2038 |
| Angle | 71.09 | 69.69 | 68.09 | 69.6 | 69.79 | 64.26 | 62.56 | 65.76 | 65.97 | 66.05 | 65.86 | 69.23 | * | 4.919 |
| Int. Dist | 0.853 | 0.581 | 0.791 | 0.841 | 1.409 | 0.711 | 0.695 | 0.665 | 0.628 | 0.668 | 1.038 | 0.746 | ** | 0.2596 |
| LAUZ | 4.41 | 6.58 | 7.25 | 5.49 | 7.11 | 5.29 | 5.43 | 6.08 | 5.77 | 5.57 | 7.49 | 8.44 | ** | 1.475 |
| LBZ | 4.31 | 18.56 | 12.03 | 11.08 | 14.73 | 14.96 | 21.15 | 23.15 | 18.88 | 19.48 | 12.46 | 31.31 | ** | 5.975 |
| SRL | 43.80 | 34.20 | 43.70 | 26.40 | 40.80 | 24.20 | 30.70 | 32.10 | 31.50 | 32.40 | 28.40 | 24.00 | * | 13.48 |
| R:S | 0.1075 | 0.1891 | 0.1492 | 0.2244 | 0.1761 | 0.2192 | 0.1546 | 0.173 | 0.1694 | 0.1725 | 0.2142 | 0.3166 | ** | 0.07332 |

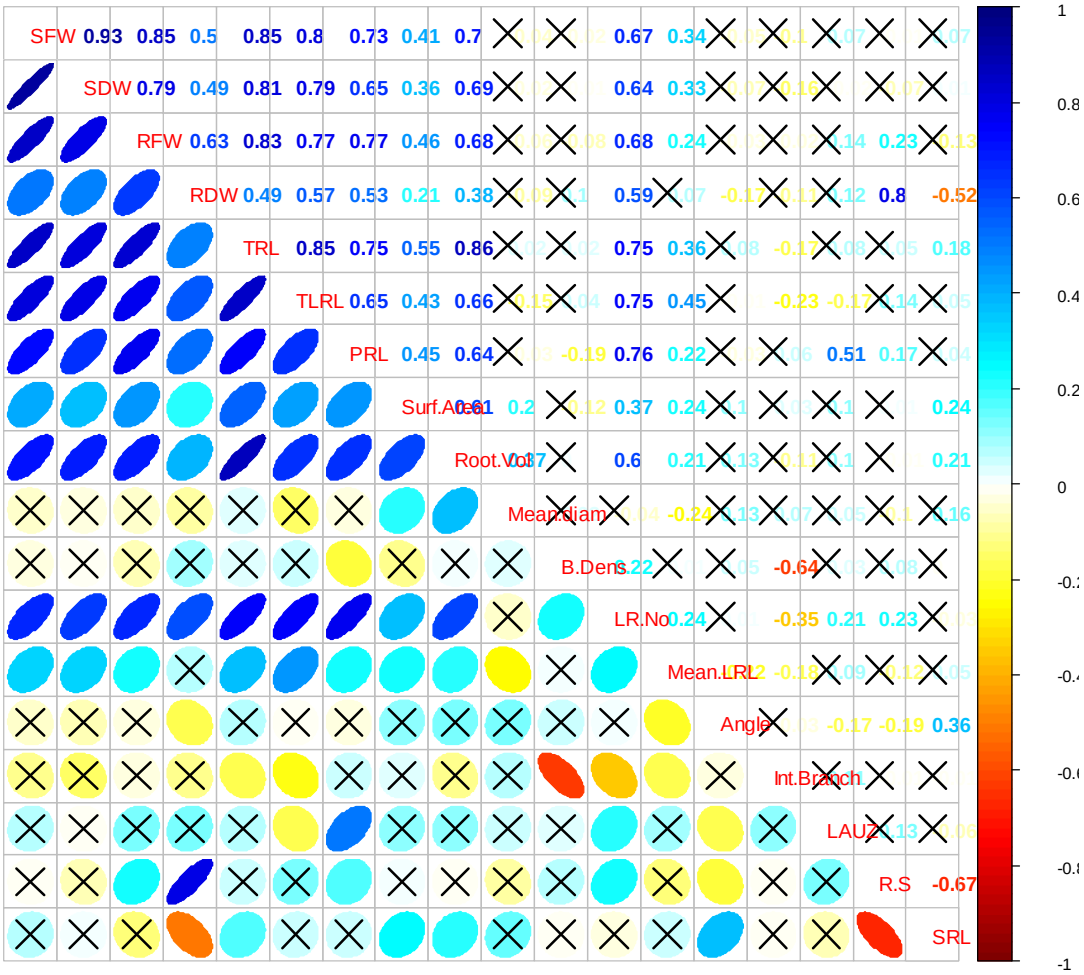


***Figure 5.5:*** *Correlations between plant traits. The correlation coefficients for linear regressions are indicated by the colour and the shape of the ellipses in the lower section below the diagonal of trait names in the matrix and the exact corresponding correlation coefficients are indicated above the diagonal of trait names in the matrix. The scale is indicated in the bar at the right of the matrix. Boxes with crosses indicate non-significant correlations (p <0.05). (Trait names from top-left to bottom-right of the diagonal are: SFW: Shoot fresh weight; SDW: Shoot dry weight; RFW: Root fresh weight; RDW: Root dry weight; TRL: Total root length; TLRL: Total length of LRs, , PRL: Primary root length; Surf Area: Root surface area; Root Vol.: Root volume; Mean Diam.: Mean root diameter; B. Dens: Branching density; LR No.: Number of LRs; Mean LRL: mean length of LRs; Angle: Mean insertion angle LRs; Int. Branch: Mean inter-branch distance of LRs; LAUZ: Length of the apical un-branched zone of the PR; R:S: Root-to-shoot ratio and , SRL: Specific root length).*

Principal component analyses (PCA) indicated five significant axes of variation, accounting for approximately 78% of the variation in the genotypes studied. Traits with eigenvalues >1.0, considered the most significant contributors to each PC, are listed in Table 5.3. The first and strongest PC was mainly associated with genotype differences in seedling biomasses (except for RDW), TRL, TLRL, and in PRL. Principal component 1 also accounted

for differences in root surface area and in the number or LRs. The second component was associated with RDW, SRL and R:S, whereas PC3 accounted for genotype differences in branching density and inter-branch distance. The fourth PC explained differences in mean LR length and root volume, whilst the PC5 explained differences in the genotypes based on LAUZ and angle (Table 5.3).

***Table 5.3:*** *Principal component analyses on 18 traits of 12 genotypes of* Brassica rapa *seedlings grown for 15 d after sowing - Rotation method: varimax with Kaiser Normalization. Components with eigenvalues >1 are considered significant (Tabachnick and Fidell, 1996). Variable loading scores with the greatest loads on each component are in bold. Genotype mean data (n = 12) were used for PCA.*

| **Trait** | **PC1** | **PC2** | **PC3** | **PC4** | **PC5** | **PC6** |
|---|---|---|---|---|---|---|
| SFW | **0.34** | -0.06 | 0.01 | -0.12 | 0.03 | -0.12 |
| SDW | **0.32** | -0.06 | -0.04 | -0.13 | 0.05 | -0.13 |
| RFW | **0.34** | 0.06 | 0.10 | -0.01 | 0.07 | -0.01 |
| RDW | 0.24 | **0.41** | 0.01 | 0.17 | 0.15 | 0.17 |
| TRL | **0.35** | -0.12 | -0.03 | 0.01 | 0.06 | 0.01 |
| Mean. Diam. | **0.21** | -0.20 | 0.14 | 0.14 | 0.03 | 0.14 |
| Surf. Area | **0.30** | -0.19 | 0.04 | 0.24 | -0.01 | 0.24 |
| PRL | **0.32** | 0.01 | 0.21 | 0.01 | -0.19 | 0.01 |
| No. of LRS | **0.31** | 0.06 | -0.17 | 0.09 | -0.03 | 0.09 |
| Mean LRL | 0.14 | -0.06 | -0.15 | **-0.52** | -0.14 | -0.52 |
| TLRL | **0.33** | -0.01 | -0.14 | -0.14 | 0.25 | -0.14 |
| LAUZ | 0.13 | 0.08 | 0.26 | 0.06 | **-0.74** | 0.06 |
| SRL | 0.00 | **-0.55** | -0.06 | -0.01 | -0.06 | -0.01 |
| B. Dens. | 0.01 | 0.07 | **-0.59** | 0.24 | -0.30 | 0.24 |
| Root. Vol. | 0.00 | -0.20 | 0.12 | **0.56** | -0.17 | 0.56 |
| Angle | -0.01 | -0.29 | -0.08 | 0.35 | **0.38** | 0.35 |
| Int. Dist. | -0.06 | -0.03 | **0.64** | -0.07 | 0.14 | -0.07 |
| R.S | 0.07 | **0.53** | 0.05 | 0.25 | 0.14 | 0.25 |
| | | | | | | |
| Eigen Value | 7.21 | 2.54 | 1.87 | 1.48 | 1.09 | 0.93 |
| % variation | 40 | 14 | 10 | 8 | 6 | 5 |
| Cumulative % variation | 40 | 54 | 64 | 72 | 78 | 83 |

Cluster analysis of root traits showed 5 distinct groups of genotypes (Figures 5.6). Two genotypes, IRRI380 and R500 were allocated to unique groups but the linkage distance between R500 and the remaining groups was wider. IMB211 clustered with IRRI030, IRRI124. The remaining clusters had 3 and 4 genotypes, respectively (Figure 5.6). Genotypes in groups 1 and 3 largely exhibited bigger biomass, increased TRL and increased number of

laterals. Genotypes in group 2 have reduced biomass and root length. Genotypes in cluster 4 appear to have root system size intermediate between that of groups 2 and 3.

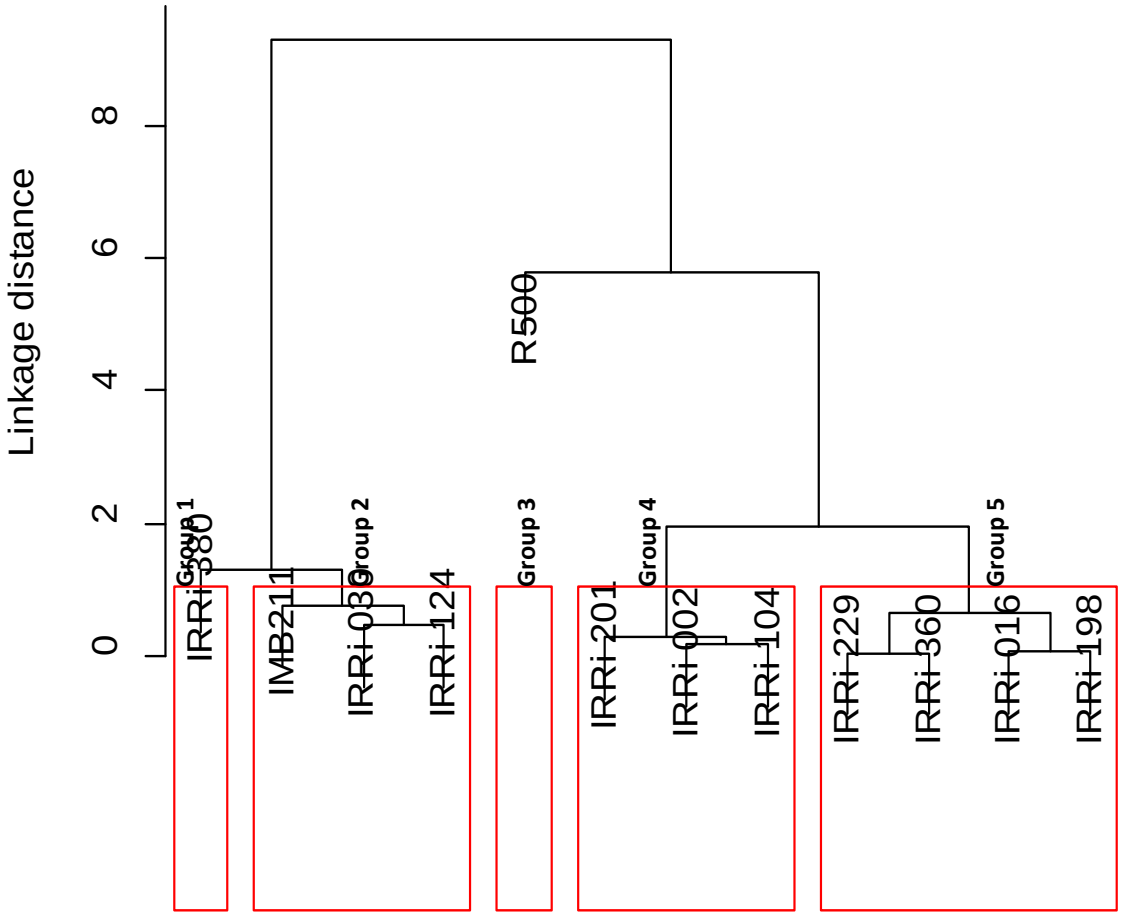


***Figure 5.6:*** *Clustering of 12* Brassica rapa *genotypes grown on soil-filled for 15 DAS. The red-lined boxes indicate groupings of the genotypes.*

Little variation in the traits assayed was attributed directly to run or block in the rhizobox experiment. The effects of genotype, and the effects of interactions between genotype x run, genotype x block and genotype x run x block accounted for most of the experimental variation (Table 5.4). The effect of genotype alone generally accounted for more variation in root traits than in shoot traits. The effect of genotype alone accounted for >35% of the variation in root biomass, but between 31-33% of the variation in shoot biomass. In some traits such as mean diameter, SRL and R:S, there was no effect of genotype alone (Table

5.4). Broad-sense heritability was highest for root biomass traits (>0.84), PRL (0.88) and TLRL (0.76), intermediate (0.40 - 0.68) for shoot biomass, mean LRL (0.65) and LAUZ (0.64), and lowest (<0.4) for branching density and root volume (Table 5.4).

Data generated in this Chapter were compared to that of Chapter 4 where plants were grown on paper but under same environmental conditions and duration. Biomasses of plants grown in soil were on average larger than that of plants grown on filter paper. However, plants grown on paper had a larger root system and more lateral roots (Figure 5.7).

***Table 5.4:*** *Sources of variation and broad sense heritability in shoot and root traits assayed 15 days after transfer to rhizoboxes among 144 seedlings of the parents (IMB211, R500) and 10 recombinant inbred lines of the* Brassica rapa *BraIRRI mapping population grown for 15 days soil-filled rhizoboxes scanner-based phenotyping platform.* $\sigma_g^2$ *= estimated variance associated with the effect of genotype,* $\sigma_{ag}^2$*= estimated covariance associated with the effect of genotype x experimental run,* $\sigma_{bg}^2$ *= estimated covariance associated with the effect of genotype x block,* $\sigma_{abg}^2$ *= estimated covariance associated with the effect of genotype x experimental run x block,* $\sigma_\varepsilon^2$ *= estimated variance associated with the residual error,* $H^2$ *= broad-sense heritability*

| Measured Trait | Standard deviations of effects | | | | | $H^2$ | Source of variation (%) | | | | |
|---|---|---|---|---|---|---|---|---|---|---|---|
| | $\sigma_g$ | $\sigma_{ag}$ | $\sigma_{bg}$ | $\sigma_{abg}$ | $\sigma$ | | Genotype | Genotype x Run | Genotype x Block | Genotype x Run x Block | Residual |
| SFW | 30.74 | 28.54 | 0.00 | 11.09 | 24.04 | 0.68 | 32.56 | 30.23 | 0.00 | 11.74 | 25.47 |
| SDW | 1.24 | 1.29 | 0.00 | 0.14 | 1.30 | 0.64 | 31.20 | 32.57 | 0.00 | 3.56 | 32.67 |
| RFW | 4.55 | 1.13 | 0.00 | 2.67 | 3.25 | 0.89 | 39.18 | 9.75 | 0.00 | 23.04 | 28.03 |
| RDW | 0.48 | 0.13 | 0.00 | 0.36 | 0.33 | 0.84 | 36.86 | 10.06 | 0.00 | 27.55 | 25.53 |
| TRL | 6.25 | 9.70 | 0.00 | 4.45 | 6.87 | 0.42 | 22.91 | 35.57 | 0.00 | 16.32 | 25.20 |
| Mean Diam. | 0.00 | 0.00 | 0.00 | 0.03 | 0.02 | 0.00 | 0.00 | 0.00 | 4.66 | 55.09 | 40.25 |
| Surf Area | 0.00 | 0.97 | 0.20 | 0.31 | 0.82 | 0.00 | 0.00 | 42.03 | 8.84 | 13.41 | 35.72 |
| Root Vol. | 2.11 | 7.72 | 0.00 | 7.56 | 5.50 | 0.09 | 9.22 | 33.74 | 0.00 | 33.03 | 24.01 |
| PRL | 3.25 | 1.17 | 0.00 | 1.61 | 2.33 | 0.88 | 38.91 | 13.98 | 0.00 | 19.23 | 27.88 |
| B. Dens. | 0.13 | 0.14 | 0.00 | 0.31 | 0.44 | 0.31 | 12.71 | 13.96 | 0.00 | 30.04 | 43.29 |
| No. of LRS | 4.69 | 1.79 | 0.70 | 1.85 | 3.79 | 0.88 | 36.60 | 13.95 | 5.47 | 14.42 | 29.56 |
| Mean LRL | 0.13 | 0.12 | 0.01 | 0.05 | 0.23 | 0.65 | 23.61 | 21.53 | 1.66 | 9.99 | 43.20 |
| Angle | 0.66 | 2.74 | 1.48 | 0.00 | 6.06 | 0.07 | 6.06 | 25.02 | 13.55 | 0.00 | 55.37 |
| Int. Dist. | 0.15 | 0.15 | 0.13 | 0.11 | 0.27 | 0.49 | 18.82 | 18.22 | 16.01 | 13.71 | 33.24 |
| LAUZ | 0.91 | 0.82 | 0.33 | 0.00 | 1.89 | 0.64 | 22.99 | 20.77 | 8.44 | 0.00 | 47.79 |
| TLRL | 6.00 | 4.14 | 0.00 | 2.81 | 6.45 | 0.76 | 30.91 | 21.32 | 0.00 | 14.51 | 33.26 |
| SRL | 0.00 | 16.66 | 0.00 | 4.96 | 10.48 | 0.00 | 0.00 | 51.91 | 0.00 | 15.45 | 32.64 |
| R:S | 0.00 | 0.07 | 0.00 | 0.05 | 0.06 | 0.00 | 0.00 | 40.78 | 0.00 | 25.50 | 33.73 |

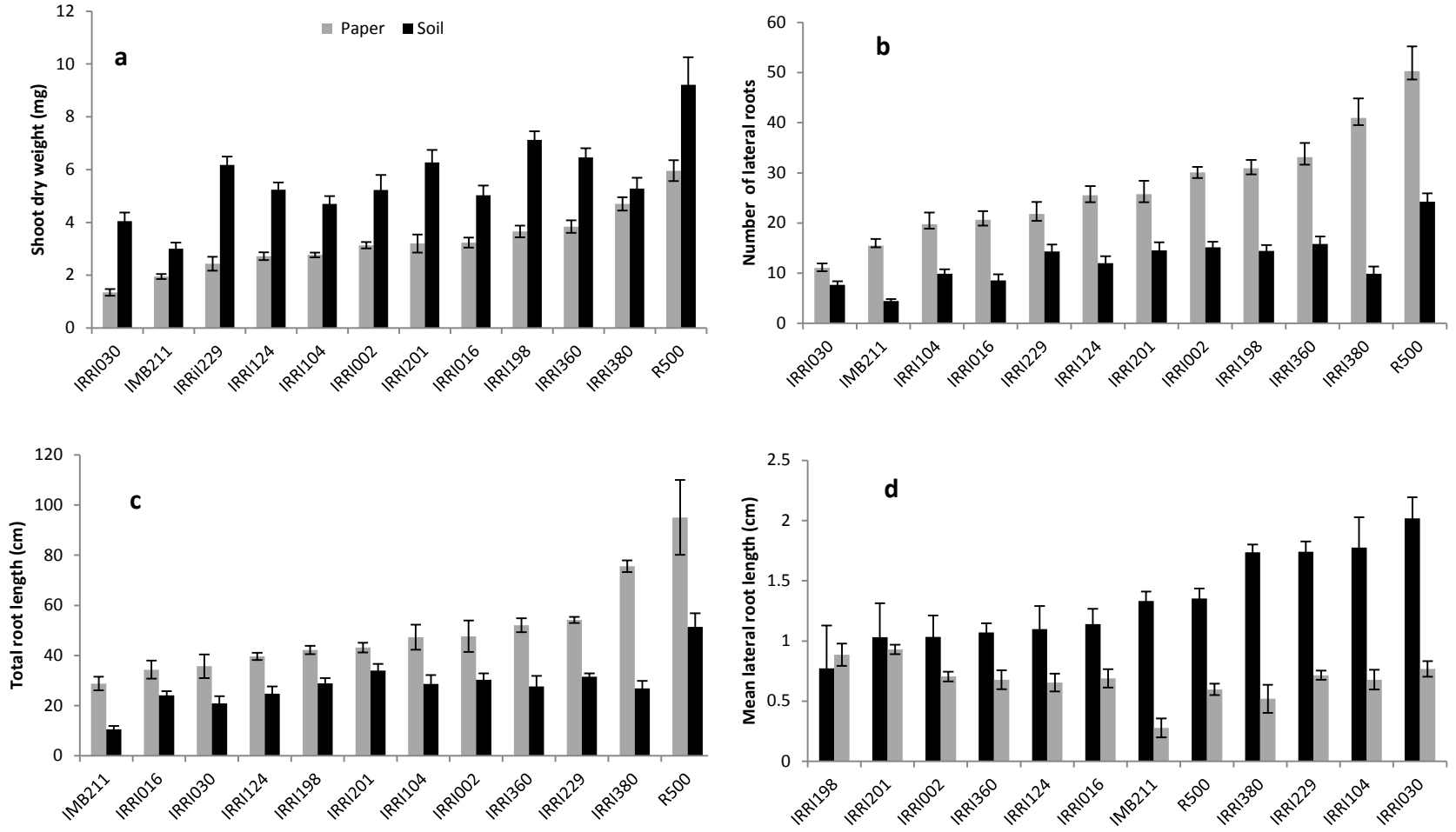


***Figure 5.7:*** *Results of shoot and root traits recorded on soil-filled rhizoboxes vs. that recorded on seed germination papers for (a) shoot dry biomass: (b) number of lateral roots; (c) length of the total root system and (d) mean length of the lateral roots.*

### 5.2.4 The dynamics of root growth

Primary root length, TRL and growth rate of lateral roots (LRGR) was observed in rhizoboxes. The length of the primary and the total root system increased sigmoidally for all genotypes in both runs (Figure 5.8). Except for two lines, root growth was more vigorous in one run due to vagaries in experimental conditions (Figure 5.8). Data also indicated considerable variability in the asymptote of root length. For the TRL, the model that best fitted the data incorporated two random-effects parameters, (the asymptote -$\emptyset_{i1}$ and Inflection point - $\emptyset_{i2}$; *Eqn. 5.2*). The estimates for the AIC, BIC and logLik for the best fit model were 528.26, 579.20 and -251.13, respectively. The AIC, BIC and logLik of a model that incorporated only one random effect (the asymptote, $\emptyset_{i1}$; *eqn. 4.4*) were 569.54, 604.81 and -275.77, respectively, suggesting that this model was not as optimal. The best fit model for PRL used only one random effect (asymptote, -$\emptyset_1$; *eqn. 4.4)* and the asymptote differed between genotypes (*P<0.05*) (Table 5.5).

***Table 5.5:*** *Estimates of the asymptotes and inflection points ($\emptyset_{i1}$, $\emptyset_{i2}$ Equation 5.2) for mixed effects models describing temporal variation in total root length and the asymptote ($\emptyset_1$ Equation 4.4) for primary root length and the intercept ($b_{i1} + \beta_1$, Equation 4.6) for mixed effects models describing the growth rate of lateral roots, among the parents (IMB211, R500) and 10 RILs of the* Brassica rapa *BraIRRI mapping population grown for 15 days in the soil-filled rhizoboxes. Percentages of total asymptotic root length made up of asymptotic primary root length are indicated brackets*

| | **IMB 211** | **R500** | **IRRI 002** | **IRRI 016** | **IRRI 030** | **IRRI 104** | **IRRI 124** | **IRRI 198** | **IRRI 201** | **IRRI 229** | **IRRI 360** | **IRRI 380** |
|---|---|---|---|---|---|---|---|---|---|---|---|---|
| **TRL Asymptote** | 9.02 | 61.59 | 35.75 | 29.45 | 23.00 | 37.20 | 35.43 | 31.84 | 41.24 | 29.69 | 42.01 | 24.52 |
| **TRL Inflection** | 8.99 | 11.33 | 10.50 | 9.10 | 9.55 | 11.63 | 11.13 | 11.19 | 12.18 | 9.22 | 11.24 | 8.69 |
| **PRL Asymptote (% of TRL)** | 8.89 (99%) | 31.91 (52%) | 17.52 (49%) | 16.44 (56%) | 15.99 (70%) | 23.73 (64%) | 18.71 (53%) | 18.61 (58%) | 18.38 (45%) | 16.95 (57%) | 20.17 (48%) | 18.53 (76%) |
| **Lateral GR** | 0.071 | 0.086 | 0.079 | 0.080 | 0.083 | 0.080 | 0.083 | 0.091 | 0.083 | 0.085 | 0.075 | 0.086 |

Asymptotes for TRL ranged from 9.0 to 62.0 cm with the parental genotypes IMB211 and R500 having an asymptote of 9.0 and 61.6 cm respectively. Asymptotes for PRL ranged from 8.9 to 31.9 cm, and these are the values recorded by the parental genotypes IMB211 and R500, respectively. For growth of both the TRL and the PRL, the parental genotypes, IMB211 and R500 recorded the least and largest asymptotes, respectively. Large proportion of the maximum TRL came from the maximum PRL (45 - 99%; Table 5.5), which might be a consequence of LRs being less visible at the surface of the rhizobox, particularly for the genotypes with smaller root system size (e.g.: IMB211) (see Figure 5.3). Inflection point of TRL ranged from 8.0 to 12 DAS with the parental genotypes, IMB211 and R500 having an inflection points of 8.99 and 11.30 DAS, respectively. The scale parameter of the logistic growth function ($\emptyset_3$) was 4.06 days across the genotypes studied for TRL. Values for the inflection point and scale parameter of the logistic growth function for PRL were constant and were 8.16 DAS and 5.0, respectively. Fitted values of the model to the measured data are shown in Figure 5.8. Adequacy of the models for TRL and PRL was assessed by logLik, AIC and BIC and also by residual and Q-Q plots (Figure 5.9).

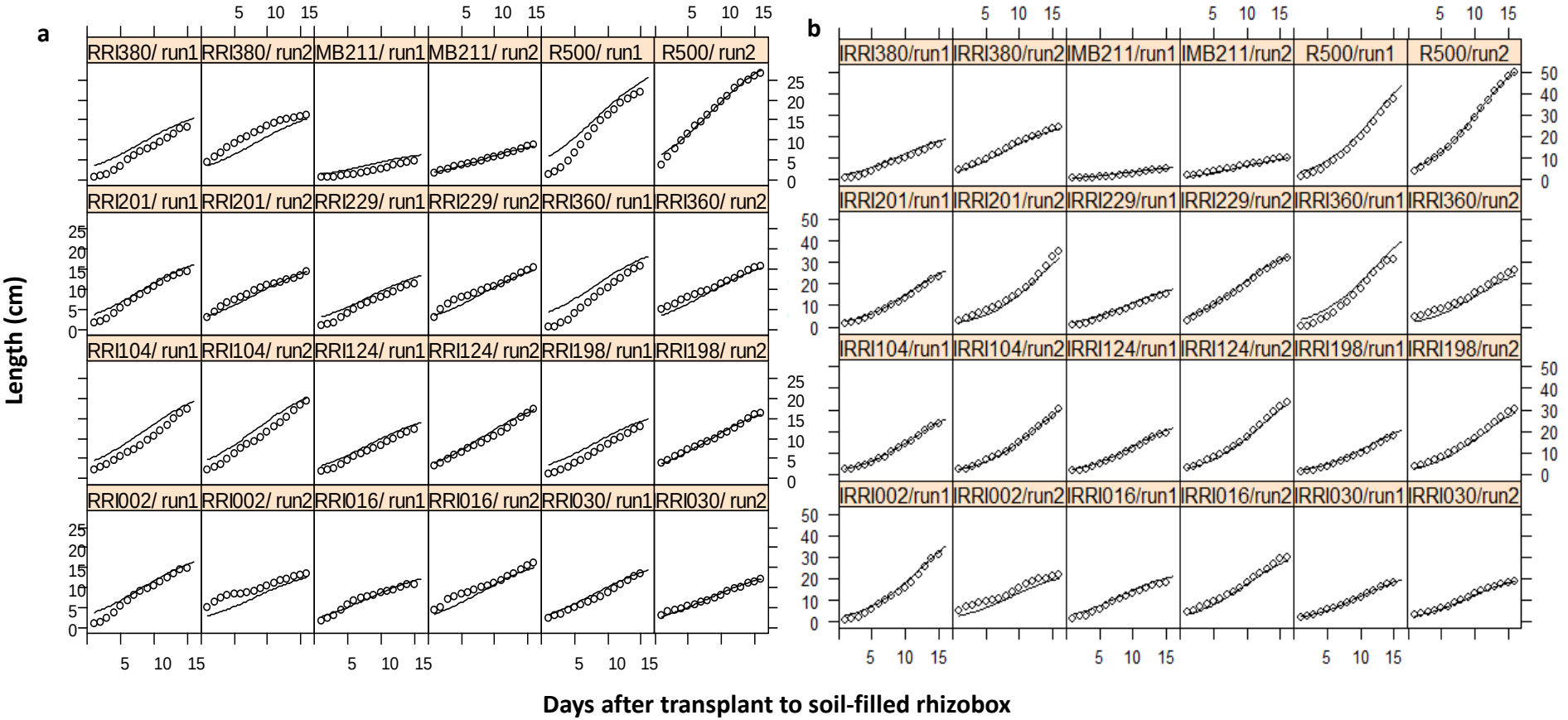


***Figure 5.8:*** *Measured (circles) and predicted (lines) values of (a) primary root and (b) total root length of the 12* Brassica rapa *genotypes measured daily for the 15 d following transfer to the phenotyping platform in two independent runs. Predicted values were estimated using a nonlinear mixed-effects model detailed in Equation 4.4.*

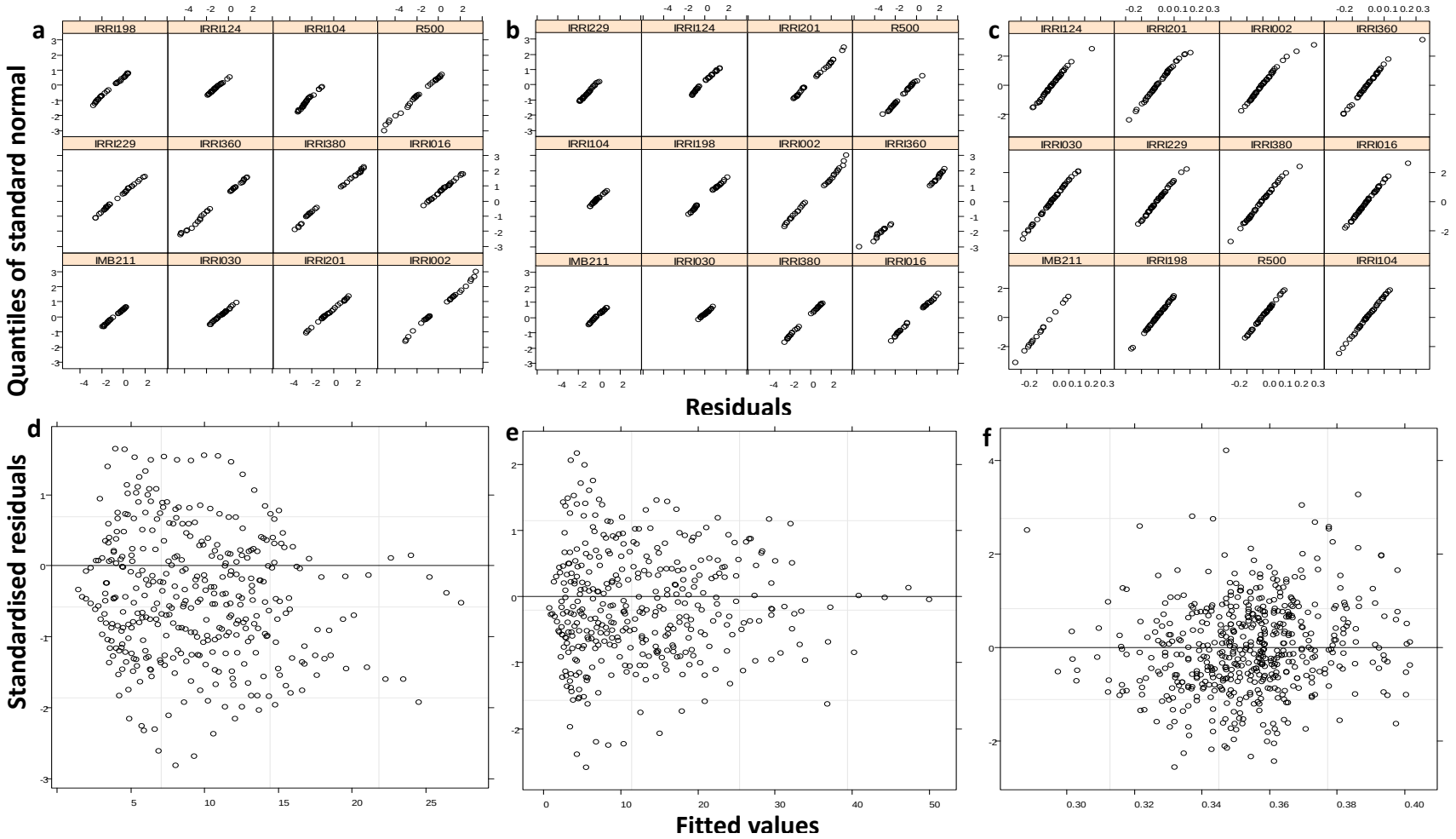


***Figure 5.9:*** *Examples of diagnostic plots for the three dynamic root traits investigated: normal plot of residuals by genotype for total root length (a), primary root length (b), lateral root growth rate (c); fitted values for standardised normal for total root length (d), primary root length (e) and lateral root growth rate (f).*

### 5.2.5 Growth rate of lateral roots

Lateral roots growth rate increased quadratically with time (DAS) for all genotypes (Figure 5.10). The most informative model included only one, random-effect parameter ($b_{i1}$, Equation 4.6) describing the effect of genotype on the initial growth rate of LRs. The model also included a correlation structure and variance function. The initial LRGR ($b_{i1}$ + $\beta_1$) differed between genotypes (Table 5.5). Values for $b_{i1}$ + $\beta_1$ ranged from 0.071 (IMB211) to 0.091 (IRRI 198) cm $d^{-1}$. The other parental genotype, R500 had a value of 0.086 cm $d^{-1}$. Model assessment with plots of residuals suggested that the model was satisfactory (Figure 5.9).

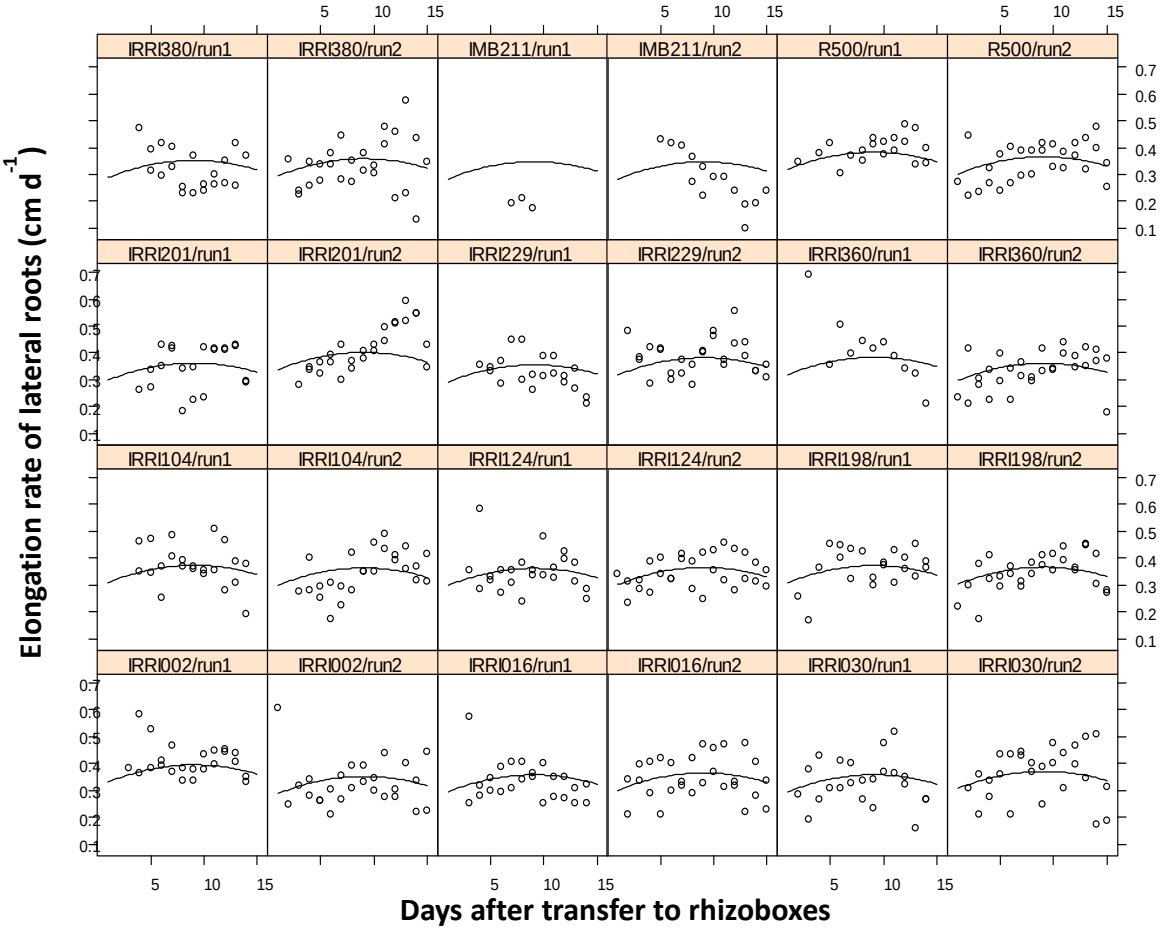


***Figure 5.10:*** *Measured (circles) and predicted (lines) values of the elongation rates of lateral roots of the two parents and ten recombinant inbred lines of the* Brassica rapa *BraIRRI mapping population as a function of the time of their emergence after transfer to the soil-filled rhizoboxes. Predicted values were estimated using a nonlinear mixed-effects model (Equation 4.6).*

### *5.3 Discussion*

Soils have complex structures. They are composed of numerous mineral and organic matter particles, whose size and arrangement is highly heterogeneous. The breeding of crop genotypes that thrives in such conditions is difficult. One way to achieve this goal is to better understand the genetic mechanisms that link root growth to soil physical conditions. Measuring RSA in naturalistic environment is thus vital for breeding of improved RSAs (Abdel-Ghani *et al.*, 2013; Richner *et al.*, 1997; Watt *et al.*, 2013; White *et al.*, 2013b; Wojciechowski *et al.*, 2009; Zhu *et al.*, 2011). Unfortunately, direct observation in soil is not possible and observations of root growth at soil-glass interface have been shown to be well suited to studies of root growth in various soil conditions. For example, rhizoboxes have been used to study the effect of nitrogen availability and ectomycorrhizal inoculation on root system architecture in seedlings of Atlas cedar (*Cedrus atlantica*), (Boukcim *et al.*, 2001, 2006). Rhizoboxes have also been adapted to study root proliferation induced by nutrient-rich patches in soils (Hodge *et al.*, 1999). Similarly, Nagel *et al.* (2012) employed rhizoboxes to detect differences in RSA induced by soil compaction.

In this chapter, the scanner-based phenotyping system has been modified to accommodate the imaging of roots grown in thin rhizoboxes. The soil provided a good medium for plant growth and gave a good contrast for root visualisation and digitisation. The system proposed is of limited complexity and is adaptable to most growth environments. The positions of root meristems can be followed in time, and therefore growth rates, spatial root distribution, root/soil concentration can be estimated from the displacement of the root meristem at consecutive time points. Statistical analysis of these values over several time periods provides root growth profiles for each genotype assessed. Although, the

washing of soil-grown root systems in rhizoboxes may also lead to the underestimation of fine roots through breakage during the washing (Glinski *et al.*, 1993; Kosola *et al.*, 2007; Mairhofer *et al.*, 2013), this is limited in this system because of the small amount of soil used for each rhizoboxes. Combining soil-filled thin rhizoboxes with optical scanner imaging could reveal root structure and development and also provide information on soil physical and chemical properties.

Similarly to experiments where roots were grown on filter paper, the size of the rhizoboxes limits application of the platform to young plants. Thus, the system has potential limitation associated to disturbance of the soil structure, the root-zone temperatures and the limited rooting volume (Neumann *et al.*, 2009). In rhizotron experiments, not all the roots of a plant are visible and accessible for digitalisation (Glinski *et al.*, 1993). In rhizoboxes, root grow at the surface of a flat surface and so roots are coerced to grow in 2-D instead of the inherent 3-D in natural environments.

Results obtained here suggest that the proportion of root system which becomes visible on the transparent surface may be related to the size of the root system. Largest percentage (45 - 99%) of the visible root length was linked to the PR which are larger and more gravitropic than LRs. Results here confirm previous results that suggest that the percentage of visible roots in rhizotrons varies between plant species. However, the observation here that root axes with bigger diameters exhibit larger percentage of their root length on the surface of rhizotrons seems inconsistent with previous results. It has been reported that the visible root length of plants with roots of relatively smaller diameters are greater than that of plants with bigger root axes (Nagel *et al.*, 2012). For example, for the root systems of

arabidopsis (*Arabidopsis thaliana*), rapeseed (*Brassica napus*), barley *(Hordeum vulgare*), rice (*Oriza sativa*), brachypodium (*Brachypodium pinnatum*) and maize (*Zea mays*), approximately 77%, 42% 33%, 32% 24% and 17%, respectively were visible on the transparent surface of rhizoboxes and accessible for digitalisation (Nagel *et al.*, 2012). It was suggested also that the fraction of visible roots may be related to specific root weight and root diameter (Nagel *et al.*, 2012; van der Weele *et al.*, 2000). High correlation between visible and harvested TRL as opposed to fraction of visible root is important in rhizobox systems. In this thesis, there were strong correlations ($R^2$ = 0.80, Figure 5.2) between the visible and harvested TRL. These results here suggest that the use of thin rhizoboxes improves the visible part of the root system that can be used as a measure for growth of total root system.

Coefficients of variation (CVs) for specific shoot and root traits measured in 144 individuals of 12 *B. rapa* lines varied between traits (Table 5.2). Examples of CVs estimated here were 43.0 for SFW, RFW and mean LRL, 38.0 for SDW, 63.5 for RDW, 47.7 for TRL, 57.7 for TLRL, 30.2 for PRL, 51.2 for number of LRs, 32.4 for branching density and 9.5% for LR angle (Table 5.2). These CVs fall within the range of CVs estimated for shoot and root traits in a single *B. rapa* genotype (R-o-18) (Chapter 3) grown on seed germination papers in multiple runs. In Chapter 3, across eight experiments, the estimated CVs for SFW, RFW, mean LRL, SDW, RDW, TRL, total LRL, PRL, number of LRs, branching density and LR angle ranged between 14.2 - 50.7, 32.4 - 64.5, 30.4 - 62.5, 12.9 - 33.4, 25.2 - 49.7, 22.8 - 66.8, 26.3 -78.7, 15.2 - 33.5, 19.8 - 34.5, 15.1- 64.6 and 5.2 and 8.0%, respectively (Table 3.2).

In this Chapter, since CVs varied for difference traits, the replication required to detect differences in these traits between genotypes also varied. For example, to detect a 50% difference in TRL and in mean LRL between two genotypes would require 10 and 39 replicates respectively (Table 5.2). The replication required largely differed between seedling grown on soil-filled rhizoboxes and seedlings cultured on seed germination paper. For example, whilst 12 and 14 replicates were estimated as adequate to detect 50% differences in TRL and mean LRL, respectively, when seedlings were grown on paper, 5 and 20 replicates, respectively were estimated for seedling grown on soil-filled rhizoboxes. Given the experimental effect, it is conceivable that another experiment could provide other estimates of needed replication. Whilst this suggests that the local environment influences the size of the variation and hence the needed replication, it also makes a strong case for preliminary analyses in all setups to determine the necessary sample size.

The effect growth media on seedling traits was also seen when traits measured here on soil-filled rhizoboxes were compared with those measured from seedlings grown on filter paper in Chapter 4. The type of media used in growing plants had significant effects on resultant shoot and RSA traits. Plant cultured on soil had greater shoot biomass but smaller root system and plant grown on germination paper had greater root system through increased lateral rooting but lower shoot biomass. The reason for the behaviour of root growth and shoot biomass accumulation on soil and paper is not immediately clear. It is speculated that since roots rarely grow through soil in complete isolation, the lack of the diversity of below-ground interactions with bacterial and fungal populations at the soil-plant interface in the paper pouch system may be implicated in the differences in root growth observed. It is also reasonable that plants grow better in soil than on paper and qualities of the rooting medium

such as aeration, temperature and water potential were more favourable in the soil media. Root systems explore the soil in order to increase surface area in order to acquire minerals and water that percolate through the soil. However, with the paper pouch system, nutrients and water may be suboptimal spatially and temporally, so the root system had to be more extensive than the soil-based plants in order to acquire the needed resources. It may also be that impedance to root growth by soil matrix resulted in smaller root system on the rhizoboxes and seedlings adapted by invested more assimilate into shoot biomass. If soil pores are not of sufficient large diameter for the roots, root tips must exert a force to deform the soil. This process may considerably decrease root elongation rates, increase the root diameter and change the pattern of lateral root initiation. The rate of root elongation decreases because of both a decrease in the rate of cell division in the meristem, and a decrease in cell length (Bengough and Mullins, 1990).

In the present study, PCA on all root traits captured 78% of RSA variation across all tested genotypes in five components (eigenvalues >1; Table 5.3). Results of PCA obtained here were similar to that of Chapter 4 (Table 4.3) when seedlings were grown on paper. Five PCs was identified in this study and PC1 which represented 40.0% of the variation was most affected by parameters essentially describing biomass, length and number of LRs and therefore related to size of the root system. High PC2 values also appear to correspond to traits describing the relationship between root and shoot biomass (R:S) or root length and biomass (SRL). PC3 was negatively affected by branching density and positively by inter-branch distance and seem to explain variation in PR related traits. PCA have been applied to investigate root trait variation among genotypes of many crop plants including narrow-leafed lupin (*Lupinus angustifolius* L., Chen *et al.*, 2011, 2012), tall fescue (*Festuca*

*arundinacea*, Sun *et al.*, 2013), rice (*Oryza sativa* L., Matsuo and Mochizuki, 2009) and arabidopsis (*Arabidopsis thaliana*, Ristova *et al.*, 2013). These studies suggested that genotypes of crop plant with intensive (i.e.: dominating PRL) and extensive (i.e.: several uniform LRs culminating into bigger root system) root systems could be distinguished as well as those with a more or less shoot biomass.

Based on results of PCA, genotypes with bigger or smaller root systems and more or less shoot biomass could be distinguished. This was supported by the results of cluster analyses where genotypes with bigger, intermediate or smaller biomass root system lengths were uniquely grouped. For example, bigger genotypes such as R500 (SDW =, 9.2 mg, TRL = 51.4 cm) is in one group; genotypes with intermediate biomass and root length such as IRRI229 (SDW = 6.2 mg, TRL =31.5 cm), IRRI360 (SDW = 6.5, TRL = 27.7) and IRRI198 (SDW = 7.1 mg, TRL = 28.9 cm) are also in the same group and genotypes with relatively smaller biomass and root system size such as IMB211 (SDW = 3.0 mg, TRL = 10.6cm), IRRI030 (SDW = 4.0mg, TRL =20.9 cm) and IRRI124 (SDW = 5.2 mg, TRL= 24.8 cm) are also grouped together (Figure 5.6). The results here largely corresponded to the cluster analyses in Chapter 4 (Figure 4.3), giving credence to the utility of the procedure in distinguishing the genotypes. For example, similar to results here, in Chapter 4, R500 and IRRI380 were each allocated to a discrete group; IMB211 and IRRI030; 360 and 198; and 016 and 229 were respectively clustered together. The differences in root system sizes observed here between groups of genotypes could be implicated in variation in foraging strategies and can therefore be exploited for improving the acquisition of resources in natural environments (White *et al.*, 2013a).

A significant effect of genotype was observed for all but one trait (Table 5.2). For a number of traits such as SRL, R:S, mean root diameter, branching density, insertion angle, root surface area and volume, broad sense heritabilities were small (<0.35, Table 5.4). It indicates that environmental vagaries, experimental errors have a strong effect on the variability in these traits (Table 5.2). However, the broad sense heritability for all other traits was large, and showed that measurements of these traits were repeatable and less affected by the environment (Fita *et al.*, 2006). It was found that traits such as PRL and RFW have high heritability and require less replication to detect significant differences from genotypic variations. Among the RSA traits, the root biomass, PRL, number of LRs and TLRL had highest heritability values (Table 5.4).

Analyses of the evolution of root growth through time showed that there were significant effects of genotype on the dynamics of root growth (Figures 5.8 & 5.10; Table 5.5). Data for PRL and TRL indicated that all genotypes follow a similar growth pattern with time, but differ in their maximum length. For the TRL only, genotypes also differ in the inflection point, the time at which the root system attains its maximum absolute growth rate. Thus, in this study, the best-fit model for TRL utilised two random effects parameters ($\emptyset_{i1}, \emptyset_{i2}$; Eqn. 5.2) as opposed to only random effect parameter ($\emptyset_i$; $\mathrm{Eqn.}\,4.4$) for the same trait in Chapter 4. This indicates strong dependence of root growth to environmental conditions (Ruts *et al.*, 2013). Data for LRGR also indicated that all genotypes follow a similar pattern with time, but differ in their maximum growth rate. Similar results have been reported by Yazdanbakhsh and Fisahn (2009) and Ruts *et al.* (2013). Root elongation rate is responsive to temporal changes in environmental conditions (Ruts *et al.*, 2013) including changes in light (Wells *et al.*, 2012), temperature (Walter *et al.*, 2002), nutrient availability (Blamey *et al.*,

1983), and soil water potential (Sharp *et al.*, 1988). Thus, insights into LR growth and development are vital to enhancing productivity of the plant in various conditions (Malamy and Benfey, 1997).

### *5.4 Summary*

- Low cost scanner-based rhizobox methodology can be employed to characterise root growth dynamics with relatively high spatial accuracy and resolution. Scanner-based rhizobox system can be scaled to screen larger populations or adapted to simulate environmental regimes that are relevant for breeding optimal RSA and root dynamic traits.
- The average proportion of roots reaching the surface of the observation window was 85.0% of the actual total root length. The visible portion of root systems could thus be considered representative of the actual total length of the entire root system.
- There were different correlation coefficients for the relationship between visible root length and actual root length for different genotypes, suggesting that visible part of the root system is not a constant fraction of the total root system. Such relationships should therefore be checked and validated prior to analysing new genotypes or when soil conditions are altered in any study.
- Coefficients of variation for the measured traits ranged between 9% and 64%.
- It was estimated that between 4 and 48 replicates, depending upon the trait, would be required to detect a significant difference in means of two lines using a 2-sided, 95% confidence interval t-test if trait means differed by 50 percent.
- The type of media used in growing plants for phenotyping studies have significant effects on resultant shoot and RSA traits. Plant cultured on soil have greater shoot

biomass but smaller root system and plant grown on germination paper have greater root system through increased lateral rooting but lower shoot biomass.

- There were strong positive correlations among biomass traits and between biomass and root architectural traits. Principal component analyses identified five significant axes of variation, accounting for approximately 78% of the variation in the genotypes studied. Genotypes with more or less shoot biomass or with bigger or smaller root system could be distinguished.
- There was a significant effect of genotype for all but one of the static root traits measured.
- Broad-sense heritability, was highest (>0.80) for traits such as root biomass, primary root length and number of lateral roots.
- There were significant effects of genotype on dynamics of on root growth. All genotypes follow a similar growth pattern with time, but differ in their maximum total root length, primary root length and lateral root growth rates. The length of the total root system required two random-effects parameters describing maximum total root length and the time at which 50% of the maximum toot root length are reached.

# CHAPTER 6 : ROOT SYSTEM RESPONSE OF *BRASSICA RAPA* SEEDLINGS TO EXTERNAL PHOSPHATE CONCENTRATION IN NON-SOIL AND SOIL ROOTING SUBSTRATE

## 6.0 Introduction

Phosphorus is an essential plant macronutrient, making up about 0.2% of a plant's dry weight (Schachtman *et al.*, 1998) and is a component of key molecules such as nucleic acids, phospholipids and ATP. Phosphorus is needed in several metabolic processes including energy transfer, signal transduction, macro-molecular biosynthesis, photosynthesis and respiration (Schachtman *et al.*, 1998; Shenoy and Kalagudi, 2005). In Chapter 1 of this thesis, challenges facing P-availability for crop production was reviewed. It was noted that P is among the least available, least mobile, mineral nutrients to plants (Shenoy and Kalagudi, 2005). While in the short to medium term, the application of P fertilizer is a common solution in intensively managed agricultural systems (White *et al.*, 2005), this leads to major environmental degradation.

To cope with low phytoavailability of P, crop plants have evolved many adaptations (Hammond *et al.*, 2009; White *et al.*, 2009; Williamson *et al.*, 2001). These adaptations could be grouped into two: (i) conservation of P use through physiological adjustments to prioritise internal P use. These adaptation mechanisms tend to focus on modifications in the plant's above-ground canopy. (ii) Enhancement in P-acquisition. This is achieved through modifications in the RSA, release of roots exudates and symbiotic association with soil microbes (Lajtha and Harrison, 1995; Lynch, 2011; Richardson *et al.*, 2009; Vance, 2001; Vance *et al.*, 2003). Alteration in RSA is a genetically-determined adaptation that enables the exploitation of the soil volume for sparingly soil available inorganic phosphate (Pi) (George *et al.*, 2011b; Hammond and White, 2008; Lynch, 2011; Lynch and Brown, 2001).

Modifications in RSA to limited P is well characterised in many plant species (White *et al.*, 2005), including arabidopsis, (*Arabidopsis thaliana*, Williamson *et al.*, 2001), common bean (*Phaseolus vulgaris* L., Liao *et al.*, 2001), maize, (*Zea mays* L., Eissenstat, 1992), wheat (*Triticum aestivum* L., Teng *et al.*, 2013), barley (*Hordeum vulgare*, Brown *et al.*, 2012), rice (*Oryza sativa*, Insalud *et al.*, 2006), lupin (*Lupinus albus* L., Watt and Evans, 2003) and brassica (*Brassica oleracea*, Hammond *et al.*, 2009).

Typically, crop plants show a reduction in the development of the PR under low Pi availability (Fang *et al.*, 2009; Sanchez-Calderon *et al.*, 2005; Shi *et al.*, 2013; Williamson *et al.*, 2001). In some plants topsoil foraging is typical (Lynch and Brown, 2001), whereas increase in length and density of root axes and/or roots hairs are observed in some other plants under low P supply (Brown, 2011; Brown *et al.*, 2012; Brown *et al.*, 2013; Ma *et al.*, 2001). Additionally, biochemical adaptations, including the release of organic anions solubilizing soil P (Shane and Lambers, 2005) and enzymes to release Pi from organic compounds are also observed (Richardson *et al.*, 2011) in P-starved environments. In *Brassica* crops, adaptation to P limiting conditions is achieved through rapid LR growth rate and development (Hammond *et al.*, 2009; Lynch and Brown, 2008; White *et al.*, 2005). *Brassicas* also develop many fine roots with many root hairs and has the tendency to increases the length and density of root hairs, under conditions of P deficiency. Moreover, in P-deficient soil, *Brassicas* have the ability to acidify soils near root tips and root hairs to enhance dissolution of P in soil, and thus increase P uptake by their roots (Bolland and Brennan, 2008).

Compared to cereals such as wheat, *Brassica* crops, including *Brassica napus (rapeseed)* and *Brassica rapa (Chinese cabbage, pak choi and turnip)* commonly referred to as canola, require less applied P to produce near-maximum yields because their roots are better able to obtain P from the soil (Bolland, 1997). Even so, these crops show yield response to P fertilizer and without an adequate P supply, yields are normally reduced (Shi *et al.*, 2013). *Brassica* crops need approximately 26.0 to 30.0 kg of P fertilizer ($P_2O_5$) per tonne of yield and are capable of removing about 18.0 to 20.0 kg of P from the soil for each tonne of seed yield. These crops tend to take up more P than many farmers apply and the amounts that are normally taken up by its roots from the soil exceed the amount that can be safely seed-placed (http://www.canolacouncil.org/).

*Brassica rapa* provides a suitable model crop for studies because it is closely related to *Arabidopsis* (Suwabe *et al.*, 2006) and also corresponds to the A genome of the widely cultivated oilseed rape (*B. napus*) (Suwabe *et al.*, 2008). There are also genomic resources available for the crop including mapping populations and diversity foundation sets (Iniguez-Luy *et al.*, 2009; White *et al.*, 2010). Also, as an important vegetable and oil crop globally (Wang *et al.*, 2011), selecting for and developing *Brassica* lines conferred with traits for efficient acquisition of P is critical. Thus, the study on the mechanisms of P uptake has important significance to the genetic improvement of P nutrition and judicious fertilization as well as reduction in nutrient loss and environmental pollution in production of *B. rapa* and other crop plants (Aziz *et al.*, 2006).

In this study, we used the parents and selected RILs from the BraIRRI mapping population (Iniguez-Luy *et al.*, 2009) to quantify RSA traits using seed germination paper and soil-filled

rhizoboxes root phenotyping system. The first aim of this Chapter was to use the developed scanner-based imaging methodology to characterise the root growth response to various changes in Pi availability and to determine if there is genetic variation existing in *B. rapa* for root system plasticity in response to external P availability. The second aim was to carry out the same study in soil and to assess the genotypic variations in the response of seedlings of *B. rapa* inbred lines.

## *6.1 Materials and methods*

Two separate experiments were conducted. Experiment 1 examined the effects of external P nutrition on the parental genotypes of the BraIRRI mapping using seed germination papers as the rooting medium. In Experiment 2, the effect of external P nutrition on RSA was examined on the parents and in addition on selected inbred lines of the BraIRRRI mapping, using roots grown in thin rhizoboxes filled with sieved soil.

### 6.1.1 Experiment 1

First, shoot and root P concentration of *B. rapa* seedlings grown previously at 250 µM were assayed. The results were compared to the critical shoot P concentration for *B. napus* in literature as reported by Major and Barraclough (2002). Subsequently, root responses of parental genotypes to external Pi concentrations ($[P]_{ext}$) were assessed at appropriate $[P]_{ext}$ levels0, 10, 30, 50 100, 150, 300 and 600 µM with applicable amounts of potassium chloride (KCl) added to balance K in solutions with no or low potassium dihydrogen phosphate ($KH_2PO_4$). Six replicates each of IMB211 and R500 were grown at these different $[P]_{ext}$.

Time-lapsed imaging of roots was performed on four $[P]_{ext}$ treatments (0, 10, 30 and 600 µM) and the remaining $[P]_{ext}$ treatments had no scanners. In treatments with no scanners, germination papers were held on plastic plates and put in the nutrient solution in the same

positions as those with scanners. Two seedlings were fixed on each germination paper by sandwiching them between a black filter paper and the germination paper (Figure 6.1). For the plants not growing on a scanner, root systems were imaged with Canon F500 flatbed scanners at the end of each experiment. In the final stage, plants were harvested to determine: (i) fresh and dry biomass of plant samples, and (ii) P concentration in root and shoot tissue as described in Chapter 2.

Eight independent runs were performed in Experiment 1. First, two short runs were carried out for 10 DAS to determine if growth responses can be triggered at an early developmental stage. In the subsequent four runs, plants were grown for 14 DAS (baseline duration of experiments in this thesis). In the last two runs, plant growth was conducted for 18 DAS to assess whether P response is triggered at a later developmental stage.

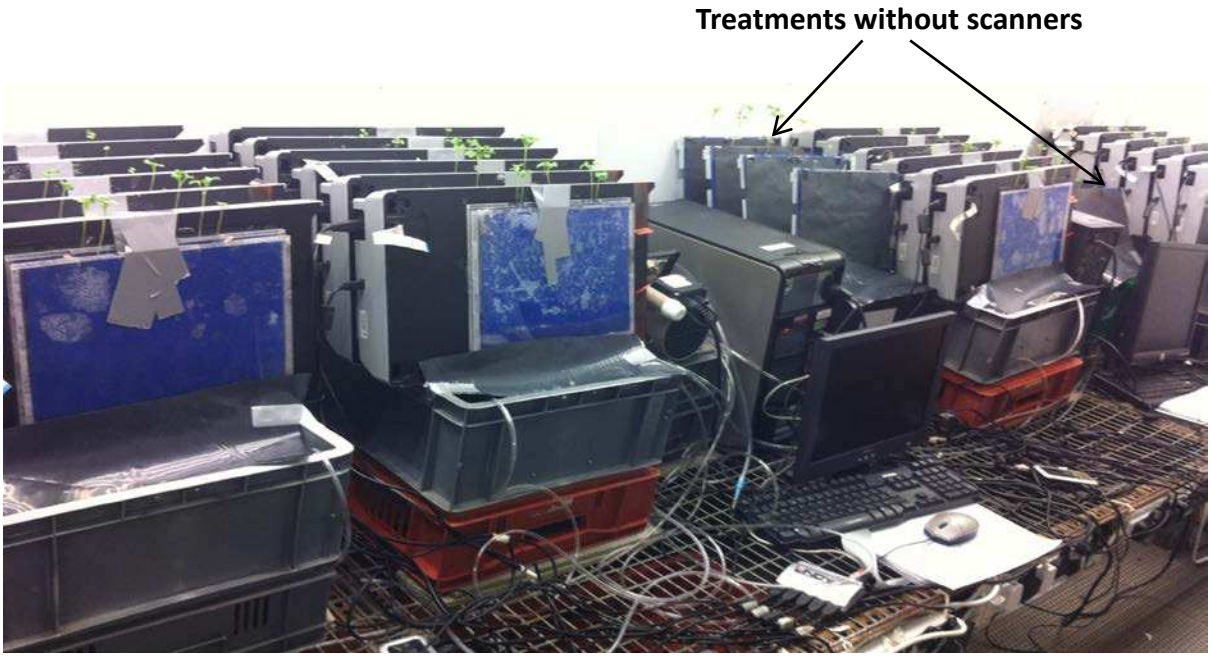


***Figure 6.1:*** *Set for Experiment 1 showing treatments with and without scanners*

### 6.1.2 Experiment 2

Six *B. rapa* genotypes exhibiting variation in root system length and other RSA traits including specific root length which also depends on variation in root diameter were selected. The selection was based on results from an experiment (Chapter 5) not reported here where ten RILs had been grown and phenotyped on soil-filled rhizoboxes at uniform $[P]_{ext}$ for 14 DAS. The genotypes selected were the parents (cv. R500, IMB211) and four RILs namely IRRI016, IRRI124, IRRI201 and IRRI229 and these had bigger, intermediate or smaller root systems. Plants were either grown at un-amended soil (low $[P]_{ext}$) or on soil amended with a solution containing 600 µM of inorganic phosphate ($KH_2PO_4$, VWR International) (high $[P]_{ext}$) and watered once to 80% field capacity on gravimetric water content basis at the onset of each run. Soil utilised was sandy loam soil collected from the 0 - 10 cm top layer of a Cambisol (FAO, 1998) near the James Hutton Institute (JHI) Dundee, Scotland (NO 456 265) as described in Section 2.1.6.2 and by Brown *et al.* (2013). General soil characteristics (Table 2.2) were measured using standard methodology (Page *et al.*, 1982). This soil contained total digestible P of 1475.0 mg P $kg^{-1}$ of which 40.8% was in organic moieties. Despite having a relatively high Olsen P of 84.5 mg P $kg^{-1}$ (probably due to presence of recently added pig manure), barley grown in this soil was responsive to the addition of P (Brown *et al.*, 2013; George *et al.*, 2011a). For each line and each $[P]_{ext}$ treatment, 6 replicates of seedlings were sown across 2 independent runs. In both runs, seedlings were grown for 21 DAS and 12 hourly images of all root systems were captured using flatbed scanners abutting soil-filled rhizoboxes. Fresh and dry biomass of plant samples as well as P concentration in root and shoot tissue samples were determined.

### 6.1.3 Data analysis

For each experiment, data from all runs were pooled together for analyses with experimental runs considered as blocks within experiments. Prior to analysis, biomass data and length of the total root system were log-transformed to linearise the data but frequency distribution indicated that the remaining traits did not require transformation (data not shown). The following mixed effect model was used to analyse the data:

$$Y_{ijk} = \mu + g_i + \beta_j + \alpha_k + g\beta_{ij} + \beta\alpha_{ik} + g\alpha_{jk} + g\beta\alpha_{ijk} + \varepsilon_{ijk} \qquad (\mathbf{6.1})$$

$$g_i \sim N(0, \sigma_g^2), \beta_j \sim N(0, \sigma_\beta^2), \alpha_k \sim N(0, \sigma_\alpha^2),\ \varepsilon_{ijk,} \sim N(0, \sigma^2)$$

where $Y_{ijk}$ is the trait value of the $i^{th}$ genotype ($i$ = 1 , 2) within the $j^{th}$ run ($j$ = 1,2 …,8) and within the $k^{th}$ $[P]_{ext}$ treatment ($k$ = 1,2 …, 8); $\mu$ the overall mean, $g$ the effect of the genotype, $\beta$ the effect of the run, $\alpha$ the effect of $[P]_{ext}$ treatment, $g\beta$ the genotype by run interaction, $\beta\alpha$ run by $[P]_{ext}$ treatment interaction, $g\alpha$ the genotype by $[P]_{ext}$ treatment interaction, $g\beta\alpha$ the genotype by run by $[P]_{ext}$ treatment interaction and $\varepsilon_{ijk}$ is the residual error. Subsequently, the mean trait value for genotypes was determined using the [Run × ($[P]_{ext}$ × Genotype)] as random factors. Broad sense heritability was subsequently calculated and for each trait and treatment heritability was calculated as the variance component attributed to genotype in the model, divided by the total variance. Data for Experiment 1 was analysed using a REML (residual maximum likelihood) procedures to allocate sources of variation (Robinson, 1987), using GenStat 14 (VSN International Oxford, UK - www.vsni.co.uk).

Initial analyses suggested that Equation 6.1 was not optimal for data in Experiment 2. A simplified version of equation 6.1 which was without $g\beta$, the genotype by run interaction; $\beta\alpha$, run by $[P]_{ext}$ treatment interaction; $g\beta\alpha$, the genotype by run by $[P]_{ext}$ was thus applied.

$$Y_{ijk} = \mu + g_i + \beta_j + \alpha_k + g\alpha_{jk} + \varepsilon_{ijk} \qquad (\mathbf{6.2})$$

$$g_i \sim N\left(0, \sigma_g^2\right), \beta_j \sim N\left(0, \sigma_\beta^2\right), \alpha_k \sim N(0, \sigma_\alpha^2),\ \varepsilon_{ijk,} \sim N(0, \sigma^2\ )$$

Definitions of parameters remained the same as in equation 6.1 but here the number of genotypes is 6 ($i$ = 1, 2…,6) the number of run is 2 ($j$ = 1,2) and the number of $[P]_{ext}$ treatments is 2 ($k$ = 1,2). Due to mortality of some seedlings, an unbalanced analysis of variance was performed on the data and in GenStat 14.

For brevity, analyses of root growth dynamics here were based only on TRL of seedlings grown for 18 and 21 DAS in Experiment 1 and Experiment 2, respectively. This is because initial examination of the data suggested that there was no effect of external P concentration on other dynamic root traits and also effect on TRL seem to be manifested in the later stages of the plants growth. Initial examination of the data also suggested that TRL over the 18 DAS (Experiment 1) or 21 DAS (Experiment 2) period followed a logistic growth curve and only the asymptotic TRL ($\emptyset_{i1}$) seem to be dependent on $[P]_{ext}$. In the model used here, DAS and $[P]_{ext}$ were treated as covariates. The asymptote of TRL which is affected by $[P]_{ext}$ is composed of an overall mean ($\beta_1$) and a random effect ($b_{i1}$) which varied among genotypes within each $[P]_{ext}$. Equation 4.4 was used here but with a modification in the formulation of $\emptyset_{i1}$:

$$y_{ij} = \frac{\emptyset_{i1}}{1 + \exp[-\left(DAS_j - \emptyset_{i2}\right)/ \emptyset_{i3}]} + \epsilon_{ij}, \qquad (\mathbf{6.3})$$

$$\emptyset_i = \begin{bmatrix} \emptyset_{i1} \\ \emptyset_{i2} \\ \emptyset_{i3} \end{bmatrix} = \begin{bmatrix} \beta_1 \\ \beta_2 \\ \beta_3 \end{bmatrix} + \begin{bmatrix} b_{i1} \\ 0 \\ 0 \end{bmatrix},$$

$$\emptyset_{i1} = \beta_1 + \gamma_1 x_{i1} + \gamma_2 x_{i2} + \gamma_3 x_{i1} x_{i2} + b_{i1},$$

$$i = \{1, \dots, s\}, j = \{1, \dots, t\},$$

$$b_{i1} \sim N\,(0, \sigma_b^2), \epsilon_{ij} \sim N\,(0, \sigma^2).$$

Definitions of all parameters remain unchanged from equation 4.4 but here, $\gamma_1$and $\gamma_2$ represent the main effects of Genotype and $[P]_{ext,}$ respectively and $\gamma_3$is the Genotype x $[P]_{ext}$ interaction; $x_{i1}$ = [(*i* = 1, 2 for Experiment 1 and 1, 2…,6 for Experiment 2); $x_{i2}$ = external P treatment (*i* = 1,2…,4 for Experiment 1 and *i* = 1,2 for Experiment 2)] and *t* is the number of time-points at which measurements were made (18 for Experiment 1 and 21 for Experiment 2). Autocorrelation was modelled with corARMA and AR1 correlation structure and a power variance function (eqn. 4.5) was used to account for heteroscedasticity.

### *6.2 Results*

During the preliminary analyses, we considered $[P]_{ext}$ in the range of 250-300 µM as adequate external P suitable for maximum shoots dry weight. This was based on critical shoot Pi of 0.67% P calculated for 95% maximum SDW in the literature (Major and Barraclough, 2002). Also in the preliminary analysis, we estimated 0.59% and 0.87% P, respectively in the shoots of R500 and IMB211 (Figure 6.2) to determine the baseline tissue P concentration under adequate P supply. However, after initial trials, 600 µM was considered here as the replete $[P]_{ext}$.

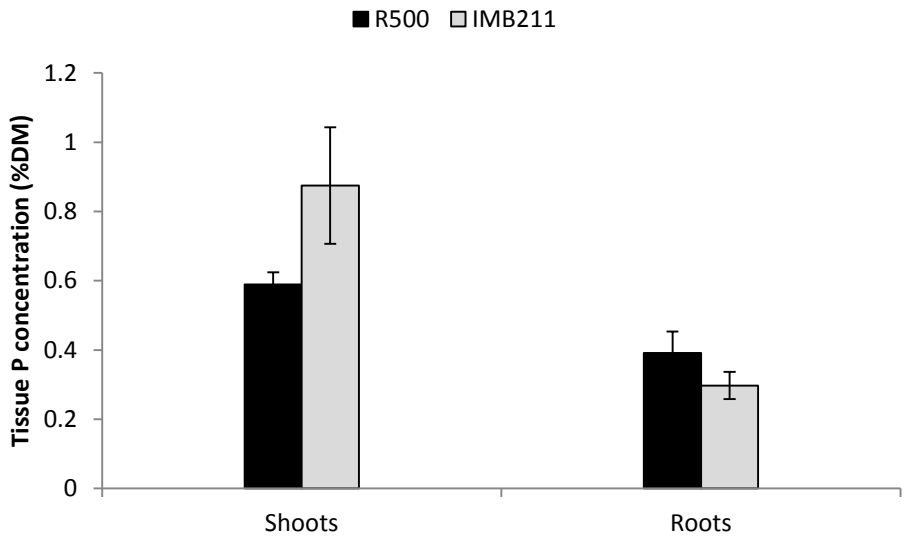


***Figure 6.2:*** *Tissue P concentrations of two genotypes of* Brassica rapa *grown at 250 µM external P concentration for 14 days.*

### 6.2.1 Experiment 1: Plant response to $[P]_{ext}$ supply on Germination papers

#### *6.2.1.1 Effect of genotype, run, external Pi concentration and their interactions*

Genotype effect accounted for the largest portion of total variance in most of the traits assayed including SFW (60%), RFW (58%), number of LRs (63%), PRL (68%), TRL (59%) and TLRL (49%) (Table 6.1). Genotype effect however recorded little or no effect in a few traits such as SDW, inter-branch distance, branching density, diameter of LRs, R:S and LAUZ (Table 6.1). Although Run accounted for some of the variability observed in the data, the amount of variability seemed small for some traits ranging from 0 - 24% except for SDW for which variability attributable to Run was inexplicably large (60%) (Table 6.1). Except for inter-branch distance (53%), for most traits assayed, little variation was attributed directly to the $[P]_{ext}$. However, the effect of $[P]_{ext}$ was significant for traits including R:S (5%), SDW (8%), PR diameter (17%), SRL (16%), and angle (14%). The effects of interactions between genotype x run, genotype x $[P]_{ext}$ and run x $[P]_{ext}$ accounted for variation ranging from 0 to 16% but the variation attributed to effect of the interactions of genotype x run x $[P]_{ext}$ was relatively

larger ranging from 0 to 41% (Table 6.1). Broad-sense heritability ($\sigma_g^2$ / $\sigma_p^2$), was highest for number of LRs (0.68),PRL (0.68), SFW (0.60), TRL (0.59) and RFW (0.58). Broad-sense heritability was intermediate for total and mean length of LRs, LAUZ (≥0.40) but low (<0.40) for remaining traits (Table 6.1).

***Table 6.1:*** *Sources of variation and broad sense heritability in shoot and root traits assayed among the parents (IMB211 and R500) of the* Brassica rapa *BraIRRI mapping population grown on seed germination paper at differential external P concentration for up to 18 days in the phenotyping platform. (Percentage contribution of sources of variation is indicated in brackets underneath variance of effects.*

| Trait | Trait means and variance effects (Percentage contribution of source of variation) | | | | | | | | | $H^2$ |
|---|---|---|---|---|---|---|---|---|---|---|
| | $\mu$ | $\sigma_\beta^2$ (%) | $\sigma_\alpha^2$ (%) | $\sigma_g^2$ (%) | $\sigma_{\beta\alpha}^2$ (%) | $\sigma_{\beta g}^2$ (%) | $\sigma_{\alpha g}^2$ (%) | $\sigma_{\beta\alpha g}^2$ (%) | $\sigma_\varepsilon^2$ (%) | |
| Int. Dist. (cm) | 0.665 | 0.0137 (1.36) | 0.5345 (53.23) | 0 (0.00) | 0.0124 (1.23) | 0 (0.00) | 0.0242 (2.41) | 0.0104 (1.04) | 0.409 (40.73) | 0.00 |
| Mean LRL (cm) | 1.434 | 0.0991 (19.09) | 0.0111 (2.14) | 0.2101 (40.47) | 0.0068 (1.31) | 0.0287 (5.53) | 0.0146 (2.81) | 0.125 (24.08) | 0.0237 (4.57) | 0.40 |
| No. of LRs | 21.48 | 8.02 (2.03) | 1.19 (0.30) | 267.64 (67.62) | 3.28 (0.83) | 30.24 (7.64) | 1.35 (0.34) | 31.57 (7.98) | 52.53 (13.27) | 0.68 |
| LR Diam (mm) | 0.3161 | 0.000799 (13.57) | 0.000047 (0.80) | 0 (0.00) | 0.000412 (7.00) | 0 (0.00) | 0.000954 (16.21) | 0.002404 (40.84) | 0.00127 (21.58) | 0.00 |
| B Dens. (root/cm) | 2.586 | 0.069 (2.98) | 0.053 (2.29) | 0 (0.00) | 0 (0.00) | 0 (0.00) | 0.019 (0.82) | 0.233 (10.06) | 1.943 (83.86) | 0.00 |
| PR Diam. (mm) | 0.4354 | 0.002738 (24.15) | 0.001974 (17.41) | 0.00115 (10.15) | 0.000958 (8.45) | 0.000022 (0.19) | 0.000187 (1.65) | 0.001239 (10.93) | 0.00307 (27.07) | 0.10 |
| PR length (cm) | 13.53 | 1.48 (1.95) | 0.66 (0.87) | 51.67 (67.93) | 2.22 (2.92) | 0.59 (0.78) | 0.11 (0.14) | 3.1 (4.08) | 16.23 (21.34) | 0.68 |
| RDW (mg) | 0.969 | 0.0806 (7.65) | 0.0075 (0.71) | 0.3801 (36.10) | 0.0334 (3.17) | 0.0936 (8.89) | 0.0643 (6.11) | 0.1725 (16.38) | 0.221 (20.99) | 0.36 |
| RFW (mg) | 12.51 | 8.38 (4.24) | 0.5 (0.25) | 114.01 (57.62) | 2.03 (1.03) | 16.29 (8.23) | 5.91 (2.99) | 17.99 (9.09) | 32.75 (16.55) | 0.58 |
| R:S | 0.2036 | 0.001527 (8.45) | 0.000911 (5.04) | 0 (0.00) | 0.000545 (3.01) | 0.000196 (1.08) | 0.001532 (8.47) | 0.003398 (18.80) | 0.00997 (55.15) | 0.00 |
| SDW (mg) | 5.56 | 0.7 (60.33) | 2.019 (8.10) | 10.844 (0.56) | 5.655 (0.04) | 0.991 (2.16) | 0 (11.23) | 2.206 (8.33) | 4.522 (9.24) | 0.01 |
| SFW (mg) | 71.3 | 53 (1.05) | 0 (0.00) | 3014 (59.74) | 73 (1.45) | 260 (5.15) | 112 (2.22) | 237 (4.70) | 1296 (25.69) | 0.60 |
| SRL (mg $cm^{-1}$) | 62.5 | 11 (0.40) | 429 (15.47) | 173 (6.24) | 131 (4.72) | 0 (0.00) | 339 (12.23) | 292 (10.53) | 1398 (50.41) | 0.06 |
| TRL (cm) | 49.1 | 158.2 (5.95) | 0 (0.00) | 1558.3 (58.58) | 37.5 (1.41) | 208 (7.82) | 64.2 (2.41) | 280.3 (10.54) | 353.7 (13.30) | 0.59 |
| TLRL (cm) | 35.6 | 130.2 (6.34) | 0 (0.00) | 1011.7 (49.25) | 34.3 (1.67) | 220.9 (10.75) | 57.4 (2.79) | 264.1 (12.86) | 335.5 (16.33) | 0.49 |
| Angle (°) | 71.57 | 4.52 (18.12) | 3.4 (13.63) | 1.03 (4.13) | 3.31 (13.27) | 0 (0.00) | 2.27 (9.10) | 7.36 (29.51) | 3.05 (12.23) | 0.04 |
| LAUZ (cm) | 6.74 | 2.4 (0.46) | 3.9 (0.74) | 0 (0.00) | 0 (0.00) | 0 (0.00) | 19.1 (3.64) | 0 (0.00) | 499.3 (95.16) | 0.00 |

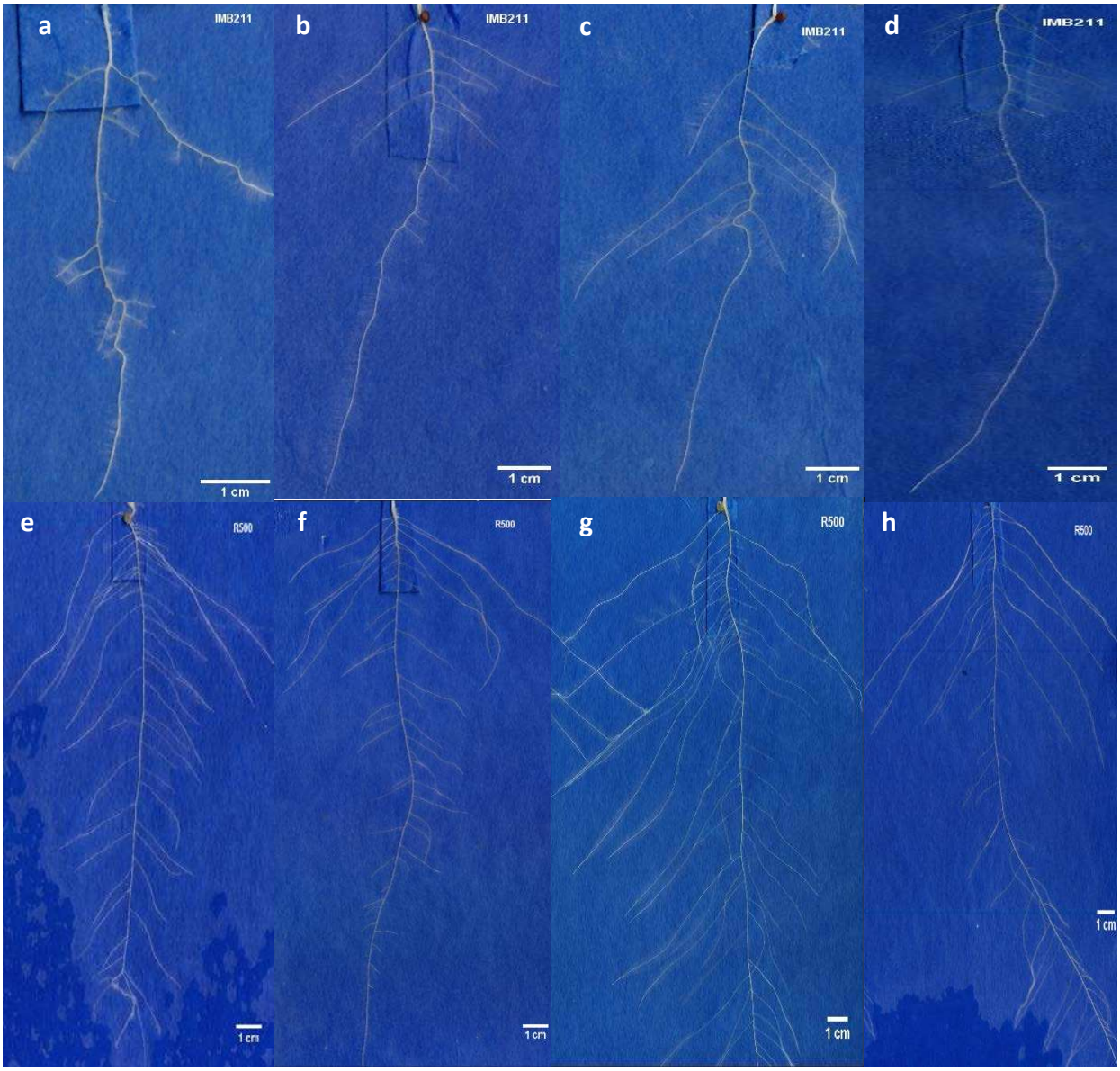


***Figure 6.3:*** *Images captured at 18 DAS for IMB211 (a-d) and R500 plants (e-h) grown on seed germination papers at 0, 10, 30 & 600 µM* $[P]_{ext}$ *respectively. Root systems g and h had overgrown the scanning window of the flatbed scanners by* $14^{th}$ *d.*

There was statistically significant differences (*p<0.05*) between IMB211 and R500 in all root architectural traits except for inter-branch distance, LAUZ, LR diameter, branching density and R:S. Importantly, significant interactions were observed between genotype (g) and $[P]_{ext}$ (Table 6.2, Figure 6.3), albeit the proportion of variation in most of these traits attributable to the interactions between genotype (g) and $[P]_{ext}$ were extremely low (Table 6.1). The effect of run was significant for all traits assayed except for the LAUZ. The effect of $[P]_{ext}$ was

significant for most traits including SDW, RDW, mean LRL, PRL and TRL, SRL and R:S (*p<0.01;* Table 6.2), as well as the number of LRs (*p <0.05*; Table 6.2). The effect of $[P]_{ext}$ was however relatively marginal for some traits including inter-branch distance and LAUZ (Table 6.2).

***Table 6.2:*** *ANOVA of traits measured on plants grown on seed germination papers as affected by experimental run, genotype (g), phosphorus treatment ($[P]_{ext}$) and g x $[P]_{ext}$.*

| Trait | Mean (IMB211) | Mean (R500) | s.e.d. (Genotype) | Run (df = 6) | Genotype (df = 1) | $[P]_{ext.}$ (df = 7) | Genotype x $[P]_{ext.}$ (df = 7) |
|---|---|---|---|---|---|---|---|
| IntBranch | 0.662 | 0.668 | 0.0503 | 0.897 | 0.011 | 0.002 | < 0.001 |
| Mean LRL | 1.103 | 1.766 | 0.0556 | < 0.001 | < 0.001 | 0.001 | < 0.001 |
| No. of LR | 9.79 | 33.16 | 0.752 | < 0.001 | < 0.001 | 0.004 | < 0.001 |
| LR Diam. | 0.3154 | 0.3167 | 0.00442 | 0.775 | < 0.001 | < 0.001 | < 0.001 |
| B. Dens. | 2.537 | 2.634 | 0.1121 | 0.384 | < 0.001 | 0.057 | < 0.001 |
| PR Diam. | 0.4105 | 0.4603 | 0.00538 | < 0.001 | < 0.001 | < 0.001 | < 0.001 |
| PR length | 8.44 | 18.62 | 0.352 | < 0.001 | < 0.001 | 0.066 | < 0.001 |
| RDW | 0.518 | 1.419 | 0.0507 | < 0.001 | < 0.001 | < 0.001 | < 0.001 |
| RFW | 4.84 | 20.17 | 0.581 | < 0.001 | < 0.001 | < 0.001 | < 0.001 |
| R:S | 0.2121 | 0.1951 | 0.0089 | 0.058 | < 0.001 | < 0.001 | < 0.001 |
| SDW | 3.21 | 7.91 | 0.258 | < 0.001 | < 0.001 | 0.021 | < 0.001 |
| SFW | 32.1 | 110.5 | 3.15 | < 0.001 | < 0.001 | < 0.001 | < 0.001 |
| SRL | 51.9 | 73.2 | 3.22 | < 0.001 | < 0.001 | < 0.001 | 0.005 |
| TRL | 20.8 | 77.4 | 2.05 | < 0.001 | < 0.001 | < 0.001 | < 0.001 |
| TLRL | 12.6 | 58.6 | 2.01 | < 0.001 | < 0.001 | < 0.001 | < 0.001 |
| Angle | 72.45 | 70.69 | 0.696 | 0.012 | < 0.001 | 0.012 | < 0.001 |
| LAUZ | 7.5 | 5.97 | 1.698 | 0.367 | 0.003 | 0.009 | 0.448 |

Estimated values for root traits either increased, decreased or showed no trend with increasing $[P]_{ext}$. At all $[P]_{ext}$ regimes, SDW of R500 was greater than that of IMB211 seedlings but increase in $[P]_{ext}$ resulted in steady increase in SDW for both genotypes. The percentage increase at 600 µM from 0 µM was 182 and 134% for IMB211 and R500, respectively (Figure 6.4a). Root biomass at 600 µM increased by 25% than at 0 µM $[P]_{ext}$ for the IMB211 genotype and by 28% at 600 µM than at 0 µM $[P]_{ext}$ for R500 (Figure 6.4b).

Total root length of IMB211 seedlings increased from 17.7 cm at 0 µM $[P]_{ext}$ to 19 cm at 600 µM $[P]_{ext}$ and from 63.44 cm at 0 µM $[P]_{ext}$ to 103.59 at 600 µM $[P]_{ext}$ for R500, (Figure 6. 4c). At all $[P]_{ext}$ regimes, the PRL of R500 was greater than the PRL of IMB211 seedlings and PRL

increased from 7.06 cm at 0 µM $[P]_{ext}$ to 9.27 cm at 600 µM $[P]_{ext}$ for IMB211 and from 16.18 cm at 0 µM $[P]_{ext}$ to 19.35 cm at 600 µM $[P]_{ext}$ for R500 (Figure 6.4d). The number of LRs increased from 32 at 0 µM $[P]_{ext}$ to 38 at 600 µM $[P]_{ext}$ for R500 but decreased from 8 at 0µM $[P]_{ext}$ to 5 at 600 µM $[P]_{ext}$ for IMB211 (Figure 6.4e). R500 recorded 47.89% increase in mean LRL at 600 µM than at 0 µM $[P]_{ext}$ but that IMB211 decreased at 600 µM $[P]_{ext}$ (Figure 6.4i). The effects of $[P]_{ext}$ on mean diameter of LRs seemed to be inconsistent for the two genotypes. IMB211 generally showed an increase in diameter with increasing $[P]_{ext,}$ recording 31.4% increase at 600µM $[P]_{ext}$ relative to mean diameter of LRs at 0 µM $[P]_{ext}$. The R500 genotype however showed a decrease of 17% at 600 µM $[P]_{ext}$ compared to mean diameter of LRs at 0 µM $[P]_{ext}$ (Figure 6.4f). The LAUZ increased significantly in response to increase in $[P]_{ext}$ (Figure 6.3). For both genotypes, LAUZ was over 120% more at 600 µM $[P]_{ext}$ than at 0 µM $[P]_{ext}$ (Figure 6. 4h).

Overall, there was no consistent trend in LR insertion angle, but that of IMB211, decreased from 75.55 ° at 0 µM $[P]_{ext}$ to 66.96 ° at 600 µM $[P]_{ext,}$ but not so much for R500 (Figure 6.4g). There was generally a decline in R:S. Root-to-shoot ratio decreased by 53.6% and 35.0% for IMB211 and R500, respectively as $[P]_{ext}$ was increased to 600 µM from 0 µM (Figure 6.4j). Oddly, there were very high SRL for both genotypes at 100 µM $[P]_{ext}$ but SRL at 600 µM $[P]_{ext}$ for IMB211 and R500 decreased by 15.2% and 11.8%, respectively from 600 µM to 0 µM $[P]_{ext}$ (not shown). There was no consistent trend in branching density for either genotype (not shown).

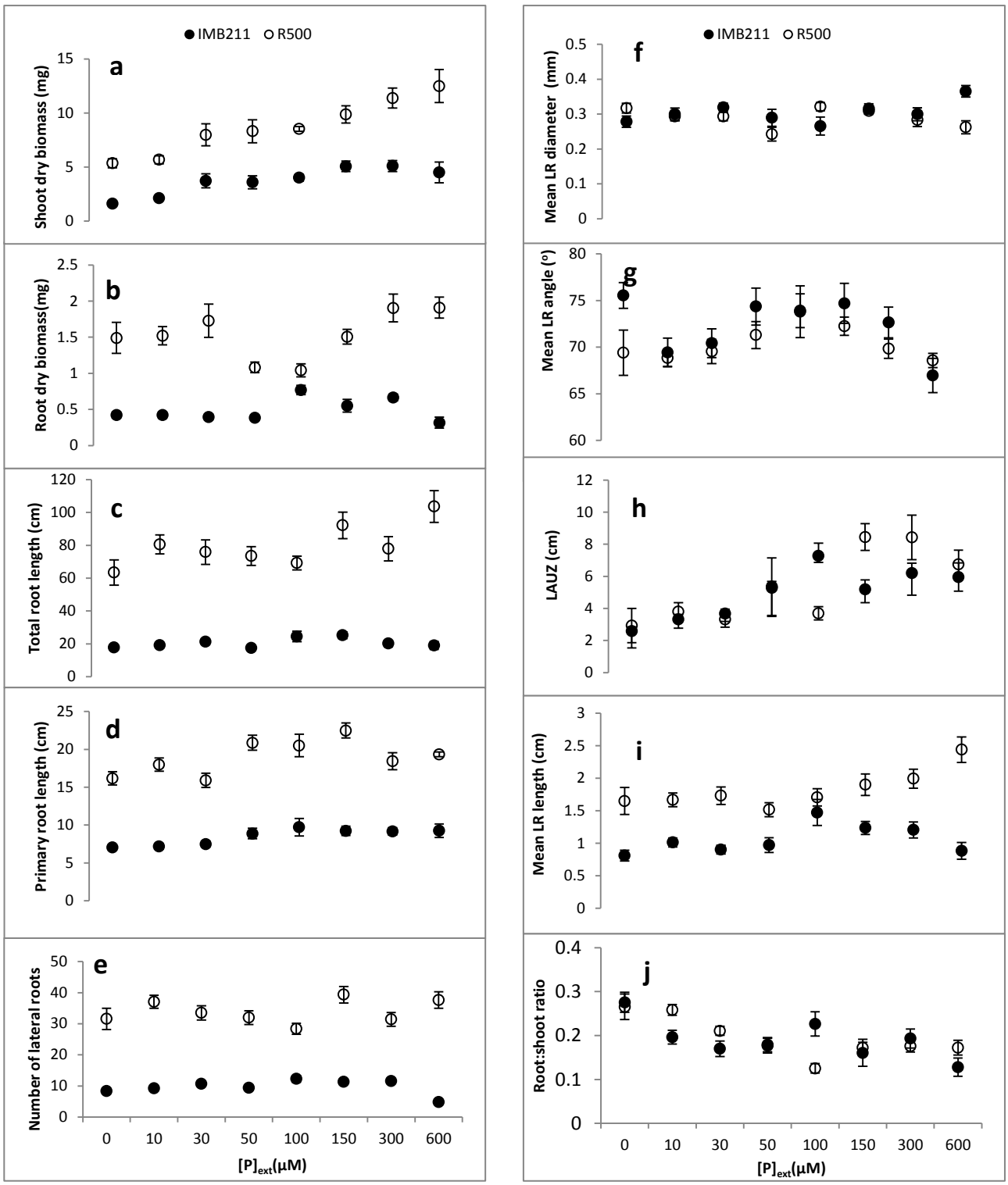


***Figure 6.4:*** *Effect of external Pi concentrations on shoot dry weight (a), root dry weight (b), total root length (c), primary root length (d), number of lateral roots (e), mean lateral root diameter (f), mean lateral root insertion angle (g), length of the apical un-branched zone of the primary root (h), mean lateral root length (i), and root-to-shoot ratio (j) in* Brassica rapa *genotypes, IMB211 and R500, grown on seed germination papers up to 18 days after sowing at different external Pi concentrations. Symbols represent means ± standard error of the mean (n = 12).*

#### *6.2.1.2 Temporal responses of root system to external P concentration*

Visually, there seemed to be no effect of $[P]_{ext}$ at the early stages, but at end of the experiment (Figure 6.5). Longer time-lapse analysis of TRL also seem to suggest that plants grown on $[P]_{ext}$ higher than 10 µM had higher TRL than when $[P]_{ext}$ was 10 µM or lower (Figure 6.5). Due to roots of seedlings outgrowing scanning panes (Figure 6.3), time lapse analyses beyond 14 DAS may be underestimated for the R500 genotype. However, ANOVA of the fitted model indicated that external P did not have significant effect on the asymptotes of TRL (Table 6.3). The overall mean (intercept, $\beta_1$) asymptotes of TRL significantly varied between genotypes and ranged between 53 and 62 cm for IMB211 and 44 and 66 cm for R500 (data not shown). The inflection point ($\emptyset_2$) and scale parameter of the logistic growth function ($\emptyset_3$) were constant across all genotypes and $[P]_{ext}$. The TRL reached the inflection point about 11 d after transfer to scanners and 4 d later (i.e.: 15 d after transfer to the scanners), TRL was about 75% of the asymptote (data not shown). The slope term describing rate of increase in the asymptote of the TRL with $[P]_{ext}$ was 0.03 (data not shown). The overall fit of the model was satisfactory based on the normal Q-Q and residual plots (Appendix 7).

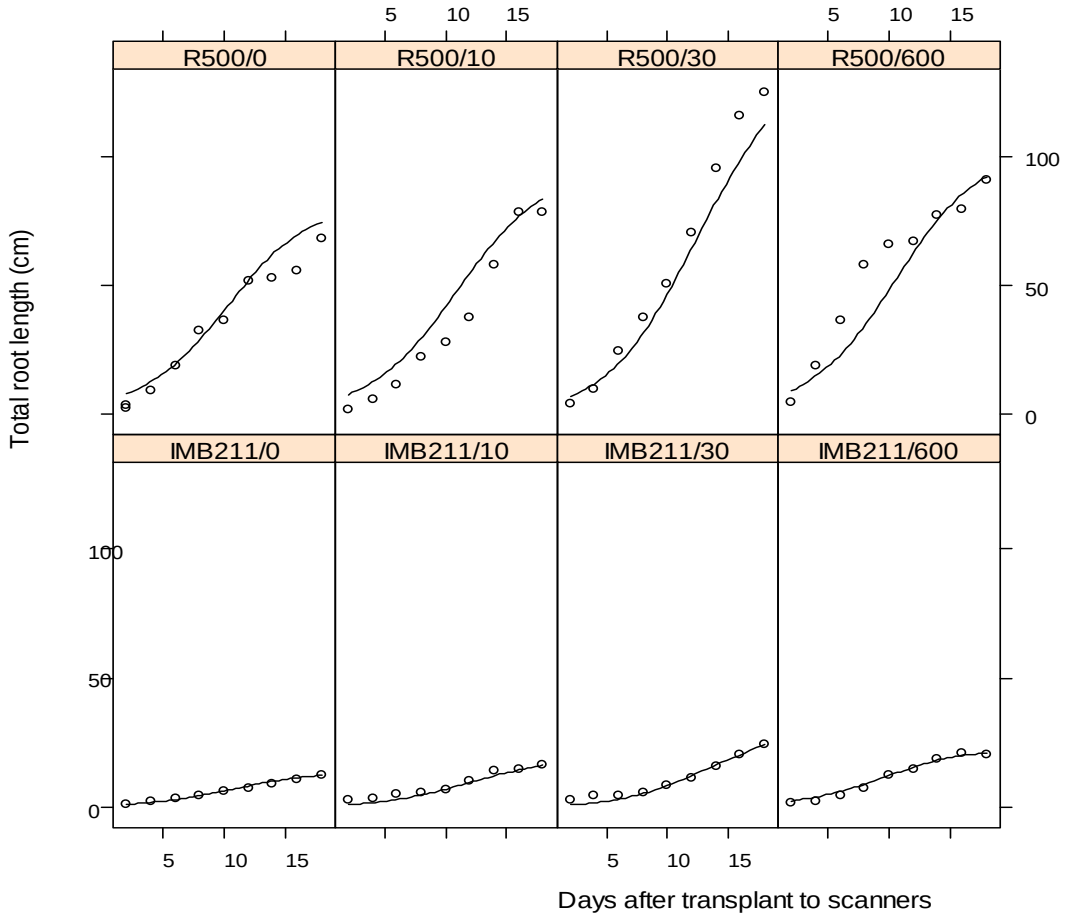


***Figure 6.5:*** *The effect of $[P]_{ext}$ on RSA growth dynamics in IMB211 and R500 seedlings grown on $[P]_{ext}$ of 0, 10, 30 and 600 µM for 18 days after sowing in seed germination papers. (Labels in the graph show name of genotype/$[P]_{ext}$)*

***Table 6.3:*** *ANOVA table for the fitted nonlinear mixed-effects model for* Brassica rapa *seedlings grown for 18 DAS on seed germination papers (Experiment 1) and 21 DAS on soil-filled rhizoboxes (Experiment 2). (numDF: numerator degrees of freedom, denDF: denominator degrees of freedom.*

| **Experiment 1** | | | | |
|---|---|---|---|---|
| **Source of variation** | **numDF** | **denDF** | **F-value** | ***p-value*** |
| Asymptote-Intercept ($\emptyset_{i1}$) | 1 | 60 | 132.99701 | *<0.0001* |
| Asymptote-$[P]_{ext}$ (Slope) | 1 | 60 | 2.94363 | *0.0914* |
| Asymptote-Genotype | 1 | 60 | 1.97032 | *<0.0001* |
| Asymptote- $[P]_{ext}$ x Genotype | 1 | 60 | 0.62130 | *0.4337* |
| Inflection point($\emptyset_{i2}$) | 1 | 60 | 87.88918 | *<0.0001* |
| Scale parameter ($\emptyset_{i3}$) | 1 | 60 | 102.28809 | *<0.0001* |
| **Experiment 2** | | | | |
| Asymptote-Intercept ($\emptyset_{i1}$) | 1 | 261 | 137.525 | *<0.0001* |
| Asymptote-$[P]_{ext}$ (Slope) | 1 | 261 | 0.352 | *0.5537* |
| Asymptote-Genotype | 5 | 261 | 6.557 | *<0.0001* |
| Asymptote- $[P]_{ext}$ x Genotype | 5 | 261 | 0.382 | *0.8611* |
| Inflection point($\emptyset_{i2}$) | 1 | 261 | 184.569 | *<0.0001* |
| Scale parameter ($\emptyset_{i3}$) | 1 | 261 | 4281.286 | *< 0.0001* |

#### *6.2.1.3 Tissue P-concentration and P-uptake in Experiment 1*

Seed P concentration was assayed for the two parental genotypes to determine the amount of P available to the seedlings at the initial stages of growth. The seed P concentration was approximately 11.5 and 14.5 mg $g^{-1}$ in the seeds of R500 and IMB211 respectively, (Figure 6.6).

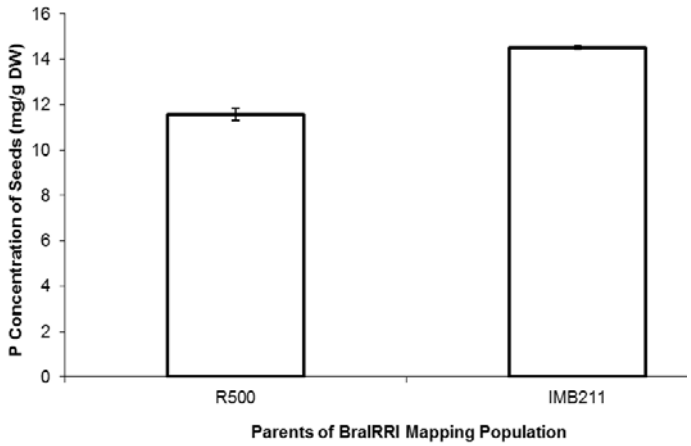


***Figure 6.6****: Seed P concentration of the parents of the BraIRRi mapping population.*

Plants grown for longer period in Experiment 1 (18 DAS) were used for tissue P analyses. Figure 6.7 show P-concentration (% dry weight) and P-uptake (µg $plant^{-1}$). P-uptake was estimated as the product of P concentration (µg P $mg^{-1}$) and dry matter (mg) in shoots and roots. Genotypes (*p<0.001*), $[P]_{ext}$ *(p<0.05)* and interactive effect of genotype and external P concentration (*p<0.001*), had significant effect on Shoot [P] but there was no consistent trend for the R500 genotype (Figure 6.7). For IMB211, Shoot [P] increased across the various $[P]_{ext}$ and there was 1.9% DW at 600 µM $[P]_{ext}$ which was over 100% greater than the 0.95 % P recorded at 0 µM $[P]_{ext}$ for that genotype (Figure 6.7). The mean shoot [P] over the different $[P]_{ext}$ for IMB211 and R500 was 1.4% DW and 1.0 %DW, respectively.

Genotype (*p<0.001*) and $[P]_{ext}$ (*p<0.05*) had significant effect on shoot P uptake but the interactive effect of genotype and $[P]_{ext}$ was statistically not significant. Shoot P uptake of

both genotypes increased with increasing $[P]_{ext}$ concentration. At all $[P]_{ext}$ regimes, uptake for R500 was greater than uptake for IMB211 (Figure 6.7). On average shoot P uptake of R500 was 64.7% greater than IMB211.

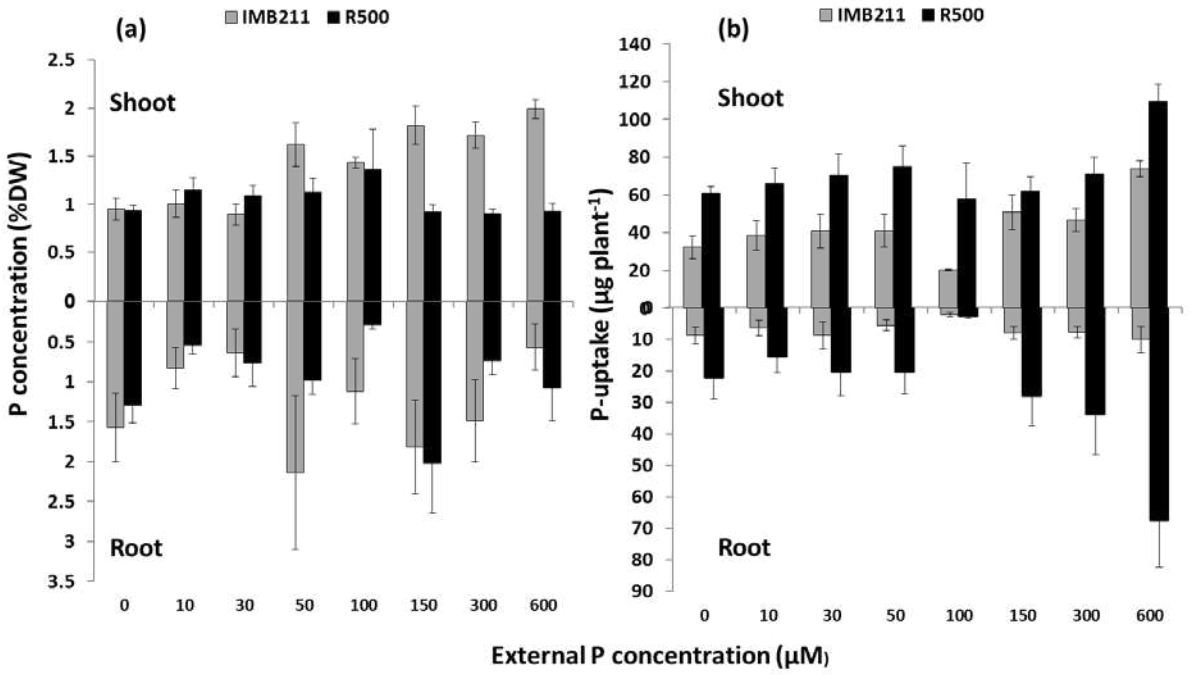


***Figure 6.7:*** *Tissue P-concentration and uptake by* Brassica rapa *genotypes, IMB211 and R500 grown for 18 DAS on seed germination papers at differential external P concentrations. (a) Shoot [P] (above) and Root [P] (below) and (b) P-uptake in shoots (above) and roots (below). Error bars show: ± standard error of the mean, n = 6.*

The effect of external P concentration was only marginally significant at $p<0.05$, ($p= 0.036$) on Root [P], but there was no noticeable trend. It appeared that seedlings which were not grown on scanners recorded greater Root [P] (Figure 6.7). Neither genotype nor the interactive effect of genotype x $[P]_{ext}$ had a significant effect on Root [P]. Genotype ($p<0.001$) and $[P]_{ext}$ ($p<0.05$) however had significant effect for P uptake in roots. Uptake in the roots of R500 was greater and increased with increasing $[P]_{ext}$ but same trend was not evident in P uptake in the roots of IMB211 (Figure 6.7).

### 6.2.2 Experiment 2: Plant response to $[P]_{ext}$ supply in soil-filled rhizoboxes

#### *6.2.2.1* Effect of genotype, run, external Pi concentration and their interactions

Genotype effect accounted for the largest portion of total variance in most of the traits assayed including SDW (78%), RDW (64%), number of LRs (76%), PRL (59%) and TRL (56 %) (Table 6.4). Genotype effect however recorded little or no effect in a few traits such as average diameter, angle, inter-branch distance, branching density, and R:S. Run accounted for little variability (0 - 23%) for majority of traits but same unusually accounted for large variability in 3 traits namely average diameter (36%), angle (99% ) and branching density (63%), (Table 6.4). For most traits assayed, little variation was attributed directly to the $[P]_{ext}$ and included 5% for SDW, 19% for average diameter, 10% for LAUZ, 23% for branching density, 30% for R:S, 18% for root area to volume ratio and 19% for root tissue density (RTD). The effects of interactions between genotype x $[P]_{ext}$ accounted for variation ranging from 0 to 11% (Table 6.4). Broad-sense heritability ($\sigma_g^2$ / $\sigma_p^2$), was highest for shoot biomass, number of LRs (> 0.75), RDW, surface area and TLRL (>0.60). Broad-sense heritability was intermediate for TRL, PRL and mean LRL (> 0.40), but low (<0.40) for remaining traits (Table 6.4).

***Table 6.4:*** *Sources of variation and broad sense heritability in shoot and root traits assayed among the parents (IMB211 and R500) and four RILs of the* Brassica rapa *BraIRRI mapping population grown on soil filled rhizoboxes at differential external P concentration for up to 21 days in the phenotyping platform. (Percentage contribution of sources of variation is indicated in brackets underneath variance of effects).*

| Trait | $\mu$ | $\sigma^2_\beta$ (%) | $\sigma^2_\alpha$ (%) | $\sigma^2_g$ (%) | $\sigma^2_{\beta\alpha}$ (%) | Residual | $H^2$ |
|---|---|---|---|---|---|---|---|
| SFW (mg) | 209.0 | 5 (0.03) | 14147 (89.13) | 83 (0.52) | 20 (0.13) | 1618 (10.19) | 0.89 |
| SDW (mg) | 11.93 | 0.383 (0.89) | 33.811 (78.47) | 1.995 (4.63) | 0 (0.00) | 6.9 (16.01) | 0.78 |
| RFW (mg) | 25.5 | 0.0132 (2.72) | 0.251 (51.80) | 0.0074 (1.53) | 0 (0.00) | 0.213 (43.95) | 0.52 |
| RDW (mg) | 1.43 | 0.0389 (4.53) | 0.5484 (63.86) | 0.0305 (3.55) | 0.012 (1.40) | 0.229 (26.67) | 0.64 |
| TRL (cm) | 61.21 | 261 (20.17) | 722.2 (55.80*) | 10.9 (0.84) | 0 (0.00) | 300.2 (23.19) | 0.56 |
| TLRL (cm) | 55.71 | 163.7 (12.78) | 801.1 (62.56) | 24.6 (1.92) | 0 (0.00) | 291.1 (22.73) | 0.63 |
| PRL (cm) | 21.42 | 0.03 (0.07) | 23.61 (58.61) | 0.33 (0.82) | 0 (0.00) | 16.31 (40.49) | 0.59 |
| Av Diam. (mm) | 0.387 | 0.001034 (36.46) | 0.000021 (0.74) | 0.00054 (18.94) | 0.000114 (4.02) | 0.00113 (39.84) | 0.01 |
| No. of LRs | 21.47 | 0 (0.00) | 1.0654 (76.02) | 0 (0.00) | 0 (0.00) | 0.336 (23.98) | 0.76 |
| Angle ($^o$) | 69.17 | 2.733457 (99.67) | 0.000167 (0.01) | 0 (0.00) | 0.000464 (0.02) | 0.00831 (0.30) | 0.00 |
| Int. Dist. (cm) | 0.95 | 0 (0.00) | 0.0098 (6.18) | 0 (0.00) | 0.0068 (4.29) | 0.142 (89.53) | 0.06 |
| Mean LRL (cm) | 1.12 | 0 (0.00) | 0.1196 (45.60) | 0.0007 (0.27) | 0 (0.00) | 0.142 (54.14) | 0.46 |
| LAUZ (cm) | 5.64 | 0.077 (0.53) | 4.341 (29.87) | 1.38 (9.50) | 0 (0.00) | 8.734 (60.10) | 0.30 |
| B. Dens. (root/cm) | 1.45 | 0.20569 (62.55) | 0.00008 (0.02) | 0.07409 (22.53) | 0 (0.00) | 0.049 (14.90) | 0.00 |
| R:S | 0.1223 | 0.000007 (0.23) | 0.000025 (0.82) | 0.00093 (30.36) | 0.000074 (2.42) | 0.00202 (66.16) | 0.01 |
| Root volume ($cm^3$) | 0.0711 | $8.4 \times 10^{-6}$ (0.58) | 0.000728 (49.92) | $4.7 \times 10^{-5}$ (3.24) | 0.000131 (8.99) | 0.000544 (37.29) | 0.50 |
| Root surface area ($cm^2$) | 7.287 | 0.811 (5.44) | 9.274 (62.19) | 0 (0.00) | 0.415 (2.78) | 4.412 (29.59) | 0.62 |
| Area: Vol. ($cm^{-1}$) | 104.0 | 57.9 (23.38) | 0.9 (0.36) | 43.3 (17.49) | 13.8 (5.57) | 131.7 (53.19) | 0.00 |
| Root Tissue density | 0.02112 | $8.1 \times 10^{-6}$ (7.41) | $1.2 \times 10^{-5}$ (11.15) | $2.0 \times 10^{-5}$ (18.53) | $1.2 \times 10^{-5}$ (11.08) | $5.7 \times 10^{-5}$ (51.83) | 0.11 |
| Root biomass (%total biomass) | 10.72 | 0 (0.00) | 0.23 (1.30) | 5.49 (31.00) | 0.48 (2.71) | 11.51 (64.99) | 0.01 |

There was statistically significant differences (*p<0.05*) between the six genotypes in all RSA traits measured except for branching density and R:S. The effect of run was significant for 50% (9 out of 18) of traits assayed including RDW, TRL, TLRL, angle, diameter, SRL, tissue density, surface area and area: volume ratio. The effect of $[P]_{ext}$ was also significant for 50%

of traits assayed including SDW, RDW, TLRL, LAUZ, diameter, R:S, RTD, surface area and area:volume ratio (*p<0.05;* Table 6.5). The interaction of Genotype and $[P]_{ext}$ was significant (*P< 0.05*) for angle, root volume and RTD (Table 6.5). Individuals within the assayed reference population showed large responses to $[P]_{ext}$. The relationship between biomass of the six lines of *B. rapa* grown in soil to which was added either 600 µM of $KH_2PO_4$ solution or 0 µM of $KH_2PO_4$ was linear and correlations between low $[P]_{ext}$ and high $[P]_{ext}$ treatments for biomass was significant (*p< 0.001*; Figure. 6.8).

***Table 6.5**: ANOVA of traits measured on plants grown on soil-filled rhizoboxes as affected by experimental run (r), genotype (g), phosphorus treatment ($[P]_{ext}$.) and g x $[P]_{ext}$*

| Trait | Overall Mean | | | | | | s.e.d (Genotype) | Run (df = 1) | Genotype (df = 5) | $[P]_{ext}$ (df = 1) | Genotype x $[P]_{ext}$ (df = 5) |
|---|---|---|---|---|---|---|---|---|---|---|---|
| | IMB211 | IRRi016 | IRRi124 | IRRi201 | IRRi229 | R500 | | | | | |
| SDW | 7.31 | 7.83 | 13.09 | 10.18 | 10.12 | 23.07 | 0.758 | 0.095 | < 0.001 | < 0.001 | 0.659 |
| RDW | 0.708 | 0.967 | 1.612 | 1.188 | 1.263 | 2.832 | 0.1382 | 0.004 | < 0.001 | 0.001 | 0.156 |
| TRL | 31.0 | 48.8 | 54.0 | 55.8 | 66.6 | 111.1 | 5.0 | < 0.001 | < 0.001 | 0.065 | 0.525 |
| TLRL | 26.4 | 42.3 | 46.3 | 48.5 | 61.9 | 108.8 | 4.93 | < 0.001 | < 0.001 | 0.011 | 0.725 |
| PRL | 13.96 | 18.14 | 23.14 | 22.06 | 22.85 | 28.34 | 1.166 | 0.293 | < 0.001 | 0.164 | 0.789 |
| LAUZ | 4.66 | 6.52 | 7.67 | 7.26 | 5.86 | 1.86 | 0.853 | 0.203 | < 0.001 | < 0.001 | 0.701 |
| No. of LRs | 10.83 | 16.04 | 21.73 | 17.58 | 22.52 | 40.08 | 1.518 | 0.335 | < 0.001 | 0.704 | 0.956 |
| Mean LRL | 0.591 | 1.026 | 1.06 | 1.281 | 1.094 | 1.635 | 0.1295 | 0.911 | < 0.001 | 0.83 | 0.85 |
| B. Dens. | 1.319 | 1.533 | 1.531 | 1.425 | 1.357 | 1.527 | 0.1843 | 0.822 | 0.746 | 0.162 | 0.604 |
| Int. Dist. | 1.175 | 0.917 | 0.867 | 1.047 | 0.904 | 0.795 | 0.1088 | 0.467 | 0.01 | 0.39 | 0.157 |
| Av Diam. | 0.3996 | 0.3897 | 0.3841 | 0.3755 | 0.3995 | 0.3743 | 0.00969 | < 0.001 | 0.026 | < 0.001 | 0.057 |
| Angle | 72.7 | 68.8 | 66.77 | 66.49 | 69.82 | 70.45 | 1.7 | < 0.001 | 0.003 | 0.825 | 0.007 |
| R:S | 0.0982 | 0.13 | 0.1293 | 0.1231 | 0.1281 | 0.1249 | 0.01297 | 0.267 | 0.13 | < 0.001 | 0.215 |
| SRL | 52.4 | 56.7 | 36.6 | 51.9 | 54 | 42.4 | 5.31 | < 0.001 | 0.001 | 0.165 | 0.351 |
| Surface area | 3.83 | 5.69 | 6.54 | 6.43 | 8.34 | 12.89 | 0.606 | < 0.001 | < 0.001 | 0.254 | 0.066 |
| Root volume | 0.0381 | 0.0572 | 0.0662 | 0.0594 | 0.085 | 0.1206 | 0.00673 | 0.148 | < 0.001 | 0.002 | 0.003 |
| Surf:vol ratio | 102.49 | 100.39 | 102.26 | 107.88 | 101.77 | 109.32 | 3.313 | <.001 | 0.038 | < 0.001 | 0.052 |
| RTD | 0.01859 | 0.01737 | 0.02815 | 0.02145 | 0.01652 | 0.02463 | 0.002178 | 0.001 | < 0.001 | < 0.001 | 0.005 |

Lines grown on high $[P]_{ext}$ soil yielded between 13 and 36% higher SDW but between 3 and 53% lesser RDW than lines grown on low $[P]_{ext}$ soil (Figures 6.8; 6.9a). External P supply decreased the biomass partitioning between shoot and root (*p<0.001*) with higher proportion of biomass invested into root at low $[P]_{ext}$ (Figure 6.9b). At high $[P]_{ext}$, approximately 8 to 10% of total biomass was of root in various lines compared to 10 to 14% at low $[P]_{ext}$ in various lines. Total root length was significantly reduced in three of the six lines assayed at high $[P]_{ext}$ compared with low $[P]_{ext}$ (Figure 6.9c). While the effect of $[P]_{ext}$ did not significantly alter PRL, same significantly (*p<0.001*) affected the LAUZ. Respectively, LAUZ were 28.43, 22.91, 11.74, 50.60, 64.19 and 81.82% higher in seedlings of IMB211, IRRI016, IRRI124, IRRI201, IRRI229 and R500 grown on high $[P]_{ext}$ soil compared to those grown on low $[P]_{ext}$ (Figure. 6.9d). Seedlings grown at high $[P]_{ext}$ recorded lesser TLRL for majority of the lines assayed (Figure. 6.9e). Whilst mean diameter and volume of roots were on the average depressed under low $[P]_{ext}$, root tissue density and the ratio of root surface area and volume were generally higher (*p<0.001*) at low $[P]_{ext}$ (Figures 6.9f -h).

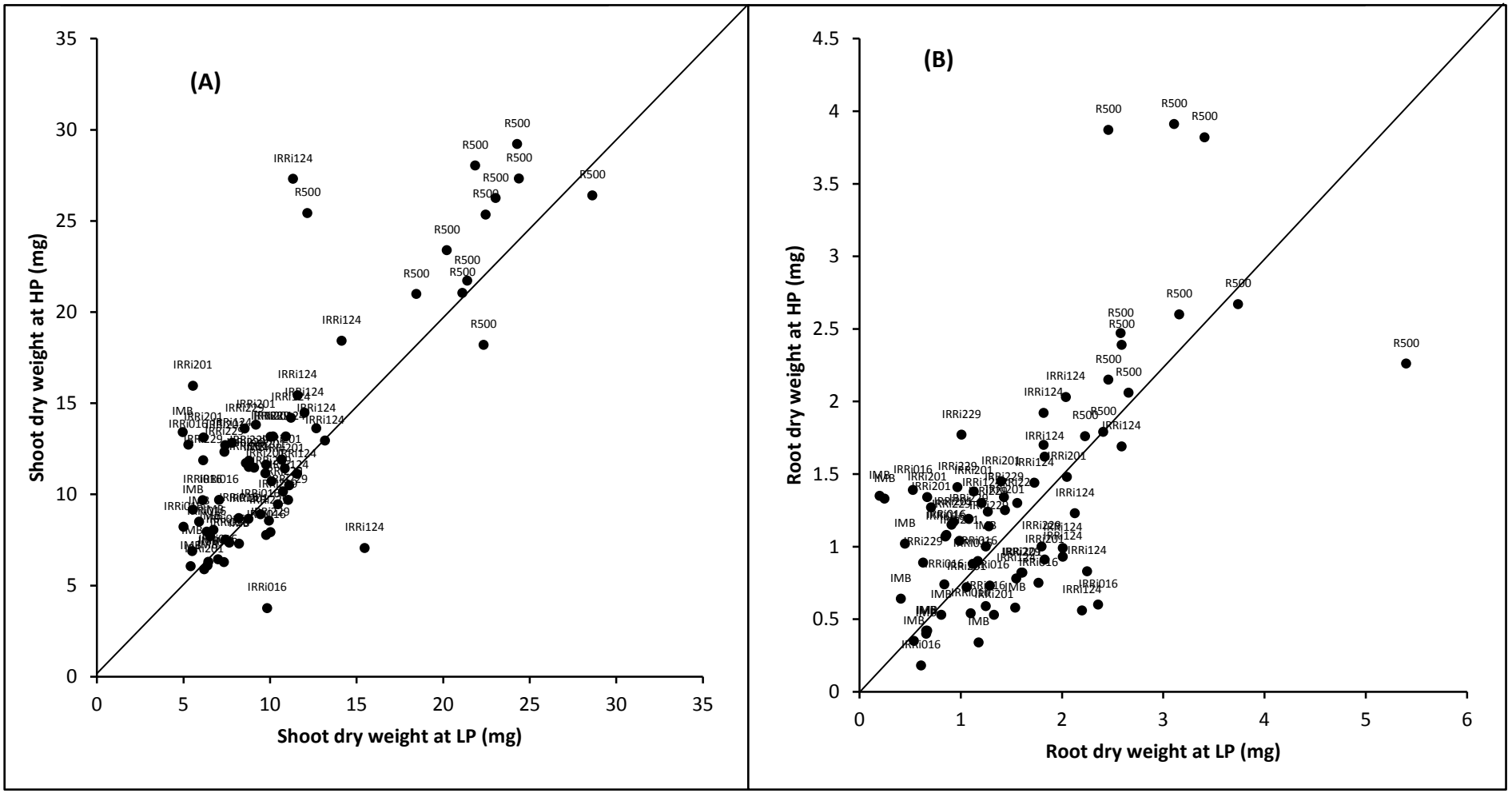


***Figure 6.8:*** *Variation in (A) shoot dry weight and (B) root dry weight in selected RILs and parents of the BraIRRI mapping population. Seedlings were grown on soil-filled rhizoboxes containing soil either un-amended or amended with solution containing 600 µM $KH_2PO_4$. Data are observed values of 12 replications per line per treatment and the continuous line represents the 1: 1 line*

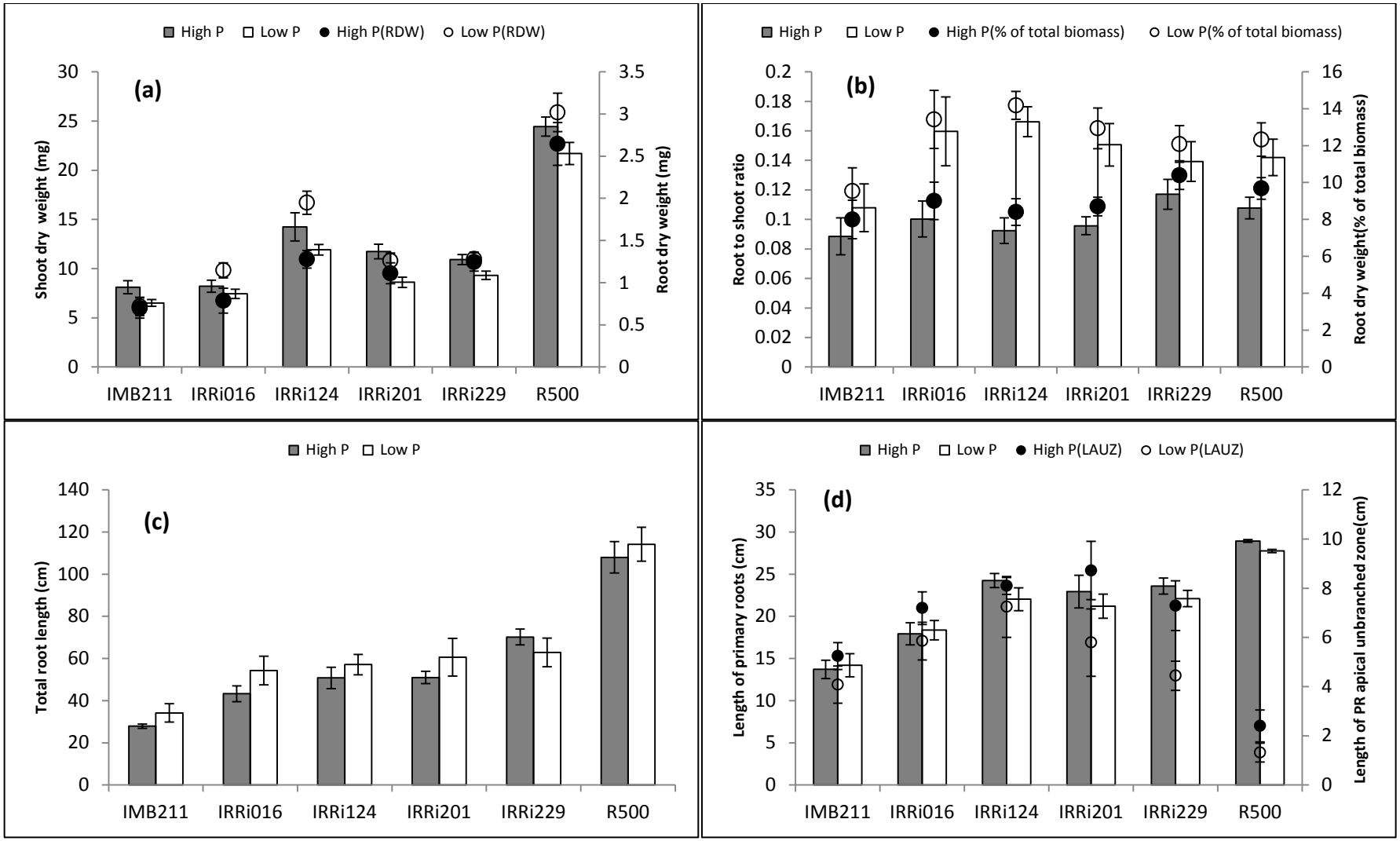
High P
Low P
High P(RDW)
Low P(RDW)
(a)
Shoot dry weight (mg)
Root dry weight (mg)
IMB211
IRRi016
IRRi124
IRRi201
IRRi229
R500
High P
Low P
High P(% of total biomass)
Low P(% of total biomass)
(b)
Root to shoot ratio
Root dry weight(% of total biomass)
(c)
Total root length (cm)
High P(LAUZ)
Low P(LAUZ)
(d)
Length of primary roots (cm)
Length of PR apical unbranched zone(cm)

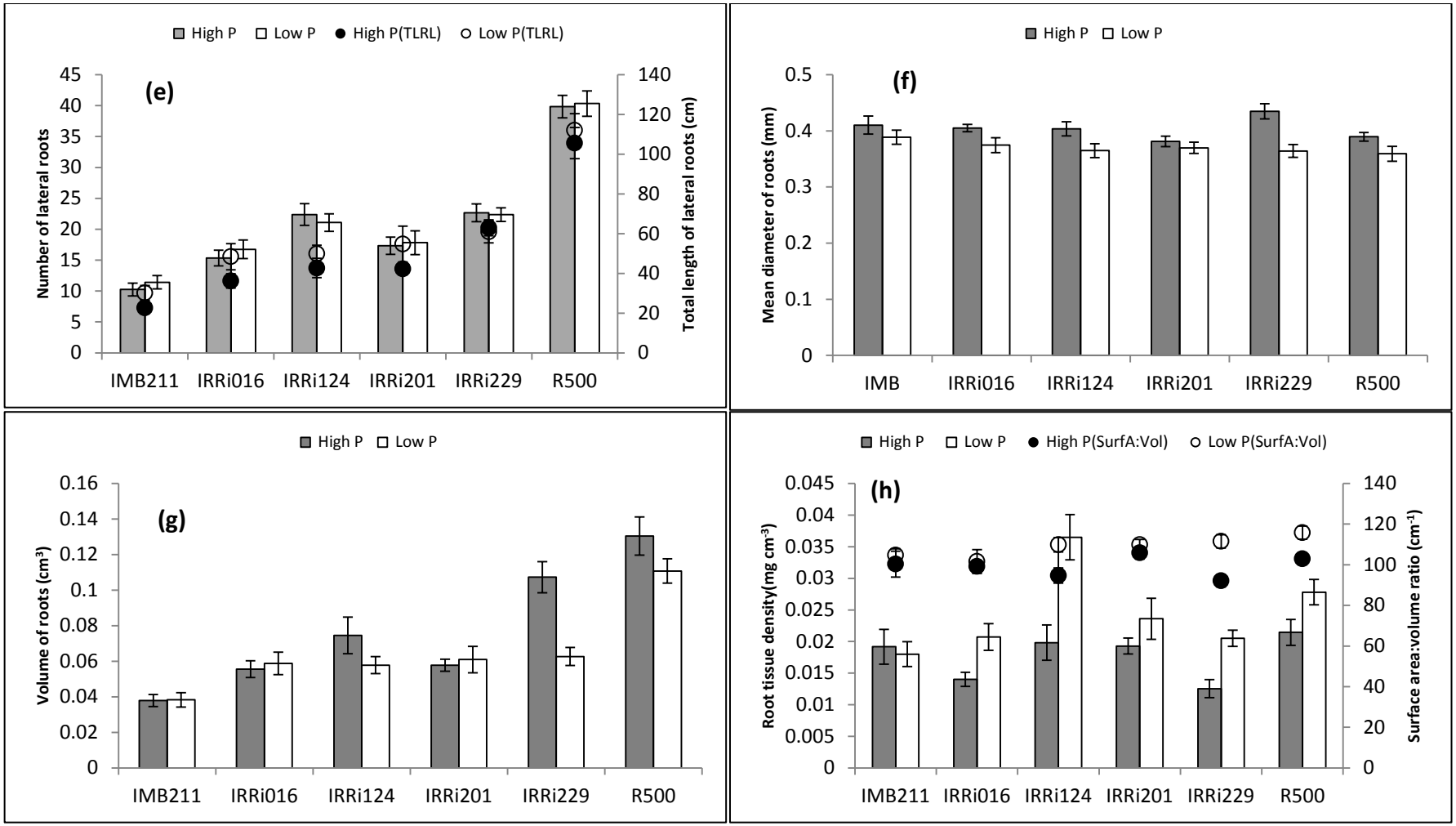


***Figure 6.9:*** *Changes in shoot and root dry weight (a), root-to-shoot ratio (b), total root length (c), primary root length and length of the apical un-branched zone of the primary root (d), number of lateral roots and total length of all laterals (e), mean diameter of all root axes (f), volume of roots (g), root tissue density and root surface area-to-volume ratio (h) in six* Brassica rapa *genotypes grown on soil-filled rhizoboxes at two* $[P]_{ext}$ *for 21 DAS. Symbols represent means ± s.e.m. (n = 12).*

#### *6.2.2.2 Temporal responses of RSA to external P concentration*

The fitted model indicated that $[P]_{ext}$ did not have significant effect on the asymptotes of TRL (Table 6.3). The overall mean (intercept, $\beta_1$) asymptotes of TRL significantly varied between genotypes and were 56.47 and 53.45 cm for IMB211, 64.63 and 63.43 cm for IRRI016, 51.88 and 35.27 cm for IRRI201, 58.68 and 56.74 cm for IRRI229, 33.60 and 39.51 cm for IRRI124, and 45.58 and 39.50 cm for R500, respectively for high and low $[P]_{ext}$ (data not shown). The inflection point ($\emptyset_2$) and scale parameter of the logistic growth function ($\emptyset_3$) were constant across all genotypes and $[P]_{ext}$. The TRL reached the inflection point about 13 d after transfer to rhizoboxes and 5 d later (i.e.: 18 d after transfer to the scanners), TRL was about 75% of the asymptote (data not shown). The slope term describing rate of increase in the asymptote of the TRL with $[P]_{ext}$ was 0.3 (data not show). To enable model convergence, the fitted model here did not incorporate an auto-correlation structure. The overall model fit (Figure 6.10) was satisfactory based on the normal Q-Q and residual plots (Appendix 7).

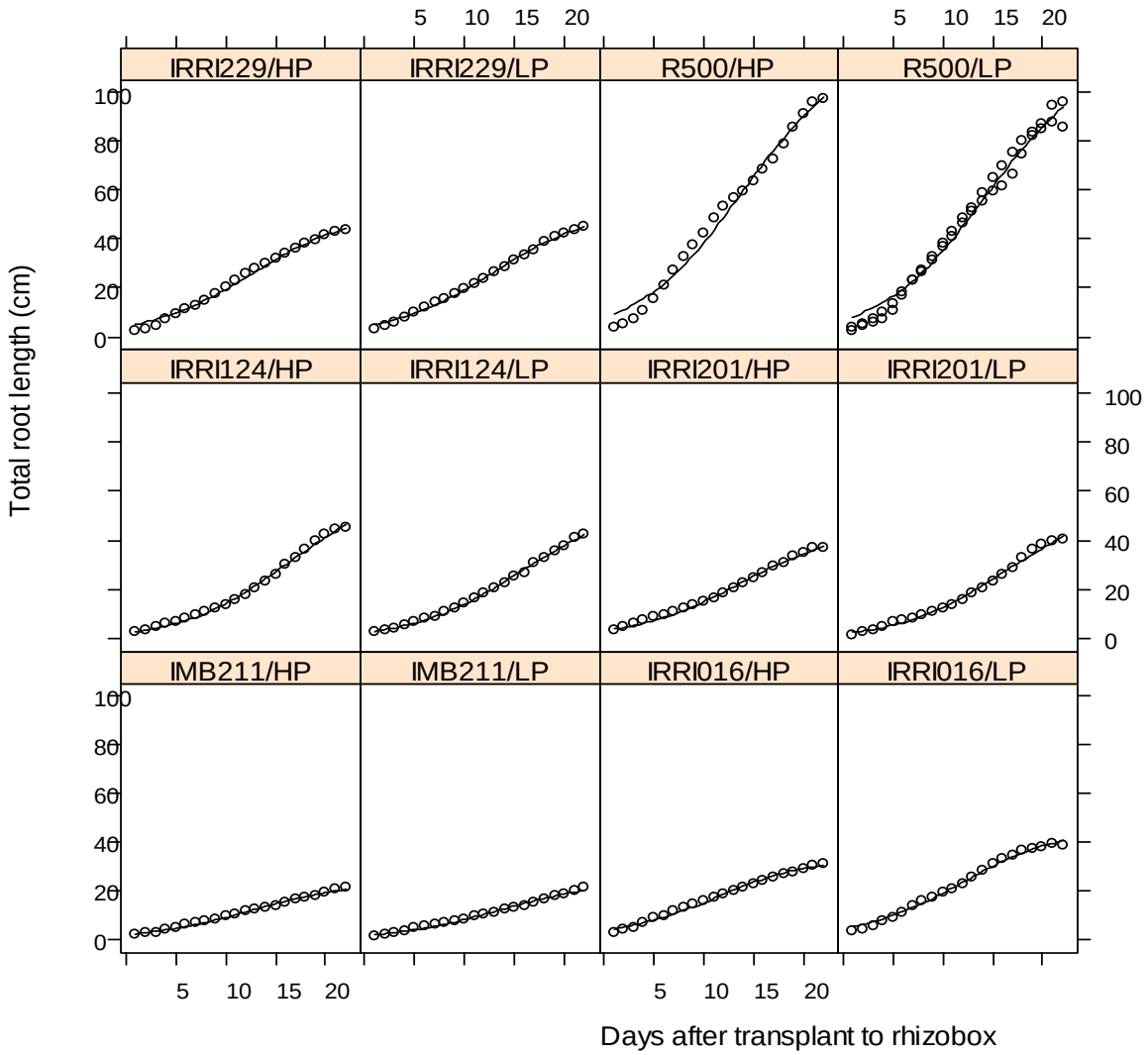


***Figure 6.10****: Plots of the fitted model (solid line) and observed values (open circles) for 6* B. rapa *genotypes grown at low or high external P concentration (LP and HP) on soil-filled rhizoboxes for 21 DAS following 3 d germination.*

#### *6.2.2.3 Tissue P-concentration in Experiment 2*

Increased P availability induced a strong increase in shoot [P] in all genotypes (*p< 0.001*, Figure 6.11A). There was also a significant interaction between the effect of $[P]_{ext}$ treatment and the genotype on Shoot [P] (*p < 0.05*). There was no clear effect of P availability on Root [P] (Figure 6.13A). Total root length (*r = 0.84, p < 0.001*), TLRL (*r = 0.79, p < 0.05*) and number of LRs (*r = 0.58, p < 0.05*) were strongly correlated with total [P] in plants grown at low $[P]_{ext}$ but not with plants grown at high $[P]_{ext}$ (Figures. 6.11B-D).

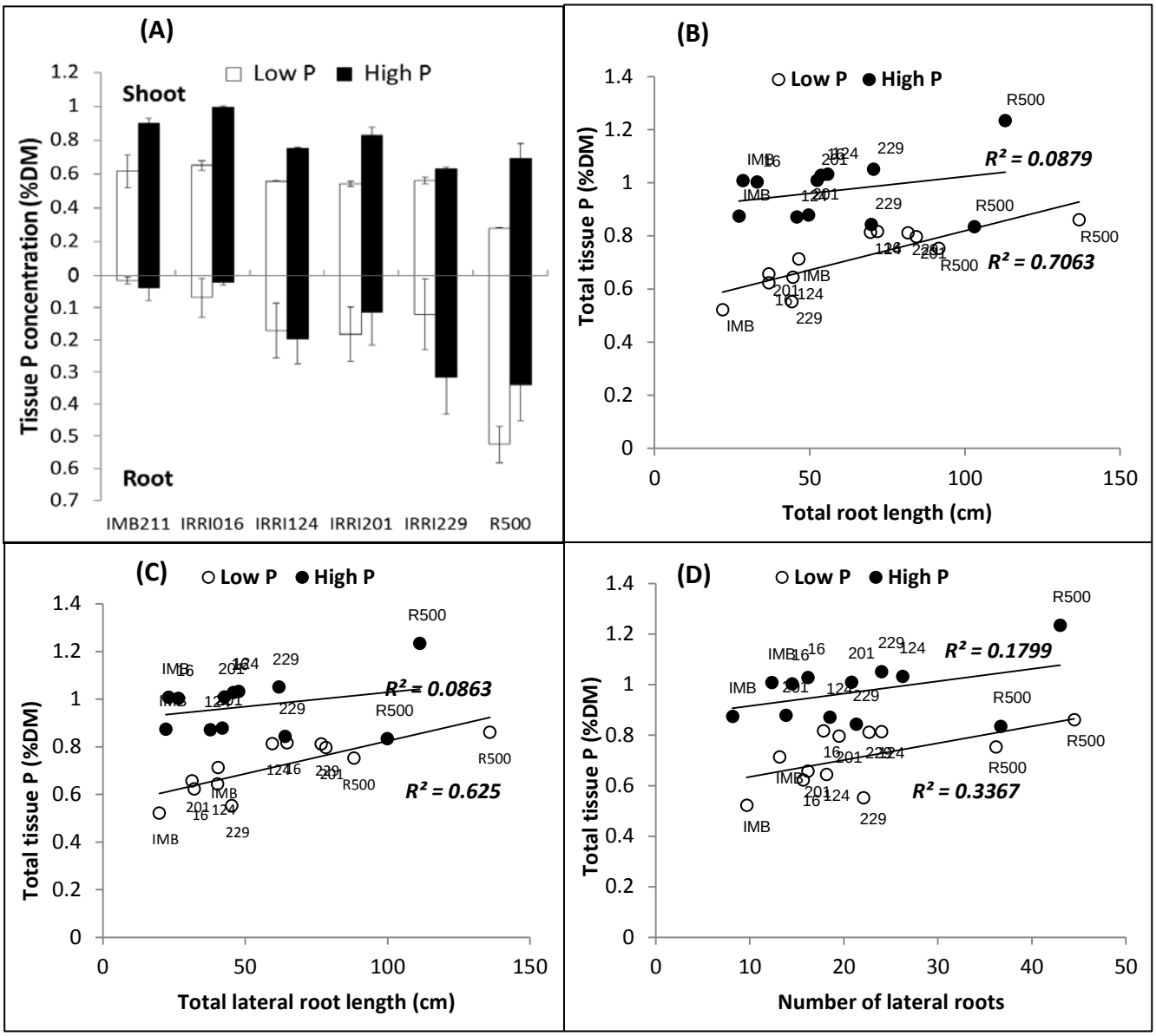


***Figure 6.11*** *(A): Tissue P-concentration by* Brassica rapa *lines at 21 DAS in soil-filled rhizoboxes amended with 0 (Low $[P]_{ext}$) or 600 µM $KH_2PO_4$ solution (High $[P]_{ext}$) and watered initially to 80% field capacity; B-D: relationship between total tissue P content and total root length (B), total tissue P content and total lateral root length (C) and total tissue P content and number of lateral roots (D) for plants grown with addition of 0 µM or 600 µM as $KH_2PO_4$ solution. Open and closed symbols are for low $[P]_{ext}$ and high $[P]_{ext}$ respectively.*

### *6.3 Discussion*

Plant adaptations to P limitation can be classified into two broad strategies: (i) strategies for the efficient use and conservation of P once it is obtained and (ii) strategies to maximise P uptake. Conservation strategies including increases in growth per unit P, re-sorption or re-translocation and increased plant leaf life span, enable plants to survive under P-limiting

environments but do not necessarily address the issue of unexploited P resources which are available in the soil (Lajtha and Harrison, 1995; Vance, 2001). Strategies which actively enhance plant P-acquisition are the most beneficial to optimal crop growth and increased yield and represent targets for crop improvement. These strategies include increases in root growth and length, R:S, SRL, root surface area, branching density and insertion angle of LRs as well as increased elongation and density of root hairs (Lynch, 2011; Richardson *et al.*, 2009; Vance, 2001). With large amounts of P fertilizer required to achieve optimal crop productivity, the identification of genotypes that can efficiently access P in P-deficient environments and precise methodology to identify those genotypes is vital to crop improvement goals. It is critical to determine the differences in the root system among selected lines to provide basic architectural information and to detect its potential correlations with the observed differences in P uptake (Narang *et al.*, 2000).

### 6.3.1 Response of shoot and root biomass to external P

In this study, response of seedlings for many traits to $[P]_{ext}$ was not consistent when seedlings were grown for shorter periods (up to 14 days after sowing) but for brevity these result are not shown here. Except for LAUZ, the analyses indicated that it is advantageous to maintain root growth at low P with reduced shoot growth. Accumulation of biomass responded to $[P]_{ext}$ concentration when seedlings were grown both on paper and rhizoboxes up to 18 and 21 DAS, respectively. In both Experiments 1 and 2, genotypes assayed under differential $[P]_{ext}$ differed in shoot and root biomass (Tables 6.2 and 6.5) but differences in shoot dry weight of plants grown on paper was marginal. Shoot biomass accumulation on high $[P]_{ext}$ was higher than on low $[P]_{ext,}$ for all genotypes (Figures 6.4a & b; 6.9a). Root-to-shoot ratio at low $[P]_{ext}$ regimes was much higher compared with at high P treatments (Figures 6.4j and 6.9b). These results are consistent with results obtained by Akhtar *et al.*

(2008a), Bolan *et al.* (1987) and Li *et al.* (2009). Increased R:S in nutrient limiting conditions is attributed to preferential assimilate distribution to the roots (Akhtar *et al.*, 2008a; Bolan *et al.*, 1987; Nielsen *et al.*, 2001; Vance *et al.*, 2003), which could be an adaptation of *B. rapa* to acquire more P under P-starvation.

The effect of $[P]_{ext}$ on root biomass was not strong in both experiments (Figures 6.4b and 6.9a). In Experiment 2, root biomasses of multiple genotypes grown in rhizoboxes containing un-amended soil (low $[P]_{ext}$) were slightly greater than that of seedlings grown in soil amended with solution $KH_2PO_4$ (high $[P]_{ext}$), but the effect was not consistent across all genotypes. There was a general decline in RDW with increasing $[P]_{ext}$ for seedlings grown on soil and non-soil media Figures 6.4b and 6.9a. For example, RDW (as percent of total plant biomass) decreased by 39% and 20% respectively for IMB211 and R500 as $[P]_{ext}$ was increased to 600 µM in Experiment 1. This result agrees with Nobel *et al.* (1989) who reported of 54% decrease in the in RDW of *Agave lechuguilla* plants when applied P was increased from 0 to 500 kg $ha^{-1}$. The proportionally greater root growth relative to shoot growth in *B. rapa* in P-limiting conditions may lead to compensating increase in P acquisition.

At the seedling stage, shoot biomass indicates economic yield and offers a reliable criterion for assessing performance under resource limiting conditions (Akhtar *et al.*, 2006). The results here indicate that on low $[P]_{ext}$, differences in biomass could be utilised in identifying efficient and inefficient genotypes. More importantly, significant variations in SDW due to $[P]_{ext}$ x genotype interaction (Tables 6.2; Figure 6.8) suggest that useful genetic variations exist among *B. rapa* for acquisition of P from limited P environments. Whilst such genotype

x environment interactions indicates high sensitivity of the trait to the environmental effect, it also has valuable implications for the development of genotypes conferred improved acquisition and use of P.

### 6.3.2 Response of root system architecture to external P

The concentration of soluble P in the soil affects root morphology of plants (Hajabbasi and Schumacher, 1994). In this thesis however, the effect of $[P]_{ext}$ was not consistently evident on RSA of plants grown for shorter periods (data not shown) and as a result growth periods had to be increased up to 21 DAS. This occurrence needs further investigation but it is possible that P concentration in the planting material, the seed, could have contributed to the non-response in the initial stages of growth. Seed P concentration can have a strong impact on P response at an early stage of the plant (White and Veneklaas, 2012). Seed P concentration of mustard seed is normally about 8.28 mg $g^{-1}$ (http://ndb.nal.usda.gov/). Seeds used in this thesis contained relatively higher concentration of P (11.5 and 14.5 mg $g^{-1}$, respectively for R500 and IMB211, Figure 6.6). Such high P value could explain why plant response to $[P]_{ext}$ in the early developmental stage was not always strong. White and Veneklaas (2012) have suggested that seed P reserves are capable of sustaining maximum growth of maize seedlings for several weeks after germination, until the plants attain an extensive root system. For a characteristic RSA response to P nutrition, plant may thus have to be grown for relatively longer periods or P-starved seeds should be used.

In this study, RSA response to external P nutrition could be observed after two weeks following germination. For example, effects of $[P]_{ext}$ in Experiment 1 were observed when seedlings were grown for 18 DAS. The results demonstrated differences in RSA between the two parental genotypes and RSA response variation to P availability. The two genotypes

showed significant and distinct RSA responses to reduced $[P]_{ext}$, and these responses were similar to changes in RSA in other crop-plant species including *Arabidopsis* (Lopez-Bucio *et al.*, 2002; Nacry *et al.*, 2005), maize (Mollier and Pellerin, 1999), common bean (Liao *et al.*, 2001) and sorghum (Al-Karaki *et al.*, 1995). In Experiment 1, the plants growing on high $[P]_{ext}$ generally had bigger root than those on lower $[P]_{ext}$ and recorded higher TRL and TLRL (*p <.001;* 6Figure 6.4c). Whilst IMB211 consistently recorded smaller root systems than R500, R500 appear to show more plasticity that IMB211. For example, R500 recorded 63.3% greater TRL on high $[P]_{ext}$ than on low $[P]_{ext}$, compared to 7.3% difference recorded by IMB211. Furthermore, many of the RSA traits that showed significant differences on differential $[P]_{ext}$ between the two genotypes also showed high broad-sense heritability values, similar to values reported by Ingram *et al.* (2012) in *Brachypodium* accessions grown under differential P supply. In contrast to results in Experiment 1, TRL of plants grown in low $[P]_{ext}$ soils in Experiment 2 rather seems to be greater (Figure 6.9c). This observation contrasts the report of Williamson *et al.* (2001) that TRL increase with increasing P. The authors however noted that the most significant effect of reduced Pi of root growth is reduced PRL, reduced internode length, and increased LRL.

Increased LRL has been observed to correlate positively with P acquisition in P-starved environments and LR formation is profitable under P limitation because it has lesser production cost compared to other root types (Eissenstat, 1992; Ingram *et al.*, 2012). Maize genotypes with increased lateral rooting, for example, had higher growth than genotypes with reduced lateral rooting (Eissenstat, 1992; Zhu *et al.*, 2005a). In Experiment 1, both common and differential responses of the genotypes' LR traits to $[P]_{ext}$ were observed. Whilst mean LRL of IMB211 seemed to increase to a point and then decline with increasing

P availability, that of R500 generally increased with increasing P availability (Figure 6.4i). A similar trend was also apparent with respect to number of LRs. This observation however appears inconsistent with the increased length and number of LRs typically observed in crops adapted to low P conditions and may have occurred due to experimental vagaries. Results obtained on soil however was generally typical of crops adapted to low P conditions with most genotypes including IRRI016 and IRRI201 showing increased lateral rooting at low P (Figure 6.9e).

Phosphorus limitation induced a reduction in LAUZ for both experiments and an increase in LR insertion angle for Experiment 1 only (Figure 6.4g-h; 6.9d). Similar genotypic variations in the adaptive response of PR growth and hence LAUZ to low P have been observed (Jain *et al.*, 2007; Linkohr *et al.*, 2002; Lopez-Bucio *et al.*, 2002; Pérez-Torres *et al.*, 2008; Williamson *et al.*, 2001). Plants grown in P-starved conditions adapt by investing into LR growth and altering LR insertion angle in favour of outward rather than downward growth, resulting in a shallower and broader root system capable of exploiting topsoil resources more efficiently (Lynch, 2011; Lynch and Brown, 2001; Woodfield and Caradus, 1990). Root angle is important to P acquisition and Bonser *et al.* (1996) for example, reported of a correlation between reduced root angle of bean cultivars in low-P soils and yield in P-poor soils.

Root traits such as mean diameter, volume and surface area have been shown to influence P uptake in plants (Gahoonia and Nielsen, 2004b; Xie and Yu, 2003). Mean diameters of low P plants decreased by 3 to 19%, with IRRI201 and IRRI229 recording the lowest and highest reduction, respectively. Similar results have been reported by Xie and Yu (2003) in water hyacinth (*Eichhornia crassipes*). The results here suggest that the genotypic variation in

diameter of *B. rapa* in response to external P concentration can be considerable. Root diameter is an important trait for P uptake. It has been shown for example, that genotypes with small root diameter can be more effective in absorbing P (Xie and Yu, 2003). This is because finer or thinner roots have increased SRL and acquisition of immobile soil-based resources depends on length (Eissenstat, 1992). Variations of root diameter in response to P could be used for breeding because the trait has also high heritability (0.54) (Woodfield and Caradus, 1990). Broad sense heritability values obtained for root diameter in this thesis were however very weak (Tables 6.1 and 6.4). It is possible that procedures employed to extract geometric features were sub optimal for such fine root features.

There are other traits associated with efficient occupation of space. In this study for example, the ratio of root surface area to root volume was influenced by P availability in three genotypes (cv. IRRI124, IRRI229 and R500). Under limited P availability, these genotypes can increase the root surface area to root volume ratio to maximise root soil contact area for a unit volume of root (Figs. 6.9g-h). Bolan *et al.* (1987) have for example reported increase of root volume with increasing external P in subterranean clover and ryegrass. Genotypes with roots of high root surface to root volume ratios have often high SRL too, so that such genotypes can also increase the volume of roots in addition to their ability to produce more fibrous root systems (Paula and Pausas, 2011).

Another trait that reflects the cost for the plant to make large root systems is the root tissue density (RTD). Root tissue density is RDW per unit fresh volume. In this study, results show that RTD declined with increasing $[P]_{ext}$ in all genotypes but one (Figure 6.9h). Root tissue density has been related to the proportion of stele and the proportion of cell wall in the

stele. Increased RTD is associated with P stressed environments, partly because roots of stressed plants tend to have thick cell walls and a large proportion of stele and sclerenchyma (Wahl *et al.*, 2001). My results are consistent with that of Zobel *et al.* (2006) in forage chicory cultivars (*Cichorium intybus* L.). A reduction in P availability mostly leads to an increased RTD and it has been suggested that plants adapted to a more nutrient rich environment normally have lower RTDs (Zobel *et al.*, 2006). Moreover, lower RTD has been associated with faster growth rates and shorter root life spans (Ryser, 1996; Wahl and Ryser, 2000; Wahl *et al.*, 2001).

### 6.3.3 Temporal pattern of root architectural responses to $[P]_{ext}$

The effects of $[P]_{ext}$ on static traits described in previous sections were not observed on the dynamic traits. No significant effects of $[P]_{ext}$ were observed on the cumulative PRL, LRGR (not shown) and TRL through time. In Experiment 1, particle analyses employed to extract root length from time-lapses images may be sup-optimal. Although $[P]_{ext}$ did not have significant effect, it seemed that responses to changes in P availability manifested several days after sowing. Response of $[P]_{ext}$ on root growth dynamics have been reported in many crop plants including arabidopsis (Al-Ghazi *et al.*, 2003; Linkohr *et al.*, 2002; Lopez-Bucio *et al.*, 2002; Williamson *et al.*, 2001) and brassicas (Akhtar *et al.*, 2008a). The non-response on root growth dynamics to $[P]_{ext}$ observed here therefore needs to be investigated further.

### 6.3.4 Tissue P

Significant genotypic variations in P-concentration and P-uptake were observed in this study. These results indicate the existence of useful genetic variations among genotypes for P acquisition from P-deficient environments. Although shoot P concentration of IMB211 was greater than that of R500 especially at higher $[P]_{ext}$ regimes, P-uptake of IMB211 was inferior to that R500. For all lines, TRL *($r = 0.84$, $p < 0.001$)*, TLRL *($r = 0.79$, $p < 0.05$)* and

number of LRs *(r = 0.58, p < 0.05)* were highly correlated with total plant tissue P. This correlation was only evident in low $[P]_{ext}$ treatments but not in high $[P]_{ext}$ or across both treatments, indicating that efficient root systems are useful for low $[P]_{ext}$. Correlations observed here agree with the results of Suriyagoda *et al.* (2012), who observed that that plant P uptake is mainly determined by root production.

In the present study, growth parameters and tissue P increased significantly with increasing levels of soil P. RSA traits also responded to $[P]_{ext}$ supply, although at a later developmental stage, indicating that the soil used in Experiment 2 was appropriate for the scanner-based screening. One of the prerequisites of varietal screening for mineral stress is that the growth medium should be deficient and/or toxic in the nutrient under study (Fageria and Baligar, 1993). In this study, not only was the soil deficient of P, but the amendment with Pi made P available to seedlings and the soil also provided physical impedance to root growth similar to soil conditions in the field . Although there were some disparities especially for certain root system traits, response of root biomass and the majority of other RSA traits on germination paper were generally similar to observations made using soil-filled rhizoboxes (Figures 6.4 and 6.9).

### *6.4 Summary*

- Shoot biomass increased with increasing external P concentrations and root-to-shoot ratio was enhanced at lower P levels.
- Length of the apical un-branched zone of the primary root (LAUZ) was significantly affected by external P concentration. LAUZ increased with increasing external P.
- Root volume was higher at high $[P]_{ext}$ regimes; low $[P]_{ext}$ availability increased lateral root insertion angle, root tissue density and root surface area to volume ratio.

- Although static root traits generally responded to $[P]_{ext}$ two weeks after sowing, root growth dynamics did not respond to external phosphorus concentration.
- Tested lines differed in P-concentration and also in P-uptake. Shoot P concentration of IMB211 was greater than that of R500 but P-uptake of IMB211 was inferior to that R500.
- Total root length, total lateral root length and number of lateral roots highly correlated with total plant tissue P at low $[P]_{ext}$ but not at high $[P]_{ext}$.
- Relationship between the observed root system length and tissue P suggest that root system size is a driver of shoot P and hence P uptake in P-deficient conditions.

## CHAPTER 7 : GENERAL DISCUSSION AND CONCLUSION

### *7.0 General discussion*

Root systems of plants are responsible for acquiring water and nutrients from the soil for plant growth. Root system architecture (RSA, the natural arrangement of the root system at a given space and time) and root growth can, therefore, have profound influence on crop productivity and yield, particularly in low-input crop production systems. Although there is substantial information on the significant role of roots in crop response to abiotic and biotic stress conditions, the mechanisms underlying such responses are poorly understood (Herrera *et al.,* 2013; Zhu *et al.,* 2011). For example, the question of how the phenotype of the root system of a given crop genotype is influenced by the concentration of phosphorus in soil solution (the environment) has attracted research attention for a long time (Hajabbasi & Schumacher, 1994). While tremendous insights have been gained about such a question, research progress is still limited mainly by factors such as the time involved, the cost and the difficulty in studying and selecting genotypes with improved RSAs in their natural environments (i.e. the soil in the field).

The availability of genomic and molecular tools has proved valuable in facilitating the identification and understanding of multiple genes and their alleles, gene expression, and the role of specific proteins in plant roots' adaptation to stress (Cobb *et al.,* 2013). It has been the expectation that modern genomic studies will enable the introduction of beneficial alleles into crop cultivars to improve adaptation to biotic and abiotic stresses (Moose and Mumm, 2008). However, this expectation has not yet been realised fully due to an incomplete understanding of the root phenotype and how genotype-environment interaction influences the evolution of the root phenotype. Prediction of root phenotypes

from genotypes has been challenging because most root phenotypes result from several genes and gene products acting jointly with complex and unpredictable environmental factors (NIFA-NSF- USDA. 2011). To bridge this gap between genomics and phenomics, considerable efforts have been made to develop different types of root phenotyping platforms (Furbank, 2009; Furbank and Tester, 2011; Zhu *et al.,* 2011). Even so, the wide use of conventional root phenotyping platforms has been limited by the fact that they are often proprietary and hence expensive, complex, and have low resolution, throughput and adaptability (Tsaftaris and Noutsos, 2009). Root phenotyping methods need to be of high precision, throughput, resolution, economical and be very simple and accessible.

### *7.1 A low-cost, high resolution optical scanner root phenotyping system*

Optical scanners have been used to study roots traits previously (Dannoura *et al.*, 2008, 2012; Dong *et al.*, 2003; Dresbøll *et al.*, 2013; Hund *et al.*, 2009). In this thesis, however, detailed description is given about the development of the root phenotyping system (Chapter 2). The testing, the subsequent data validation using models (Chapters 3 - 6), and the potential to scale the system for higher throughput is novel. The system developed in this thesis enables remote image acquisition and is novel because it is coupled with a software interface for simultaneous management of multiple scanners. The root phenotyping system described in this thesis was sited in controlled environment (Chapter 2) but scanner setups are not unique to *ex situ* applications (Clark *et al.*, 2011). The use of scanners in root imaging is also applicable to *in situ* protocols (Dannoura *et al.*, 2012).

Scanners, and other simple imaging devices such as digital cameras are most common in *ex situ* applications where they are usually combined with experimental systems in which

plants are grown or cultured on moist germination papers (Hund *et al.*, 2009), in hydroponic systems (Chen *et al.*, 2011) and in aeroponic systems (Waisel, 1996, 2002). Other experimental setups applicable to imaging with scanners or cameras include growing plants on agar in petri dishes (Bengough *et al.*, 2004) or in small 2D rhizotrons (Devienne-Barret *et al.*, 2006). For example, Bengough *et al.* (2004) used a scanner based 2D gel chambers to predict which barley seedlings in landraces would develop shallow and deep root distributions. Similarly, genetic loci associated with RSA traits in *Brassica napus* under contrasting phosphate supply have been identified in high-throughput root phenotyping screens employing trays and flatbed scanners (Shi *et al.*, 2013).

Scanners are becoming popular in high throughput root imaging because such devices are cheap and readily accessible. Image acquisition with scanners is technically simple. Scanners also provide opportunity for high-throughput imaging because of their image acquisition speed and their compactness so that many can be fitted into a small growth room (Ortiz-Ribbing and Eastburn, 2003). Furthermore, scanners offer relatively large viewing or imaging area at high resolution which provides flexibility to study growth of root systems for extended period and also to study fine root features such as root hairs (Dong *et al.*, 2003; Pierret *et al.*, 2003a). In this thesis, the *ArchiScan* software enabled remote and time-lapse image acquisition, providing an added advantage of studying growth dynamics of undisturbed live roots. Breeding crops with improved RSA is currently constrained by difficulties associated with observing root traits. The scanner-based phenotyping system described in this thesis could have potential implications for selecting and developing crop root system ideotypes conferred with efficient resource acquisition and to screen several plants for multiple dynamic root traits, a vital requirement for breeding (Gregory *et al.*,

2009; White *et al.*, 2009). For example, if the scanner-based phenotyping system is a scaled up, it can be used to rapidly screen mapping populations of several lines for root growth and its response to various environmental stimuli such as phosphate starvation. Not only can this speed up the determination of candidate genes for a root growth QTLs but it can also aid in estimating the stability of these QTLs under single environmental differences such as low versus high P supply.

The majority of previous root system studies have been carried out solely in non-soil rooting media, raising questions about their applicability to field conditions (Pacheco-Villalobos and Hardtke, 2012). It is difficult to study the effects of soil physical characteristics and soil biota on RSA and root growth in non-soil rooting media. These aforementioned limitations apply to studies presented in Chapters 3, 4 and part of Chapter 6 where plants were grown on seed germination paper. Root systems of seedling were also coerced to grow on flat surfaces and were therefore not typical of the inherent 3D form of root growth in natural environments.

However, it was useful to work with germination paper to develop the system because it is quicker than in soil and nutrient supply could be controlled. The data presented in Chapters 5 and 6, demonstrate, however, that scanner-based phenotyping can be adapted to provide data on RSA from near-naturalistic environment, of soil-filled rhizoboxes. Similar results were observed when seedlings were grown on soil-filled rhizoboxes (Chapter 5) and on paper (Chapter 4), which points to the robustness of the phenotyping platform. For example, in both Chapters, root growth followed similar pattern. Data for most static root traits (traits measured ones at the end of experiments) also had high broad sense

heritability or repeatability suggesting that the system is robust and data produced were repeatable between runs. Besides, Dannoura *et al.* (2008, 2012) showed that scanners could be used *in situ* in the field to study roots but on a limited scale as image acquisition was by mouse clicks and field computer keyboard. Such methodologies could be coupled with the *ArchiScan* interface to automatically and remotely acquire images as well as manage numerous scanners simultaneously and thereby increase the throughput of data on RSA in the field.

### *7.2 Root phenotyping through imaging may be constrained by time taken for image analyses, not image acquisition*

At a scanner resolution of 300 dots per inch (dpi), A4 size flatbed scanner system described in this thesis takes approximately 5 s to capture the images of up to 3 root systems. With 24 scanners in operation, images of 72 root systems were captured per scan, with the possibility of capturing hundreds or even thousands of images per day depending on the operational number of scanners and scanning periodicity. For optimal performance, it must be noted, however, that increasing the operational number of scanners should be done in concert with increase in the number computers to manage them. Scanners employed in this thesis were managed by 3 computers but we also observed that 16 scanners could adequately be managed by a computer. In this thesis images were generally captured 12 hourly, but time between successive image acquisitions by the scanners could be seconds, minutes, hours or days. Whilst short time span between sequential image acquisitions may be apt for observing transient changes in root growth, it can also significantly increase time and efforts required for image analyses and also increase the space and facilities required to store images.

After evaluating a number of root analysis software programmes, *SmartRoot* (Lobet *et al.*, 2011) was the most useful. Not only was installation of *SmartRoot* straightforward, a detailed manual accompanied the software and its developers almost immediately responded to queries (http://www.uclouvain.be/en-smartroot). Moreover, the software could be used to extract dynamic (growth measurements), static (single time-point measurements), global (measurements from the entire root system) and local (measurements from a section of the root system) traits from images with almost the same procedure. Even so, this software however could take up to 30 minutes to extract data from an image of the root system of a 14 d old seedling and even longer when the image was of poor quality. Approximately one week was needed to extract static root data from images captured in a single experiment. Time taken for image analysis was therefore the main limitation to throughput in root phenotyping.

These observations are consistent with the results of a survey conducted by the National Science Foundation (USA) to determine the limitations of plant phenotyping (https://phenocept.discovery.wisc.edu/). In this survey, 56% of respondents (scientist involved in phenotyping) indicated that data analyses rather than data acquisition limit their phenotyping process. Over 52% of respondents also indicated that inadequacies in automation of image analysis rather than inadequacies in automation of acquisition impede their phenotyping. In this thesis, to automate and speed up extraction of data from time-lapse images, an *ImageJ* macro was developed (Chapter 2). However, the macro was not robust enough to extract all fine root features.

Addressing constraints to root phenotyping requires a collaborative, multidisciplinary approach from plant physiology and agronomy, engineering, computer science, statistics and mathematics (Figure 7.1) (NRC, 2013; NIFA-NSF- USDA, 2011). Integration of disciplines allows bottlenecks at every level of the phenotyping pipeline to potentially be addressed. For example, computer scientists and software developers can partner with root researchers to develop robust software dedicated to root system analyses. Such software can incorporate algorithms capable of discriminating roots from soil or other media artefacts based on simple shape or texture descriptors other than pixel or voxel intensity gradients alone. Shape descriptor-based filters are capable of searching for geometrical structures which can be regarded as tubular and would be less affected by the presence of noise of different shape orientations (Frangi *et al.*, 1998).

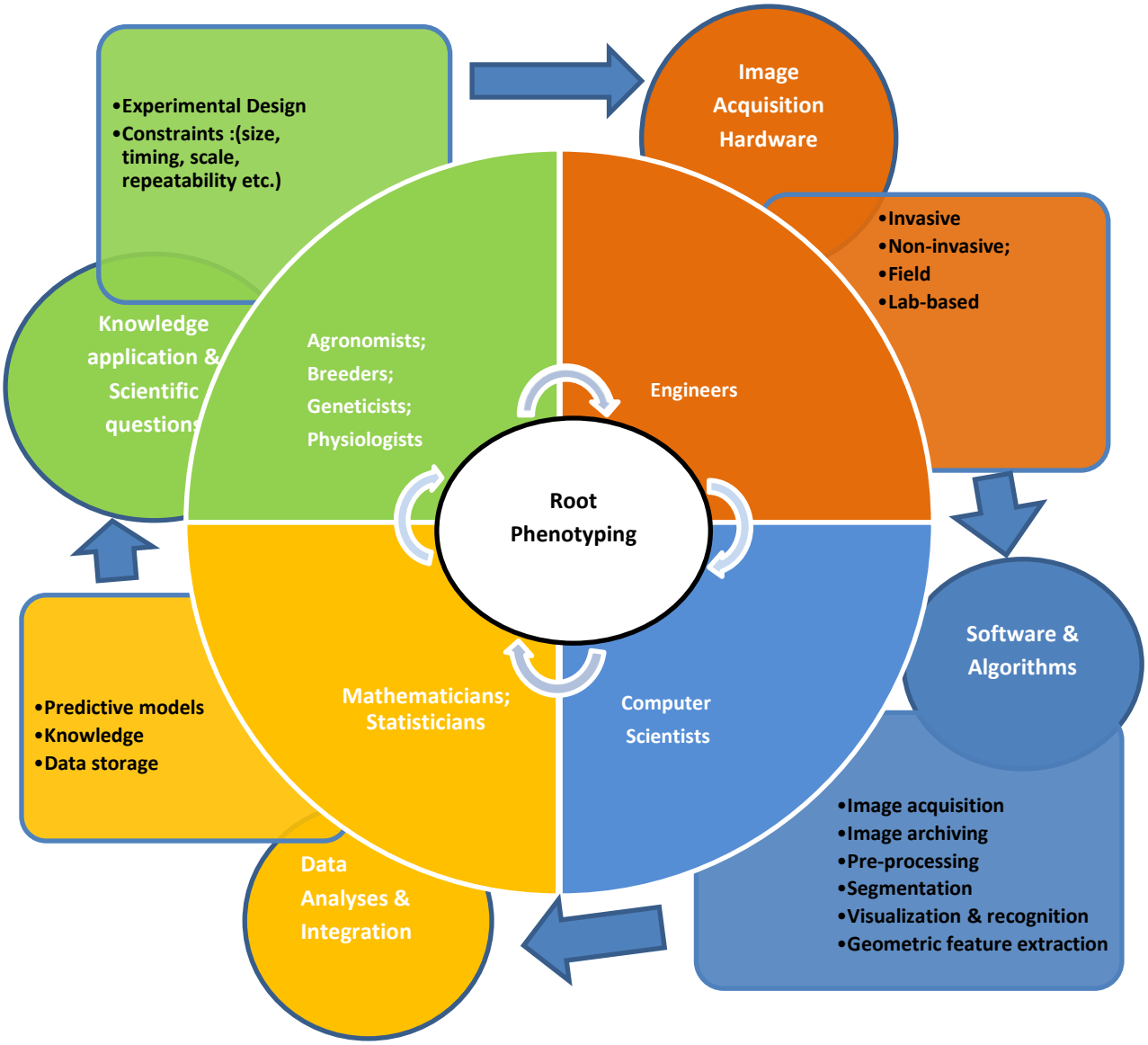


***Figure 7.1:*** *Schematic of different areas involved in root system phenotyping*

Until full automation in root analyses is achieved, semi-automated software like *SmartRoot* (Lobet *et al.*, 2011) are essential. It is also conceivable that tracing techniques can be improved so that the time required to characterise a root is reduced. Techniques such as Livewire or Intelligent Scissors algorithms which have been developed in medical sciences could for example be tested on root data (Falcao *et al.*, 1998). In these algorithms, users initiate image segmentation by seeding points manually on the image and optimal shapes

are then derived from these points (Poon *et al.*, 2007). These algorithms are usually improved by a pre-processing routine that utilises specialised filters (Poon *et al.*, 2007). For example, livewire-assisted semiautomatic segmentation was recently employed to analyse root growth dynamics of *Phaseolus vulgaris* and *Cicer arietinum* from 2D time series images, from which spatio-temporal 3D structures were constructed to reveal multimodal transient growth zone in basal roots (Basu and Pal, 2012).

### *7.3 Large replication is required to detect significant differences in RSA*

Root system phenotyping can be used to analyse trait variation within or between species or across environments. Given the constraints of cost, labour and time, this sometimes results in conflicts between scale and precision (Cornelissen *et al.*, 2003). To reduce the inherent cost and time in screening roots, there is the tendency for scientists to minimise the number of samples (replicates) in root system studies. However, such tendencies must be tempered by statistical considerations essential to characterise variations in RSA between and within species. It is very vital that researchers check coefficients of variation (CVs) in their setups prior to undertaking any study (Pérez-Harguindeguy *et al.*, 2013). Unfortunately, limited attention has been given to intra-genotypic variability (ITGV) for many crops. It has been argued that ITGV is negligible compared to interspecific or inter-genotypic variability, so plants of the same genotype can be characterised by mean trait values (Albert *et al.*, 2010). Intra-genotypic variability could however be as large as inter-genotypic variation in some RSA traits and cannot be discounted as negligible (Peter *et al.,* 2013). Identifying ITGV is particularly relevant to roots because roots tend to show more plasticity and their phenotypes are less stable than those of shoots (Garnier and Navas, 2012).

In this thesis, CVs of various root traits of a single *B. rapa* genotype R-o-18, ranged between 5 and 103% (Chapter 3, Table 3.2). These variations represent environmental effects since plants were from a single genotype although all plants were grown in same environment. Lesser CV values (15 - 24%) have been reported for root system traits but these CV values were estimated from several studies involving a low number of replicates and are likely to increase with increasing replication (Cornelissen *et al.*, 2003; Pérez-Harguindeguy *et al.*, 2013). The number of replicates to detect significant differences between means of root traits increases proportionally with CV to the power of two. Since the CVs for many root traits are large, large numbers of replicates are therefore required to detect differences in these traits between genotypes. Here, depending on the trait, 4 to 37 replicates would be sufficient to detect a 50% significant difference in trait means in a 2-sided 95% CI t-test (Table 3.3). For example, to detect a 50% difference in TRL between two genotypes would require 12 replicates (Table 3.3). In soil, and depending on the trait, between 4 and 48 replicates would generally be required to detect a similar difference between two means at statistical power of 0.80 (Table 5.2). For some traits such as diameter and LR insertion angle, there was less ITGV and so the replication could be reduced. This low variability in LR insertion angle within a genotype may explain why root angle is one of the few root traits that has been successfully bred in crops, for enhanced topsoil foraging for P acquisition (Lynch, 2011).

Employing the appropriate replication is particularly pertinent in studies aimed at detecting QTLs. To avoid the detection of false-positive QTLs, it is important that many individuals per line are screened from a population of numerous lines, particularly for traits that show high coefficient of variation in their phenotypic means. Large replication provides the

opportunity to observe recombinant events and facilitates the estimation of parameters with greater accuracy and, therefore, a greater ability to detect QTL (Doerge 2002).

### *7.4 Low-cost optical scanner-based imaging provides reliable data for modelling root growth dynamics*

The results from this study show that scanner-based root phenotyping can be greatly beneficial to the construction of mathematical models of root systems. Using *SmartRoot* (Lobet *et al.*, 2011), it was possible to generate root "nodes" (the intersection of successive segments of a segmented root axis) and their coordinates (Chapters 2 and 3), enabling the validation of a previously reported density-based root system model (Dupuy *et al.*, 2005; Dupuy *et al.*, 2010a; Dupuy *et al.*, 2010b; Dupuy and Vignes, 2012). It was shown in Chapter 3 that root length distributions between modelled and real root systems were similar. These results suggest that simple basic information taken from few root samples, as opposed to the measurement of complex topological data, could be employed to reconstruct a realistic root system (Dupuy *et al.*, 2005). Also, because the model was density-based and root morphology is analysed aggregately, the same approach could be developed for plants grown in soil using densities such as biomass, volume or root length (Dupuy *et al.*, 2005).

The combination of modelling (both statistical and mechanistic) and data provided by scanners have the potential to deliver significant information on the functioning of soil systems, and enhance understanding of biological mechanisms and dynamics underlying root growth. The complementation of scanner-based imaging with density-based modelling approaches could generate relevant data describing not only root dynamics but also biological soil processes. Root growth cannot be easily visualised yet in the soil, so data generated from scanners could be used to train a set of elementary developmental rules to

reproduce the morphogenetic behaviour of individual roots and how it responds to various environmental factors (de Dorlodot *et al.,* 2007). This can be used to simulate the inherent 3D dynamic structure of RSA in the soil and improve the understanding of root-soil interactions and other soil processes, such as the effects of soil strength, water and nutrient availability on root system growth. With some modifications, it may be possible to couple optical imaging by scanners in two-dimensional soil-filled rhizoboxes, with luciferase reporter assays including bioluminescence-based reporters (Michelini *et al.*, 2008) or plants that produce fluorescent proteins to identify specific genes or gene expression (Faget *et al.*, 2012; Faget *et al.*, 2010; Federici *et al.*, 2012; Kurup *et al.*, 2005). For example, a root imaging platform was recently reported in *Arabidopsis* (*GLO-Roots*), using bioluminescence-based reporters for simultaneous observation of root growth and biological activity in a 2-D soil-filled chamber (Rellán-Álvarez *et al.*, 2013).

### *7.5 RSA traits exhibit temporal dynamics*

The growth of a root system is an irreversible and ontogenetic change in its biomass measured in size, or form (Hunt, 2003; Paine *et al.*, 2012). Growing root systems explore their local environment enabling acquisition of resources at different locations in the rhizosphere. Quantification of temporal changes in root growth provides important information about how root systems adapt to different biotic and abiotic stimuli (Basu *et al.*, 2007; Wells *et al.*, 2012). Dynamic analyses of root systems have, for example, been employed to study the influence of phosphorus starvation on the elongation rate of the PR of *Arabidopsis* (Ma *et al.*, 2003).

It is generally believed that typical root growth in a productive environment is initially slow, and then accelerates to a maximum before slowing again when the plants mature followed

by senescence and decay (Hunt, 2003). This growth pattern reflects resource availability and also arises because the rate of biomass accumulation per total biomass slows as plants grow (Hunt, 2003). Paine *et al.* (2012) have, therefore, argued that analysing root system growth with assumptions of constant growth rate may be unrealistic because such assumptions indicate that resources are never limiting. Results obtained in this thesis are consistent with this assertion. Dynamic analyses performed on growth of the total root system, the primary and first order lateral roots showed that these exhibit temporal variation with significant effects of genotype (Chapters 4 and 5). Total length of the root system followed a logistic growth function. There was significant variation between genotypes in the total root length attained (asymptote) (Chapter 4 & 5) and in the symmetry of the predicted curves (Chapter 5).

One advantage of the logistic mixed-effects approach to analysing root growth is that the behaviour of the model is biologically plausible and is due to the nonlinear characteristics of root growth curves (Calegario *et al.*, 2005; Guan *et al.*, 2006; Paine *et al.*, 2012). The experiments conducted in this thesis utilised seedlings and since there could be resource limitation and ontogenetic development in seedlings, parameters in the mixed-effects logistic model can be interpreted biologically. The asymptote in the model may represent root growth limitation due to either finite resources or changes in the seedlings' ontogeny. In mature plants', the asymptote may represent changes in the plants' ontogeny such as the start of flowering or grain development and the inflection point may represents the age at which absolute root growth is maximised within a growing period. The scale parameter could indicate the time when root growth begins to slow down within a growing period (Calegario *et al.*, 2005; Guan *et al.*, 2006; Paine *et al.*, 2012). Such information could be vital

in understanding the plant's phenology and could facilitate predicting root growth limitation within a growing season. For example, genotypes with a bigger asymptotes but smaller inflection points and scale parameters could suggest that growth was limited in the initial stages of the plants' life. Mixed-effects logistic modelling for example may answer biologically relevant questions such as the resource acquisition capacity of different lines at different position along the inflection point.

Growth of primary roots also followed a logistic growth function, although the non-linearity was less pronounced (Chapter 4). Previous results have reported approximately linear growth of PRs over a period of time (Erickson, 1976; Torrion *et al.*, 2012). Torrion *et al.* (2012) for example indicated that until the full-seed stage, PR growth of soybean (*Glycine max* L.) plants followed a linear function. Similarly, the PR of maize elongated in length linearly at approximately 2 mm $hr^{-l}$ for 3 d or more (Erickson, 1976). The analysis of LR growth is more complex than that of total and PR growth (Armengaud *et al.,* 2009). This is because there are usually many LRs on each PR and individual LRs may show different growth rates depending on their time of emergence (Armengaud *et al.*, 2009). In this thesis, growth rate of LRs generally increased quadratically to a maximum for all types of LRs (Figure 3.5). Older LRs generally had faster elongation rates than those that emerged later but the growth of all LRs seemed to peak roughly at the same DAS. Quadratic increase in LR growth observed (Chapters 3 and 4) may be attributable to steady increase in emergence of LRs on the PR. Hund *et al.,* (2009) and McCully *et al.,* (1999) have suggested that growth of LRs of a single root system follow an exponential function during the initial phase of its development. This growth pattern continues until the final length and densities of the oldest

proximal LRs are attained after which LRs growth may follow a linear function (Hund *et al.,* 2009; McCully *et al.,* 1999).

### *7.6 Genotypic variation in seedling root architectural traits and implications for phosphorus acquisition efficiency in Brassica rapa*

Genotypic variation in adaptive response to P stress and P-acquisition efficiency have been widely reported in many crops (Gahoonia and Nielsen, 2004a, b; Li *et al.*, 2007; Lynch and Beebe, 1995; Lynch and Brown, 2008; Miller *et al.*, 2003; White *et al.*, 2005; White and Hammond, 2008b; Zobel *et al.*, 2006) but has not been fully exploited in breeding (Lynch and Brown, 2012). This is because crop breeding has typically focused on crop adaptation to high-input systems and has not used root traits as selection criteria (Gahoonia and Nielsen, 2004b; Lynch and Brown, 2012). *Brassicas* have been noted to be relatively more efficient at acquiring and utilising P in P-limiting environments than many crops (Hoffland, 1992; White *et al.*, 2005). However, information on the genetic variability in their root systems is not common. Genetic diversity in *Brassicas* in response to phosphate limitation has been reported (Akhtar *et al.,* 2007; Akhtar *et al.,* 2008a, b; Akhtar *et al.,* 2009; Akhtar *et al.,* 2006; Hammond *et al.,* 2009; Shi *et al.,* 2013a; Shi *et al.,* 2012).

This thesis has determined the genetic variation in *B. rapa* for root system plasticity in response to external P availability. The genotypes studied showed differential biomass accumulation when grown on germination paper and on soil-filled rhizoboxes (Chapter 6). However, in the present study, shoot P concentration was not directly proportional to biomass accumulation. It has been suggested that shoot P concentration may not be a reliable criterion in assessing genotypes for P use efficiency (PUE) (Fageria and Baligar, 1999; Ozturk *et al.*, 2005). This assertion however depends on how PUE is defined. Shoot P

concentration would be critical if PUE is defined as the equivalent of P efficiency ratio, (PER; g DM $g^{-1}$ P; Table 1.1), calculated as yield divided by the amount of P in the plant. PER is equivalent to the reciprocal of tissue P concentration of a wholly harvested plant (Hammond *et al.,* 2009; White *et al.,* 2005). On the other hand, increased yield is a significant component of all measures of PUE (Table 1.1). Increasing yield, whilst maintaining or decreasing shoot-P will lead to increased PUE (Hammond *et al.,* 2009).

Variation in specific RSA traits and plasticity in response to P availability were observed among the studied genotypes in both soil and non-soil media (Chapter 6). Greater root system length enables greater exploration of the soil volume, and is thus associated with enhanced performance and improved P-acquisition of crop plants on P-limited soils (Brasil *et al.*, 2003; Gahoonia and Nielsen, 2004b; Lambers et al., 2006; Lynch and Brown, 2001). Results presented in Chapter 6 from seedlings cultured on both germination paper and in rhizoboxes support this observation. Genotypes with bigger root system were superior in P uptake. Total root length has been found to correlate with seed yield in many crop plants including chickpea (*Cicer arietinum* L., Kashiwagi *et al.*, 2006), wheat (*Triticum aestivum*, Barraclough, 1984), oats (*Avena sativa*) and barley (*Hordeum vulgare*, Léon and Schwarz, 1992). In this thesis, analysis of correlations of correlation of quantitative RSA traits showed significant positive correlations between RSA traits and physiological growth indices such as shoot biomass (SDW) and root biomass (RDW) (Figures 3.4, 4.2, 5.5). Whilst trait correlations shown in Chapter 3 (Figure 3.4), represents only phenotypic correlations, those shown in chapters 4 and 5 (Figures 4.2 and 5.5) represents both phenotypic and genotypic correlations and may have greater significance in breeding. According to all the correlations, it can be concluded that shoot and root biomass and hence, total biomass increased with

the increase in TRL, TLRL and LR number (Figures 4.2 and 5.5). Given that P uptake increased with the increase TRL (Figure 6.7), cultivars with bigger roots with many and highly dense laterals are expected to acquire relatively more soil resources in deficiency soil conditions than cultivars with smaller RSAs with few and sparsely distributed laterals. So, in order to increase P acquisition and hence yield in breeding programs, breeders should opt for cultivars with bigger RSAs with many laterals. Thus, the differences in root system size observed in this thesis between the *B. rapa* genotypes suggest that selection and breeding of *B. rapa* genotypes conferred with larger root systems may contribute to more efficient use of soil P and lead to improved seed yield.

Moreover, the strong positive correlations observed in this thesis between the root parameters are central to this type of analysis. For example, it suggests that selection for a trait such as PR length will not be detrimental to other traits such as number of LR (Seiler, 2008). However, in some cases, low correlation between traits may also be beneficial in permitting independent manipulation of such traits without large predictive value for a change in other traits (Gifford et al., 2013). For example, weak relationships between LR insertion angle with TRL (r = - 0.35) or number of LRs (r = -0.29) observed in Chapter 3 suggest that root angle could be independently changed without affecting TRL or number of LRs.

Results in this thesis confirmed the observations of other researchers, on various plant species, that a decrease in LR insertion angle (Fig. 6.5h) is a root system response to P availability (Bonser *et al.*, 1996; Ingram *et al.*, 2012; Lynch and Brown, 2001). Both IMB211 and R500 genotypes exhibited a reduced R:S and increased LAUZ with increasing P

availability (Figs. 6.5i & 6.9d). However, responses for traits including number of LRs and mean LR length to P nutrition on paper rooting media (Figs. 6.5d & 6.5e) were not consistent between the two parental genotypes. Similar results have been reported in *Brachypodium* by Ingram *et al.* (2012) and in *Brassica napus* by Shi *et al.* (2013b) who suggested that mapping QTL for LR growth in P deficient conditions could enhance our understanding of plant low-P adaptation. This is because the ability to reliably link phenotypic data on RSA under low P conditions to genotypic information would better explain the genetic basis of variation in RSA traits in response to P starvation.

### *7.7 Effect of rooting media on the root phenotype*

The responses of several RSA traits to P nutrition on germination paper were generally similar to observations made using soil-filled rhizoboxes but some differences were also observed. The results presented in Chapter 6 indicated that the root system phenotype can be influenced by the rooting media, an observation made previously for LRs in maize RILs grown in sand culture (Zhu and Lynch, 2004). For example, in Chapter 2, characteristics of root system morphology and topological indices differed between the rooting media for the two parental genotypes. Moreover, in Chapter 4, mixed effect modelling of TRL indicated that the best-fit model for seedlings grown on paper required only one random effect parameter, the asymptote $(\emptyset_1, \mathrm{Eqn.}\,4.4)$ to describe the effect of genotype (Figure 4.6). Two random effects parameters, the asymptote and inflection point $(\emptyset_{i1}, \emptyset_{i2}, \mathrm{Eqn.}\,5.2)$ were, however, required to describe the effects of genotype on TRL when plants were grown in soil-filled rhizoboxes (Chapter 5; Figure 5.8; Table 5.5). These suggest that root growth dynamics are affected by local environmental conditions. Indeed, seed germination papers and other non-soil growth media provide an effective rooting media to phenotype a

large number of plants, but root phenotypes must subsequently be evaluated and confirmed in soil media.

### *7.8 Areas for future study*

The A4 size of scanning window of scanners employed in the experiments described in this thesis could restrict the platform to studying the root system of seedlings. This raises some concern because root traits of seedlings may not always be well correlated with those of mature plants (Abdel-Ghani *et al.*, 2013; Arihara and Crosbie, 1982; Shipley *et al.*, 1989; Watt *et al.*, 2013; White *et al.*, 2013b; Wojciechowski *et al.*, 2009; Zhu *et al.*, 2011; Šmilauerová and Šmilauer, 2007). The ability to image root systems of mature plants grown in soil is likely to improve the correlations between traits obtained in the phenotyping platform and measurements made in the field. The root systems of larger plants might be accommodated by growing plants in larger pouches, which might be imaged in overlapping sectors and these images combined to reconstruct an image of the entire root system as described by Lobet and Draye (2013).

Further studies could also incorporate scanners with increased scanning window such as A3 scanners (admittedly, these may be much expensive than A4 scanners) and determine if useful breeding material can be identified on the basis of seedling root traits recorded on the optical scanners. It is also important to determine if seedling traits are beneficial in detecting yield or yield stability in the field and so, seedling root traits recorded on the scanners should be correlated with yield of mature plants. The system could also be scaled up and employed to screen plants grown at varying P regimes to generate high throughput root growth data for dynamic modelling of root system response to P availability with density-based models.

### *7.9 Summary*

This thesis described the development of a low cost, high-resolution root phenotyping system (HRP) and its application to studying genotypic variations in RSA traits between *Brassica rapa* genotypes. The thesis also studied root system response of *Brassica rapa* seedlings to external P concentration. The low-cost scanner-based root phenotyping system allowed the acquisition of information, in a short period of time, about the complex root architecture of seedlings of *Brassica rapa* genotypes. Limited engineering and financial inputs were required. Assessment of various rooting media and its effect on RSA traits indicated that the type of rooting media could affect the RSA data that is generated from it. A non-soil rooting medium, seed germinating paper was a more suitable substrate for screening seedling root traits but root phenotypes must be validated *in situ* in the field, or failing that, in soil media in controlled environments.

Significant differences were observed in RSA traits but replication must be high to identify differences in root architectural traits between *Brassica rapa* genotypes. Root traits showed temporal dynamics with strong genotypic effect. A logistic model adequately described total and primary root growth, and a quadratic model described temporal changes in growth rate of first order lateral roots of *Brassica rapa* seedlings. Density-based mechanistic model reproduced experimental results accurately by simulating PR length and cumulative length of all LRs.

Many RSA traits that showed significant differences when plants were grown with different P supply between *Brassica rapa* genotypes also showed high broad-sense heritability and significant phenotypic correlations between shoot biomass and several other root traits. The

high genetic contributions and heritability observed are promising measures for the manipulation of various root system traits and presents great opportunity for developing crops with multiple desirable traits including improved P acquisition and yield.

Overall, scanner-based phenotyping of RSA provides economical and readily available means of studying the mechanisms underlying the plant-soil interactions. Further developments in accurate and quicker means of images analyses and the extraction of geometric information from root images should permit more efficient RSA phenotyping with optical scanners and facilitate analyses of variations in RSA and root growth dynamics. Scanner-based root system phenotyping also provides a promising opportunity in generating high resolution root system data in developing models for predicting root phenotypes performance in breeding populations.

**REFERENCES**


**Abdel-Ghani AH, Kumar B, Reyes-Matamoros J, Gonzalez-Portilla PJ, Jansen C, San Martin JP, Lee M, Lubberstedt T**. 2013. Genotypic variation and relationships between seedling and adult plant traits in maize (*Zea mays* L.) inbred lines grown under contrasting nitrogen levels. *Euphytica* **189**, 123-133.

**Acuña TLB, Wade LJ**. 2013. Use of genotype × environment interactions to understand rooting depth and the ability of wheat to penetrate hard soils. *Annals of Botany* **112**, 359-368.

**Adu MO, Chatot A, Wiesel L, Bennett MJ, Broadley MR, White PJ, Dupuy LX.** (2014). A scanner system for high-resolution quantification of variation in root growth dynamics of *Brassica rapa* genotypes. *Journal of Experimental Botany* **65**, 2039-2048.

**Akhtar MS, Oki Y, Adachi T, Murata Y, Gill MA, Khan MHR, Hiroyuki K**. 2006. Inter-cultivar variations of phosphorus deficiency stress tolerance in hydrponically grown *Brassica*. *Songklanakarin Journal of Science and Technology* **28**, 601- 613.

**Akhtar MS, Oki Y, Adachi T**. 2007. Genetic diversity in *Brassica* cultivars under deficiently buffered P-stress environment: II. Percent distribution of biomass and P-concentration, P-stress factor and P-utilization efficiency. *Journal of American Science* **3**, 64-72.

**Akhtar MS, Oki Y, Adachi T**. 2008a. Genetic variability in phosphorus acquisition and utilization efficiency from sparingly soluble P-sources by *Brassica* cultivars under P-stress environment. *Journal of Agronomy and Crop Science* **194**, 380-392.

**Akhtar MS, Oki Y, Adachi T**. 2008b. Intraspecific variations of phosphorus absorption and remobilization, P forms, and their internal buffering in *Brassica* cultivars exposed to a P-stressed environment. *Journal of Integrative Plant Biology* **50**, 703-716.

**Akhtar MS, Oki Y, Adachi T**. 2009. Mobilization and acquisition of sparingly soluble P-sources by *Brassica* cultivars under P-starved environment II. Rhizospheric pH changes, redesigned root architecture and Pi-uptake kinetics. *Journal of Integrative Plant Biology* **51**, 1024-1039.

**Akhtar MS, Oki Y, Adachi T, Murata Y, Gill MA, Khan MHR, Hiroyuki K**. 2006. Inter-cultivar variations of phosphorus deficiency stress tolerance in hydrponically grown *Brassica*. *Songklanakarin Journal of Science and Technology* **28**, 601-613.

**Akinrinde EA, Gaizer T**. 2006. Differences in the performance and phosphorus-use efficiency of some tropical rice (*Oryza sativa* L.) varieties. *Pakistan Journal of Nutrition* **5**, 206-211.

**al Hagrey SA**. 2007. Geophysical imaging of root-zone, trunk, and moisture heterogeneity. *Journal of Experimental Botany* **58**, 839-854.

**Albert CH, Thuiller W, Yoccoz NG, Douzet R, Aubert S, Lavorel S**. 2010. A multi-trait approach reveals the structure and the relative importance of intra- vs. interspecific variability in plant traits. *Functional Ecology* **24**, 1192-1201.

**Al-Ghazi Y, Muller B, Pinloche S, Tranbarger TJ, Nacry P, Rossignol M, Tardieu F, Doumas P**. 2003. Temporal responses of Arabidopsis root architecture to phosphate starvation: evidence for the involvement of auxin signalling. *Plant, Cell & Environment* **26**, 1053-1066.

**Ali ML, Pathan MS, Zhang J, Bai G, Sarkarung S, Nguyen HT**. 2000. Mapping QTLs for root traits in a recombinant inbred population from two indica ecotypes in rice. *Theoretical and Applied Genetics* **101**, 756-766.

**Al-Karaki GN, Clark RB, Sullivan CY**. 1995. Effects of phosphorus and water stress levels on growth and phosphorus uptake of bean and sorghum cultivars. *Journal of Plant Nutrition* **18**, 563-578.

**Alonso-Blanco C, Aarts MGM, Bentsink L, Keurentjes JJB, Reymond M, Vreugdenhil D, Koornneef M**. 2009. What has natural variation taught us about plant development, physiology, and adaptation? *Plant Cell* **21**, 1877-1896.

**Amtmann A, Hammond JP, Armengaud P, White PJ**. 2005. Nutrient sensing and signalling in plants: potassium and phosphorus. In: Callow JA, ed. *Advances in Botanical Research*, Volume 43: Academic Press, 209-257.

**Araujo AP, Fernandes AM, Kubota FY, Brasil FC, Teixeira MG**. 2004. Sample size for measurement of root traits on common bean by image analysis. *Pesquisa Agropecuaria Brasileira* **39**, 313-318.

**Arihara J, Crosbie TM**. 1982. Relationships among seedling and mature root system traits of maize. *Crop Science.* **22**, 1197-1202.

**Armengaud P, Zambaux K, Hills A, Sulpice R, Pattison RJ, Blatt MR, Amtmann A**. 2009. *EZ-Rhizo*: integrated software for the fast and accurate measurement of root system architecture. *Plant Journal* **57**, 945-956.

**Arsenault J-L, Poulcur S, Messier C, Guay R**. 1995. *WinRHlZO*™, a Root-measuring system with a unique overlap correction method. *HortScience* **30**, 906-906.

**Asseng S, Aylmore LAB, MacFall JS, Hopmans JW, Gregory PJ**. 2000. Computer-assisted tomography and magnetic resonance imaging. In: Smit AL, Bengough AG, Engels C, van Noordwijk M, Pellerin S, van de Geijn SC, eds. *Root Methods: a Handbook*. Heidelberg: Springer, 343-363.

**Atkinson D**. 2000. Root characteristics: why and what to measure. In: Smit AL, Bengough AG, Engels C, van Noordwijk M, Pellerin S, van de Geijn SC, eds. *Root Methods: a Handbook*. Heidelberg: Springer, 1-32.

**Aziz T, Rahmatullah, Maqsood MA, Tahir MA, Cheema MA, Ahmad I.** 2006. Phosphorus utilization by six brassica cultivars (*Brassica juncea* L.) from tri-calcium phosphate; a relatively insoluble P compound. *Pakistan Journal of Botany* **38**, 1529-1538.

**Bai C, Liang Y, Hawkesford MJ.** 2013. Identification of QTLs associated with seedling root traits and their correlation with plant height in wheat. *Journal of Experimental Botany* **64,** 1745-1753.

**Bai H, Murali B, Barber K, Wolverton C**. 2013. Low phosphate alters lateral root setpoint angle and gravitropism. *American Journal of Botany* **100**, 175-182.

**Barber SA**. 1984. *Soil Nutrient Bioavailability*. USA: John Wiley and Sons.

**Barraclough PB**. 1984. The growth and activity of winter wheat roots in the field: root growth of high-yielding crops in relation to shoot growth. *The Journal of Agricultural Science* **103**, 439-442.

**Barrow HG, Tenenbaum JM**. 1978. Recovering intrinsic scene characteristics from images. In: Hanson A, Riseman E, eds. *Computer Vision Systems*. New York: Academic Press, 3-26.

**Basu P, Anupam P, Lynch JP, Brown KM, Pal A**. 2007. A novel image-analysis technique for kinematic study of growth and curvature. *Plant Physiology* **145**, 305-316.

**Basu P, Pal A**. 2012. A new tool for analysis of root growth in the spatio-temporal continuum. *New Phytologist* **195**, 264-274.

**Bates GH**. 1937. A Device for the observation of root growth in the soil. *Nature* **139**, 966-967.

**Bates TR, Lynch JP**. 2000. The efficiency of *Arabidopsis thaliana* (*Brassicaceae*) root hairs in phosphorus acquisition. *American Journal of Botany* **87**, 964-970.

**Beebe SE, Rojas-Pierce M, Yan X, Blair MW, Pedraza F, Muñoz F, Tohme J, Lynch JP**. 2006. Quantitative trait loci for root architecture traits correlated with phosphorus acquisition in common bean. *Crop Science.* **46**, 413-423.

**Bell DL, Sultan SE**. 1999. Dynamic phenotypic plasticity for root growth in Polygonum: A comparative study. *American Journal of Botany* **86**, 807-819.

**Bengough AG, Bransby MF, Hans J, McKenna SJ, Roberts TJ, Valentine TA**. 2006. Root responses to soil physical conditions; growth dynamics from field to cell. *Journal of Experimental Botany* **57**, 437-447.

**Bengough AG, Castrignano A, Pagès L, van Noordwijk M**. 2000. Sampling strategies, scaling, and statistics. In: Smit AL, Bengough AG, Engels C, van Noordwijk M, Pellerin S, van de Geijn SC, eds. *Root Methods: a Handbook*. Heidelberg: Springer, 147-173.

**Bengough AG, Gordon DC, Al-Menaie H, Ellis RP, Allan D, Keith R, Thomas WTB, Forster BP**. 2004. Gel observation chamber for rapid screening of root traits in cereal seedlings. *Plant and Soil* **262**, 63-70.

**Bengough AG, McKenzie BM, Hallett PD, Valentine TA**. 2011. Root elongation, water stress, and mechanical impedance: a review of limiting stresses and beneficial root tip traits. *Journal of Experimental Botany* **62**, 59-68.

**Bengough AG, Mullins CE**. 1990. Mechanical impedance to root growth: a review of experimental techniques and root growth responses. *Journal of Soil Science* 41, 341-358.

**Berger A**. 2002. Magnetic resonance imaging. *British Medical Journal* **324**, 35.

**Bingham IJ, Bengough AG**. 2003. Morphological plasticity of wheat and barley roots in response to spatial variation in soil strength. *Plant and Soil* **250**, 273-282.

**Bingham IJ, Rees RM, Bengough AG**. 2009. Influence of soil compaction on the dynamics of root growth and mortality in spring barley. Abstract book: *International Symposium "Root Research and Applications" RootRAP*. , 2-4 September 2009. Boku - - Vienna ,pp 148-4.

-**Blamey FPC, Edwards DG, Asher CJ**. 1983. Effects of aluminum, OH: Al and P: Al molar ratios, and ionic strength on soybean root elongation in solution culture. *Soil Science* **136**, 197-207.

**Bohm W**. 1979. *Methods of Studying Root Systems. Ecological Studies*. Heidelberg: Springer.

**Bois JF, Couchat**. 1983. Comparison of the effects of water stress on the root systems of two cultivars of upland rice (*Oryza sativa* L.). *Annals of Botany* **52**, 479-487.

**Bolan NS, Robson AD, Barrow NJ**. 1987. Effects of phosphorus application and mycorrhizal inoculation on root characteristics of subterranean clover and ryegrass in relation to phosphorus uptake. *Plant and Soil* **104**, 294-298.

**Bolland M**. 2007. Tissue testing for phosphorus. Vol. 2011. http://www.agric.wa.gov.au/objtwr/imported_assets/content/lwe/land/fert/fn2006_tissue phos_mbolland.pdf Government of Western Australia Department of Agriculture and Food farm Note 251, July 2007, Accessed on 3rd October, 2012.

**Bolland MDA, Brennan RF**. 2008. Comparing the phosphorus requirements of wheat, lupin, and canola. *Australian Journal of Agricultural Research* **59**, 983-998.

**Bolland MDA**. 1997. Comparative phosphorus requirement of canola and wheat. *Journal of Plant Nutrition* **20**, 813-829.

**Bonser AM, Lynch J, Snapp S**. 1996. Effect of phosphorus deficiency on growth angle of basal roots in *Phaseolus vulgaris*. *New Phytologist* **132**, 281-288.

**Boroujeni FZ, Wirza R, Mustapha N, Affendey LS, Maskon O, Khalilian M**. 2010. A new tracing algorithm for automatic boundary extraction from coronary cineangiograms. In: *Proceedings of the International MultiConference of Engineers and Computer Scientists 2010 Vol. II, IMECS 2010*, March 17 - 19, 2010, Hong Kong, 1431-1435.

**Bottema MJ**. 2000. Circularity of objects in images. In:*Proceedings* of the *IEEE International Conference on Acoustics, Speech, and Signal Processing, 2000.* IEEE Xplore, pp.2247-2250.

**Boukcim H, Pagès L, Mousain D**. 2006. Local $NO_3^-$ or $NH_4^+$ supply modifies the root system architecture of *Cedrus atlantica* seedlings grown in a split-root device. *Journal of Plant Physiology* **163**, 1293-1304.

**Boukcim H, Pagès L, Plassard C, Mousain D**. 2001. Root system architecture and receptivity to mycorrhizal infection in seedlings of *Cedrus atlantica* as affected by nitrogen source and concentration. *Tree Physiology* **21**, 109-115.

**Box JE, Johnson JW**. 1987. Minirhizotron rooting comparisons of three wheat cultivars. In: Box JE, Johnson JW, eds. *Minirhizotron Observation Tubes: Methods and Applications for Measuring Rhizosphere Dynamics*, ASA Special Publication 50, American Society of Agronomy, Crop Science Society of America, Soil Science Society of America,USA: Madison, Wisconsin, 123-130.

**Brasil EC, Marriel IE, Carvalho JG, Pitta GVE, ParentonI SN, Schaffert RE, Alves VMC**. 2003. Morphological characteristics of the root system of contrasting maize genotypes in relation to phosphorus efficiency under phosphorus stress. In: Rengel Z, ed. *International Symposium on Phosphorus Dynamics in the Soil-Plant Continuum*. Perth, W. Australia, 96-97.

**Breeze VG, Hopper MJ**. 1987. The uptake of phosphate by plants from flowing nutrient solution: IV. Effect of phosphate concentration on the growth of *Trifolium repens* L. supplied with nitrate, or dependent upon symbiotically fixed nitrogen. *Journal of Experimental Botany* **38**, 618-630.

**Broadley MR, Bowen HC, Cotterill HL, Hammond JP, Meacham MC, Mead A, White PJ**. 2003. Variation in the shoot calcium content of angiosperms. *Journal of Experimental Botany* **54**, 1431-1446.

**Broadley MR, Bowen HC, Cotterill HL, Hammond JP, Meacham MC, Mead A, White PJ**. 2004. Phylogenetic variation in the shoot mineral concentration of angiosperms. *Journal of Experimental Botany* **55**, 321-336.

**Broadley MR, Lochlainn SO, Hammond JP, Bowen HC, Cakmak I, Eker S, Erdem H, King GJ, White PJ**. 2010. Shoot zinc (Zn) concentration varies widely within *Brassica oleracea* L. and is affected by soil Zn and phosphorus (P) levels. *Journal of Horticultural Science & Biotechnology* **85**, 375-380.

**Bros EW, Cowell CB**. 1987. A technique for optimizing sample size (replication). *Journal of Experimental Marine Biology and Ecology* **114**, 63-71.

**Brown LK, George TS, Dupuy LX, White PJ**. 2013. A conceptual model of root hair ideotypes for future agricultural environments: what combination of traits should be targeted to cope with limited P availability? *Annals of Botany* **112**, 317-330.

**Brown LK, George TS, Thompson JA, Wright G, Lyon J, Dupuy L, Hubbard SF, White PJ**. 2012. What are the implications of variation in root hair length on tolerance to phosphorus deficiency in combination with water stress in barley (*Hordeum vulgare*)? *Annals of Botany* **110**, 319-328.

**Brown LK**. 2011. *Understanding the impact of root hairs on phosphorus acquisition by barley (*Hordeum vulgare *L.),* MSc thesis, University of Dundee, UK.

**Budinger T, Wwhrli F, Blumenfeld SM, Grunbaum AA, Lauterbur PC, Loeffler W, Natterer F, Nelson AJ, Shepp L, Shulman RG, Tsui BMW, Weidman ST, Riemer RL, Perchura CM**. 1996. *Mathematics and Physics of Emerging Biomedical Imaging*. Washington, D.C.: National Academy Press.

**Buman RA, Schumacher TE, Riedell WE**. 1994. A modified soil monolith technique for characterizing root systems. *Crop Science* **34**, 296-299.

**Burton A, Williams M, Lynch J, Brown K**. 2012. RootScan: Software for high-throughput analysis of root anatomical traits. *Plant and Soil* **357**, 189-203.

**Calegario N, Daniels RF, Maestri R, Neiva R**. 2005. Modeling dominant height growth based on nonlinear mixed-effects model: a clonal Eucalyptus plantation case study. *Forest Ecology and Management* **204**, 11-21.

**Chen J, Xu L, Cai Y, Xu J**. 2009. Identification of QTLs for phosphorus utilization efficiency in maize (*Zea mays* L.) across P levels. *Euphytica* **167**, 245-252.

**Chen Y, Zhou X**. 2010. Plant root image processing and analysis based on 2D scanner. *5th International. Conference on Bio-Inspired Computing: Theories and Application*. Ghangsha, China: IEEE, 1216-1220.

**Chen YL, Dunbabin VM, Diggle AJ, Siddique KHM, Rengel Z**. 2011. Development of a novel semi-hydroponic phenotyping system for studying root architecture. *Functional Plant Biology* **38**, 355-363.

**Chen YL, Dunbabin VM, Diggle AJ, Siddique KHM, Rengel Z**. 2012. Assessing variability in root traits of wild *Lupinus angustifolius* germplasm: basis for modelling root system structure. *Plant and Soil* **354**, 141-155.

**Cheng W, Kuzyakov Y**. 2005. Root effects on soil organic matter decomposition. In: Zobel RW, Wright SF, eds. *Roots and Soil Management: Interactions between Roots and the Soil*. Madison: American Society of Agronomy, Crop Science Society of America, Soil Science, 119 - 143.

**Clark RT, MacCurdy RB, Jung JK, Shaff JE, McCouch SR, Aneshansley DJ, Kochian LV**. 2011. Three-dimensional root phenotyping with a novel imaging and software platform. *Plant Physiology* **156**, 455-465.

**Cobb J, DeClerck G, Greenberg A, Clark R, McCouch S**. 2013. Next-generation phenotyping: requirements and strategies for enhancing our understanding of genotype-phenotype relationships and its relevance to crop improvement. *Theoretical and Applied Genetics* **126**, 867-887.

**Cock WRS, Teixeira do AJA, Bressan-Smith RE, Monnerat PH**. 2002. Biometrical analysis of phosphorus use efficiency in lettuce cultivars adapted to high temperatures. *Euphytica* **126**, 299-308.

**Connelly A, Lohman JAB, Loughman BC, Quiquampoix H, Ratcliffe RG**. 1987. High-resolution imaging of plant-tissues by NMR. *Journal of Experimental Botany* **38**, 1713-1723.

**Cope KR, Bugbee B**. 2013. Spectral effects of three types of white light-emitting diodes on plant growth and development: absolute versus relative amounts of blue light. *HortScience* **48**, 504-509.

**Cordell D, Drangert J-O, White S**. 2009. The story of phosphorus: Global food security and food for thought. *Global Environmental Change* **19**, 292-305.

**Cornelissen JHC, Lavorel S, Garnier E, Diaz S, Buchmann N, Gurvich DE, Reich PB, Steege HT, Morgan HD, Heijden MGAvd, Pausas JG, Poorter H**. 2003. A handbook of protocols for standardised and easy measurement of plant functional traits worldwide. *Australian Journal of Botany* **51**, 335-380.

**Costa C, Dwyer LM, Hamilton RI, Hamel C, Nantais L, Smith DL**. 2000. A sampling method for measurement of large root systems with scanner-based image analysis. *Agronomy Journal* **92**, 621-627.

**Crush JR, Care DA, Gourdin A, Woodfield DR**. 2005. Root growth media effects on root morphology and architecture in white clover. *New Zealand Journal of Agricultural Research* **48**, 255-263.

**Dai X, Wang Y, Yang A, Zhang W-H**. 2012. OsMYB2P-1, an R2R3 MYB transcription factor, is involved in the regulation of phosphate-starvation responses and root architecture in rice. *Plant Physiology* **159**, 169-183.

**Daniel TC, Sharpley AN, Lemunyon JL**. 1998. Agricultural phosphorus and eutrophication: A symposium overview. *Journal of Environmental Quality* **27**, 251-257.

**Dannoura M, Kominami Y, Makita N, H. O**. 2012. Flat optical scanner method and root dynamics. In: Mancuso S, ed. *Measuring Roots: An Updated Approach*. Heidelberg: Springer, 127-133.

**Dannoura M, Kominami Y, Oguma H, Kanazawa Y**. 2008. The development of an optical scanner method for observati on of plant root dynamics. *Plant Root* **2**, 14-18.

**Dawson CJ, Hilton J**. 2011. Fertiliser availability in a resource-limited world: production and recycling of nitrogen and phosphorus. *Food Policy* **36,** S14-S22.

**de Dorlodot S, Forster B, Pagès L, Price A, Tuberosa R, Draye X**. 2007. Root system architecture: opportunities and constraints for genetic improvement of crops. *Trends in Plant Science* **12**, 474-481.

**de Graaff M-A, Van Kessel C, Six J**. 2009. Rhizodeposition-induced decomposition increases N availability to wild and cultivated wheat genotypes under elevated $CO_2$. *Soil Biology and Biochemistry* **41**, 1094-1103.

**De Smet I, White PJ, Bengough AG, Dupuy L, Parizot B, Casimiro I, Heidstra R, Laskowski M, Lepetit M, Hochholdinger F, Draye X, Zhang HM, Broadley MR, Peret B, Hammond JP, Fukaki H, Mooney S, Lynch JP, Nacry P, Schurr U, Laplaze L, Benfey P, Beeckman T, Bennett M**. 2012. Analyzing lateral root development: How to move forward. *Plant Cell* **24**, 15-20.

**Des Marais DL, Hernandez KM, Juenger TE.** 2013. Genotype-by-Environment Interaction and Plasticity: Exploring Genomic Responses of Plants to the Abiotic Environment. *Annual Review of Ecology, Evolution, and Systematics* 44, 5-29.

**Devienne-Barret F, Richard-Molard C, Chelle M, Maury O, Ney B**. 2006. Ara-rhizotron: An effective culture system to study simultaneously root and shoot development of *Arabidopsis*. *Plant and Soil* **280**, 253-266.

**Dickison WC**. 2000. *Integrative Plant Anatomy*. U.S.A.: Academic Press.

**Doerge RW.** 2002. Mapping and analysis of quantitative trait loci in experimental populations. *Nature Reviews Genetics* **3,** 43-52.

**Dong S, Neilsen D, Neilsen GH, Weis M, Dong SF**. 2003. A scanner-based root image acquisition technique for measuring roots on a rhizotron window. *HortScience* **38**, 1385-1388.

**Doussan C, Pierret A, Garrigues E, Pagès L**. 2006. Water uptake by plant roots: II - Modelling of water transfer in the soil root-system with explicit account of flow within the root system - comparison with experiments. *Plant and Soil* **283**, 99-117.

**Downie H, Holden NJ, Otten W, Spiers AJ, Valentine TA, Dupuy LX**. 2012. Transparent soil for imaging the rhizosphere. PLoS ONE 7(9): e44276. doi:10.1371/journal.pone.0044276.

**Dresbøll DB, Thorup-Kristensen K, McKenzie BM, Dupuy L, Bengough AG**. 2013. Timelapse scanning reveals spatial variation in tomato (*Solanum lycopersicum* L.) root elongation rates during partial waterlogging. *Plant and Soil* **369**, 467-477.

**Dubrovsky JG, Forde BG**. 2012. Quantitative analysis of lateral root development: Pitfalls and how to avoid them. *Plant Cell* **24**, 4-14.

**Duncan JS, Ayache N**. 2000. Medical image analysis: progress over two decades and the challenges ahead. *IEEE Transactions on Pattern Analysis and Machine Intelligence* **22**, 85-106.

**Dupuy L, Fourcaud T, Stokes A, Danjon F**. 2005. A density-based approach for the modelling of root architecture: application to Maritime pine (*Pinus pinaster* Ait.) root systems. *Journal of Theoretical Biology* **236**, 323-334.

**Dupuy L, Gregory PJ, Bengough AG**. 2010a. Root growth models: towards a new generation of continuous approaches. *Journal of Experimental Botany* **61**, 2131-2143.

**Dupuy L, Vignes M, McKenzie BM, White PJ**. 2010b. The dynamics of root meristem distribution in the soil. *Plant Cell and Environment* **33**, 358-369.

**Dupuy LX, Vignes M**. 2012. An algorithm for the simulation of the growth of root systems on deformable domains. *Journal of Theoretical Biology* **310**, 164-174.

**Dutt D, Lal M, Malik RS, Upadhyay MK**. 2005. Development of specialty papers is an art: seed germination paper from indigenous raw materials- Part XIII. *Journal of Scientific and Industrial Research* **64**, 440-442.

**Eapen D, Barroso ML, Ponce G, Campos ME, Cassab GI**. 2005. Hydrotropism: root growth responses to water. *Trends in Plant Science* **10**, 44-50.

**Eissenstat DM**. 1992. Costs and benefits of constructing roots of small diameter. *Journal of Plant Nutrition* **15**, 763-782.

**Eng J**. 2003. Sample size estimation: how many individuals should be studied? *Radiology* **227**, 309 -313.

**Erickson RO**. 1976. Modeling of plant-growth. *Annual Review of Plant Physiology and Plant Molecular Biology* **27**, 407-434.

**Fageria NK, Baligar VC, Li YC**. 2008. The role of nutrient efficient plants in improving crop yields in the twenty first century. *Journal of Plant Nutrition* **31**, 1121-1157.

**Fageria NK, Baligar VC**. 1993. Screening crop genotypes for mineral stresses. *Proceedings of the Workshop on Adaptation of Plants to Soil Stress*. University of Nebraska, Lincoln, NE.: INTSORMIL Publication, 142-159.

**Fageria NK, Baligar VC**. 1997. Upland rice genotypes evaluation for phosphorus use efficiency. *Journal of Plant Nutrition* **20**, 499-509.

**Fageria NK, Baligar VC**. 1999. Phosphorus-use efficiency in wheat genotypes. *Journal of Plant Nutrition* **22**, 331-340.

**Fageria NK, Morais OP, Baligar VC, Wright RJ**. 1988. Response of rice cultivars to phosphorus supply on an oxisol. *Fertilizer Research* **16**, 195-206.

**Fageria NK, Moreira A**. 2011. The role of mineral nutrition on root growth of crop plants. In: Sparks DL, ed. *Advances in Agronomy*, Vol. 110: Academic Press, 251-331.

**Faget M, Liedgens M, Feil B, Stamp P, Herrera JM**. 2012. Root growth of maize in an Italian ryegrass living mulch studied with a non-destructive method. *European Journal of Agronomy* **36**, 1-8.

**Faget M, Liedgens M, Stamp P, Flutsch P, Herrera JM**. 2010. A minirhizotron imaging system to identify roots expressing the green fluorescent protein. *Computers and Electronics in Agriculture* **74**, 163-167.

**Faget M, Nagel KA, Walter A, Herrera JM, Jahnke S, Schurr U, Temperton VM**. 2013. Root-root interactions: extending our perspective to be more inclusive of the range of theories in ecology and agriculture using *in-vivo* analyses. *Annals of Botany* **112,** 253-266.

**Falcao AX, Udupa JK, Samarasekera S, Sharma S, Hirsch BE, Lotufo RDA**. 1998. User-steered image segmentation paradigms: Live wire and Live lane. *Graphical Models and Image Processing* **60**, 233-260.

**Fang SQ, Yan XL, Liao H**. 2009. 3D reconstruction and dynamic modeling of root architecture *in situ* and its application to crop phosphorus research. *Plant Journal* **60**, 1096-1108.

**Farley RA, Fitter AH**. 1999. The responses of seven co-occurring woodland herbaceous perennials to localised nutrient-rich patches. *Journal of Ecology* **87**, 849-859.

**Federici F, Dupuy L, Laplaze L, Heisler M, Haseloff J**. 2012. Integrated genetic and computation methods for in planta cytometry. *Nature Methods* **9**, 483-485.

**Fiorani F, Schurr U**. 2013. Future scenarios for plant phenotyping. *Annual Review of Plant Biology* **64**, 267-291.

**Fita A, Picó B, Monforte AJ, Nuez F**. 2008. Genetics of root system architecture using near-isogenic lines of melon. *Journal of the American Society for Horticultural Science* **133**, 448-458.

**Fita A, Pico B, Nuez F**. 2006. Implications of the genetics of root structure in melon breeding. *Journal of American Soceity of Horticultural Science* **372**, 379-379.

**Fitter AH, Stickland TR, Harvey ML, Wilson GW**. 1991. Architectural analysis of plant-root systems 1. Architectural correlates of exploitation efficiency. *New Phytologist* **118**, 375-382.

**Fitter AH**. 1985. Functional significance of root morphology and root system architecture. In: Fitter AH, Atkinson D, Read DJ, Usher MB, eds. *Ecological Interactions in Soil. Plants, Microbes and Animals*. Oxford: Blackwell Scientific Publications, 87-106.

**Fitter AH**. 1986. The topology and geometry of plant-root systems - influence of watering rate on root-system topology in *Trifolium pratense*. *Annals of Botany* **58**, 91-101.

**Fitter AH**. 1987. An architectural approach to the comparative ecology of plant-root systems. *New Phytologist* **106**, 61-77.

**Fitter AH**. 1991. The ecological significance of root system architecture: an economic approach. In: Atkinson D, ed. *Plant Root Growth: An Ecological Perspective* Oxford: Blackwell Scientific Publications, 229 - 243.

**Fitter AH**. 2002. Characteristics and functions of root systems. In: Waisel Y, Eshel A, Kafkafi L, eds. *Plant Roots The Hidden Half*. New York: Marcel Dekker, 15 - 32.

**Foehse D, Jungk A**. 1983. Influence of phosphate and nitrate supply on root hair formation of rape, spinach and tomato plants. *Plant and Soil* **74**, 359-368.

**Ford KE, Gregory PJ, Gooding MJ, Pepler S**. 2006. Genotype and fungicide effects on late-season root growth of winter wheat. *Plant and Soil* **284**, 33-44.

**Forde B, Lorenzo H**. 2001. The nutritional control of root development. *Plant and Soil* **232**, 51-68.

**Frangi AF, Niessen WJ, Vincken KL, Viergever MA**. 1998. Multiscale vessel enhancement filtering. *Medical Image Computing and Computer-Assisted Intervention - Miccai'98* **1496**, 130-137.

**French A, Ubeda-Tomas S, Holman TJ, Bennett MJ, Pridmore T**. 2009. High-throughput quantification of root growth using a novel image-analysis tool. *Plant Physiology* **150**, 1784-1795.

**Furbank RT, Tester M**. 2011. Phenomics-technologies to relieve the phenotyping bottleneck. *Trends in Plant Science* **16**, 635-644.

**Futsaether C, Oxaal U**. 2002. A growth chamber for idealised studies of seedling root growth dynamics and structure. *Plant and Soil* **246**, 221-230.

**Gahoonia TS, Nielsen NE**. 1996. Variation in acquisition of soil phosphorus among wheat and barley genotypes. *Plant and Soil* **178**, 223-230.

**Gahoonia TS, Nielsen NE**. 2004a. Barley genotypes with long root hairs sustain high grain yields in low-P field. *Plant and Soil* **262**, 55-62.

**Gahoonia TS, Nielsen NE**. 2004b. Root traits as tools for creating phosphorus efficient crop varieties. *Plant and Soil* **260**, 47-57.

**Galkovskyi T, Mileyko Y, Bucksch A, Moore B, Symonova O, Price C, Topp C, Iyer-Pascuzzi A, Zurek P, Fang S, Harer J, Benfey P, Weitz J**. 2012. *GiA Roots*: software for the high throughput analysis of plant root system architecture. *BMC Plant Biology* **12**, 116.

**Garnier E, Navas M-L**. 2012. A trait-based approach to comparative functional plant ecology: concepts, methods and applications for agroecology. A review. *Agronomy for Sustainable Development* **32**, 365-399.

**Garrigues E, Doussan C, Pierret A**. 2006. Water uptake by plant roots: I - Formation and propagation of a water extraction front in mature root systems as evidenced by 2D light transmission imaging. *Plant and Soil* **283**, 83-98.

**Gaudin AC, McClymont SA, Holmes BM, Lyons E, Raizada MN**. 2011. Novel temporal, fine-scale and growth variation phenotypes in roots of adult-stage maize (*Zea mays* L.) in response to low nitrogen stress. *Plant Cell and Environment* **34**, 2122-2137.

**Ge ZY, Rubio G, Lynch JP**. 2000. The importance of root gravitropism for inter-root competition and phosphorus acquisition efficiency: results from a geometric simulation model. *Plant and Soil* **218**, 159-171.

**George TS, Brown LK, Newton AC, Hallett PD, Sun BH, Thomas WTB, White PJ**. 2011a. Impact of soil tillage on the robustness of the genetic component of variation in phosphorus (P) use efficiency in barley (*Hordeum vulgare* L.). *Plant and Soil* **339**, 113-123.

**George TS, Fransson A-M, Hammond JP, White PJ**. 2011b. Phosphorus nutrition: rhizosphere processes, plant response and adaptations. In: Bünemann E, Oberson A, Frossard E, eds. *Phosphorus in Action*: *Soil Biology, Vol 26*,Springer: Heidelberg, 245-271.

**Gerald JNF, Lehti-Shiu MD, Ingram PA, Deak KI, Biesiada T, Malamy JE**. 2006. Identification of quantitative trait loci that regulate *Arabidopsis* root system size and plasticity. *Genetics* **172**, 485-498.

**Gifford ML, Banta JA, Katari MS, Hulsmans J, Chen L, Ristova D, Tranchina D, Purugganan MD, Coruzzi GM, Birnbaum KD**. 2013. Plasticity regulators modulate specific root traits in discrete nitrogen environments. *PLoS Genetics **9**: doi:10.1371/journal.pgen.1003760s*.

**Glimskar A**. 2000. Estimates of root system topology of five plant species grown at steady-state nutrition. *Plant and Soil* **227**, 249-256.

**Glinski DS, Karnok KJ, Carrow RN**. 1993. Comparison of reporting methods for root growth data from transparent-interface measurements. *Crop Science.* **33**, 310-314.

**Graham EA, Nobel PS**. 1999. Root water uptake, leaf water storage and gas exchange of a desert succulent: implications for root system redundancy. *Annals of Botany* **84**, 213-223.

**Greenwood DJ, Barnes A, Liu KF, Hunt J, Cleaver TJ, Loquens SMH**. 1980. Relationships between the critical concentrations of nitrogen, phosphorus and potassium in 17 different vegetable crops and duration of growth. *Journal of the Science of Food and Agriculture* **31**, 1343-1353.

**Gregory PJ, Bengough AG, Grinev D, Schmidt S, Thomas WTB, Wojciechowski T, Young IM**. 2009. Root phenomics of crops: opportunities and challenges. *Functional Plant Biology* **36**, 922-929.

**Gregory PJ, Hutchison DJ, Read DB, Jenneson PM, Gilboy WB, Morton EJ**. 2003. Non-invasive imaging of roots with high resolution X-ray micro-tomography. *Plant and Soil* **255**, 351-359.

**Gregory PJ**. 2006. *Plant Roots: Their Growth, Activity and Interaction with Soils*. Oxford: Blackwell Publishing Ltd.

**Gruber BD, Giehl RFH, Friedel S, von Wirén N**. 2013. Plasticity of the *Arabidopsis* root system under nutrient deficiencies. *Plant Physiology* **163**, 161-179.

**Grzesiak S, Grzesiak MT, Felek W, Hura T, Stabryla J**. 2002. The impact of different soil moisture and soil compaction on the growth of triticale root system. *Acta Physiologiae Plantarum* **24**, 331-342.

**Guan BT, Chang T-Y, Shih P-C, Lin S-T**. 2006. Application of a nonlinear mixed-effects model to assess the effects of nursery nitrogen fertilization on seedling height growth of Taiwan yellow false cypress. *Taiwan Journal for Science* **21**, 67-74.

**Hainsworth J, Aylmore L**. 1983. The use of computer assisted tomography to determine spatial distribution of soil water content. *Soil Research* **21**, 435-443.

**Hajabbasi MA, Schumacher TE**. 1994. Phosphorus effects on root growth and development in two maize genotypes. *Plant and Soil* **158**, 39-46.

**Hammond JP, Bennett MJ, Bowen HC, Broadley MR, Eastwood DC, May ST, Rahn C, Swarup R, Woolaway KE, White PJ**. 2003. Changes in gene expression in *Arabidopsis* shoots during phosphate starvation and the potential for developing smart plants. *Plant Physiol* **132**, 578-596.

**Hammond JP, Broadley MR, White PJ, King GJ, Bowen HC, Hayden R, Meacham MC, Mead A, Overs T, Spracklen WP, Greenwood DJ**. 2009. Shoot yield drives phosphorus use efficiency in *Brassica oleracea* and correlates with root architecture traits. *Journal of Experimental Botany* **60**, 1953-1968.

**Hammond JP, Broadley MR, White PJ**. 2004. Genetic responses to phosphorus deficiency. *Annals of Botany* **94**, 323-332.

**Hammond JP, White PJ**. 2008. Sucrose transport in the phloem: integrating root responses to phosphorus starvation. *Journal of Experimental Botany* **59**, 93-109.

**Hamza MA, Aylmore LAG**. 1992. Soil solute concentration and water uptake by single lupin and radish plant roots. *Plant and Soil* **145**, 197-205.

**Haralick R, Shapiro L**. 1992. *Computer and Robot Vision*: Addison-Wesley Publishing Company.

**Hargreaves CE, Gregory PJ, Bengough AG**. 2009. Measuring root traits in barley (*Hordeum vulgare* ssp *vulgare* and ssp *spontaneum*) seedlings using gel chambers, soil sacs and X-ray microtomography. *Plant and Soil* **316**, 285-297.

**Harrington CA, Brissette JC, Carlson WC**. 1989. Root system structure in planted and seeded loblolly and shortleaf pine. *Forest Science* **35**, 469-480.

**Herrera JM, Noulas C, Feil B, Stamp P, Liedgens M.** 2013. Nitrogen and genotype effects on root growth and root survivorship of spring wheat. *Plant Nutrition and Soil Science* **176**, 561-571.

**Herrera J, Verhulst N, Govaerts B**. 2012. Strategies to identify genetic diversity in root traits. In: Reynolds MP, Pask AJD, Mullan D, eds. *Physiological Breeding I: Interdisciplinary Approaches to Improve Crop Adaptation*. Mexico: CIMMYT, 97-108.

**Hiltner, L. 1904.** On recent experiences and problems in the field of Bodenbakteriologie with special emphasis on green manure and fallow (translated from German). *German Agricultural Society)* **98**, 59-78.

**Hinsinger P**. 2001. Bioavailability of soil inorganic P in the rhizosphere as affected by root-induced chemical changes: a review. *Plant and Soil* **237**, 173-195.

**Hochholdinger F, Park WJ, Sauer M, Woll K**. 2004a. From weeds to crops: genetic analysis of root development in cereals. *Trends in Plant Science* **9**, 42-48.

**Hochholdinger F, Tuberosa R**. 2009. Genetic and genomic dissection of maize root development and architecture. *Current Opinion in Plant Biology* **12**, 172-177.

**Hochholdinger F, Woll K, Sauer M, Dembinsky D**. 2004b. Genetic dissection of root formation in maize (*Zea mays*) reveals root-type specific developmental programmes. *Annals of Botany* **93**, 359-368.

**Hodge A, Berta G, Doussan C, Merchan F, Crespi M**. 2009. Plant root growth, architecture and function. *Plant and Soil* **321**, 153-187.

**Hodge A, Robinson D, Griffiths BS, Fitter AH**. 1999. Why plants bother: root proliferation results in increased nitrogen capture from an organic patch when two grasses compete. *Plant, Cell & Environment* **22**, 811-820.

**Hodge A, Stewart J, Robinson D, Griffiths BS, Fitter AH**. 2000a. Competition between roots and soil micro-organisms for nutrients from nitrogen-rich patches of varying complexity. *Journal of Ecology* **88**, 150-164.

**Hodge A, Stewart J, Robinson D, Griffiths BS, Fitter AH**. 2000b. Spatial and physical heterogeneity of N supply from soil does not influence N capture by two grass species. *Functional Ecology* **14**, 645-653.

**Hodge A**. 2004. The plastic plant: root responses to heterogeneous supplies of nutrients. *New Phytologist* **162**, 9-24.

**Hoecker N, Keller B, Piepho HP, Hochholdinger F**. 2006. Manifestation of heterosis during early maize (*Zea mays* L.) root development. *Theoretical and Applied Genetics* **112**, 421-429.

**Hoffland E**. 1992. Quantitative evaluation of the role of organic acid exudation in the mobilization of rock phosphate by rape. *Plant and Soil* **140**, 279-289.

**Hornak JP**. 2008. The basics of MRI [Online]. Interactive learning software. Vol. 2013. http://www.cis.rit.edu/htbooks/mri/index.html.

**Huisken J, Stainier DYR**. 2009. Selective plane illumination microscopy techniques in developmental biology. *Development* **136**, 1963-1975.

**Huisken J, Swoger J, Del Bene F, Wittbrodt J, Stelzer EHK**. 2004. Optical sectioning deep inside live embryos by selective plane illumination microscopy. *Science* **305**, 1007-1009.

**Hund A, Trachsel S, Stamp P**. 2009. Growth of axile and lateral roots of maize: I. Development of a phenotying platform. *Plant and Soil* **325**, 335-349.

**Hunt R**. 2003. Growth and development/growth analysis, individual plants. In: Thomas B, Murphy DJ, Murray D, eds. *Encyclopaedia of Applied Plant Sciences*. London: Academic Press, 579-588.

**Hutchings MJ, John EA**. 2004. The effects of environmental heterogeneity on root growth and root/shoot partitioning. *Annals of Botany* **94**, 1-8.

**Ingram KT, Leers GA**. 2001. Software for measuring root characters from digital images. *Agronomy Journal* **93**, 918-922.

**Ingram PA, Zhu JM, Shariff A, Davis IW, Benfey PN, Elich T**. 2012. High-throughput imaging and analysis of root system architecture in *Brachypodium distachyon* under differential nutrient availability. *Philosophical Transactions of the Royal Society B-Biological Sciences* **367**, 1559-1569.

**Iniguez-Luy FL, Lukens L, Farnham MW, Amasino RM, Osborn TC**. 2009. Development of public immortal mapping populations, molecular markers and linkage maps for rapid cycling *Brassica rapa* and *B. oleracea*. *Theoretical and Applied Genetics* **120**, 31-43.

**Insalud N, Bell RW, Colmer TD, Rerkasem B**. 2006. Morphological and physiological responses of rice (*Oryza sativa*) to limited phosphorus supply in aerated and stagnant solution culture. *Annals of Botany* **98**, 995-1004.

**Iqbal RJ, Ranjha AM, Waheed T, Iftikhar A**. 2001. Genotypic differences among cotton genotypes for phosphorus use efficiency and stress factor. *International Journal of Agriculture and Biology* **3**, 186-187.

**Ivanov K, Zaprjanov P, Angelov V, Bekjaro G, Dospatliev L**. 2010. ICP determination of phosphorous in soils and plants. *19th World Congress of Soil Science, Soil Solutions for a Changing World*. Brisbane, Australia: World Congress of Soil Science, 71-74.

**Iyer-Pascuzzi AS, Symonova O, Mileyko Y, Hao YL, Belcher H, Harer J, Weitz JS, Benfey PN**. 2010. Imaging and analysis platform for automatic phenotyping and trait ranking of plant root systems. *Plant Physiology* **152**, 1148-1157.

**Jackson LE**. 1995. Root architecture in cultivated and wild lettuce (*Lactuca* spp.). *Plant, Cell & Environment* **18**, 885-894.

**Jackson SA, Iwata A, Lee SH, Schmutz J, Shoemaker R**. 2011. Sequencing crop genomes: approaches and applications. *New Phytologist* **191**, 915-925.

**Jain A, Poling MD, Karthikeyan AS, Blakeslee JJ, Peer WA, Titapiwatanakun B, Murphy AS, Raghothama KG**. 2007. Differential effects of sucrose and auxin on localised phosphate deficiency-induced modulation of different traits of root system architecture in arabidopsis. *Plant Physiology* **144**, 232-247.

**Jain A, Poling MD, Smith AP, Nagarajan VK, Lahner B, Meagher RB, Raghothama KG**. 2009. Variations in the composition of gelling agents affect morphophysiological and molecular responses to deficiencies of phosphate and other nutrients. *Plant Physiology* **150**, 1033-1049.

**Kaestner A, Schneebeli M, Graf F**. 2006. Visualizing three-dimensional root networks using computed tomography. *Geoderma* **136**, 459-469.

**Kashiwagi J, Krishnamurthy L, Crouch JH, Serraj R**. 2006. Variability of root length density and its contributions to seed yield in chickpea (*Cicer arietinum* L.) under terminal drought stress. *Field Crops Research* **95**, 171-181.

**King GJ**. 2005. Brassica: Harvesting the genome, diversity and products. In: King GJ, ed. *A (draft) "White Paper for the multinational brassica genome project*: The multinational brassica genome project. http://brassica.nbi.ac.uk/pdf/mbgp_white_paper_v110.pdf. Accessed 14 - 12 - 2012.

**Kirbas C, Quek F**. 2004. A review of vessel extraction techniques and algorithms. *ACM Computing Surveys* **36,** 81-121.

**Kolawole GO, Tian G, Singh BB**. 2002. Differential response of cowpea lines to application of P fertilizer. In: Fatokun CA, ed. *Challenges and Opportunities for Enhancing Sustainable Cowpea Production*, 319-328.

**Kosola KR, Workmaster BAA, Busse JS, Gilman JH**. 2007. Sampling damage to tree fine roots: comparing air excavation and hydropneumatic elutriation. *HortScience* **42**, 728-731.

**Kramer PJ, Boyer JS**. 1995. *Water Relations of Plants and Soils*. San Diego, CA.: Academic Press.

**Kücke M, Schmid H, Spiess A**. 1995. A comparison of four methods for measuring roots of field crops in three contrasting soils. *Plant and Soil* **172**, 63-71.

**Kumar A, Kusuma P, Gowda MVC**. 2009. Genotypic variation in root traits in groundnut germplasm under phosphorus stress condition. *Journal of SAT Agricultural Research* **7**, 1-4.

**Kumar B, Abdel-Ghani AH, Reyes-Matamoros J, Hochholdinger F, Lübberstedt T**. 2012. Genotypic variation for root architecture traits in seedlings of maize (*Zea mays* L.) inbred lines. *Plant Breeding* **131**, 465-478.

**Kurup S, Runions J, Kohler U, Laplaze L, Hodge S, Haseloff J**. 2005. Marking cell lineages in living tissues. *Plant Journal* **42**, 444-453.

**Kutschera L**. 1960. *Wurzelatlas mitteleuropäischer Ackerunkräuter und Kulturpflanzen. (Root Atlas Central European arable weeds and crops)*. Frankfurt-Germany: DLG-Verlag.

**Lajtha K, Harrison AF**. 1995. Strategies of phosphorus acquisition and conservation by plant species and communities. In: Tiessen H, ed. *Phosphorus in the Global Environment*. Chichester, UK: John Wiley Sons, 140-147.

**Lambers H, Mougel C, Jaillard B, Hinsinger P**. 2009. Plant-microbe-soil interactions in the rhizosphere: an evolutionary perspective. *Plant and Soil* **321**, 83-115.

**Lambers H, Shane MW, Cramer MD, Pearse SJ, Veneklaas EJ**. 2006. Root structure and functioning for efficient acquisition of phosphorus: matching morphological and physiological traits. *Annals of Botany* **98**, 693-713.

**Le Bot J, Serra V, Fabre J, Draye X, Adamowicz S, Pagès L**. 2010. *DART*: a software to analyse root system architecture and development from captured images. *Plant and Soil* **326**, 261-273.

**Lecompte F, Ozier-Lafontaine H, Pagès L**. 2001. The relationships between static and dynamic variables in the description of root growth. Consequences for field interpretation of rooting variability. *Plant and Soil* **236**, 19-31.

**Lecompte F, Pagès L, Ozier-Lafontaine H**. 2005. Patterns of variability in the diameter of lateral roots in the banana root system. *New Phytologist* **167**, 841-850.

**Lee D-H**. 1998. Phosphorus use efficiency in anthocyanin-free tomato (*Lycopersicon esculentum* Mill.). *Journal of Plant Biology* **41**, 86-92.

**Lee JA, Woolhouse HW**. 1969. A comparative study of bicarbonate inhibition of root growth in calcicole and calcifuge grasses. *New Phytologist* **68**, 1-11.

**Lee K, Avondo J, Morrison H, Blot L, Stark M, Sharpe J, Bangham A, Coen E**. 2006. Visualizing plant development and gene expression in three dimensions using optical projection tomography. *Plant Cell* **18**, 2145-2156.

**Leitner D, Felderer B, Vontobel P, Schnepf A**. 2013. Recovering root system traits using image analysis - exemplified by 2-dimensional neutron radiography images of lupine. *Plant Physiology*. DOI:10.1104/pp.113.227892.

**Léon J, Schwarz KU**. 1992. Description and application of a screening method to determine root morphology traits of cereal cultivars. *Journal of Agronomy and Crop Science* **169**, 128-134.

**Li CH, Lee CK**. 1993. Minimum cross entropy thresholding. *Pattern Recognition* **26**, 617-625.

**Li CH, Tam PKS**. 1998. An iterative algorithm for minimum cross entropy thresholding. *Pattern Recognition Letters* **19**, 771-776.

**Li J, Xie Y, Dai A, Liu L, Li Z**. 2009. Root and shoot traits responses to phosphorus deficiency and QTL analysis at seedling stage using introgression lines of rice. *Journal of Genetics and Genomics* **36**, 173-183.

**Li YF, Luo AC, Wei XH, Yao XG**. 2007. Genotypic variation of rice in phosphorus acquisition from iron phosphate: contributions of root morphology and phosphorus uptake kinetics. *Russian Journal of Plant Physiology* **54**, 230-236.

**Liao H, Rubio G, Yan X, Cao AQ, Brown KM, Lynch JP**. 2001. Effect of phosphorus availability on basal root shallowness in common bean. *Plant and Soil* **232**, 69-79.

**Liao H, Yan X, Rubio G, Beebe SE, Blair MW, Lynch JP**. 2004. Genetic mapping of basal root gravitropism and phosphorus acquisition efficiency in common bean. *Functional Plant Biology* **31**, 959-970.

**Liedgens M, Richner W, Stamp P, Soldati A**. 2000. A rhizolysimeter facility for studying the dynamics of crop and soil processes: description and evaluation. *Plant and Soil* **223**, 87-97.

**Linkohr BI, Williamson LC, Fitter AH, Leyser HM**. 2002. Nitrate and phosphate availability and distribution have different effects on root system architecture of arabidopsis. *Plant Journal* **29**, 751-760.

**Liu M**. 2007. *Phosphorus requirement of St. Augustine grass*, PhD thesis, University of Florida, USA.

**Lobet G, Draye X**. 2013. Novel scanning procedure enabling the vectorization of entire rhizotron-grown root systems. *Plant Methods* **9**, 1, doi:10.1186/1746-4811-9-1.

**Lobet G, Draye X, Perilleux C.** (2013) An online database for plant image analysis software tools. *Plant Methods*, 9, 38. doi:10.1186/1746-4811-9-38.

**Lobet G, Pagès L, Draye X**. 2011. A novel image-analysis toolbox enabling quantitative analysis of root system architecture. *Plant Physiology* **157**, 29-39.

**Lopez-Bucio J, Hernandez-Abreu E, Sanchez-Calderon L, Nieto-Jacobo MF, Simpson J, Herrera-Estrella L**. 2002. Phosphate availability alters architecture and causes changes in hormone sensitivity in the *Arabidopsis* root system. *Plant Physiology* **129**, 244-256.

**Lu G, Cao J, Yu X, Xiang X, Chen H**. 2008. Mapping QTLs for root morphological traits in *Brassica rapa* L. based on AFLP and RAPD markers. *Journal of Applied Genetics* **49**, 23-31.

**Luster J, Gottlein A, Nowack B, Sarret G**. 2009. Sampling, defining, characterising and modeling the rhizosphere-the soil science tool box. *Plant and Soil* **321**, 457-482.

**Lynch JP, Beebe SE**. 1995. Adaptation of beans (*Phaseolus vulgaris* L.) to low phosphorus availability. *HortScience* **30**, 1165-1171.

**Lynch JP, Brown KM**. 2001. Topsoil foraging - an architectural adaptation of plants to low phosphorus availability. *Plant and Soil* **237**, 225-237.

**Lynch JP, Brown KM**. 2008. Root strategies for phosphorus acquisition. In: White PJ, Hammond JP, eds. *The Ecophysiology of Plant-Phosphorus Interactions*. Dordrecht: Springer, 83-116.

**Lynch JP, Brown KM**. 2012. New roots for agriculture: exploiting the root phenome. *Philosophical Transactions of the Royal Society B: Biological Sciences* **367**, 1598-1604.

**Lynch JP**. 1995. Root architecture and plant productivity. *Plant Physiology* **109**, 7-13.

**Lynch JP**. 2011. Root phenes for enhanced soil exploration and phosphorus acquisition: Tools for future crops. *Plant Physiology* **156**, 1041-1049.

**Ma Z, Baskin TI, Brown KM, Lynch JP**. 2003. Regulation of root elongation under phosphorus stress involves changes in ethylene responsiveness. *Plant Physiology* **131**, 1381-1390.

**Ma Z, Bielenberg DG, Brown KM, Lynch JP**. 2001. Regulation of root hair density by phosphorus availability in *Arabidopsis thaliana*. *Plant, Cell & Environment* **24**, 459-467.

**Mahesh M**. 2002. The AAPM/RSNA physics tutorial for residents - search for isotropic resolution in CT from conventional through multiple-row detector. *Radiographics* **22**, 949-962.

**Maini R, Aggarwal H**. 2010. A comprehensive review of image enhancement techniques. *Journal of Computing* **2**, 8 - 13.

**Mairhofer S, Zappala S, Tracy SR, Sturrock C, Bennett M, Mooney SJ, Pridmore TP**. 2013. Recovering complete plant root system architectures from soil via X-ray µ-Computed Tomography. *Plant Methods* **9**, 1-7, doi:10.1186/1746-4811-9-8.

**Major BJ, Barraclough PB**. 2002. Critical phosphate (P) and inorganic phosphate (Pi) concentrations for the growth of winter oilseed rape (*Brassica napus*). In: Horst WJ, Schenk MK, Bürkert A, Claassen N, Flessa H, Frommer WB, Goldbach H, Olfs HW, Römheld V, Sattelmacher B, Schmidhalter U, Schubert S, Wirén N, Wittenmayer L, eds. *Plant Nutrition*: Food Security and Sustainability of Agro-Eecosystems through Basic and Applied Research. Vol. 92, New York: Springer, 714-715.

**Malamy JE, Benfey PN**. 1997. Down and out in *Arabidopsis*: the formation of lateral roots. *Trends in Plant Science* **2**, 390-396.

**Malamy JE, Ryan KS**. 2001. Environmental regulation of lateral root initiation in *Arabidopsis*. *Plant Physiology* **127**, 899-909.

**Malamy JE**. 2005. Intrinsic and environmental response pathways that regulate root system architecture. *Plant Cell and Environment* **28**, 67-77.

**Manschadi AM, Hammer GL, Christopher JT, deVoil P**. 2008. Genotypic variation in seedling root architectural traits and implications for drought adaptation in wheat (*Triticum aestivum* L.). *Plant and Soil* **303**, 115-129.

**Marion A**. 1991. *An Introduction to Image Processing*: Chapman & Hall Computing.

**Marschner H**. 1995. *Mineral Nutrition of Higher Plants*. London: Academic Press.

**Martinez-Ortiz C**. 2010. *2D and 3D Shape Descriptors*, PhD thesis, University of Exeter, UK.

**Materechera SA, Alston AM, Kirby JM, Dexter AR**. 1992. Influence of root diameter on the penetration of seminal roots into a compacted subsoil. *Plant and Soil* **144**, 297-303.

**Matsuo N, Mochizuki T**. 2009. Genotypic differences in root traits of rice (*Oryza sativa* L.) seedlings grown under different soil environments. *Plant Root* **3**, 17-25.

**May LH, Chapman F, Aspinall D**. 1965. Quantitative studies of root development I. The influence of nutrient concentration. *Australian Journal of Biological Sciences* **18**, 25-35.

**May LH, Randles F, Aspinall D, Paleg LG**. 1967. Quantitative studies of root development II. Growth in the early stages of development. *Australian Journal of Biological Sciences* **20**, 273-284.

**McCully ME**. 1999. Roots in soil: Unearthing the complexities of roots and their rhizospheres. *Annual Review of Plant Physiology and Plant Molecular Biology* **50**, 695-718.

**Megahed FM**. 2012. *The Use of Image and Point Cloud Data in Statistical Process Control*, PhD thesis, Virginia Polytechnic Institute and State University, USA.

**Mian MAR, Nafziger ED, Kolb FL, Teyker RH**. 1994. Root size and distribution of fieldgrown wheat genotypes. *Crop Science.* **34**, 810-812.

**Michelini E, Cevenini L, Mezzanotte L, Ablamsky D, Southworth T, Branchini BR, Roda A**. 2008. Combining intracellular and secreted bioluminescent reporter proteins for multicolor cell-based assays. *Photochemical and Photobiological Sciences* **7**, 212-217.

**Miller CR, Ochoa I, Nielsen KL, Beck D, Lynch JP**. 2003. Genetic variation for adventitious rooting in response to low phosphorus availability: potential utility for phosphorus acquisition from stratified soils. *Functional Plant Biology* **30**, 973-985.

**Modaihsh AS, Abdallah AE, Mahjoub MO**. 2001. Accumulation of cadmium in arid soils as affected by intensive phosphorus fertilization. *Arid Land Research and Management* **15**, 173-181.

**Mollier A, Pellerin S**. 1999. Maize root system growth and development as influenced by phosphorus deficiency. *Journal of Experimental Botany* **50**, 487-497.

**Montagu KD, Conroy JP, Atwell BJ**. 2001. The position of localised soil compaction determines root and subsequent shoot growth responses. *Journal of Experimental Botany* **52**, 2127-2133.

**Mooi E, Sarstedt M**. 2011. *A Concise Guide to Market Research*. Springer: Heidelberg, 237-284.

**Mooney SJ, Pridmore TP, Helliwell J, Bennett MJ**. 2012. Developing X-ray Computed Tomography to non-invasively image 3-D root systems architecture in soil. *Plant and Soil* **352**, 1-22.

**Moose SP, Mumm RH**. 2008. Molecular plant breeding as the foundation for 21$^{st}$ century crop improvement. *Plant Physiology* **147**, 969-977.

**Moradi A, Conesa H, Robinson B, Lehmann E, Kuehne G, Kaestner A, Oswald S, Schulin R**. 2009. Neutron radiography as a tool for revealing root development in soil: capabilities and limitations. *Plant and Soil* **318**, 243-255.

**Nacry P, Canivenc G, Muller B, Azmi A, Van OH, Rossignol M, Doumas P**. 2005. A role for auxin redistribution in the responses of the root system architecture to phosphate starvation in arabidopsis. *Plant Physiology* **138**, 2061-2074.

**Nadelhoffer KJ, Raich JW**. 1992. Fine root production estimates and belowground carbon allocation in forest ecosystems. *Ecology* **73**, 1139-1147.

**Naeem A, French AP, Wells DM, Pridmore TP**. 2011. High-throughput feature counting and measurement of roots. *Bioinformatics* **27**, 1337-1338.

**Nagel KA, Kastenholz B, Jahnke S, Van Dusschoten D, Aach T, Muhlich M, Truhn D, Scharr H, Terjung S, Walter A, Schurr U**. 2009. Temperature responses of roots: impact on growth, root system architecture and implications for phenotyping. *Functional Plant Biology* **36**, 947-959.

**Nagel KA, Putz A, Gilmer F, Heinz K, Fischbach A, Pfeifer J, Faget M, Blossfeld S, Ernst M, Dimaki C, Kastenholz B, Kleinert A-K, Galinski A, Scharr H, Fiorani F, Schurr U**. 2012. *GROWSCREEN-Rhizo* is a novel phenotyping robot enabling simultaneous measurements of root and shoot growth for plants grown in soil-filled rhizotrons. *Functional Plant Biology* **39**, 891-904.

**Narang RA, Bruene A, Altmann T**. 2000. Analysis of phosphate acquisition efficiency in different arabidopsis accessions. *Plant Physiology* **124**, 1786-1799.

**Neumann G, George TS, Plassard C**. 2009. Strategies and methods for studying the rhizosphere - the plant science toolbox. *Plant and Soil* **321**, 431-456.

**Nielsen KL, Eshel A, Lynch JP**. 2001. The effect of phosphorus availability on the carbon economy of contrasting common bean (*Phaseolus vulgaris* L.) genotypes. *Journal of Experimental Botany* **52**, 329-339.

**Nobel PS, Quero E, Linares H**. 1989. Root versus shoot biomass: responses to water, nitrogen, and phosphorus applications for *Agave lechuguilla*. *Botanical Gazette* **150**, 411 - 416.

**National Research Council (NRC)** 2013. *Frontiers in Massive Data Analysis*. National Research Council, Washington, D.C: The National Academies Press.

**Ober ES, Sharp RE**. 2007. Regulation of root growth responses to water deficit. In: Jenks MA, Hasegawa PM, Jain SM, eds. *Advances in Molecular Breeding Toward Drought and Salt Tolerant Crops*. Springer: Dordrecht, 33-53.

**Oborny B**. 2004. External and internal control in plant development. *Complexity* **9**, 22-28.

**Ortiz-Ribbing LM, Eastburn DM**. 2003. Evaluation of digital image acquisition methods for determining soybean root characteristics. *Crop Management,* doi:10.1094/CM-2003-0702-01-RS, http://www.plantmanagementnetwork.org/pub/cm/research/2003/digital/.

**Osivand M, Azizi P, Kavoosi M, Davatgar N, Razavipour T**. 2009. Increasing phosphorus availability from rock phosphate using organic matter in rice ( *Oryza sativa* L ). *Philippine Agricultural Scientist* **92**, 301-307.

**Osmont KS, Sibout R, Hardtke CS**. 2007. Hidden branches: developments in root system architecture. *Annual Review of Plant Biology* **58**, 93-113.

**O'Toole JC, Bland WL**. 1987. Genetic variation in crop plant root systems. *Advances in Agronomy*, **41,** 91-145.

**Otsu N**. 1979. Threshold selection method from gray-level histograms. *IEEE Transactions on Systems, Man, and Cybernetics* **9**, 62-66.

**Ozturk L, Eker S, Torun B, Cakmak I**. 2005. Variation in phosphorus efficiency among 73 bread and durum wheat genotypes grown in a phosphorus-deficient calcareous soil. *Plant and Soil* **269**, 69-80.

**Pacheco-Villalobos D, Hardtke CS**. 2012. Natural genetic variation of root system architecture from *Arabidopsis* to *Brachypodium*: towards adaptive value. *Philosophical Transactions of The Royal Society B: Biological Sciences* **367**, 1552-1558.

**Page AL, Miller RH, Keeney DR**. 1982. *Methods of Soil Analysis*. Madison: American Society of Agronomy.

**Pagès L, Asseng S, Pellerin S, Diggle A**. 2000. Modelling root system growth and architecture. In: In: Smit AL, Bengough AG, Engels C, van Noordwijk M, Pellerin S, van de Geijn SC, eds. *Root Methods: A Handbook*. Heidelberg: Springer, 113-146.

**Pagès L, Bengough AG**. 1997. Modelling minirhizotron observations to test experimental procedures. *Plant and Soil* **189**, 81-89.

**Pagès L**. 1995. Growth patterns of the lateral roots of young oak (*Quercus robur*) tree seedlings-relationship with apical diameter. *New Phytologist* **130**, 503-509.

**Paine CET, Marthews TR, Vogt DR, Purves D, Rees M, Hector A, Turnbull LA**. 2012. How to fit nonlinear plant growth models and calculate growth rates: an update for ecologists. *Methods in Ecology and Evolution* **3**, 245-256.

**Parentoni SN, Mendes FF, Lauro Guimarães JM** (2012) Breeding for phosphorus use efficiency. *In* Fritsche-Neto R, Borém A (e*ds*.). Plant Breeding for Abiotic Stress Tolerance. Heidelberg. Springer pp 67- 86.

**Paula S, Pausas JG**. 2011. Root traits explain different foraging strategies between resprouting life histories. *Oecologia* **165**, 321-331.

**Peek M, Russek-Cohen E, Wait A, Forseth I**. 2002. Physiological response curve analysis using nonlinear mixed models. *Oecologia* **132**, 175-180.

**Pérez-Harguindeguy N, Díaz S, Garnier E, Lavorel S, Poorter H, Jaureguiberry P, Bret-Harte MS, Cornwell WK, Craine JM, Gurvich DE, Urcelay C, Veneklaas EJ, Reich PB, Poorter L, Wright IJ, Ray P, Enrico L, Pausas JG, de Vos AC, Buchmann N, Funes G, Quétier F, Hodgson JG, Thompson K, Morgan HD, ter Steege H, van der Heijden MGA, Sack L, Blonder B, Poschlod P, Vaieretti MV, Conti G, Staver AC, Aquino S, Cornelissen JHC**. 2013. New handbook for standardised measurement of plant functional traits worldwide. *Australian Journal of Botany* **61**, 167-234.

**Pérez-Torres C-A, López-Bucio J, Cruz-Ramírez A, Ibarra-Laclette E, Dharmasiri S, Estelle M, Herrera-Estrella L**. 2008. Phosphate availability alters lateral root development in arabidopsis by modulating auxin sensitivity via a mechanism involving the TIR1 auxin receptor. *Plant Cell* **20**, 3258-3272.

**Perret JS, Al-Belushi ME, Deadman M**. 2007. Non-destructive visualization and quantification of roots using computed tomography. *Soil Biology and Biochemistry* **39**, 391-399.

**Peter H, Dietrich H, Christoph L.** 2013. Intraspecific variation in root and leaf traits and leaf-root trait linkages in eight aspen demes (*Populus tremula* and *P. tremuloides*). *Frontiers in Plant Science* **4**: 415. doi: 10.3389/fpls.2013.00415.

**Pierret A, Doussan C, Garrigues E, Mc Kirby J**. 2003a. Observing plant roots in their environment: current imaging options and specific contribution of two-dimensional approaches. *Agronomie* **23**, 471-479.

**Pierret A, Gonkhamdee S, Jourdan C, Maeght J-L**. 2013. *IJ_Rhizo*: an open-source software to measure scanned images of root samples. *Plant and Soil* **373**, 531-539.

**Pierret A, Kirby M, Moran C**. 2003b. Simultaneous X-ray imaging of plant root growth and water uptake in thin-slab systems. *Plant and Soil* **255**, 361-373.

**Pilet PE, Ney D.** 1978. Rapid, localized light effect on root growth in maize. *Planta* **144,** 109-110.

**Pinheiro J, Bates D, DebRoy S, Sarkar D, Team. TRC**. 2008. nlme: Linear and Nonlinear Mixed Effects Models. R package version 3.1-89. Vienna: R Foundation for Statistical Computing.

**Pinheiro JC, Bates DM**. 2000. *Mixed-Effects Models in S and S-PLUS*. New York: Springer.

**Poon K, Hamarneh C, Abugharbieh R**. 2007. Live-vessel: extending Livewire for simultaneous extraction of optimal medial and boundary paths in vascular images. *Medical Image Computing and Computer-Assisted Intervention- MICCAI 2007, Pt 2, Proceedings* **4792**, 444-451.

**Posada D, Buckley TR**. 2004. Model selection and model averaging in phylogenetics: advantages of akaike information criterion and bayesian approaches over likelihood ratio tests. *Systematic Biology* **53**, 793-808.

**Pound MP, French AP, Atkinson JA, Wells DM, Bennett MJ, Pridmore T**. 2013. *RootNav*: navigating images of complex root architectures. *Plant Physiology* **162**, 1802-1814.

**Qi XJ, Qi J, Wu YJ**. 2007. *RootLM*: a simple color image analysis program for length measurement of primary roots in *Arabidopsis. Plant Root* **1**, 10-16, doi:10.3117/plantroot.1.10.

**Rafiq N, Maqsood ZT, Parveen Z**. 2006. Lead and cadmium in wheat grain. *Bulletin of Environmental Contamination and Toxicology* **76**, 1044-1052.

**Raghothama KG**. 1999. Phosphate acquisition. *Annual Review of Plant Physiology and Plant Molecular Biology* **50**, 665-693.

**Rahman L, Aspinall D, Paleg L**. 1975. Quantitative studies on root development. III. Further observations on growth in the seedling phase. *Functional Plant Biology* **2**, 425-434.

**Ramaekers L, Remans R, Rao IM, Blair MW, Vanderleyden J**. 2010. Strategies for improving phosphorus acquisition efficiency of crop plants. *Field Crops Research* **117**, 169-176.

**Raven JA**. 2008. Phosphorus and the future. In: White PJ, Hammond JP, eds. *The Ecophysiology of Plant-Phosphorus Interactions*. New York: Springer, 271-279.

**R Core Team**. 2008. *R:* A Language and Environment for Statistical Computing. Vienna, Austria: R Foundation for Statistical Computing.

**Redjala T, Zelko I, Sterckeman T, Legue V, Lux A**. 2011. Relationship between root structure and root cadmium uptake in maize. *Environmental and Experimental Botany* **71**, 241-248.

**Rellán-Álvarez R, Yee M-C, Yu G, Dinneny JR**. 2013. Growth and luminescence observatory for roots (*GLO-Roots*): a platform for high-resolution analysis of root structure and physiology in soil. Proceedings of XVII International Plant Nutrition Colloquium, 19-22 August 2013 Istanbul - Turkey, 13-14.

**Rewald B, Ephrath JE**. 2013. Minirhizotron techniques. In: Eshel A, Beeckman T, eds. *Plant Roots: The Hidden Half*. New York: CRC Press, 42.1-42.15.

**Richardson AE, Hocking PJ, Simpson RJ, George TS**. 2009. Plant mechanisms to optimise access to soil phosphorus. *Crop and Pasture Science* **60**, 124-143.

**Richardson AE, Lynch JP, Ryan PR, Delhaize E, Smith FA, Smith SE, Harvey PR, Ryan MH, Veneklaas EJ, Lambers H, Oberson A, Culvenor RA, Simpson RJ**. 2011. Plant and microbial strategies to improve the phosphorus efficiency of agriculture. *Plant and Soil* **349**, 121-156.

**Richner W, Kiel C, Stamp P**. 1997. Is seedling root morphology predictive of seasonal accumulation of shoot dry matter in maize? *Crop Science* **37**, 1237-1241.

**Ridler TW, Calvard S**. 1978. Picture thresholding using an iterative selection method. *IEEE Transactions onSystems, Man, and Cybernetics,* **8**, 630-632.

**Ristova D, Rosas U, Krouk G, Ruffel S, Birnbaum KD, Coruzzi GM**. 2013. *RootScape*: a landmark-based system for rapid screening of root architecture in arabidopsis. *Plant Physiology* **161**, 1086-1096.

**Roberts T, McKenna S, Du C-J, Wuyts N, Valentine T, Bengough AG**. 2010. Estimating the motion of plant root cells from in vivo confocal laser scanning microscopy images. *Machine Vision and Applications* **21**, 921-939.

**Robertson BM, Waines JG, Gill BS**. 1979. Genetic variability for seedling root numbers in wild and domesticated wheats. *Crop Science* **19**, 843-847.

**Robinson DL**. 1987. Estimation and use of variance-components. *Statistician* **36**, 3-14.

**Rodgers HL, Day FP, Atkinson R**. 2004. Root dynamics in restored and naturally regenerated Atlantic white cedar wetlands. *Restoration Ecology* **12**, 401-411.

**Roy RN, Finck A, Blair GJ, Tandon HLS**. 2006. *Plant Nutrition for Food Security: A Guide to Integrated Nutrient Management*. Food and Agriculture Organization of the United Nations, Fertilizer and Plant Nutrition Bulletin 16, Rome, Italy.

**Ruts T, Matsubara S, Walter A**. 2013. Synchronous high-resolution phenotyping of leaf and root growth in *Nicotiana tabacum* over 24-h periods with *GROWMAP*-plant. *Plant Methods* **9**, 2, doi:10.1186/1746-4811-9-2.

**Ryser P**. 1996. The importance of tissue density for growth and life span of leaves and roots: a comparison of five ecologically contrasting grasses. *Functional Ecology* **10**, 717-723.

**Sadhu D, Bhaduri PN**. 1984. Variable traits of root and shoot of wheat under different cultural conditions and ages. *Journal of Agronomy and Crop Science* **153**, 216-224.

**Sanchez-Calderon L, Lopez-Bucio J, Chacon-Lopez A, Cruz-Ramirez A, Nieto-Jacobo F, Dubrovsky JG, Herrera-Estrella L**. 2005. Phosphate starvation induces a determinate developmental program in the roots of *Arabidopsis thaliana*. *Plant Cell and Physiology* **46**, 174-184.

**Schachtman DP, Reid RJ, Ayling SM**. 1998. Phosphorus uptake by plants: from soil to cell. *Plant Physiology* **116**, 447-453.

**Seiler GJ**. 2008. Root growth of interspecific sunflower seedlings derived from wild perennial sunflower species. *Canadian Journal of Plant Science* **88**, 705-712.

**Sekulska-Nalewajko J, Goclawski J**. 2009. Segmentation and geometry identification of white roots in two-dimensional scanner images. *5th International Conference on Perspective Technologies and Methods in MEMS Design, 2009. MEMSTECH 2009,* 73-76.

**Sena G, Frentz Z, Birnbaum KD, Leibler S**. 2011. Quantitation of cellular dynamics in growing arabidopsis roots with light sheet microscopy. *PLoS ONE **6**: e21303.doi:10.1371/journal.pone.0021303*

**Sezgin M, Sankur B**. 2004. Survey over image thresholding techniques and quantitative performance evaluation. *Journal of Electronic Imaging* **13**, 146-168.

**Shane MW, Lambers H**. 2005. Cluster roots: a curiosity in context. *Plant and Soil* **274**, 101-125.

**Sharp RE, Davies WJ**. 1985. Root-growth and water-uptake by maize plants in drying soil. *Journal of Experimental Botany* **36**, 1441-1456.

**Sharp RE, Silk WK, Hsiao TC**. 1988. Growth of the maize primary root at low water potentials: I. Spatial distribution of expansive growth. *Plant Physiology* **87**, 50-57.

**Sharpe J, Ahlgren U, Perry P, Hill B, Ross A, Hecksher-Sorensen J, Baldock R, Davidson D**. 2002. Optical Projection Tomography as a tool for 3D microscopy and gene expression studies. *Science* **296**, 541-545.

**Sharpe J**. 2004. Optical Projection Tomography. *Annual Review of Biomedical Engineering* **6**, 209-228.

**Sharpley AN, Daniel T, Sims T, Lemunyon J, Stevens R, Parry R**. 2003. Agricultural phosphorus and eutrophication, 2nd ed. In: U.S. Department of Agriculture, Agricultural Research Service, ARS-149, 44.

**Shendure J, Ji HL**. 2008. Next-generation DNA sequencing. *Nature Biotechnology* **26**, 1135-1145.

**Shenoy VV, Kalagudi GM**. 2005. Enhancing plant phosphorus use efficiency for sustainable cropping. *Biotechnology Advances* **23**, 501-513.

**Shi L, Shi T, Broadley MR, White PJ, Long Y, Meng J, Xu F, Hammond JP**. 2013a. High-throughput root phenotyping screens identify genetic loci associated with root architectural traits in *Brassica napus* under contrasting phosphate availabilities. *Annals of Botany* **112,** 381-389.

**Shi T, Li R, Zhao Z, Ding G, Long Y, Meng J, Xu F, Shi L**. 2013b. QTL for yield traits and their association with functional genes in response to phosphorus deficiency in *Brassica napus*. *Plos One* **8**, e54559. doi:10.1371/journal.pone.0054559.

**Shi TX, Zhao DY, Li DX, Wang N, Meng JL, Xu FS, Shi L.** 2012. *Brassica napus* root mutants insensitive to exogenous cytokinin show phosphorus efficiency. *Plant and Soil* **358**, 57-70.

**Shipley B, Keddy P, Moore D, Lemky K**. 1989. Regeneration and establishment strategies of emergent macrophytes. *Journal of Ecology* **77**, 1093-1110.

**Siddique KHM, Belford RK, Tennant D**. 1990. Root:shoot ratios of old and modern, tall and semi-dwarf wheats in a mediterranean environment. *Plant and Soil* **121**, 89-98.

**Silverman B**. 1996. *Density Estimation for Statistics and Data Analysis*. London: Chapman & Hall.

**Šmilauerová M, Šmilauer P**. 2007. What youngsters say about adults: seedling roots reflect clonal traits of adult plants. *Journal of Ecology* **95**, 406-413.

**Smit AL, Bengough AG, Engels C, van Noordwijk M, Pellerin S, van de Geijn SC**. eds. 2000. *Root Methods: A Handbook*. Heidelberg: Springer.

**Smith CL**. 2008. Basic Confocal Microscopy. *Current Protocols in Molecular Biology* **81S**, 14.11.11-14.11.18, doi: 10.1002/0471142727.mb1411s81.

**Smith S, De Smet I**. 2012. Root system architecture: insights from *Arabidopsis* and cereal crops. *Philosophical Transactions of The Royal Society B: Biological Sciences* **367**, 1441-1452.

**Smucker AJM**. 1993. Soil and environmental modifications of root dynamics measurement. *Annual Review of Phytopathology* **31**, 191-218.

**Song K, Osborn TC, Williams PH**. 1990. *Brassica* taxonomy based on nuclear restriction fragment length polymorphisms (RFLPs): 3. Genome relationships in *Brassica* and related genera and the origin of *B. oleracea* and *B. rapa* (syn. *campestris*). *Theoretical and Applied Genetics* **79**, 497-506.

**Song KM, Osborn TC, Williams PH**. 1988. *Brassica* taxonomy based on nuclear restriction fragment length polymorphisms (RFLPs). Preliminary analysis of subspecies within *B. rapa* (syn *campestris*) and *B. oleracea. Theoretical and Applied Genetics* **76**, 593-600.

**Stefanelli D, Fridman Y, Perry RL**. 2009. *DigiRoot*: new software for root studies. *European Journal of Horticultural Science* **74**, 169-174.

**Stephenson P, Baker D, Girin T, Perez A, Amoah S, King GJ, Ostergaard L**. 2010. A rich TILLING resource for studying gene function in *Brassica rapa*. *BMC Plant Biology* **10**:62, doi:10.1186/1471-2229-10-62

**Stingaciu L, Schulz H, Pohlmeier A, Behnke S, Zilken H, Javaux M, Vereecken H**. 2013. *In situ* root system architecture extraction from Magnetic Resonance Imaging for water uptake modeling. *Vadose Zone Journal* **12**, 1-9.

**Subramanian R**. 2012. *High Throughput Automated Seedling Phenotyping System*. PhD thesis, University of Wisconsin - Madison, USA.

**Sun J, Meyer W, Cross J, Huang B**. 2013. Growth and physiological traits of canopy and root systems associated with drought resistance in tall fescue. *Crop Science* **53**, 575-584.

**Suriyagoda LD, Ryan MH, Renton M, Lambers H**. 2012. Adaptive shoot and root responses collectively enhance growth at optimum temperature and limited phosphorus supply of three herbaceous legume species. *Annals of Botany* **110**, 959-968.

**Suwabe K, Morgan C, Bancroft I**. 2008. Integration of *Brassica* A genome genetic linkage map between *Brassica napus* and *B. rapa*. *Genome* **51**, 169-176.

**Suwabe K, Tsukazaki H, Iketani H, Hatakeyama K, Kondo M, Fujimura M, Nunome T, Fukuoka H, Hirai M, Matsumoto S**. 2006. Simple Sequence Repeat-based comparative genomics between *Brassica rapa* and *Arabidopsis thaliana:* The genetic origin of clubroot resistance. *Genetics* **173**, 309-319.

**Syers JK, Johnston AE, Curtin D**. 2008. *Efficiency of Soil and Fertilizer Phosphorus Use: Reconciling Changing Concepts of Soil Phosphorus Behaviour with Agronomic Information*. Food and Agriculture Organization of the United Nations, Fertilizer and Plant Nutrition Bulletin *18*, Rome, Italy.

**Tabachnick BG, Fidell LS**. 1996. *Using Multivariate Statistics (3rd ed.).* New York: Harper Collins College Publishers.

**Tan ZX, Lal R, Wiebe KD**. 2005. Global soil nutrient depletion and yield reduction. *Journal of Sustainable Agriculture* **26**, 123-146.

**Taylor HM, Upchurch DR, McMichael BL**. 1990. Applications and limitations of rhizotrons and minirhizotrons for root studies. *Plant and Soil* **129**, 29-35.

**Teng W, Deng Y, Chen XP, Xu XF, Chen RY, Lv Y, Zhao YY, Zhao XQ, He X, Li B, Tong YP, Zhang FS, Li ZS**. 2013. Characterization of root response to phosphorus supply from morphology to gene analysis in field-grown wheat. *Journal of Experimental Botany* **64**, 1403-1411.

**Tennant D**. 1975. A test of a modified line intersect method of estimating root length. *Journal of Ecology* **63**, 995-1001.

**Tennant D**. 1976. Root growth of wheat. I early patterns of multiplication and extension of wheat roots including effects of levels of nitrogen, phosphorus and potassium. *Australian Journal of Agricultural Research* **27**, 183-196.

**Thaler P, Pagès L**. 1996. Root apical diameter and root elongation rate of rubber seedlings (*Hevea brasiliensis*) show parallel responses to photoassimilate availability. *Physiologia Plantarum* **97**, 365-371.

**Thorndike R**. 1953. Who belongs in the family? *Psychometrika* **18**, 267-276.

**Tinker PB, Nye PH**. 2000. *Solute Movement in the Rhizosphere*. Oxford: Oxford University Press.

**Torrion JA, Setiyono TD, Cassman KG, Ferguson RB, Irmak S, J.E. S**. 2012. Soybean root development relative to vegetative and reproductive phenology. *Agronomy Journal* **104**, 1702-1709.

**Trachsel S, Kaeppler SM, Brown KM, Lynch JP**. 2011. Shovelomics: high throughput phenotyping of maize (*Zea mays* L.) root architecture in the field. *Plant and Soil* **341**, 75-87.

**Tracy SR, Roberts JA, Black CR, McNeill A, Davidson R, Mooney SJ**. 2010. The X-factor: visualizing undisturbed root architecture in soils using X-ray computed tomography. *Journal of Experimental Botany* **61**, 311-313.

**Tsaftaris SA, Noutsos C**. 2009. Plant phenotyping with low cost digital cameras and image analytics. In: Allan R, Forstner U, Salomons W, eds. *Information Technologies in Environmental Engineering, Environmental Science and Engineering*. Springer: Heidelberg, 238-251.

**Tsai WH**. 1985. Moment-preserving thresolding: a new approach. *Computer Vision, Graphics, and Image Processing* **29**, 377-393.

**NIFA-NSF- USDA**. 2011. Phenomics : genotype to phenotype. Phenomics workshop report of the National Institute of Food and Agriculture and the National Science Foundation of the United States Department of Agrivulture, (NIFA-NSF-USDA Phenomics Workshop Report).

http://www.nsf.gov/bio/pubs/reports/phenomics_workshop_report.pdf. Accessed on 02-09-2013.

**van der Weele CM, Jiang HS, Palaniappan KK, Ivanov VB, Palaniappan K, Baskin TI**. 2003. A new algorithm for computational image analysis of deformable motion at high spatial and temporal resolution applied to root growth. Roughly uniform elongation in the meristem and also, after an abrupt acceleration, in the elongation zone. *Plant Physiology* **133**, 423-423.

**van der Weele CM, Spollen WG, Sharp RE, Baskin TI**. 2000. Growth of *Arabidopsis thaliana* seedlings under water deficit studied by control of water potential in nutrient-agar media. *Journal of Experimental Botany* **51**, 1555-1562.

**Van Veldhoven PP, Mannaerts GP**. 1987. Inorganic and organic phosphate measurements in the nanomolar range. *Analytical Biochemistry* **161**, 45-48.

**Vance CP, Uhde-Stone C, Allan DL**. 2003. Phosphorus acquisition and use: critical adaptations by plants for securing a nonrenewable resource. *New Phytologist* **157**, 423-447.

**Vance CP**. 2001. Symbiotic nitrogen fixation and phosphorus acquisition. Plant nutrition in a world of declining renewable resources. *Plant Physiology* **127**, 390-397.

**Volkmar KM**. 1993. A Comparison of minirhizotron techniques for estimating root length density in soils of different bulk densities. *Plant and Soil* **157**, 239-245.

**Wahbi A, Gregory PJ**. 1995. Growth and development of young roots of barley (*Hordeum vulgare* L.) genotypes. *Annals of Botany* **75**, 533-539.

**Wahl S, Ryser P, Edwards PJ**. 2001. Phenotypic plasticity of grass root anatomy in response to light intensity and nutrient supply. *Annals of Botany* **88**, 1071-1078.

**Wahl S, Ryser P**. 2000. Root tissue structure is linked to ecological strategies of grasses. *New Phytologist* **148**, 459-471.

**Waisel Y**. 1996. Aeroponics: a tool for root research. In: Waisel Y, Eshel A, Kafkafi U, eds. *Plant Roots: The Hidden Half*. New York: Mercel Dekker, 239-245.

**Waisel Y**. 2002. Aeroponics: a tool for root research under minimal environmental restrictions. In: Waisel Y, Eshel A, Kafkafi U, eds. *Plant Roots: The Hidden Half*. New York: Marcel Dekker, 323-331.

**Walter A, Schurr U**. 2005. Dynamics of leaf and root growth: endogenous control versus environmental impact. *Annals of Botany* **95**, 891-900.

**Walter A, Spies H, Terjung S, Küsters R, Kirchgeßner N, Schurr U**. 2002. Spatio-temporal dynamics of expansion growth in roots: automatic quantification of diurnal course and temperature response by digital image sequence processing. *Journal of Experimental Botany* **53**, 689-698.

**Walter A, Studer B, Kölliker R**. 2012. Advanced phenotyping offers opportunities for improved breeding of forage and turf species. *Annals of Botany* **110,** 1271-1279.

**Wang X, Wang H, Wang J, Sun R, Wu J, Liu S, Bai Y, Mun J-H, Bancroft I, Cheng F, Huang S, Li X, Hua W, Wang J, Wang X, Freeling M, Pires JC, Paterson AH, Chalhoub B, Wang B, Hayward A, Sharpe AG, Park B-S, Weisshaar B, Liu B, Li B, Liu B, Tong C, Song C, Duran C, Peng C, Geng C, Koh C, Lin C, Edwards D, Mu D, Shen D, Soumpourou E, Li F, Fraser F, Conant G, Lassalle G, King GJ, Bonnema G, Tang H, Wang H, Belcram H, Zhou H, Hirakawa H, Abe H, Guo H, Wang H, Jin H, Parkin IAP, Batley J, Kim J-S, Just J, Li J, Xu J, Deng J, Kim JA, Li J, Yu J, Meng J, Wang J, Min J, Poulain J, Wang J, Hatakeyama K, Wu K, Wang L, Fang L, Trick M, Links MG, Zhao M, Jin M, Ramchiary N, Drou N, Berkman PJ, Cai Q, Huang Q, Li R, Tabata S, Cheng S, Zhang S, Zhang S, Huang S, Sato S, Sun S, Kwon S-J, Choi S-R, Lee T-H, Fan W, Zhao X, Tan X, Xu X, Wang Y, Qiu Y, Yin Y, Li Y, Du Y, Liao Y, Lim Y, Narusaka Y, Wang Y,**

**Wang Z, Li Z, Wang Z, Xiong Z, Zhang Z**. 2011. The genome of the mesopolyploid crop species *Brassica rapa*. *Nature Genetics* **43**, 1035-1039.

**Wang XR, Yan XL, Liao H**. 2010. Genetic improvement for phosphorus efficiency in soybean: a radical approach. *Annals of Botany* **106**, 215-222.

**Watt M, Evans JR**. 2003. Phosphorus acquisition from soil by white lupin (*Lupinus albus* L.) and soybean (*Glycine max* L.), species with contrasting root development. *Plant and Soil* **248**, 271-283.

**Watt M, Moosavi S, Cunningham S, Kirkegaard JA, Rebetzke GJ, Richards RA**. 2013. A rapid, controlled-environment root seedling screen for wheat correlates well with rooting depths at young vegetative, but not reproductive, stages in the field. *Annals of Botany* **112**, 447-455.

**Weaver JE, Bruner WE**. 1927. *Root Development of Vegetable Crops*. New York: McGraw-Hill.

**Weaver JE**. 1919. *The Ecological Relations of Roots*. Washington: Carnegie Institute Washington Publication.

**Weaver JE**. 1920. *Root Development in the Grassland Formation*. Washington: Canegie Institute Washington Publication.

**Weaver JE**. 1925. Investigations on the root habits of plants. *American Journal of Botany* **12**, 502-509.

**Weaver JE**. 1926. *Root Development of Field Crops*. New York: The McGraw-Hill Book Company, INC.

**Webb DT. 1982**. Light induced callus formation and root growth inhibition of *Dioon edule Lindl*. Seedlings in Sterile Culture. *Zeitschrift für Pflanzenphysiologie*, **106**, 223-228.

**Wells DM, French AP, Naeem A, Ishaq O, Traini R, Hijazi H, Bennett MJ, Pridmore TP**. 2012. Recovering the dynamics of root growth and development using novel image acquisition and analysis methods. *Philosophical Transactions of the Royal Society B-Biological Sciences* **367**, 1517-1524.

**White JW, Andrade-Sanchez P, Gore MA, Bronson KF, Coffelt TA, Conley MM, Feldmann KA, French AN, Heun JT, Hunsaker DJ, Jenks MA, Kimball BA, Roth RL, Strand RJ, Thorp KR, Wall GW, Wang GY**. 2012. Field-based phenomics for plant genetics research. *Field Crops Research* **133**, 101-112.

**White PJ, Bengough AG, Bingham IJ, George TS, Karley AJ, Valentine TA**. 2009. Induced mutations affecting root architecture and mineral acquisition in barley. In: *Proceedings of the joint FAO/IAEA programme, international symposium on induced mutations in plants. Paper IAEA-CN.* pp. 167-244*,* International Atomic Energy Agency: Vienna, Austria.

**White PJ, Broadley MR, Greenwood DJ, Hammond JP**. 2005. *Proceedings of the International Fertiliser Society 568: Genetic Modifications to Improve Phosphorus Acquisition by Roots*. International Fertiliser Society : York, UK.

**White PJ, Brown PH**. 2010. Plant nutrition for sustainable development and global health. *Annals of Botany* **105**, 1073-1080.

**White PJ, George TS, Dupuy LX, Karley AJ, Valentine TA, Wiesel L, Wishart J**. 2013a. Root traits for infertile soils. *Frontiers in Plant Science* **4**, 193. doi: 10.3389/fpls.2013.00193

**White PJ, George TS, Gregory PJ, Bengough AG, Hallett PD, McKenzie BM**. 2013b. Matching roots to their environment. *Annals of Botany* **112,** 207-222.

**White PJ, Hammond JP, King GJ, Bowen HC, Hayden RM, Meacham MC, Spracklen WP, Broadley MR**. 2010. Genetic analysis of potassium use efficiency in *Brassica oleracea*. *Annals of Botany* **105**, 1199-1210.

**White PJ, Hammond JP**. 2008a. Diagnosing phosphorus deficiency in crop plants. In: White PJ, Hammond JP, eds. *The Ecophysiology of Plant-Phosphorus Interactions*, Springer: New York, 225-246.

**White PJ, Hammond JP**. 2008b. Phosphorus nutrition of terrestrial plants. In: White PJ, Hammond JP, eds. *The Ecophysiology of Plant-Phosphorus Interactions*. Springer: New York, 51-81.

**White PJ, Veneklaas EJ**. 2012. Nature and nurture: the importance of seed phosphorus content. *Plant and Soil* **357**, 1-8.

**Whitman DW, Agrawal AA.** 2009. What is phenotypic plasticity and why is it important? Whitman DW, Ananthakrishnan TN (Eds.), Phenotypic Plasticity of Insects, Science Publishers: London, 1- 63.

**Whitmore AP, Whalley WR**. 2009. Physical effects of soil drying on roots and crop growth. *Journal of Experimental Botany* **60**, 2845-2857.

**Willatt ST, Struss RG**. 1979. Germination and early growth of plants studied using neutron radiography. *Annals of Botany* **43**, 415-422.

**Williams CH, David DJ**. 1973. The effect of superphosphate on the cadmium content of soils and plants. *Soil Research* **11**, 43-56.

**Williamson LC, Ribrioux SPCP, Fitter AH, Leyser HMO**. 2001. Phosphate availability regulates root system architecture in *Arabidopsis*. *Plant Physiology* **126**, 875-882.

**Wojciechowski T, Gooding MJ, Ramsay L, Gregory PJ**. 2009. The effects of dwarfing genes on seedling root growth of wheat. *Journal of Experimental Botany* **60**, 2565-2573.

**Woodfield DR, Caradus JR**. 1990. Estimates of heritability for, and relationships between, root and shoot characters of white clover II. Regression of progeny on mid-parent. *Euphytica* **46**, 211-215.

**Xie YJ, Yu D**. 2003. The significance of lateral roots in phosphorus (P) acquisition of water hyacinth (*Eichhornia crassipes*). *Aquatic Botany* **75**, 311-321.

**Xu XD, Xie QG, McClung CR**. 2010. Robust circadian rhythms of gene expression in *Brassica rapa* tissue culture. *Plant Physiology* **153**, 841-850.

**Xuecheng Z, Xiwen L**. 2009. Advances in non-destructive measurement and 3D visualization methods for plant root based on machine vision. *2nd International Conference on Biomedical Engineering and Informatics, 2009. BMEI '09,* 1-5.

**Yang XJ, Finnegan PM**. 2010. Regulation of phosphate starvation responses in higher plants. *Annals of Botany* **105**, 513-526.

**Yang Z, Downie H, Rozbicki E, Dupuy LX, Macdonald MP**. 2013. Light Sheet Tomography (LST) for *in situ* imaging of plant roots. *Optics Express* **21**, 16239-16247.

**Yazdanbakhsh N, Fisahn J**. 2009. High throughput phenotyping of root growth dynamics, lateral root formation, root architecture and root hair development enabled by *PlaRoM*. *Functional Plant Biology* **36**, 938-946.

**Yazdanbakhsh N, Fisahn J**. 2012. High-throughput phenotyping of root growth dynamics. In: Normanly J, ed. *High-Throughput Phenotyping in Plants*. Vol. 918, New York: Humana Press, 21-40.

**Yorke JS, Sagar GR**. 1970. Distribution of secondary root growth potential in the root system of *Pisum sativum*. *Canadian Journal of Botany* **48**, 699-704.

**Yu Q, Kuo J, Tang C**. 2001. Using confocal laser scanning microscopy to measure apoplastic pH change in roots of *Lupinus angustifolius* L. in response to high pH. *Annals of Botany* **87**, 47-52.

**Zack GW, Rogers WE, Latt SA**. 1977. Automatic measurement of sister chromatid exchange frequency. *Journal of Histochemistry & Cytochemistry* **25**, 741-753.

**Zeng G, Birchfield ST, Wells CE**. 2008. Automatic discrimination of fine roots in minirhizotron images. *New Phytologist* **177**, 549-557.

**Zeng G, Birchfield ST, Wells CE**. 2010. Rapid automated detection of roots in minirhizotron images. *Machine Vision and Applications* **21**, 309-317.

**Zhang BG, De Reffye P, Liu L, Kang MZ, B.G. L**. 2003. Analysis and modeling of the root system architecture of winter wheat seedling. *International Symposium on Plant Growth Modeling, Simulation, Visualization and their Applications*. PMA'03, Beijing China, 321-328. http://hal.inria.fr/docs/00/12/25/03/PDF/PMA03_321_328_ZBG.pdf. Accessed on 27-09-2012.

**Zhang D, Cheng H, Geng L, Kan G, Cui S, Meng Q, Gai J, Yu D**. 2009. Detection of quantitative trait loci for phosphorus deficiency tolerance at soybean seedling stage. *Euphytica* **167**, 313-322.

**Zhang H, Fritts JE, Goldman SA**. 2008. Image segmentation evaluation: A survey of unsupervised methods. *Computer Vision and Image Understanding* **110**, 260-280.

**Zhang HM, Jennings A, Barlow PW, Forde BG**. 1999. Dual pathways for regulation of root branching by nitrate. *Proceedings of the National Academy of Sciences of the United States of America* **96**, 6529-6534.

**Zhang TY, Suen CY**. 1984. A fast parallel algorithm for thinning digital patterns. *Communications of the ACM* **27**, 236-239.

**Zhao J, Fu JB, Liao H, He Y, Nian H, Hu YM, Qiu LJ, Dong YS, Yan XL**. 2004. Characterization of root architecture in an applied core collection for phosphorus efficiency of soybean germplasm. *Chinese Science Bulletin* **49**, 1611-1620.

**Zhu J, Kaeppler SM, Lynch JP**. 2005a. Mapping of QTLs for lateral root branching and length in maize (*Zea mays* L.) under differential phosphorus supply. *Theoretical and Applied Genetics* **111**, 688-695.

**Zhu J, Kaeppler SM, Lynch JP**. 2005b. Topsoil foraging and phosphorus acquisition efficiency in maize (*Zea mays* L.). *Functional Plant Biology* **32**, 749-762.

**Zhu J, Lynch JP**. 2004. The contribution of lateral rooting to phosphorus acquisition efficiency in maize (*Zea mays* L.) seedlings. *Functional Plant Biology* **31**, 949-958.

**Zhu JM, Ingram PA, Benfey PN, Elich T**. 2011. From lab to field, new approaches to phenotyping root system architecture. *Current Opinion in Plant Biology* **14**, 310-317.

**Zobel RW, Alloush GA, Belesky DP**. 2006. Differential root morphology response to no versus high phosphorus, in three hydroponically grown forage chicory cultivars. *Environmental and Experimental Botany* **57**, 201-208.

**Zobel RW, Waisel Y**. 2010. A plant root system architectural taxonomy: a framework for root nomenclature. *Plant Biosystems* **144**, 507-512.

## APPENDICES

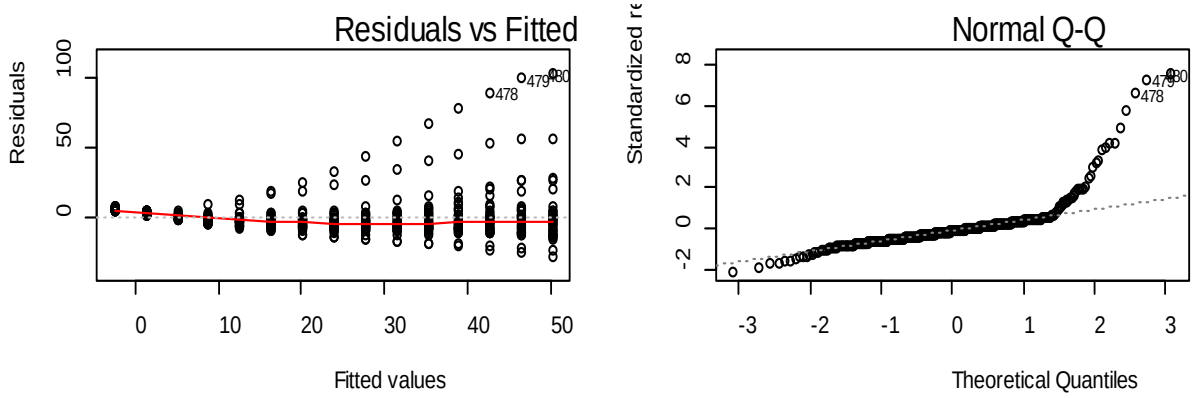


***Appendix1:*** *Diagnostic plots for the simple linear regression model fitted on total root length vs DAS for 16* Brassica rapa *genotypes*

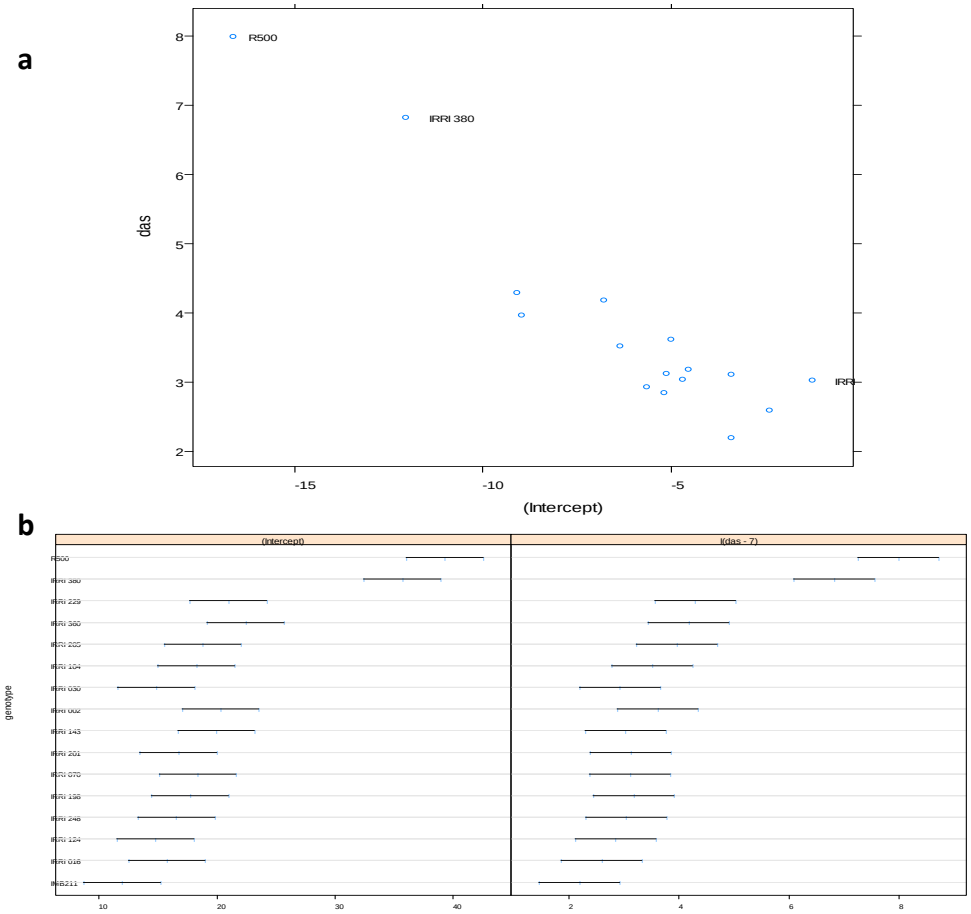


***Appendix 2:*** *Pairs plot relationship between intercept and slope fitted by genotype for non-centred total root length data; (b) Ninety-five percent confidence intervals on intercept and slope for each genotype to the centred total root length data.*

***Appendix 3:*** *Linear model structural adequacy assessments based on a hierarchical likelihood ratio test*

| Model | df | AIC | BIC | LogLik | LR test (P value) |
|---|---|---|---|---|---|
| Total root length | | | | | |
| 1 | 11 | 158.3237 | 204.1433 | -68.1618 | |
| 2 | 7 | 880.7606 | 909.9185 | -433.3803 | *<0.0001* |
| 3 | 7 | 260.7611 | 289.9191 | -123.3806 | |
| 4 | 22 | 203.4312 | 295.0704 | -79.7156 3 | *<0.0001* |
| Primary root length | | | | | |
| 1 | 11 | 1256.469 | 1302.289 | -617.2346 | |
| 2 | 7 | 1728.736 | 1757.893 | -857.3678 | *<0.0001* |
| 3 | 7 | 1449.513 | 1478.671 | -717.7567 | |
| 4 | 22 | 1346.115 | 1437.754 | -651.0574 | *<0.0001* |

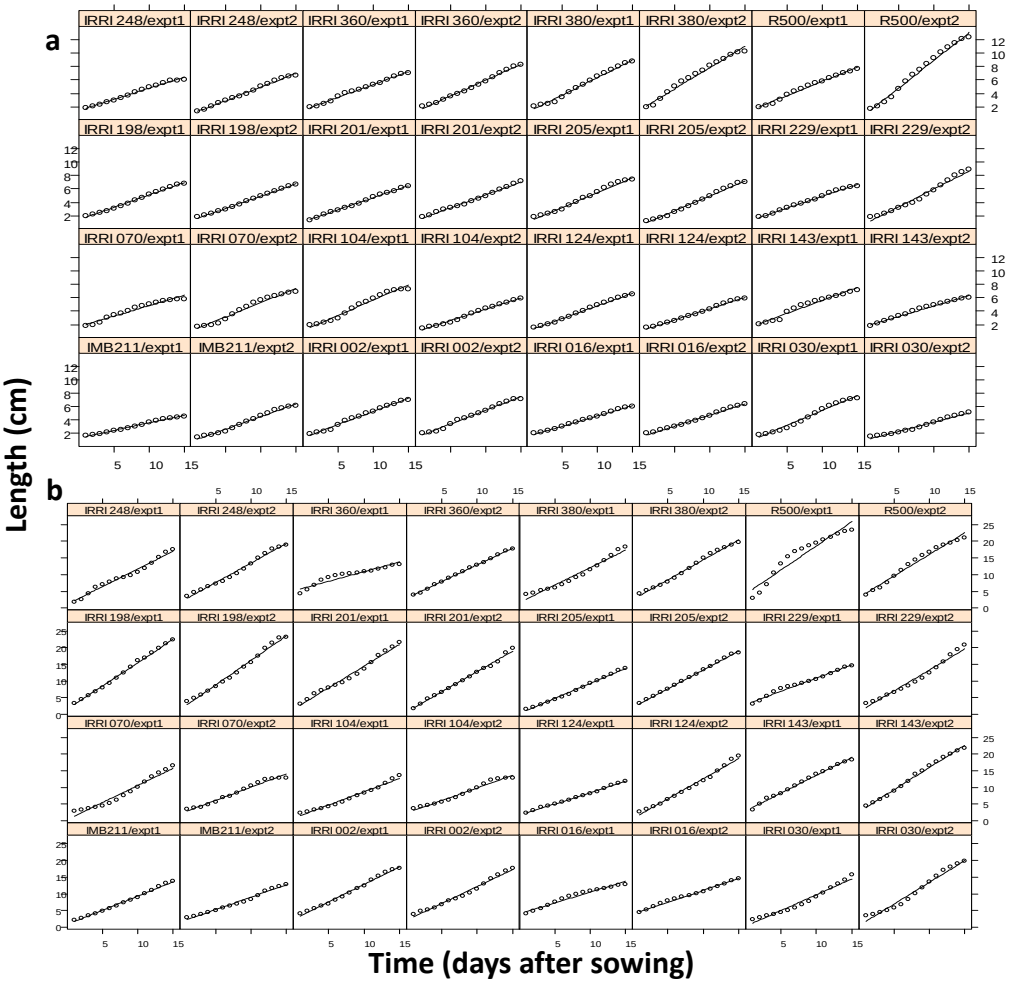


***Appendix 4:*** *Measured (circles) and predicted (lines) values from linear mixed-effects model for (a) total root length (data was square rooted ) and (b) primary root length of 15 DAS Brassica rapa seedlings of the parents and 14 recombinant inbred lines of the cross of IMB211 X R500 across two independent experimental runs.*

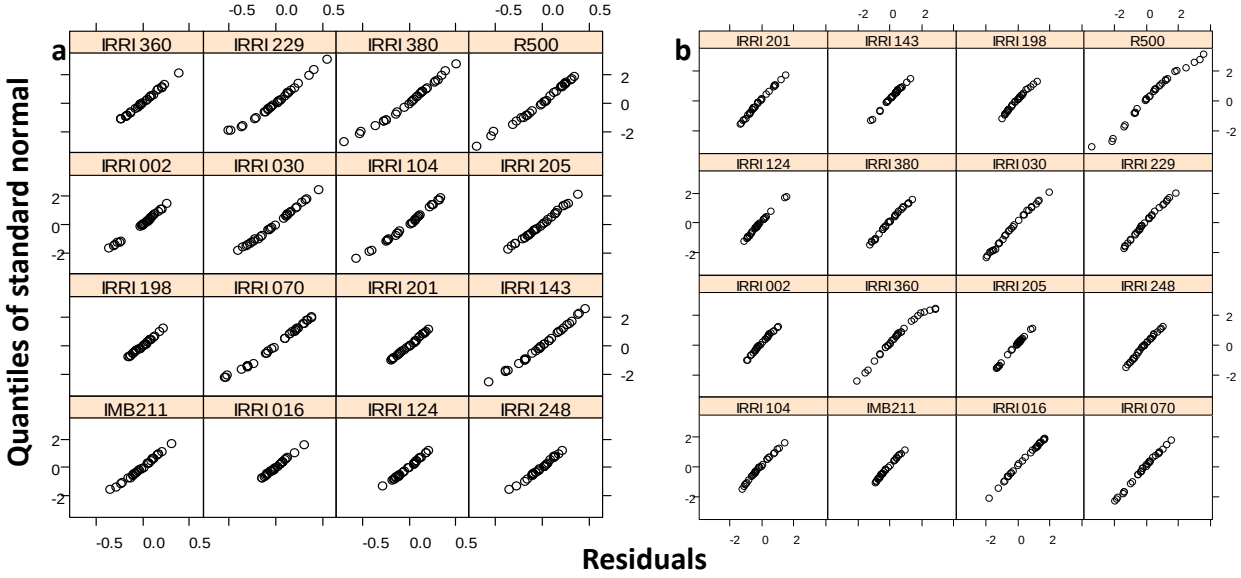


***Appendix 5:*** *Normal plot of residuals by genotype from the linear model for (a) total root length and (b) primary root length*

***Appendix 6:*** *Parameters estimates for the final model for Total and Primary root length*

| Genotype | Run # | Fixed Intercept | Random intercept | Fixed Slope | Random Slope | Fixed Intercept | Random intercept | Fixed Slope | Random Slope |
|---|---|---|---|---|---|---|---|---|---|
| | | Total Root Length | | | | Primary Root Length | | | |
| IMB211 | 1 | 0.0505 | 1.3105 | -0.2548 | 0.2302 | 0.1238 | 0.8040 | -0.0232 | 0.8523 |
| IMB211 | 2 | 0.0505 | 1.0526 | -0.2548 | 0.3277 | 0.1238 | 1.5068 | -0.0232 | 0.6270 |
| IRRI 002 | 1 | 0.0505 | 1.3914 | -0.2548 | 0.3897 | 0.1238 | 2.3329 | -0.0232 | 1.0460 |
| IRRI 002 | 2 | 0.0505 | 1.6097 | -0.2548 | 0.3586 | 0.1238 | 2.0537 | -0.0232 | 0.8911 |
| IRRI 016 | 1 | 0.0505 | 1.5622 | -0.2548 | 0.3063 | 0.1238 | 3.9904 | -0.0232 | 0.6516 |
| IRRI 016 | 2 | 0.0505 | 1.6990 | -0.2548 | 0.2802 | 0.1238 | 3.9922 | -0.0232 | 0.5805 |
| IRRI 030 | 1 | 0.0505 | 0.9545 | -0.2548 | 0.4429 | 0.1238 | 0.2422 | -0.0232 | 0.9478 |
| IRRI 030 | 2 | 0.0505 | 1.2435 | -0.2548 | 0.2238 | 0.1238 | 0.4483 | -0.0232 | 1.1785 |
| IRRI 070 | 1 | 0.0505 | 1.6667 | -0.2548 | 0.3153 | 0.1238 | 0.3208 | -0.0232 | 1.0273 |
| IRRI 070 | 2 | 0.0505 | 1.2782 | -0.2548 | 0.3785 | 0.1238 | 2.1500 | -0.0232 | 0.6713 |
| IRRI 104 | 1 | 0.0505 | 1.1393 | -0.2548 | 0.4528 | 0.1238 | 0.7207 | -0.0232 | 0.7966 |
| IRRI 104 | 2 | 0.0505 | 1.1464 | -0.2548 | 0.3122 | 0.1238 | 2.2881 | -0.0232 | 0.6336 |
| IRRI 124 | 1 | 0.0505 | 1.0294 | -0.2548 | 0.3801 | 0.1238 | 1.5821 | -0.0232 | 0.6875 |
| IRRI 124 | 2 | 0.0505 | 1.2491 | -0.2548 | 0.2893 | 0.1238 | 0.6332 | -0.0232 | 1.0770 |
| IRRI 143 | 1 | 0.0505 | 1.7235 | -0.2548 | 0.3887 | 0.1238 | 2.9464 | -0.0232 | 1.0694 |
| IRRI 143 | 2 | 0.0505 | 1.9600 | -0.2548 | 0.2617 | 0.1238 | 2.6795 | -0.0232 | 1.2093 |
| IRRI 198 | 1 | 0.0505 | 1.3752 | -0.2548 | 0.3716 | 0.1238 | 1.4445 | -0.0232 | 1.4053 |
| IRRI 198 | 2 | 0.0505 | 1.5331 | -0.2548 | 0.3160 | 0.1238 | 1.4041 | -0.0232 | 1.3526 |
| IRRI 201 | 1 | 0.0505 | 1.1068 | -0.2548 | 0.3588 | 0.1238 | 1.4679 | -0.0232 | 1.2982 |
| IRRI 201 | 2 | 0.0505 | 1.5010 | -0.2548 | 0.3335 | 0.1238 | 0.6898 | -0.0232 | 1.0938 |
| IRRI 205 | 1 | 0.0505 | 1.0386 | -0.2548 | 0.4460 | 0.1238 | 0.2627 | -0.0232 | 0.9023 |
| IRRI 205 | 2 | 0.0505 | 0.7635 | -0.2548 | 0.3970 | 0.1238 | 2.0595 | -0.0232 | 1.0031 |
| IRRI 229 | 1 | 0.0505 | 1.3879 | -0.2548 | 0.3579 | 0.1238 | 2.9506 | -0.0232 | 0.7948 |
| IRRI 229 | 2 | 0.0505 | 0.9647 | -0.2548 | 0.4808 | 0.1238 | 0.8131 | -0.0232 | 1.1300 |
| IRRI 248 | 1 | 0.0505 | 1.4282 | -0.2548 | 0.3334 | 0.1238 | 1.0797 | -0.0232 | 1.0623 |
| IRRI 248 | 2 | 0.0505 | 1.1593 | -0.2548 | 0.3549 | 0.1238 | 1.7259 | -0.0232 | 1.0517 |
| IRRI 360 | 1 | 0.0505 | 1.5004 | -0.2548 | 0.3820 | 0.1238 | 5.1101 | -0.0232 | 0.5776 |
| IRRI 360 | 2 | 0.0505 | 1.4735 | -0.2548 | 0.4265 | 0.1238 | 2.9043 | -0.0232 | 0.8795 |
| IRRI 380 | 1 | 0.0505 | 1.1791 | -0.2548 | 0.5212 | 0.1238 | 1.6013 | -0.0232 | 1.0508 |
| IRRI 380 | 2 | 0.0505 | 1.7804 | -0.2548 | 0.5835 | 0.1238 | 2.4937 | -0.0232 | 1.0705 |
| R500 | 1 | 0.0505 | 1.5795 | -0.2548 | 0.4231 | 0.1238 | 4.1206 | -0.0232 | 1.4503 |
| R500 | 2 | 0.0505 | 0.9592 | -0.2548 | 0.7758 | 0.1238 | 3.1344 | -0.0232 | 1.1707 |

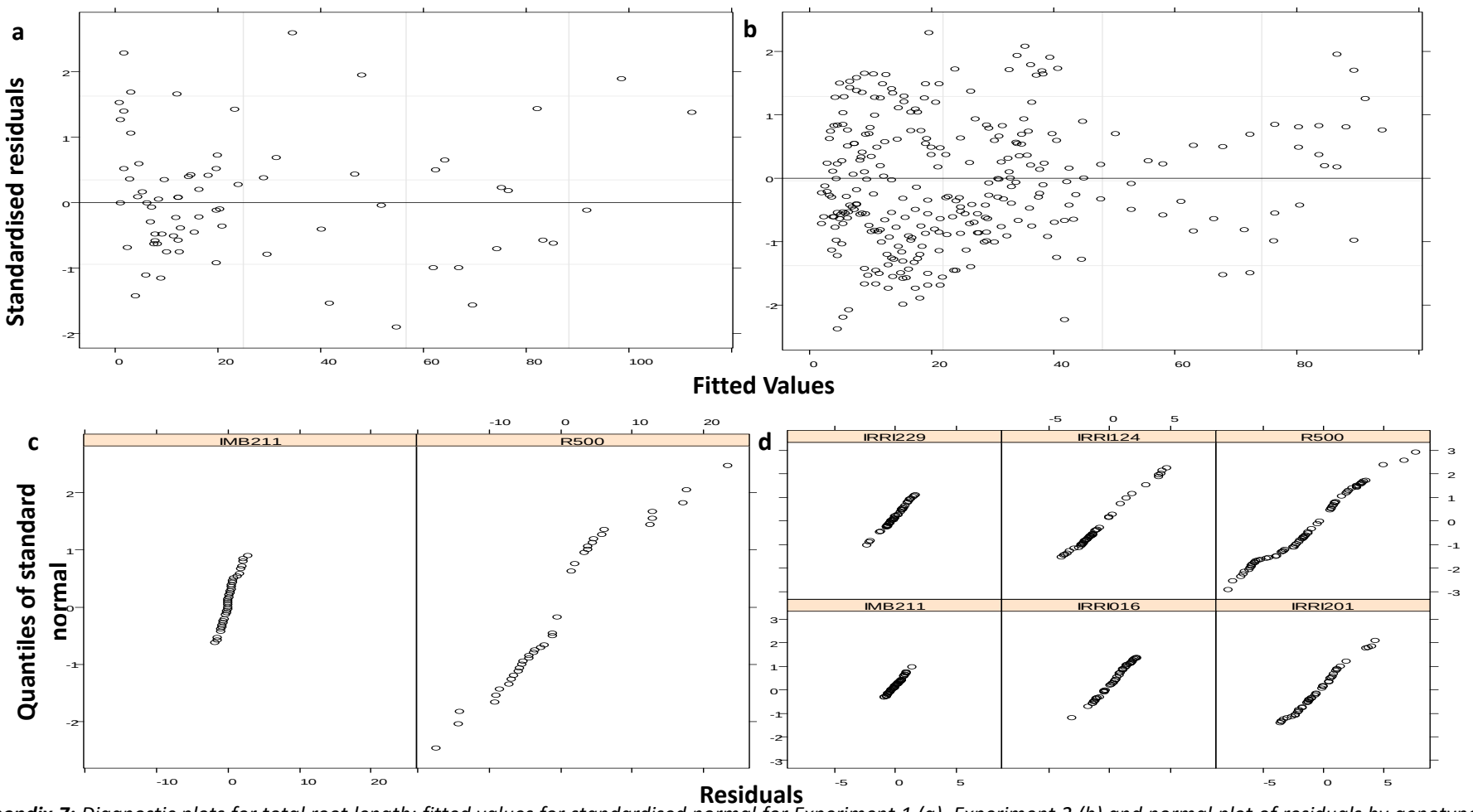


***Appendix 7:*** *Diagnostic plots for total root length: fitted values for standardised normal for Experiment 1 (a), Experiment 2 (b) and normal plot of residuals by genotype for Experiment 1 (c) and Experiment 2 (d)*

**Appendix 8 – Research article**

*Journal of Experimental Botany*, Vol. 65, No. 8, pp. 2039–2048, 2014
doi:10.1093/jxb/eru048 Advance Access publication 6 March, 2014
This paper is available online free of all access charges (see http://jxb.oxfordjournals.org/open_access.html for further details)

Journal of Experimental Botany
www.jxb.oxfordjournals.org

RESEARCH PAPER

# A scanner system for high-resolution quantification of variation in root growth dynamics of *Brassica rapa* genotypes

**Michael O. Adu[1,2], Antoine Chatot[1,*], Lea Wiesel[1], Malcolm J. Bennett[2], Martin R. Broadley[2], Philip J. White[1] and Lionel X. Dupuy[1,†]**

[1] Department of Ecological Sciences, The James Hutton Institute, Invergowrie, Dundee, DD2 5DA, Scotland, UK
[2] Plant and Crop Sciences Division, School of Biosciences, University of Nottingham, Sutton Bonington Campus, Leicestershire, LE12 5RD, UK

* Current address: Daphnestraße 32, 81925 München, Germany
† To whom correspondence should be addressed. E-mail: lionel.dupuy@hutton.ac.uk

Received 2 September 2013; Revised 22 November 2013; Accepted 20 January 2014



## Abstract

**The potential exists to breed for root system architectures that optimize resource acquisition. However, this requires the ability to screen root system development quantitatively, with high resolution, in as natural an environment as possible, with high throughput. This paper describes the construction of a low-cost, high-resolution root phenotyping platform, requiring no sophisticated equipment and adaptable to most laboratory and glasshouse environments, and its application to quantify environmental and temporal variation in root traits between genotypes of *Brassica rapa* L. Plants were supplied with a complete nutrient solution through the wick of a germination paper. Images of root systems were acquired without manual intervention, over extended periods, using multiple scanners controlled by customized software. Mixed-effects models were used to describe the sources of variation in root traits contributing to root system architecture estimated from digital images. It was calculated that between one and 43 replicates would be required to detect a significant difference (95% CI 50% difference between traits). Broad-sense heritability was highest for shoot biomass traits (>0.60), intermediate (0.25–0.60) for the length and diameter of primary roots and lateral root branching density on the primary root, and lower (<0.25) for other root traits. Models demonstrate that root traits show temporal variations of various types. The phenotyping platform described here can be used to quantify environmental and temporal variation in traits contributing to root system architecture in *B. rapa* and can be extended to screen the large populations required for breeding for efficient resource acquisition.**

**Key words:** Architecture, high-resolution, high throughput, model, nitrogen, phenotyping, phosphorus, root.

## Introduction

Breeding crops with better root system architectures (RSAs) for the acquisition of water and mineral elements and, thereby, greater resource-use efficiency, requires the ability to screen root system development quantitatively, in high resolution, nondestructively, in as natural an environment as possible, on a large number of genotypes in a short time (de Dorlodot *et al.*, 2007; Walter *et al.*, 2007; Zhu *et al.*, 2011; Fiorani and Schurr, 2013). Traditional techniques used in the field include soil coring (Box and Ramsuer, 1993), trenching (Vepraskas and Hoyt, 1988), and pinboard excavation (Oliveira *et al.*, 2000), followed by washing substrate from the roots and quantification of root length and diameters. These techniques are slow and laborious, destructive, prone to inaccuracy (because small roots are lost during washing), and ill suited to screening large genetic populations (Smit *et al.*, 2000; Trachsel *et al.*, 2010).

To overcome some of the limitations of phenotyping root systems in the field, researchers have developed methods to phenotype the root systems of plants growing in artificial substrates under controlled conditions in the laboratory or glasshouse. Various translucent, artificial media have been employed, including water (Drew and Saker, 1975; Tuberosa *et al.*, 2002), aeroponics (Waisel, 2002; Eshel and Grunzweig, 2013), gels (Bengough *et al.*, 2004; Shi *et al.*, 2013), and transparent soils (Downie *et al.*, 2012). The use of transparent artificial substrates has many advantages. First, the homogeneity of the media is controlled, and therefore it is possible to minimize the inherent variability of the root traits observed. Imaging is facilitated in clear media, and the application of automated algorithms for the extraction of root features is, therefore, possible (French *et al.*, 2009). The light spectrum can be exploited to improve image quality and reduce the effects of high light doses on root growth (Yazdanbakhsh and Fisahn, 2009). Using dyes and fluorescence imaging, it is also possible to characterize functional traits, such as apoplastic pH (Bibikova *et al.*, 1998). Biospeckle laser imaging, a more recent technique, provides new opportunities to screen for functional traits without the use of a dye (Ribeiro *et al.*, 2014). Finally, transparent substrates allow 3D descriptions of RSAs using a range of techniques such as laser scanning (Fang *et al.*, 2009), optical (Iyer-Pascuzzi *et al.*, 2010; Clark *et al.*, 2011), or light sheet tomography (Yang *et al.*, 2013).

Although these techniques facilitate nondestructive analyses of RSAs, root traits of plants grown in these substrates are not always well correlated with those of plants grown in the field (Wojciechowski *et al.*, 2009; Schmidt *et al.*, 2012). Another common technique is to observe roots growing at the interface between soil and a transparent barrier. This includes observations from belowground rhizotrons (Bland *et al.*, 1990) or minirhizotrons inserted into the soil (Zeng *et al.*, 2008; Dupuy *et al.*, 2010) and observations of plants growing in rhizotubes or rhizoboxes (Nagel *et al.*, 2012; Dresbøll *et al.*, 2013). However, these techniques provide only partial information about RSAs and can affect plant growth by physical interactions (Wenzel *et al.*, 2001).

Recently, radiation-based techniques, such as nuclear magnetic resonance imaging (Rascher *et al.*, 2011) and neutron and X-ray computed tomography (Oswald *et al.*, 2008; Flavel *et al.*, 2012; Mairhofer *et al.*, 2013), have become popular because they allow noninvasive measurements of RSAs in soils. However, instrumentation costs are generally high and the acquisition of data is often too slow to enable dynamic measurements of root system development or the screening of large genetic populations (Iyer-Pascuzzi *et al.*, 2010; Smith and De Smet, 2012; Fiorani and Schurr, 2013).

This paper describes a low-cost, high-resolution root phenotyping platform that requires no sophisticated equipment and is adaptable to most laboratory and glasshouse environments. It is based on a traditional pouch-and-wick system (Liao *et al.*, 2001; Hund *et al.*, 2009) in which roots are grown on the surface of germination paper and imaged in high resolution using flatbed scanners. Images were acquired without manual intervention, over extended periods, using multiple scanners controlled by customized software. The platform was used to screen RSAs of up to 48 plants simultaneously and has the potential to be expanded. The platform was used to estimate the number of replicates required to detect differences in traits contributing to RSAs between genotypes of *Brassica rapa* L. and to quantify genotypic, environmental, and temporal variation in these traits.

## Materials and methods

### *Genetic material*

The variability of root architectural traits was studied in a diploid inbred line of *B. rapa* L. subsp. *trilocularis* cv. R-o-18 (Stephenson *et al.*, 2010). Two parents (cv. IMB211 and cv. R500) and 14 recombinant inbred lines (RILs) of the BraIRRI mapping population were used to study variations in root traits caused by genetic factors. The BraIRRI population is an immortal mapping population consisting of 160 RILs derived from the cross between IMB211 and R500 (Iniguez-Luy *et al.*, 2009). Genotype IMB211 is a highly inbred rapid cycling Chinese cabbage *B. rapa* subsp. *pekinensis* and R500 is a highly inbred annual yellow sarson *B. rapa* subsp. *trilocularis* (Iniguez-Luy *et al.*, 2009; Xu *et al.*, 2010).

### *Growth conditions*

Plants were grown using a pouch-and-wick system (Liao *et al.*, 2001; Hund *et al.*, 2009). Seeds were sown on 12 × 12 cm germination papers (Anchor Paper, Saint Paul, MN, USA) sprayed with deionized water and placed vertically in a Sanyo MIR153 incubator at 20 °C. Three days after sowing (DAS), seedlings of similar size with radicles 2–3 cm in length were transferred to large sheets of germination paper (30 × 42 cm) attached to flatbed scanners using 30 × 20 cm clear-Perspex plates (Fig. 1a). The germination paper surrounding each radicle was cut and transferred with the seedling to minimize disturbance during this process. Two seedlings were placed on each large sheet of germination paper. Scanners were fixed in near-vertical positions 5 cm above 20 l of nutrient solution contained in opaque polyvinyl plastic tanks, each supplying six scanners (Fig. 1b). Approximately 10 cm of the germination paper was submerged in the nutrient solution.

Nutrient solution was prepared with deionized water and contained 2 mM $Ca(NO_3)_2$, 2 mM $NH_4NO_3$, 0.75 mM $MgSO_4$, 0.5 mM KOH, 0.25 mM $KH_2PO_4$, 0.1 mM FeNaEDTA, 30 mM $H_3BO_3$, 25 mM $CaCl_2$, 10 mM $MnSO_4$, 3 mM $CuSO_4$, 1 mM $ZnSO_4$, and 0.5 mM $Na_2MoO_4$ (Broadley *et al.*, 2003). The nutrient solution was adjusted to pH 6 at the start of the experiment using $H_2SO_4$. Plants were grown under a 16/8 h day/night cycle. Temperature in the growth room was kept constant at 15 °C. Light intensity during the day was maintained at 100 µmol $m^{-2}$ $s^{-1}$ at plant height. Relative humidity was approximately 60%. Seedlings were removed from scanners at 18 DAS. Roots were excised from the shoot base and freshweight (FW) of roots and shoots was recorded. Shoot and root samples were dried at 60 °C for 72 h and dry weight (DW) was determined. The single genotype experiment on R-o-18 was performed in five independent runs, each run comprising eight scanners with two plants per scanner. Trait data was collected on 72 plants. The multiple-genotype experiment on the 16 BraIRRI lines was performed in two independent runs, each run comprising two consecutive assays of a subset of eight genotypes grown in four banks of six scanners with two plants per scanner. Trait data was collected on 190 plants.

### *Time-lapse imaging of roots*

Images were taken daily from 3 to 18 DAS using flatbed scanners. Scanners were chosen for this purpose because their resolution is high compared to standard cameras. Thus, fine roots and root hairs have the potential to be resolved. In this study, 24 A4 CanoScan

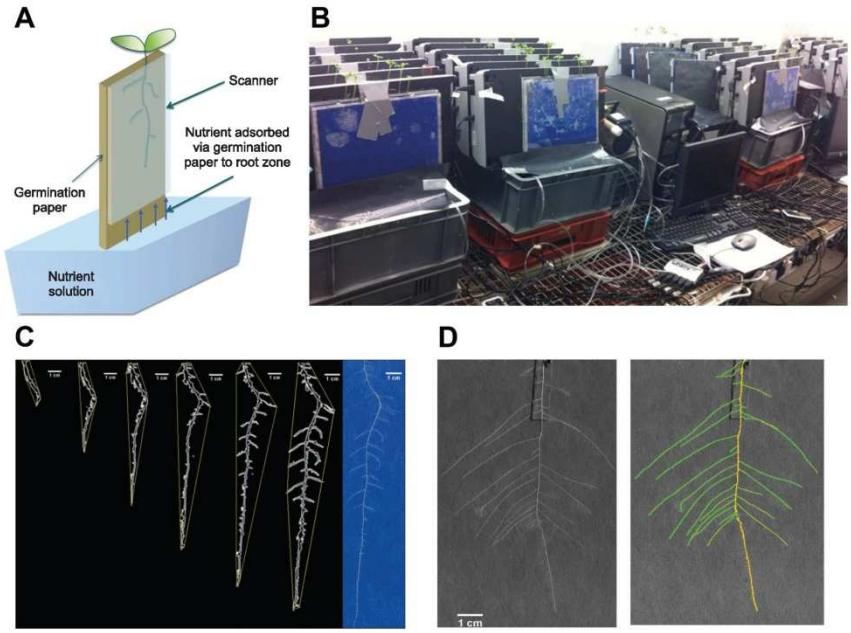


**Fig. 1.** (A) Schematic representation of the pouch-and-wick system used to grow plants in the phenotyping platform. Roots grew on the surface of germination paper held between a clear-Perspex plate and the glass window of a scanner. Scanners were fixed in near-vertical positions 5 cm above 20 l of nutrient solution contained in opaque polyvinyl plastic tanks each supplying six scanners. Approximately 10 cm of the germination paper was submerged in the nutrient solution. (B) The phenotyping platform comprising 24 scanners assembled in four banks of six scanners. (C) The features of a root system, including the convex hull, at successive timepoints obtained using customized ImageJ macros, including the root system at the last timepoint. (D) The features of a root system at a specific timepoint obtained using the SmartRoot plugin for ImageJ.

5600F scanners (Canon UK, Reigate, UK) were assembled in four banks of six scanners (Fig. 1b). This allowed the root systems of 48 seedlings to be imaged simultaneously. The frequency of image acquisition, scanning resolution, and file format was controlled by three computers using in-house software (ArchiScan). ArchiScan was programmed in Python and employs the TWAIN module (http://twainmodule.sourceforge.net/) for communicating between computers and scanners. The program is distributed under the GPL2 open source license and can be downloaded from the ArchiRoot website (http://www.archiroot.org.uk). ArchiScan is generic software and can be used with any scanner provided a TWAIN driver is available.

### *Image segmentation and extraction of root features*

Features of a root system at specific timepoints were determined using ImageJ (http://rsbweb.nih.gov/ij/), using either in-house macros that can be downloaded from the ArchiRoot website (Fig. 1c) or the SmartRoot plugin (Fig. 1d; http://www.uclouvain.be/en-smartroot). Image analysis was carried out on greyscale images obtained from the red channel of the colour images. Median and Gaussian filters were applied to remove noise resulting from, for example, condensation on the surface of scanners or differences in the texture of the germination paper. Variations in pixel intensity over longer distances than the root diameter resulting from, for example, nonuniform moisture content of the germination paper were removed by subtracting the mean background pixel intensity of neighbouring pixels from the pixel intensity of the original image. Macros implemented: (1) the moment-preserving threshold algorithm of (Tsai, 1985), which was used for segmentation of the restored image; (2) an edge-tracing algorithm to define the boundary (perimeter) of root tissues; (3) an algorithm to remove objects external to the root system from the image; and (4) algorithms to estimate global traits of the root system (total root length, total root cross-sectional area, total root perimeter, convex hull of the root system) on 2D images (Fig. 1c). SmartRoot was used to produce a skeleton of interconnected individual roots that defines RSAs (Lobet *et al.*, 2011). Throughout the text, root traits are referred to as 'static' if the measure is obtained at a single timepoint, such as at the end of an experiment, or 'dynamic' if the measure integrates multiple timepoints during an experiment. Root traits are termed 'global' when derived from an entire root system or 'local' when the measurement refers only to a portion of the root system.

### *Statistical analysis*

The experiment with a single genotype (*B. rapa* subsp. *trilocularis* cv. R-o-18) was used to calculate the number of replicates (R) that would be required to detect a significant difference between two populations with identical standard deviations in a trait using a two-sided 95% confidence interval (CI) t-test if the trait means differed by 50% (Supplementary Data Equation S1 available at *JXB* online; Eng, 2003).

The sources of variation in static root traits in the single-genotype experiment were determined using a mixed-effects model with experimental run and scanner considered as random factors (Supplementary Data Equation S2). The sources of variation in static root traits in the multiple-genotype experiment were determined using a mixed-effects model with experimental run, scanner,

and genotype considered as random factors (Supplementary Data Equation S3). The sources of variation in dynamic root traits were determined using mixed-effects models with genotype and DAS considered as random factors. Logistic growth functions were used to model the increase in total root length and primary root length with time (Supplementary Data Equation S4). The growth rate of a lateral root was expressed as the quotient of the lateral root length divided by the length of time after its emergence from the primary root. A quadratic function was used to model the growth rate of lateral roots (Supplementary Data Equation S6).

Statistical analyses of static root traits were performed using GenStat release 14.1 (VSN International, Oxford, UK). Statistical analyses of all mixed-effects models were performed using R software and the nlme library (Pinheiro and Bates, 2000; R Development Core Team, 2012; Pinheiro *et al.*, 2013).

## Results

### *A new platform for high-resolution quantification of root architectural development*

Plants grew vigorously for up to 15 days in the pouch-and-wick system and showed no symptoms of mineral deficiencies when provided with an appropriate nutrient solution through the wick. Images of roots were acquired daily with no manual intervention. The custom-written ArchiScan software was used to control the acquisition of images by multiple scanners and computers. Using the customized macros, it was possible to measure global RSA traits from these images and detailed architectural parameters of root systems at the end of experiments were extracted using SmartRoot (Lobet *et al.*, 2011). Total root length estimated using the custom-written macros was highly correlated with total root length estimated using SmartRoot ($R^2$=0.77, $n$=20; data not shown). However, the macros generally underestimated total root length, probably because they did not detect extremely fine root features.

### *Sources of variation in static root traits of a single* B. rapa *genotype*

The root system of the genotype studied in detail, *B. rapa* L. subsp. *trilocularis* cv. R-o-18, consisted of a single primary root and several first-order lateral roots which emerged from the primary root. The emergence of second-order laterals was rarely observed and these roots were therefore not included in any analyses. Coefficients of variation (CVs) for root traits ranged from 5.8 for lateral root insertion angle to 83.2 for lateral root length. Most of the variation in all the traits examined, except for lateral root insertion angle and lateral root length, could be attributed to vagaries in experimental conditions (i.e. run and scanner). Using Supplementary Data Equation S1, it can be calculated that between one and 43 replicates, depending upon the trait, would be required to detect a significant difference using a two-sided 95% CI t-test if trait means differed by 50% (Table 1).

### *Genotypic variation in root traits*

A significant effect of genotype ($P$<0.001) was observed for all root traits measured on parents and RILs of the BraIRRI population (Table 2). The parental genotypes exhibited extreme values for many biomass and root length traits. The R500 genotype had the largest values for the majority of root and shoot traits assayed. However, although the IMB211 genotype had the smallest values for total lateral root length and total root length, it did not have the lowest values for all root and shoot traits, providing some evidence for transgressive segregation. Neither parental genotype had the most extreme values for lateral branching density, length or diameter of lateral roots, or lateral root insertion angle.

There were strong positive correlations among biomass traits among the 190 plants studied (Fig. 2). Total root length

**Table 1.** *Sources of variation in shoot and root traits assayed at 18 DAS among 72 surviving seedlings of* Brassica rapa *L. subsp.* trilocularis *cv. R-o-18 grown for 15 days in the phenotyping platform*

The experiment was performed in five runs employing eight scanners per run and two plants per scanner. mean, mean trait value; CV, coefficient of variation (n=72 seedlings); $\sigma_a^2$, estimated variance associated with the effect of the run; $\sigma_b^2$ estimated variance associated with the effect of the scanner; $\sigma^2$, estimated variance associated with the residual error; R, number of replicates required to detect a significant difference in a measured trait between two populations with identical standard deviations in the trait using a two-sided 95% confidence interval t-test.

| Trait | Trait means, coefficients of variation, and standard deviations of effects | | | | | Source of variation (%) | | | R |
|---|---|---|---|---|---|---|---|---|---|
| | Mean | CV (%) | $\sigma_a^2$ | $\sigma_b^2$ | $\sigma^2$ | Run | Scanner | Residual | |
| Shoot fresh weight (mg) | 116.6 | 23.1 | 27.22 | 18.36 | 19.22 | 42.0 | 28.3 | 29.7 | 3.3 |
| Shoot dry weight (mg) | 9.1 | 19.9 | 0.68 | 1.20 | 1.32 | 21.4 | 37.5 | 41.1 | 2.4 |
| Root fresh weight (mg) | 35.4 | 40.7 | 4.17 | 10.91 | 9.31 | 17.1 | 44.7 | 38.2 | 10.2 |
| Root dry weight (mg) | 3.2 | 33.5 | 0.62 | 0.79 | 0.70 | 29.3 | 37.6 | 33.1 | 6.9 |
| Primary root length (cm) | 12.0 | 31.4 | 3.05 | 1.83 | 3.17 | 37.9 | 22.7 | 39.4 | 6.1 |
| Primary root diameter (mm) | 0.49 | 9.7 | 0.070 | 0.000 | 0.047 | 60.1 | 0.0 | 39.9 | 0.6 |
| Lateral branching density ($cm^{-1}$) | 2.61 | 36.8 | 0.451 | 0.613 | 0.713 | 25.4 | 34.5 | 40.1 | 8.3 |
| Lateral root length (cm) | 2.90 | 83.2 | 1.96 | 0.00 | 2.33 | 45.7 | 0.0 | 54.3 | 42.5 |
| Lateral root diameter (mm) | 0.38 | 7.6 | 0.080 | 0.010 | 0.026 | 68.6 | 8.9 | 22.5 | 0.4 |
| Lateral root insertion angle (°) | 77.3 | 5.8 | 1.58 | 1.45 | 4.15 | 22.0 | 20.2 | 57.8 | 0.2 |
| Total lateral root length (cm) | 101.3 | 40.3 | 29.7 | 27.6 | 29.9 | 34.1 | 31.7 | 34.3 | 10.0 |
| Total root length (cm) | 112.0 | 37.1 | 29.5 | 28.4 | 30.2 | 33.5 | 32.2 | 34.3 | 8.5 |

**Table 2.** *Genotypic variation in shoot and root traits assayed at 18 DAS among the parents (IMB211, R500) and 14 recombinant inbred lines of the* Brassica rapa *BraIRRI mapping population grown for 15 days in the phenotyping platform*

A significant effect of genotype was observed for all traits measured (P<0.001, n=190 plants). LSD=least significant difference.

| | IMB 211 | R 500 | IRRI 002 | IRRI 016 | IRRI 030 | IRRI 070 | IRRI 104 | IRRI 124 | IRRI 143 | IRRI 198 | IRRI 201 | IRRI 205 | IRRI 229 | IRRI 248 | IRRI 360 | IRRI 380 | LSD |
|---|---|---|---|---|---|---|---|---|---|---|---|---|---|---|---|---|---|
| Shoot fresh weight (mg) | 29.4 | 104.1 | 55.9 | 56.3 | 21.3 | 41.6 | 44.4 | 47.1 | 60.3 | 74.0 | 62.6 | 34.8 | 36.9 | 40.9 | 64.8 | 75.3 | 9.63 |
| Shoot dry weight (mg) | 2.0 | 5.8 | 3.1 | 3.2 | 1.4 | 2.6 | 2.8 | 2.7 | 3.3 | 3.7 | 3.2 | 2.1 | 2.4 | 2.6 | 4.1 | 4.7 | 0.63 |
| Root fresh weight (mg) | 8.2 | 22.6 | 13.0 | 12.2 | 6.7 | 9.2 | 12.2 | 11.5 | 10.0 | 13.2 | 12.3 | 9.3 | 10.7 | 10.2 | 16.1 | 21.9 | 4.05 |
| Root dry weight (mg) | 0.8 | 2.0 | 2.4 | 1.0 | 0.6 | 1.4 | 0.9 | 1.1 | 1.0 | 1.1 | 1.0 | 0.8 | 0.9 | 0.8 | 1.4 | 1.9 | 0.8 |
| Primary root length (cm) | 13.1 | 20.4 | 17.7 | 11.9 | 17.2 | 14.3 | 13.4 | 15.9 | 18.5 | 19.5 | 18.8 | 16.3 | 15.1 | 16.4 | 18.2 | 17.9 | 2.04 |
| Primary root diameter (mm) | 0.36 | 0.41 | 0.37 | 0.40 | 0.33 | 0.36 | 0.38 | 0.35 | 0.35 | 0.35 | 0.36 | 0.35 | 0.34 | 0.35 | 0.38 | 0.38 | 0.003 |
| Lateral branching density ($cm^{-1}$) | 2.65 | 3.15 | 3.23 | 2.46 | 1.68 | 3.43 | 3.04 | 2.71 | 2.79 | 2.12 | 2.25 | 2.79 | 2.83 | 2.59 | 3.07 | 3.81 | 0.540 |
| Lateral root length (cm) | 1.33 | 1.35 | 1.03 | 1.14 | 2.02 | 1.37 | 1.78 | 1.10 | 0.69 | 0.77 | 1.03 | 1.34 | 1.74 | 0.76 | 1.07 | 1.74 | 0.487 |
| Lateral root diameter (mm) | 0.26 | 0.26 | 0.33 | 0.31 | 0.23 | 0.24 | 0.24 | 0.27 | 0.28 | 0.29 | 0.26 | 0.23 | 0.24 | 0.25 | 0.31 | 0.27 | 0.036 |
| Lateral root insertion angle (°) | 70.1 | 70.8 | 72.9 | 63.3 | 75.1 | 66.8 | 65.9 | 65.6 | 73.4 | 62.8 | 63.8 | 68.8 | 65.1 | 65.2 | 63.3 | 71.0 | 4.12 |
| Total lateral root length (cm) | 15.7 | 74.7 | 30.0 | 22.5 | 18.5 | 24.7 | 33.9 | 23.8 | 22.3 | 22.8 | 24.4 | 32.4 | 39.1 | 19.4 | 31.8 | 57.7 | 13.01 |
| Total root length (cm) | 28.8 | 95.0 | 47.7 | 34.4 | 35.8 | 38.9 | 47.3 | 39.7 | 40.7 | 42.2 | 43.2 | 48.4 | 54.2 | 36.3 | 52.1 | 75.6 | 13.47 |

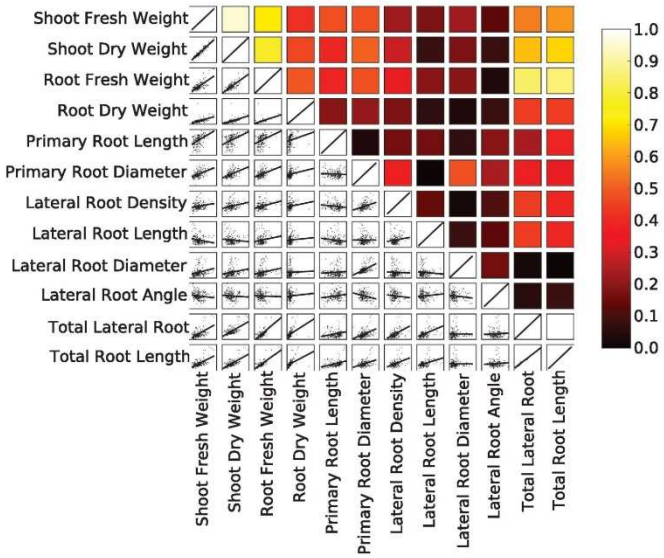


**Fig. 2.** Correlations between plant traits. The plots below the diagonal show linear regressions (red lines) of the data (black points) for different traits. The correlation coefficients for these linear regressions are indicated by the colour of the boxes above the diagonal. The scale of colour codes indicates the correlation coefficients between two traits.

was strongly positively correlated with shoot and root biomass, total lateral root length, lateral root branching density on the primary root, and lateral root length. The diameter of the primary root was also correlated with shoot and root biomass and with the diameter of lateral roots. Little correlation was found between either primary root length or lateral root insertion angle and any other trait.

Little variation in the traits assayed was attributed directly to run or scanner in the multiple-genotype experiment. The effects of genotype, and the effects of interactions between genotype×run, genotype×scanner, and genotype×run×scanner accounted for most of the experimental variation (Table 3). The effect of genotype alone accounted for more variation in shoot traits than in root traits. The effect of genotype alone accounted for >44% of the variation in shoot biomass, but only 15–23% of the variation in root biomass. Broad-sense heritability, estimated as the quotient of the estimated variance associated with the genotypic effect and the total variance for the trait ($\sigma_g^2/\sigma_p^2$), was largest for shoot biomass traits (>0.60), intermediate (0.25–0.60) for length and diameter of primary

**Table 3.** *Sources of variation and broad-sense heritability in shoot and root traits assayed at 18 DAS among 190 surviving seedlings of the parents (IMB211, R500) and 14 recombinant inbred lines of the* Brassica rapa *BrailRIl mapping population grown for 15 days in the phenotyping platform*

m=mean trait value; $\sigma^2_g$, estimated variance associated with the effect of genotype; $\sigma^2_{ag}$, estimated covariance associated with the effect of genotype×experimental run; $\sigma^2_{bg}$, estimated covariance associated with the effect of genotype×scanner; $\sigma^2_{abg}$, estimated covariance associated with the effect of genotype×experimental run×scanner; $\sigma^2_{bg}$, estimated variance associated with the residual error, $H^2$, broad-sense heritability.

| Trait | Trait means and standard deviations of effects | | | | | | | Source of variation (%) | | | | |
|---|---|---|---|---|---|---|---|---|---|---|---|---|
| | Mean | $\sigma_g$ | $\sigma_{ag}$ | $\sigma_{bg}$ | $\sigma_{abg}$ | $\sigma$ | $H^2$ | Genotype | Genotype× Run | Genotype× Scanner | Genotype× Run×Scanner | Residual |
| Shoot fresh weight (mg) | 53.4 | 19.58 | 9.17 | 1.38 | 0.00 | 10.10 | 0.72 | 48.7 | 22.8 | 3.4 | 0.0 | 25.1 |
| Shoot dry weight (mg) | 3.1 | 1.02 | 0.66 | 0.00 | 0.00 | 0.61 | 0.60 | 44.4 | 28.9 | 0.0 | 0.0 | 26.7 |
| Root fresh weight (mg) | 12.5 | 2.94 | 4.44 | 0.00 | 2.30 | 3.32 | 0.21 | 22.6 | 34.1 | 0.0 | 17.7 | 25.6 |
| Root dry weight (mg) | 1.2 | 0.32 | 0.26 | 0.00 | 0.88 | 0.56 | 0.12 | 15.7 | 13.0 | 0.0 | 43.5 | 27.7 |
| Primary root length (cm) | 16.4 | 2.19 | 1.18 | 0.00 | 1.24 | 2.34 | 0.41 | 31.4 | 17.0 | 0.0 | 17.8 | 33.7 |
| Primary root diameter (mm) | 0.36 | 0.019 | 0.014 | 0.007 | 0.011 | 0.019 | 0.36 | 27.8 | 19.6 | 9.5 | 15.4 | 27.7 |
| Lateral branching density ($cm^{-1}$) | 2.82 | 0.454 | 0.322 | 0.155 | 0.000 | 0.666 | 0.28 | 28.4 | 20.1 | 9.7 | 0.0 | 41.7 |
| Lateral root length (cm) | 1.28 | 0.16 | 0.44 | 0.14 | 0.16 | 0.48 | 0.06 | 11.9 | 31.7 | 10.1 | 11.6 | 34.7 |
| Lateral root diameter (mm) | 0.27 | 0.000 | 0.040 | 0.007 | 0.022 | 0.023 | 0.00 | 0.0 | 43.6 | 7.6 | 24.0 | 24.8 |
| Lateral root insertion angle (°) | 67.6 | 3.12 | 3.48 | 1.62 | 0.36 | 4.18 | 0.24 | 24.4 | 27.3 | 12.7 | 2.8 | 32.7 |
| Total lateral root length (cm) | 31.3 | 8.09 | 18.35 | 1.99 | 1.25 | 9.15 | 0.14 | 20.8 | 47.3 | 5.1 | 3.2 | 23.6 |
| Total root length (cm) | 47.8 | 9.73 | 18.75 | 1.23 | 2.15 | 9.45 | 0.18 | 23.6 | 45.4 | 3.0 | 5.2 | 22.9 |

roots and lateral root branching density on the primary root, and smallest (<0.25) for root biomass traits, lateral root length, lateral root diameter, lateral root insertion angle, total lateral root length, and total root length (Table 3).

### *The dynamics of root growth*

Primary root length and total root length were measured daily during the course of the experiment (Fig. 3). The increases in primary root length and total root length with time followed a sigmoidal shape for all genotypes and the data showed no irregularities. The model that fitted the combined data for all genotypes best was a logistic growth function. The most informative model included only a single, random-effect parameter (the asymptote, $Ø_1$, Supplementary Data Equation S4) describing the effect of genotype on the growth in primary root length or total root length. Both the inflection point ($Ø_2$) and scale parameter of the logistic growth function ($Ø_3$) were constants across all genotypes studied. Values for the inflection point and scale parameter of the logistic growth function describing primary root length were 8.82 DAS and 0.211, respectively. Values for the inflection point and scale parameter of the logistic growth function describing total root length were 10.4 DAS and 0.310, respectively. Asymptotes for primary root length and total root length differed between genotypes (Table 4). The parental genotype IMB211 had an asymptote of 17.4 cm and the parental genotype R500 had an asymptote of 28.3 cm for primary root length. The parental genotype IMB211 had the smallest asymptote (37.3 cm) and the parental genotype R500 had the largest asymptote (126.6 cm) of all the genotypes assayed for total root length. These observations are consistent with the measurements of primary root length and total root length assayed at 18 DAS (Table 2).

The relationship between the growth rate of first-order lateral roots and their day of emergence after transfer to the phenotyping platform followed a quadratic function for all genotypes (Fig. 4). The lateral roots that emerged first (the basal lateral roots) generally had faster elongation rates than those that emerged later. The maximum lateral root elongation rate predicted by the model fitted to the data was 0.35 cm $d^{-1}$. The most informative model included only one, random-effect parameter ($b_{i1}$, Supplementary Data Equation S6) describing the effect of genotype on the initial growth rate of first-order lateral roots. The maximum initial growth rate ($b_{i1} + \beta_1$) of first-order lateral roots ranged from 0.216 to 0.307 cm $d^{-1}$, with IMB211 having a value of 0.255 cm $d^{-1}$ and R500 having a value of 0.290 cm $d^{-1}$. Unexplained residual errors in the model for lateral root elongation rate (Fig. 4) were greater than those for the models for either primary root length or total root length (Fig. 3).

## Discussion

### *Screening for root traits that improve crop yield*

The efficient acquisition of a particular mineral element requires a specific set of root traits, many of which have been identified (Dunbabin *et al.*, 2003; Lynch, 2007, 2013;

White *et al.*, 2013a,b). However, breeding for such root traits, either directly through screening for the traits themselves or indirectly through the identification of molecular-markers associated with the traits, requires observations on large populations of genotypes, which necessitates high-throughput, low-cost phenotyping platforms. Imaging is the central component of high-throughput phenotyping. Images contain detailed quantitative information on plant shape and morphologies. Images can be acquired rapidly and without manual intervention using, for example, motorized positioners and conveyors to move samples and/or image capture equipment (Yazdanbakhsh and Fisahn, 2009; Hartmann *et al.*, 2011). Image data can be obtained at regular time intervals for a large number of samples. Image analysis algorithms can then be used to extract biologically meaningful traits automatically from image data (Armengaud *et al.*, 2009; Lobet *et al.*, 2011). Unfortunately, the development of such systems requires considerable expertise in engineering and computer programming and large monetary investments in infrastructure. These prerequisites are often lacking in plant research laboratories. Root images are also noisier that shoot images and the image resolution obtained with conventional cameras can be a limitation to phenotyping.

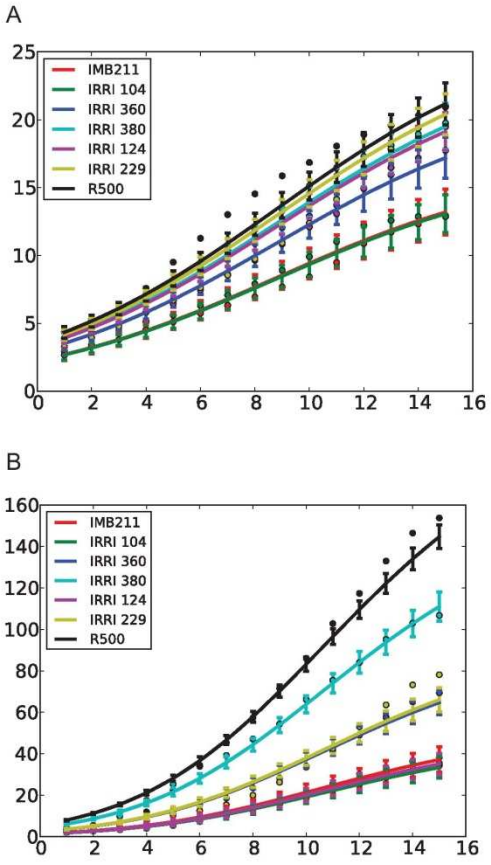


**Fig. 3.** Measured (circles) and predicted (lines) values of primary root length (A) and total root length (B) of the two parents and five recombinant inbred lines of the *Brassica rapa* BrapRRI mapping population over the 15 d following transfer to the phenotyping platform. Predicted values were estimated using a nonlinear mixed-effects model (Supplementary Data Equation S4). Error bars indicate standard error of the predicted means.

The phenotyping platform developed for the experiments reported here can overcome some of these limitations. The platform requires no sophisticated equipment and is adaptable to most laboratory and glasshouse environments. The utility of flatbed scanners for high-resolution imaging of roots was recently demonstrated by Dresbøll *et al.* (2013) in their study of the responses of tomato root growth to anoxia. The quality of the images obtained when roots were imaged against the uniform background of the germination paper using the scanners enabled efficient image analysis (Fig. 1). The ability to control multiple scanners automatically allowed the acquisition of images over extended periods without manual intervention and will enable the extension of phenotyping platform to the simultaneous screening of larger populations of genotypes.

### *Variation in root growth among* B. rapa *genotypes*

Coefficients of variation for specific shoot and root traits measured in 72 individuals of R-o-18 varied considerably (Table 1). The relationship between the CV for a trait and the number of replicates required to detect a significant difference follows a quadratic function. Since the CVs for many root traits were large, many replicates would be required to detect differences in these traits between genotypes. Since plants were grown on the surface of a germination paper with homogeneous

**Table 4.** *Estimates of the asymptotes ($\emptyset_2$, Supplementary Data Equation S4) for mixed-effects models describing temporal variation in total root length and primary root length, and the intercept ($b_{ll} + \beta_1$, Supplementary Data Equation S6) for the mixed-effects model describing the growth rate of first-order lateral roots among the parents (IMB211, R500) and 14 recombinant inbred lines of the* Brassica rapa *BrapRRI mapping population grown for 15 days in the phenotyping platform*

| | IMB 211 | R 500 | IRRI 002 | IRRI 016 | IRRI 030 | IRRI 070 | IRRI 104 | IRRI 124 | IRRI 143 | IRRI 198 | IRRI 201 | IRRI 205 | IRRI 229 | IRRI 248 | IRRI 360 | IRRI 380 |
|---|---|---|---|---|---|---|---|---|---|---|---|---|---|---|---|---|
| Total root length | 37.3 | 126.6 | 64.2 | 49.4 | 47.8 | 56.8 | 55.9 | 47.5 | 61.1 | 56.1 | 53.5 | 61.3 | 67.6 | 52.6 | 71.5 | 113.7 |
| Primary root length | 17.4 | 28.3 | 22.3 | 17.0 | 22.9 | 19.1 | 17.1 | 20.3 | 25.4 | 29.0 | 26.5 | 21.1 | 22.5 | 23.5 | 19.1 | 24.0 |
| Lateral growth rate | 0.255 | 0.290 | 0.255 | 0.273 | 0.307 | 0.285 | 0.326 | 0.262 | 0.216 | 0.234 | 0.263 | 0.296 | 0.295 | 0.233 | 0.281 | 0.297 |

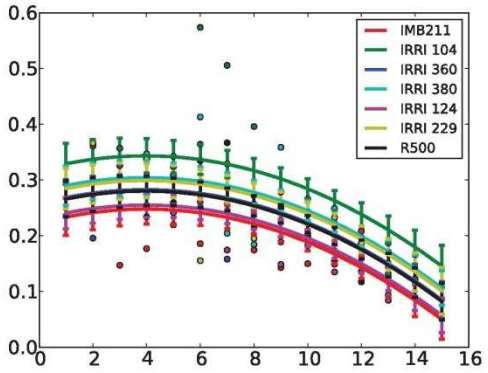


**Fig. 4.** Measured (circles) and predicted (lines) values of the elongation rates of lateral roots of the two parents and five recombinant inbred lines of the *Brassica rapa* BraIRRI mapping population as a function of the time of their emergence after transfer to the phenotyping platform. Predicted values were estimated using a nonlinear mixed-effects model (Supplementary Data Equation S6). Error bars indicate standard error of the predicted means.

distribution of water and mineral nutrients, most of the variability observed in root traits is intrinsic to the processes of root development. Intrinsic noise, or developmental stochasticity, is particularly significant in plant roots. It has been shown, for example, that innate changes in lateral root growth rates can exceed by up to 5-fold those observed in response to nitrate availability (Forde, 2009). It is essential therefore to develop ways to characterize developmental stochasticity in order to minimize residual variations in root phenotyping experiments.

The phenotyping platform developed here was used to quantify variation in shoot and root morphological traits from a selection of genotypes (Table 2). A significant effect of genotype was observed for all traits. It is usually observed that shoot biomass traits have larger broad-sense heritability that root biomass traits (Arraouadi *et al.*, 2012; Bouteillé *et al.*, 2012), and the results obtained with the pouch-and-wick system confirm these observations (Table 3). Broad-sense heritability of root length typically ranges from 0.15 to 0.80 (Gahoonia and Nielsen, 2004; Bouteillé *et al.*, 2012). Although shoot biomass, primary root length, and lateral root branching density have large CVs, their heritability is high. Traits with large differences between genotypes and small variation within a genotype (i.e. high hereditability) require less replication to detect significant differences between genotypes than traits with either small differences between genotypes or low hereditability.

Many of the static traits described above show temporal variation. For example, primary root length and total root system length follow a sigmoidal growth function with time (Fig. 3). This has been observed in many crop species (Merrill *et al.*, 2002). It is also common to observe fastest growth rates of lateral roots emerging a few days after sowing (Nacry *et al.*, 2005). This behaviour was best modelled on the current data using a quadratic relationship between lateral root growth rate and day of emergence from the primary root (Fig. 4). However, lateral root growth rate within a single plant was highly variable and the residual variances in models were higher than in primary and total root length models. Although run was not a significant factor, there were large differences in the variance of the residual between two runs for the total root length models, and different models might be required in the future for the analysis of such data. There were significant effects of genotype on the dynamics of root growth (Table 4 and Figs 3 and 4). Data for primary root length and total root length indicate that all genotypes follow a similar growth pattern with time but differ in their absolute growth rate. Data for the elongation rate of lateral roots also indicate that all genotypes follow a similar pattern with time, but differ in their maximum growth rate.

### *The application of scanner-based high-resolution root phenotyping*

Identifying chromosomal loci affecting a particular root trait (quantitative trait loci) requires evaluation of many hundreds of genotypes with high replication (Qu *et al.*, 2008; Sharma *et al.*, 2011; Shi *et al.*, 2013). The phenotyping platform described here can automatically image the root systems of 48 plants grown simultaneously (Fig. 1). It is, therefore, not of a sufficient size to phenotype the root systems of a genetic mapping population within a short time period. However, since it has no moving parts, it is relatively simple to extend the platform, although achieving the required throughput might necessitate a reduction in the cost of the equipment. This could be achieved for example with a more economical imaging technology such as contact image sensors (Dannoura *et al.*, 2012).

Real soil environments are also difficult to reproduce in laboratories and glasshouses. Roots grow in three dimensions and experience a range of physical conditions that influence their growth in various ways (Bengough *et al.*, 2011). Interactions with a range of biological organisms, such as bacteria and arbuscular mycorrhizal fungi, can also have a strong impact on the acquisition of water and mineral elements (Bucher, 2007). The ability to image root systems of mature plants growing in soil is likely to improve the correlations between traits obtained in the phenotyping platform and measurements made in the field. The platform described here can be used to image the roots of plants growing in other substrates, including soil (Dresbøll *et al.*, 2013). Furthermore, although the platform described here could only accommodate young seedlings because of the size of the scanner window, root systems of larger plants might be accommodated by growing plants in larger pouches, which could be imaged in overlapping sectors and these images combined to reconstruct an image of the entire root system, as described recently by Lobet and Draye (2013).

Root systems of plants grown in soil respond dynamically to changes in their local environment. For example, the development of RSAs alters in response to vagaries in the availability of water (Taylor and Ratliff, 1969; Rostamza *et al.*, 2013), the root distribution within the soil profile responds to the presence of macropores and the depth at which a compacted subsoil is formed (Valentine *et al.*, 2012; Acuña and

Wade, 2013), lateral roots proliferate in patches of soil with high availability of various essential mineral elements (Forde and Walch-Liu, 2009; Hodge *et al.*, 2009), and root systems develop to avoid exposure to toxic elements, such as cadmium (Lux *et al.*, 2011). The platform described here can be used to investigate responses of the root systems to environmental variables and, if scaled to accommodate genetic mapping populations, to identify genetic factors affecting root responses to the environment. The ability to characterize dynamic responses to environmental variables will allow researchers to identify quantitative trait loci influencing the plasticity of the root system, which is required for marker-assisted selection of genotypes adapted to multiple soil types and environmental conditions (de Dorlodot *et al.*, 2007; Hochholdinger and Tuberosa, 2009; Hodge *et al.*, 2009; Acuña and Wade, 2013). The application of scanner-based, high-resolution root phenotyping of mature plants grown in soil could, therefore, facilitate the development of crop varieties that are better adapted to future environmental conditions.

## Supplementary material

Supplementary data are available at *JXB* online.

Supplementary Data. Statistical models of root systems.

## Acknowledgements

This work was supported by the Rural and Environment Science and Analytical Services Division (RESAS) of the Scottish Government through Work Package 3.3, 'The soil, water and air interface and its response to climate and land use change' (2011–2016). Funding for this study was provided in part by the UK Biotechnology and Biological Sciences Research Council (BBSRC) Crop Improvement Research Club (grant BB/J019631/1) and a BBSRC Professorial Fellowship (to M.J.B.). M.O.A. was supported by the University of Nottingham Vice-Chancellor's Scholarship for Research Excellence. Jim Anderson, Amy Gibson, Sophie Hiel, Ken Loades, Linda Ford, and Gill Banks provided invaluable help for laboratory work. The authors are grateful for advice from Jim McNichol and Christine Hackett on the statistical analyses.

## References

**Acuña TLB, Wade LJ.** 2013. Use of genotype × environment interactions to understand rooting depth and the ability of wheat to penetrate hard soils. *Annals of Botany* **112,** 359–368.

**Armengaud P, Zambaux K, Hills A, Sulpice R, Pattison RJ, Blatt MR, Amtmann A.** 2009. EZ-Rhizo: integrated software for the fast and accurate measurement of root system architecture. *The Plant Journal* **57,** 945–956.

**Arraouadi S, Badri M, Abdelly C, Huguet T, Aouani ME.** 2012. QTL mapping of physiological traits associated with salt tolerance in *Medicago truncatula* recombinant inbred lines. *Genomics* **99,** 118–125.

**Bengough AG, Gordon DC, Al-Menaie H, Ellis RP, Allan D, Keith R, Thomas WTB, Forster BP.** 2004. Gel observation chamber for rapid screening of root traits in cereal seedlings. *Plant and Soil* **262,** 63–70.

**Bengough AG, McKenzie BM, Hallett PD, Valentine TA.** 2011. Root elongation, water stress, and mechanical impedance: a review of limiting stresses and beneficial root tip traits. *Journal of Experimental Botany* **62,** 59–68.

**Bibikova TN, Jacob T, Dahse I, Gilroy S.** 1998. Localized changes in apoplastic and cytoplasmic pH are associated with root hair development in *Arabidopsis thaliana*. *Development* **125,** 2925–2934.

**Bland WL, Mesarch MA, Wolfe JE.** 1990. A controlled-temperature rhizotron. *Crop Science* **30,** 1142–1145.

**Bouteillé M, Rolland G, Balsera C, Loudet O, Muller B.** 2012. Disentangling the intertwined genetic bases of root and shoot growth in *Arabidopsis*. *PLoS One* **7,** e32319.

**Box JE, Ramsuer EL.** 1993. Minirhizotron wheat root data: comparisons to soil core root data. *Agronomy Journal* **85,** 1058–1060.

**Broadley MR, Bowen HC, Cotterill HL, Hammond JP, Meacham MC, Mead A, White PJ.** 2003. Variation in the shoot calcium content of angiosperms. *Journal of Experimental Botany* **54,** 1431–1446.

**Bucher M.** 2007. Functional biology of plant phosphate uptake at root and mycorrhiza interfaces. *New Phytologist* **173,** 11–26.

**Clark RT, MacCurdy RB, Jung JK, Shaff JE, McCouch SR, Aneshansley DJ, Kochian LV.** 2011. Three-dimensional root phenotyping with a novel imaging and software platform. *Plant Physiology* **156,** 455–465.

**Dannoura M, Kominami Y, Makita N, Hiroyuki, O.** 2012. Flat optical scanner method and root dynamics. In: Mancuso S, ed, *Measuring roots: an updated approach*. New York: Springer, pp 127–133.

**de Dorlodot S, Forster B, Pagès L, Price A, Tuberosa R, Draye X.** 2007. Root system architecture: opportunities and constraints for genetic improvement of crops. *Trends in Plant Science* **12,** 474–481.

**Downie H, Holden N, Otten W, Spiers AJ, Valentine TA, Dupuy LX.** 2012. Transparent soil for imaging the rhizosphere. *PLoS One* **7** e44276.

**Dresbøll DB, Thorup-Kristensen K, McKenzie BM, Dupuy L, Bengough AG.** 2013. Timelapse scanning reveals spatial variation in tomato (*Solanum lycopersicum* L.) root elongation rates during partial waterlogging. *Plant and Soil* **369,** 467–477.

**Drew MC, Saker LR.** 1975. Nutrient supply and the growth of the seminal root system in barley: II. Localized, compensatory increases in lateral root growth and rates of nitrate uptake when nitrate supply is restricted to only part of the root system. *Journal of Experimental Botany* **26,** 79–90.

**Dunbabin V, Diggle A, Rengel Z.** 2003. Is there an optimal root architecture for nitrate capture in leaching environments? *Plant, Cell and Environment* **26,** 835–844.

**Dupuy L, Vignes M, McKenzie BM, White PJ.** 2010. The dynamics of root meristem distribution in the soil. *Plant, Cell and Environment* **33,** 358–369.

**Eng J.** 2003. Sample size estimation: how many individuals should be studied? *Radiology* **227,** 309–313.

**Eshel A, Grunzweig JM.** 2013. Root-shoot allometry of tropical forest trees determined in a large-scale aeroponic system. *Annals of Botany* **112,** 291–296.

**Fang S, Yan X, Liao H.** 2009. 3D reconstruction and dynamic modeling of root architecture in situ and its application to crop phosphorus research. *The Plant Journal* **60,** 1096–1108.

**Fiorani F, Schurr U.** 2013. Future scenarios for plant phenotyping. *Annual Review of Plant Biology* **64,** 267–291.

**Flavel RJ, Guppy CN, Tighe M, Watt M, McNeill A, Young IM.** 2012. Non-destructive quantification of cereal roots in soil using high-resolution X-ray tomography. *Journal of Experimental Botany* **63,** 2503–2511.

**Forde BG.** 2009. Is it good noise? The role of developmental instability in the shaping of a root system. *Journal of Experimental Botany* **60,** 3989–4002.

**Forde BG, Walch-Liu P.** 2009. Nitrate and glutamate as environmental cues for behavioural responses in plant roots. *Plant, Cell and Environment* **32,** 682–693.

**French A, Ubeda-Tomas S, Holman TJ, Bennett MJ, Pridmore T.** 2009. High-throughput quantification of root growth using a novel image-analysis tool. *Plant Physiology* **150,** 1784–1795.

**Gahoonia TS, Nielsen NE.** 2004. Root traits as tools for creating phosphorus efficient crop varieties. *Plant and Soil* **260,** 47–57.

**Hartmann A, Czauderna T, Hoffmann R, Stein N, Schreiber F.** 2011. HTPheno: an image analysis pipeline for high-throughput plant phenotyping. *BMC Bioinformatics* **12,** 148.

**Hochholdinger F, Tuberosa R.** 2009. Genetic and genomic dissection of maize root development and architecture. *Current Opinion in Plant Biology* **12,** 172–177.

**Hodge A, Berta G, Doussan C, Merchan F, Crespi M.** 2009. Plant root growth, architecture and function. *Plant and Soil* **321,** 153–187.

**Hund A, Trachsel S, Stamp P.** 2009. Growth of axile and lateral roots of maize: I development of a phenotying platform. *Plant and Soil* **325,** 335–349.

**Iniguez-Luy FL, Lukens L, Farnham MW, Amasino RM, Osborn TC.** 2009. Development of public immortal mapping populations, molecular markers and linkage maps for rapid cycling *Brassica rapa* and *B. oleracea*. *Theoretical and Applied Genetics* **120,** 31–43.

**Iyer-Pascuzzi AS, Symonova O, Mileyko Y, Hao YL, Belcher H, Harer J, Weitz JS, Benfey PN.** 2010. Imaging and analysis platform for automatic phenotyping and trait ranking of plant root systems. *Plant Physiology* **152,** 1148–1157.

**Liao H, Rubio G, Yan XL, Cao AQ, Brown KM, Lynch JP.** 2001. Effect of phosphorus availability on basal root shallowness in common bean. *Plant and Soil* **232,** 69–79.

**Lobet G, Draye X.** 2013. Novel scanning procedure enabling the vectorization of entire rhizotron-grown root systems. *Plant Methods* **9,** 1.

**Lobet G, Pagès L, Draye X.** 2011. A novel image-analysis toolbox enabling quantitative analysis of root system architecture. *Plant Physiology* **157,** 29–39.

**Lux A, Martinka M, Vaculík M, White PJ.** 2011. Root responses to cadmium in the rhizosphere: a review. *Journal of Experimental Botany* **62,** 21–37.

**Lynch JP.** 2007. Roots of the Second Green Revolution. *Australian Journal of Botany* **55,** 493–512.

**Lynch JP.** 2013. Steep, cheap and deep: an ideotype to optimize water and N acquisition by maize root systems. *Annals of Botany* **112,** 347–357.

**Mairhofer S, Zappala S, Tracy S, Sturrock C, Bennett M, Mooney S, Pridmore T.** 2013. Recovering complete plant root system architectures from soil via X-ray μ-computed tomography. *Plant Methods* **9,** 1–7.

**Merrill SD, Tanaka DL, Hanson JD.** 2002. Root length growth of eight crop species in haplustoll soils. *Soil Science Society of America Journal* **66,** 913–923.

**Nacry P, Canivenc G, Muller B, Azmi A, Van Onckelen H, Rossignol M, Doumas P.** 2005. A role for auxin redistribution in the responses of the root system architecture to phosphate starvation in arabidopsis. *Plant Physiology* **138,** 2061–2074.

**Nagel KA, Putz A, Gilmer F, *et al*.** 2012. GROWSCREEN-Rhizo is a novel phenotyping robot enabling simultaneous measurements of root and shoot growth for plants grown in soil-filled rhizotrons. *Functional Plant Biology* **39,** 891–904.

**Oliveira RGM, Noordwijk M, Gaze SR, Brouwer G, Bona S, Mosca G, Hairiah K.** 2000. Auger sampling, ingrowth cores and pinboard methods. In: Smit A, Bengough AG, Engels C, Noordwijk M, Pellerin S, Geijn S, eds, *Root methods: a handbook*. Berlin: Springer, pp 175–210.

**Oswald SE, Menon M, Carminati A, Vontobel P, Lehmann E, Schulin R.** 2008. Quantitative imaging of infiltration, root growth, and root water uptake via neutron radiography. *Vadose Zone Journal* **7,** 1035–1047.

**Pinheiro JC, Bates DM.** 2000. *Mixed-effects models in S and S-PLUS* . New York: Springer-Verlag.

**Pinheiro J, Bates D, DebRoy S, Sarkar D**, R Development Core Team. 2013. nlme: linear and nonlinear mixed effects models. R package version 3.1–113. Vienna, Austria: R Development Core Team.

**Qu YY, Mu P, Zhang HL, Chen CY, Gao YM, Tian YX, Wen F, Li ZC.** 2008. Mapping QTLs of root morphological traits at different growth stages in rice. *Genetica* **133,** 187–200.

**Rascher U, Blossfeld S, Fiorani F, *et al*.** 2011. Non-invasive approaches for phenotyping of enhanced performance traits in bean. *Functional Plant Biology* **38,** 968–983.

R Development Core Team. 2012. *R: a language and environment for statistical computing* . Vienna, Austria: R Foundation for Statistical Computing.

**Ribeiro KM, Barreto B, Pasqual M, White PJ, Braga RA, Dupuy LX.** 2014. Continuous, high-resolution biospeckle imaging reveals a discrete zone of activity at the root apex that responds to contact with obstacles. *Annals of Botany*, **113,** 555–563.

**Rostamza M, Richards RA, Watt M.** 2013. Response of millet and sorghum to a varying water supply around the primary and nodal roots. *Annals of Botany* **112,** 439–446.

**Schmidt S, Bengough AG, Gregory PJ, Grinev DV, Otten W.** 2012. Estimating root–soil contact from 3D X-ray microtomographs. *European Journal of Soil Science* **63,** 776–786.

**Sharma S, Xu S, Ehdaie B, Hoops A, Close T, Lukaszewski A, Waines JG.** 2011. Dissection of QTL effects for root traits using a chromosome arm-specific mapping population in bread wheat. *Theoretical and Applied Genetics* **122,** 759–769.

**Shi L, Shi T, Broadley MR, White PJ, Long Y, Meng J, Xu F, Hammond JP.** 2013. High-throughput root phenotyping screens identify genetic loci associated with root architectural traits in *Brassica napus* under contrasting phosphate availabilities. *Annals of Botany* **112,** 381–389.

**Smit AL, Bengough AG, Engels C, van Noordwijk M, Pellerin S, van de Geijn SC.** 2000. *Root methods: a handbook*. Berlin: Springer-Verlag.

**Smith S, De Smet I.** 2012. Root system architecture: insights from *Arabidopsis* and cereal crops. *Philosophical Transactions of the Royal Society B* **367,** 1441–1452.

**Stephenson P, Baker D, Girin T, Perez A, Amoah S, King GJ, Ostergaard L.** 2010. A rich TILLING resource for studying gene function in *Brassica rapa*. *BMC Plant Biology* **10,** 62.

**Taylor HM, Ratliff LF.** 1969. Root elongation rates of cotton and peanuts as a function of soil strength and soil water content. *Soil Science* **108,** 113–119.

**Trachsel S, Kaeppler SM, Brown KM, Lynch JP.** 2010. Shovelomics: high throughput phenotyping of maize (*Zea mays* L.) root architecture in the field. *Plant and Soil* **341,** 75–87.

**Tsai WH.** 1985. Moment-preserving thresholding—a new approach. *Computer Vision Graphics and Image Processing* **29,** 377–393.

**Tuberosa R, Sanguineti MC, Landi P, Giuliani MM, Salvi S, Conti S.** 2002. Identification of QTLs for root characteristics in maize grown in hydroponics and analysis of their overlap with QTLs for grain yield in the field at two water regimes. *Plant Molecular Biology* **48,** 697–712.

**Valentine TA, Hallett PD, Binnie K, Young MW, Squire GR, Hawes C, Bengough AG.** 2012. Soil strength and macropore volume limit root elongation rates in many UK agricultural soils. *Annals of Botany* **110,** 259–270.

**Vepraskas MJ, Hoyt GD.** 1988. Comparison of the trench-profile and core methods for evaluating root distributions in tillage studies. *Agronomy Journal* **80,** 166–172.

**Waisel Y.** 2002. Aeroponics: a tool for root research under minimal environmental restrictions. In: Waisel Y, Eshel A, Kafkafi U, eds, *Plant roots: the hidden half*. New York: Marcel Dekker, pp 323–331.

**Walter A, Scharr H, Gilmer F, *et al*.** 2007. Dynamics of seedling growth acclimation towards altered light conditions can be quantified via GROWSCREEN: a setup and procedure designed for rapid optical phenotyping of different plant species. *New Phytologist* **174,** 447–455.

**Wenzel W, Wieshammer G, Fitz W, Puschenreiter M.** 2001. Novel rhizobox design to assess rhizosphere characteristics at high spatial resolution. *Plant and Soil* **237,** 37–45.

**White PJ, George TS, Dupuy LX, Karley AJ, Valentine TA, Wiesel L, Wishart J.** 2013a. Root traits for infertile soils. *Frontiers in Plant Science* **4,** 193.

**White PJ, George TS, Gregory PJ, Bengough AG, Hallett PD, McKenzie BM.** 2013b. Matching roots to their environment. *Annals of Botany* **112,** 207–222.

**Wojciechowski T, Gooding MJ, Ramsay L, Gregory PJ.** 2009. The effects of dwarfing genes on seedling root growth of wheat. *Journal of Experimental Botany* **60,** 2565–2573.

**Xu XD, Xie QG, McClung CR.** 2010. Robust circadian rhythms of gene expression in *Brassica rapa* tissue culture. *Plant Physiology* **153,** 841–850.

**Yang Z, Downie H, Rozbicki E, Dupuy LX, MacDonald MP.** 2013. Light sheet tomography (LST) for *in situ* imaging of plant roots. *Optics Express* **21,** 16239–16247.

**Yazdanbakhsh N, Fisahn J.** 2009. High throughput phenotyping of root growth dynamics, lateral root formation, root architecture and root hair development enabled by PlaRoM. *Functional Plant Biology* **36,** 938–946.

**Zeng G, Birchfield ST, Wells CE.** 2008. Automatic discrimination of fine roots in minirhizotron images. *New Phytologist* **177,** 549–557.

**Zhu JM, Ingram PA, Benfey PN, Elich T.** 2011. From lab to field, new approaches to phenotyping root system architecture. *Current Opinion in Plant Biology* **14,** 310–317.

## Supplementary Data

**High-resolution quantification of variation in root growth dynamics of *Brassica rapa* genotypes.** *Michael O Adu, Antoine Chatot, Lea Wiesel, Malcolm J Bennett, Martin R Broadley, Philip J White, and Lionel X Dupuy*

**SUPPLEMENTARY DATA**

**Statistical models of root systems**

The experiment with a single genotype (*B. rapa* subsp. *trilocularis* cv. R-o-18) was used to calculate the number of replicates (*R*) that would be required to detect a significant difference between two populations with identical standard deviations in a trait using a two-sided, 95% confidence interval (CI), t-test, if the trait means differed by 50% (Eng, 2003):

$$R = \left(\frac{CV\ Z_{crit}}{25}\right)^2, \tag{S1}$$

where *CV* is coefficient of variation for the trait in the reference population and $Z_{crit}$ is the standard normal deviate corresponding to a confidence interval of 95% (1.96).

The sources of variation in static root traits in the single-genotype experiment were determined using a mixed effects model with experimental run and scanner considered as random factors:

$$\begin{gathered} y_{ij} = m + a_i + b_j + \epsilon_{ij}\ , \\ i \in \{1, \dots, n\}, j \in \{1, \dots, r\}\ , \\ a_i \sim N(0, \sigma_a^2), \qquad b_j \sim N(0, \sigma_b^2), \qquad \epsilon_{ij,} \sim N(0, \sigma^2\ ), \end{gathered} \tag{S2}$$

where $y_{ij}$ represents the root trait from the $i^{th}$ run and $j^{th}$ scanner, *m* is the mean trait value, $a_i$ is the effect of $i^{th}$ run, $b_j$ is the effect of the $j^{th}$ scanner, $\epsilon_{ij}$ is the residual error, *n* is the number of runs (5), *r* is the total number of scanners (8), $\sigma_a^2$ is the estimated variance associated with the effect of the run, $\sigma_b^2$ is the estimated variance associated with the effect of the scanner, and), $\sigma^2$ is the estimated variance associated with the residual error.

The sources of variation in static root traits in the multiple-genotype experiment were determined using a mixed effects model with experimental run, scanner and genotype considered as random factors:

$$\begin{gathered} y_{ijk} = m + g_k + ag_{ik} + bg_{jk} + abg_{ijk} + \epsilon_{ijk}, \\ i \in \{1, \dots, n\}, j \in \{1, \dots, r\}, k \in \{1, \dots, s\}, \\ g_k / ag_{ik} / bg_{jk} / abg_{ijk} \sim N\left(0, \sigma^2_{g/ag/bg/abg}\right), \epsilon_{ij}\ \sim N(0, \sigma^2\ ), \end{gathered} \tag{S3}$$

where $y_{ijk}$ represents the root trait from the $i^{th}$ experimental run, $j^{th}$ scanner and $k^{th}$ genotype, $m$ is the mean trait value, $g_k$ is the effect of the genotype, $ag_{ik}$ is the effect of interactions

between experimental run and genotypic factors, $bg_{jk}$ is the effect of interactions between scanner and genotypic factors, $abg_{ijk}$ is the effect of interactions between experimental run, scanner and genotypic factors, $\epsilon_{ijk}$ is the residual error, $n$ is the number of runs (2), $r$ is the total number of scanners (24) and $s$ is the number of genotypes (16). Broad-sense heritability ($H^2$) was estimated as $\sigma_g^2$ / $\sigma_p^2$, where $\sigma_g^2$ is the estimated variance associated with the genotypic effect and $\sigma_p^2$ is the total variance for the trait.

The sources of variation in dynamic root traits were determined using mixed effects models with genotype and day after sowing (DAS) considered as random factors. To account for non-linearity in growth curves, a logistic growth function was used to model the increase in total root length and primary root length with time. The three parameters of the logistic function were the asymptote ($\emptyset_1$), inflection point ($\emptyset_2$), and scale parameter ($\emptyset_3$). These models were used to describe sources of temporal variation in (i) total root length, (ii) primary root length, and (iii) the growth rate of first order lateral roots:

$$y_{ij} = \frac{\emptyset_{i1}}{1+\exp\left[-\left(DAS_j - \emptyset_{i2}\right)/\emptyset_{i3}\right]} + \epsilon_{ij}, \quad \text{(S4)}$$

$$\emptyset_i = \begin{bmatrix}\emptyset_{i1}\\ \emptyset_{i2}\\ \emptyset_{i3}\end{bmatrix} = \begin{bmatrix}\beta_1\\ \beta_2\\ \beta_3\end{bmatrix} + \begin{bmatrix}b_i\\ 0\\ 0\end{bmatrix},$$

$$i = \{1, \dots, s\}, j = \{1, \dots, t\},$$

$$b_i \sim N\left(0, \sigma_b^2\right),\ \epsilon_{ij} \sim N\left(0, \sigma^2\right).$$

where $y_{ij}$ is the total root length or primary root length for the $i^{th}$ genotype, on the $j^{th}$ DAS, and $t$ is the number of timepoints at which measurements were made (15). The parameters $\beta_1$, $\beta_2$ and $\beta_3$ are the mean values of the individual logistic parameters $\emptyset_{i1}$, $\emptyset_{i2}$ and $\emptyset_{i3}$, respectively, and $b_i$, is the random effect on the asymptote of the logistic function and $\epsilon_{ij}$ is the residual error. A likelihood ratio test was used to select the final model, which had the three parameters as fixed effects and only the asymptote as a random effect. For the total root length model, data were normalised by square root transformation before analyses. Autocorrelation in the data was modelled using the moving average (corARMA) and autoregressive model of an order 1 (AR1) correlation structure (Pinheiro and Bates, 2000). To account for heteroscedasticity a power variance function was used of the form:

$$Var\left(\epsilon_{ij} \middle| DAS\right) = \sigma^2\left(\delta_1 + |DAS|^{\delta_2}\right), \quad \text{(S5)}$$

where $\sigma^2$ is the variance when $j$=0 and $\delta_1$ and $\delta_2$ are the two parameters for the power variance function (Pinheiro and Bates, 2000).

The growth rate of a lateral root was expressed as the quotient of the lateral root length divided by the length of time after its emergence from the primary root. Data for growth rates of lateral roots were normalized by square root transformation and the sources of variation in the growth rate of lateral roots were determined using mixed effects models with genotype and day after sowing (DAS) considered as random factors:

$$y_{ij} = b_{i1} + \beta_1 + \beta_2 DAS_j + \beta_3 DAS_j^2 + \epsilon_{ij}\,, \quad i = \{1, \ldots, s\}, j = \{1, \ldots, t\}, \quad b_{i1} \sim N(0, \sigma_{b1}^2), \epsilon_{ijk} \sim N(0, \sigma^2). \tag{S6}$$

where $y_{ij}$ is the lateral root growth rate for genotype $i$ on the $j^{th}$ day of the experiment, $\beta_1$, $\beta_2$ and $\beta_3$ are the fixed effect parameters for the quadratic function and $b_{i1}$ is the random effects on the intercept of the quadratic function.

The sources of variation in the mixed effects models described in Equations 2, 3, 5, 7, and 8 were chosen based on Akaike and Bayesain information criteria (Pinheiro and Bates, 2000). The quality of the mixed effects models was also assessed visually using quantile-quantile plots to check for normality and residual plots to check that the variance of residuals was constant (Pinheiro and Bates, 2000). ANOVA was used to determine the significance of differences in fixed and random effects.

**References**

**Eng J**. 2003. Sample size estimation: how many individuals should be studied? *Radiology* **227**, 309 -313.

**Pinheiro JC, Bates DM**. 2000. *Mixed-Effects Models in S and S-PLUS*. New York: Springer-Verlag.